Ultra Structurally Based Impedance Model for Oral Cancer Detection

by

Peter Robert Pelletier

A Dissertation Presented in Partial Fulfillment
of the Requirements for the Degree
Doctor of Philosophy

Approved April 2010 by the
Graduate Supervisory Committee:

Michael Kozicki, Chair
Bruce Towe
Marco Saraniti
Michael Goryll

ARIZONA STATE UNIVERSITY

May 2012

ABSTRACT

This research investigated using impedance as a minimally invasive oral cancer-screening tool by modeling healthy and diseased tissue. This research developed an ultra-structurally based tissue model for oral mucosa that is versatile enough to be easily modified to mimic the passive electrical impedance responses of multiple benign and cancerous tissue types. This new model provides answers to biologically meaningful questions related to the impedance response of healthy and diseased tissues. This model breaks away from the old empirical top down “black box” Thèvinin equivalent model. The new tissue model developed here was created from a bottom up perspective resulting in a model that is analogous to having a “Transparent Box” where each network element relating to a specific structural component is known. This new model was developed starting with sub cellular ultra-structural components such as membranes, proteins and electrolytes. These components formed the basic network elements and topology of the organelles. The organelle networks combine to form the cell networks. The cell networks combine to make networks of cell layers and the cell layers were combined into tissue networks. This produced the complete “Transparent Box” model for normal tissue. This normal tissue model was modified for disease based on the ultra-structural pathology of each disease. The diseased tissues evaluated include cancers type one through type three; necrotic-inflammation, hyperkeratosis and the compound condition of hyperkeratosis over cancer type two. The impedance responses for each of the disease were compared side by side with the response of normal healthy tissue. Comparative evidence from the models showed the structural changes in cancer produce a unique identifiable impedance “finger print.” The evaluation of the “Transparent Box” model for normal tissues and diseased tissues show clear support for using comparative impedance measurements as a clinical tool for oral cancer screening.

ACKNOWLEDGMENTS

The development of this research project was very challenging because of its multidisciplinary nature. A fair amount of time was spent on gathering knowledge outside my traditional discipline of electrical engineering. The study of cell biology, electrochemistry and medical pathology was required. I am very grateful to the many people who helped me work my way through the difficult problems I encountered along the way.

First and foremost, I would like to thank Dr. Michael Kozicki, my research advisor and my source of inspiration for entrepreneurial activities. Dr. Kozicki has provided me the freedom to approach problems in my own way while still providing expert guidance and suggestions over the course of many insightful conversations.

I would like to thank each member of my committee who provided an invaluable source of expert knowledge, talent and fresh perspective on my chosen topic. Each member easily provided me with their valuable time when there was very little to spare.

I would like to thank John Iannuzzi and Phil Altomare of Core technology group in Pennsylvania for lending me their most capable frequency response analyzer for exploring the commercial development of impedance based cancer detection.

Finally, I am grateful to Dr. Don Coffey, Professor of Oncology at the Johns Hopkins University School of Medicine who inspired me to develop a better way of detecting cancer through his lectures and conversations. I would also like to thank Dr. Stewart Lindsay, and Dr. Paul Davies who gave me an opportunity to join the research discussions for the National Cancer Institute's Center for Convergence of Physical Science and Cancer Biology at Arizona State University. Without this opportunity I would never have went to the Cancer Lecture by Dr. Don Coffey which inspired many years of research leading to many new and exciting discoveries.

TABLE OF CONTENTS

Page

CHAPTER Page

LIST OF TABLES

Table Page

LIST OF FIGURES

Figure Page

Figure Page

I. INTRODUCTION

A. Introduction

This research is focused on a small part of a larger goal. The larger goal is to reduce cancer deaths by increasing the availability and effectiveness of non-invasive impedance based early cancer screening tools. The small part that this research focuses on is the development of an ultra-structurally based tissue model for oral mucosa that is versatile enough to be easily modified to mimic the passive electrical impedance response of multiple benign and cancerous cell tissue types. This new model will provide answers to biological meaningful questions related to the impedance response of healthy and diseased tissues. It should provide a measure of confidence for the further development of impedance based measurement tools as a diagnostic and screening aid for oral tissue abnormalities.

The current state of the art passive element models for non-reactive cells and tissues are empirically based “Black Box” models. These models can approximate actual cell and tissue impedance responses but they can’t answer detailed questions about the systems they model. The lumped parameter elements within these models do not represent any single biological, chemical or physical attribute. These electrical elements represent a combination of all the attributes affecting impedance response, which also includes the electrode electrolyte interface effects.

B. The Modeling Goal

The goal of this research is to produce and explore a detailed “Transparent Box” passive element electrical model for both healthy and diseased oral mucosal tissues, where an electrical network represents the passive physical and ionic makeup of each cell structure. All the electrical networks for each cell structure will be combined into the organelle networks then further combined into the cell and then tissue networks. This

model will allow for the manipulation of structurally based details analogous to having knowledge and access to all the circuit elements that were previously hidden in the "Black Box." With this approach there is a structural and biochemical connection with each element within the model so that detailed questions can be answered when certain cell structures are affected by disease.

C. Analytical Questions

Construction of the detailed ultra structurally based "Transparent Box" passive element electrical model for both healthy and diseased tissues is just the first part of the project. Using the model when applied to various diseased tissues is the second part. The third part of the project is to finally answer the important questions that have both medical and scientific significance for using impedance in a clinical setting for the screening of cancer and other oral tissue diseases.

List of ten analytical questions to be asked by the "Transparent Box" model

1) What factors dominate the apparent decrease in impedance response of cancer tissue compared to the impedance response of normal healthy tissue?
2) What changes in the cells and tissues are responsible for decreasing impedance are they structurally related?
3) Are the observed impedance differences in cancer solely dominated by electrolyte increases as a result of increased cell signaling as suggested by [1-3]?
4) Are the impedance differences mainly because of biochemical differences in the various membranes of the cells and the organelles [4-7]?
5) Are the numbers, sizes and structures of the organelles within the cell responsible for the observed lower impedance responses [8-12]?

6) Does the large nuclear to cytoplasmic ratio feature common in all cancer cell tissues cause the observed decrease in impedance [13]?
7) Can impedance be used to differentiate between other benign diseases that often get misdiagnosed as cancer because their lesions have similar physical appearances to cancer [14]?
8) Can impedance be used to screen for and detect innocuous lesions before they become apparent by a visual inspection for the earliest detection of oral cancer?
9) What frequency or frequencies would be best for impedance based oral cancer-screening tool?
10) What methods of data display or manipulation would provide the best identification of tissue anomalies for possible disease identification?

D. Organization of the Dissertation

This dissertation is broken into fifteen major sections and one appendix. Each section has an introduction and a review. In general the first three sections introduce the problem, justify the need for the research and formulate the questions to be answered by the models. The first section is an introduction about the analytical questions this research will attempt to answer. The second section introduces the need for this research by introducing the greater goal of decreasing oral cancer deaths and by proposing impedance as an effective minimally invasive cancer-screening tool. The third section is a review of the empirically based models used to describe tissue impedance response; it outlines the need for a new model and introduces the foundation of how the models will be developed. The middle sections four through eleven develop the model. Section four is a brief introduction to the cell and the organelles it is meant to provide a little summary to

non-biologists. Readers interested in learning more in-depth about cell biology should reference [9]. Section five is a brief introduction to AC circuit theory for biologists. These readers interested in learning more about impedance spectroscopy should reference [50], and [51]. Section six introduces the development of the “Transparent Box” model starting from the membrane. Section seven covers the development of the organelle level models. Section eight covers the development of the cell level models it shows the integration of the organelle networks into the cell network. Section nine develops the tissue level model it shows how the individual cells are combined into layers of cells and into layers of tissue. Section ten covers the integration of Monte Carlo method into the “Transparent Box” model. Section eleven completes the transparent box model electrical elements and network for oral mucosal tissue with normal healthy cells. The last sections use the model and provide the answers to the problems. Section twelve is the development and comparative evaluation of diseased tissues using the “transparent box” model. Section twelve is the most important section and contains the majority of the scientifically valuable data. This is where impedance spectroscopy waveforms for each disease are compared and evaluated. Section thirteen provides an electrical element comparison between diseases. Section fourteen provides network evaluation for the transparent box models. Section fifteen provides the conclusion and the answers to the analytical questions. The appendix covers general notes on using and manipulating all the tissue models in Excel® spread sheets for the calculation of network elements.

II. CANCER

A. Introduction to Cancer

Cancer refers to any one of a large number of diseases characterized by the development of abnormal cells that divide uncontrollably, referred to as a neoplasm or tumor [9, pp. 1113-1320]. A tumor is said to be benign if it remains clustered together. The neoplasm is not a true cancer until the neoplastic cells gain the ability to infiltrate and colonize other tissues; this is the trait of malignancy [9, p. 1320], [11], [12], [14]. Invasiveness implies the cells have an ability to enter the bloodstream or lymphatic vessels and form secondary tumors called metastases, in other parts of the body [9, p. 1324]. Carcinomas are cancers arising from the epithelial cells [14]. Oral cancers are predominantly carcinomas with origins in the mouth [14]. Most cancers start from a single abnormal cell, but by the time it is first detected a typical tumor may already contain a billion or more cells [9], [14].

B. Background on Oral Cancer

In the United States squamous cell carcinoma of the oral cavity and pharynx accounts for over 34,000 cases annually which results in about 8,000 deaths per year [14], [15], [16]? Unfortunately, the diagnosis continues to rely on patient presentation and physical examination with biopsy confirmation. Often times no pain or discomfort is associated with the development of cancer. This can result in delayed diagnosis and that accounts for the fact that the majority of these cancers are diagnosed in the late stages of development [10], [15], [16]. Studies confirm that survival does correlate with stage thereby making it imperative that diagnosis and treatment begin early for increased survival rates [16]. Advances in surgical techniques, radiation therapy technology and the addition of combined chemotherapy and radiation therapy, has done very little to increase

survival rates [14]. The CDC has determined early screening is the key to decreasing the sobering statistics.

C. Evolving Demographics of Oral Cancer

Oral cancer has traditionally been thought of as a risk for older people over 50 who have used alcohol and or tobacco. But recently it has been discovered that young people who have contracted certain strains of human papillomavirus (HPV) are at great risk of developing oral cancer as early as there mid 20's. The problem with HPV in most people is it can manifest no symptoms at all [14]. HPV related cancers are the fastest growing segment of the oral cancer population. The numbers of oral cancers are increasing each year despite the continuous drop in tobacco use. This highlights the importance of annual screenings by a dentist or doctor for all patents regardless of age or history of tobacco and alcohol use.

D. State of the Science, Methods of Oral Cancer Detection

Currently most cancer screening is performed visually by conventional oral examination (COE). Unfortunately on average a COE will miss a cancer diagnosis in 25% of cancer cases [14-16]. Although COE may be effective as a screening test, there are still many problems with this approach. First, approximately 5–15% of the general populations have oral mucosal abnormalities [14], [17–19]. Without question, the vast majority of these lesions are clinically and biologically benign [14], [20]. This is difficult for two reasons. First, once a neoplastic lesion is large enough to be seen and manifest symptoms it may be in the late stages of development. Second there are several harmless benign lesions and growths that have very similar physical appearances to cancer making visual diagnosis very difficult [20]. Compounding the problem is early lesions of oral cancer and pre-cancer are often innocuous and rarely demonstrate the clinical characteristics observed in advanced cases such as: ulceration, induration, pain, or

associated swelling of the lymph nodes [14], [20]. Healthcare providers commonly take a wait and see approach to oral lesions since a majority of oral lesions and growths are harmless and biopsies can be extremely expensive and painful.

E. State of Diagnostic Aides

There are some adjunctive diagnostic aids to the COE with the most popular being fluorescent-based dyes and mouthwashes to assist the dentist in the examination of oral cancer [21]. The dyes help highlight surface anomalies; they do not actually diagnose cancer. They assist the dentist or physician to determine if and where to take a scalpel biopsy [22]. The florescent-based systems are not fool proof as they indicate high false positives on many benign mucosal alterations including leukoedemas and keratoses. A pathologist would make the diagnosis based on a microscopic analysis of the scalpel biopsies. Another diagnostic aid is the brush biopsy. A soft brush collects surface cells that are then examined microscopically. The brush biopsy has the advantage of being minimally invasive but it can only detect the cells at the surface and cannot pinpoint a precise location [21]. Cells from deeper layers of the oral mucosa are not sampled therefore it cannot distinguish cancer from dysplasia. A positive brush biopsy would still necessitate a scalpel biopsy. Current adjunct diagnostic aids do not give instant results, the results are visually based so affected oral lesions must be large enough to be seen. Current adjuncts can only inspect the surface cells. A new diagnostic aid that can instantly and non invasively determine the depth, size and progression of a neoplastic tissue would be valuable for both diagnosis and for monitoring the properties of a suspicious tissue [14].

F. Structural Properties of Cancer

Cancer is diagnosed by a pathologist based on microscopic examination of the cells from a tissue biopsy. The traits that indicate a cell is cancerous are numerous. The first

distinct trait is general disorder. Cells are called anaplsatic and loose differentiation. The cells no longer have a regular and ordered arrangement. In cancer cells there is a striking increase in cell volume. The cells have markedly irregular surfaces, the tissue arranged haphazardly and there are a greater number of cells in mitosis throughout the tissue. Whereas normal cells are arranged orderly with predictable transitions, the cell mitosis is restricted to the basal surface unlike cancer where cell mitosis can be found anywhere [9]. In cancer cells the nucleus is large and irregular shaped and some cells are multi nucleated. The nuclear envelope is often convoluted, irregular and doubled over on itself. Fig. 2-1 Structure differences between normal cells and cancerous cells, illustrates the dramatic nuclear changes that identify cancer cells. Other differences in cancer cells are difficult to visualize such as abnormal nuclear pores and a defective filament system that is not properly connected to the membrane [69, pg 242]. The membranes of the endoplasmic reticulum are typically smaller in area in neoplastic cells[9]. The numbers of mitochondria are increased to meet the growing energy demands of rapidly growing and dividing cancer cells [9], [70, pg 51]. The mitochondria in neoplastic cells also show smaller deformed inner membranes as compared to normal cells. Cancer cells often show virons and virous like particles in the ultra structural analysis of neoplastic tissue [71]. There is a general increase in the number of small organelles [9], [70-72]. The main feature that separates a dysplasia (sometimes referred to as pre-cancer) from cancer is the inability of the cells to become invasive these contained cells are often referred to as carcinoma in situ (in position) [9]. Cancer is a neoplasm that is not contained by membranes or connective tissue barriers such as the basal lamina [9], [11]. The un assisted eye shows cancer lesions tend to spread out like a crabs legs from a crabs body. This is how cancer (Latin for crab) received its name by bearing a resemblance this constellation of the zodiac.

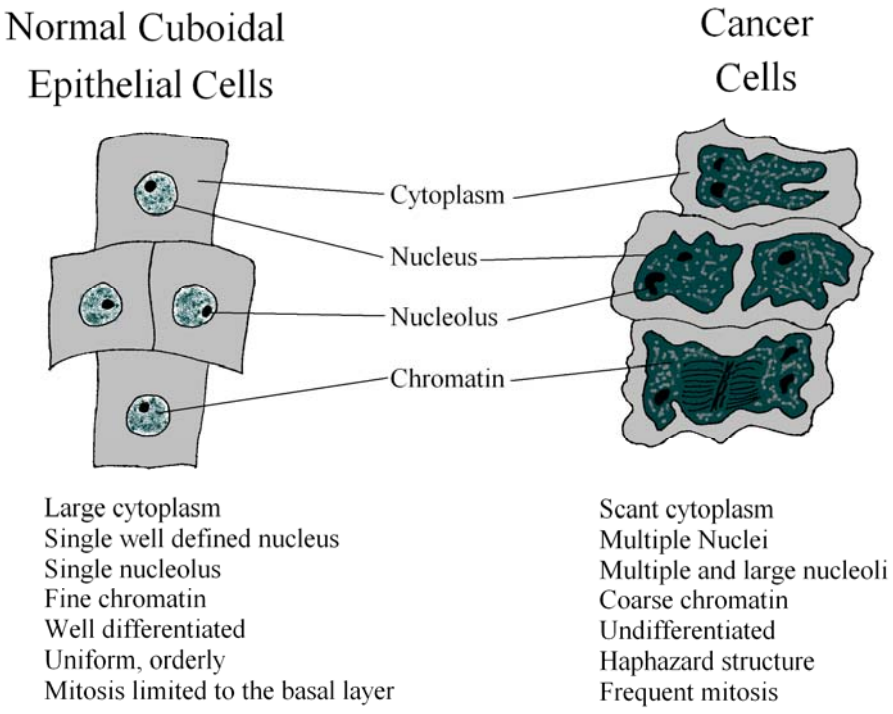

Fig. 2-1 Structure differences between normal cells and cancerous cells

G. Impedance Properties of Cancer

What is known is that diseases like cancer alter the number, size, shape, structure and chemistry of the cells and their organelles [9]. There is substantial evidence that shows cancer cells and tissues have different impedance responses than that of healthy cells and tissues [23-36]. This impedance response difference may be used to create an impedance based diagnostic tool [23-36]. The problem with using impedance, as a diagnostic tool is it is non-specific; it is unknown what exact features cause the decrease in impedance measured [37]. Furthermore if impedance is used in diagnostics are there any other benign conditions that have similar impedance responses to cancer that would complicate diagnosis [38]. This is why a detailed “transparent Box” model that includes all the membrane microstructure that affects electrical properties of the cell and tissue are

required. The great classical cell biologist, E.B. Wilson, in 1925 wrote, "The key to every biological problem must finally be sought in the cell [39].” The only way to legitimately create a more useful impedance spectroscopy model for the study of healthy and diseased tissue is to build the model from the bottom up by using the actual ultra structure of the cell. Today’s electron micrographs of healthy and diseased cells allows for an unprecedented view of the ultra structure of the cell, this detail will allow for the construction of the detailed cell model [74].

H. Why Model Cancer

Why model oral cancer tissue using impedance methods? There are multiple reasons to model the tissue that include economic, practical and compassionate reasons. With a model you can change things in cells that you cannot practically do in a lab. You can instantly see the effect to the impedance response caused by changing any cell structure, organelle or electrolyte conductivity. Working with actual tissue is difficult because of expense and availability. In the medical research community there is a vivid and unforgettable saying expressed by many researchers “Tissue is the issue.” Getting healthy and cancerous tissue is nearly impossible. The few tissue samples that are available are small 3mm square and typically cost $600 to $1000 [40]. If the research requires both healthy and diseased tissue from the same organ and patient it becomes even more difficult to obtain. Currently there are no oral tissues available, cancer or otherwise [40].

For compassionate reasons cancer is one of the deadliest diseases affecting young people and early screening will save lives [14]. The economic reasons for modeling cancer include both direct and indirect cost savings from early cancer screening. Economically the United States market for impedance based oral cancer diagnostic tool is greater than two hundred thousand units, this number is based on the approximate number of dentists in the United States as of 2009 [41]. The oral health community needs

a quick noninvasive method to screen patients for oral cancer. Impedance can be the answer if differentiation between cancer and other diseases can be assured.

I. Impedance for Oral Cancer Detection

Impedance has been proposed, as a method to diagnose and screen for cancer since the mid 1980s [42]. The earliest studies used skin cancer; unfortunately problems arose with variability of the impedance of the outer skin layer related to lesion size and from contact resistance variability [36]. Our non-mucosal skin (outer skin) is a fairly good insulator because of the high amounts of keratin [43-45]. The keratin protein functions as a waterproof and abrasion resistant outer protective layer in the dead or dying squamous cells [9]. Impedance was used to screen for melanoma and other skin cancers but high contact resistance and variability from sweat made the readings unreliable [36]. For these reasons it increased the difficulty of getting good measurements and prevented the commercial development of impedance spectroscopy for cancer screening. High contact resistance becomes a problem when the contact resistance is orders of magnitude larger than the sample resistance [46]. For example if the electrode contact resistance is in the 20k ohm range and the intracellular resistance changes are in the hundred-ohm range, then the signal of merit will be half a percent of the overall signal. This will make the intracellular signal lost in the noise created by the contact resistance. To make matters worse sweat and other metabolic conditions may decrease contact resistance creating unreliable swings in data [46]. Oral mucosa has less keratin in the outer layers of epithelia compared to keratinized squamous epithelial skin cells, therefore it has lower contact resistance making the measurement more ideal [9], [20]. The contact resistance of oral mucosa has a much lower range of variability as compared to keratinized squamous epithelial skin cells [43-45]. Tumor or lesion size becomes less of a variable also because electrode spacing can be small to preserve resolution while maintaining low contact

resistance and good signal to noise ratios. Other mucosal tissues with similar properties to the oral mucosa such as the cervix tissues and colon tissues were successfully measured using impedance [23-35].

J. Cancer Review

This section covered what cancer is and more specifically about oral cancers. This section discussed the growth of oral cancer in younger populations due to the increase in HPV infections. The current methods of cancer detection and the challenge of early detection were covered. The pathology and the structural properties of cancer were discussed and how these structural properties begin to relate to the impedance properties of cancer. This section finishes with the reasons to model cancer impedance properties and how the field of impedance measurements for cancer has evolved and developed.

III. LITERATURE REVIEW OF TISSUE MODELS

A. Modeling Background

Relatively little modern research has been done for modeling the electrical differences between normal and diseased tissues. Many contemporary researchers still use an empirical approach when dealing with cell and tissue impedance modeling [47]. There have been attempts to make more structurally based tissue models that employ finite element techniques but they still do not attempt to include the interior cell structures [56]. These newer models do not provide more information for their increased complexity [57]. The models for diseased tissue are empirically based simple modifications to the Cole model.

B. Cole Model

The nearly 80-year-old Cole model is the most popular empirical model used in the literature [47-50]. It has been the standard to describe the impedance responses of various non-polarized non-excitable cell tissues [50]. The Cole model is attractive because it is simple and can approximate impedance measurements displayed as Nyquist plots from many tissues and electrode-electrolyte interfaces. Fig. 3-1 Cole model, shows how very few parameters are required to estimate the impedance response of various tissues.

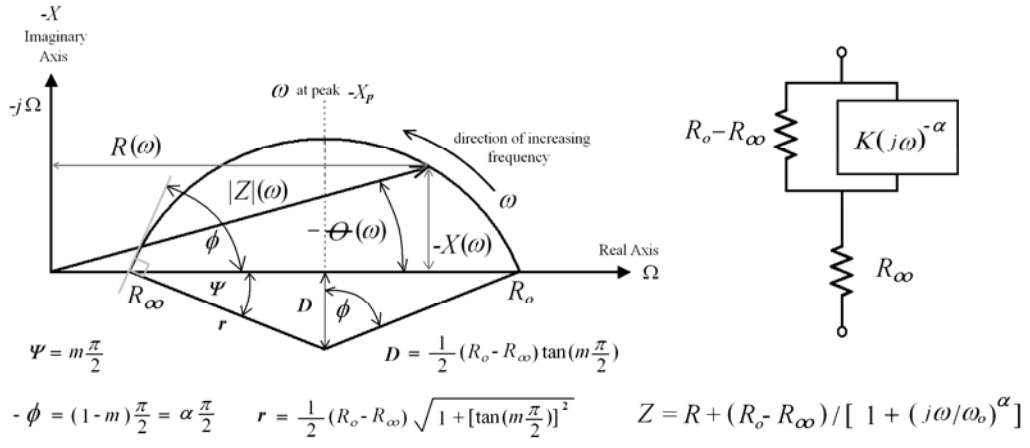

Fig. 3-1 Cole model

The equivalent series resistance, R_s, and series Reactance X_s, when plotted on the complex impedance plane produce a minor arc of a circle with a center that often lies below the real axis. The circular arc has a high frequency intercept at R_{inf} and a low-frequency intercept at R_o. Both the high frequency and zero frequency intercepts form a 90-degree angle from the radial vector *r.* The angle between the real axis and the radius vector *r* is ψ when $\psi = 0$ then $\alpha = 1$ the impedance locus is center lies on the real axis. If $\alpha < 1$ the impedance locus is a depressed semicircular arc whose center lies below the real axis. The original Cole model uses as few as three electrical elements to approximate actual measured cell responses [50].

The drawback of the standard Cole model is the electrical elements obtained from experimentation do not correlate directly to actual cell structure and composition. With the Cole model there is no practical way to specifically attribute a change in the impedance output of a tissue to a specific structural or electrochemical change within the cells of a tissue [47]. The model lacks detail required to evaluate sub-cellular structural changes such as changes in the sizes and numbers of organelles.

C. Network Structure Follows Physical Structure

The criticism of most models used in electrochemical impedance spectroscopy (EIS), is that they are not necessarily based on the physical structure so the element values have little additional meaning [37], [51]. This is a problem because there are an infinite number of combinations of network elements, values and topologies that can be assembled to create virtually the same output waveform that was measured in an actual tissue impedance measurement [37], [51]. Unless these network topologies and values for a model are based on structure, they are nearly useless to describe or investigate disease even if they reproduce the Nyquist and bode plots perfectly. Fig. 3-2 Three equivalent

circuits show different electrical circuits possessing the same number of time constants that can yield mathematically equivalent frequency responses.

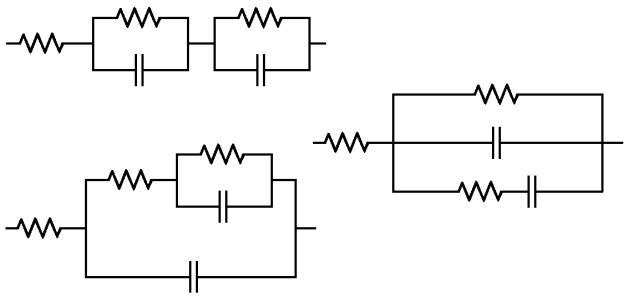

Fig. 3-2 Three equivalent circuits

It is evident then that all the EIS experimentation in the world will not produce a model with detail of what is actually happening in the cells of healthy or diseased tissues. In the absence of any satisfactory explanation of the features of a model, its function is nothing more than a way of expressing experimental results [37], [47], [51]. A different approach is needed instead of fitting the data to an arbitrary model; a model must be developed based on the actual structure of the cell and tissues similar to what Fricke developed in 1925. Fricke developed a theory for the resistance of suspensions of spherical cells based on findings from Fricke and Morse [52], [53]. They found that their measurements on suspensions of red blood cells at various frequencies could be accurately fitted to a circuit shown in Fig. 3-3 Electrical properties of cell suspensions. The variable *Re* was thought to represent the resistive properties of the suspending medium the extracellular fluid resistance, *Ri* was the resistance of the intracellular fluid of the corpuscles and *Cm* was the capacitances of the membranes [105]. Hence at low frequencies the membranes have a high reactance; the lines of current are considered to flow round the corpuscles and the total impedance is relatively high and equal to *Re*.

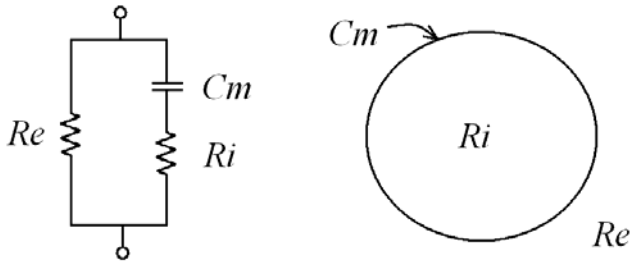

Fig. 3-3 Electrical properties of cell suspensions

At high frequencies the reactance of the membranes is low, the current flows through the membrane and the limiting resistive value is due to that of the intracellular fluid *Ri* in parallel with the extracellular fluid *Re.* The transition range between these two extremes is dominated by the capacitive properties of the membrane [53], [105]. Fricke had shown that his model incorporating a pure frequency-independent capacitance was satisfactory in representing the electrical properties of suspensions of red blood cells; other tissues show a more complex behavior and require a frequency dependent reactance to be added to the model [47]. The need for a frequency dependent reactance is in part due to the electrode electrolyte interface [47], [52] and the distribution of relaxation times [47]. The interest here is in the structural nature of the variables for the Frick model. The resistances and capacitances both have a geometric and biological meaning where they previously did not have either. Many of the circuit model analogs ignore the internal structures of the cell and simply use one or two RC time constants as fitting parameters [48], [50], [54-64], [105]. The first RC time constant represents the outer membrane and the second time constant represents the nuclear membrane or more accurately: the composite time constant of the largest organelles. These RC time constants are arrived at by empirical methods and not by structure [47]. Researchers have long ignored the

electrical contributions of small organelles such as the endosome, perioxosome and lysosome, primarily for the fact that the RC time constant for such a small individual organelle will be on the order of femto seconds [43], [55-66]. But an individual cell does not just contain a few of these organelles it may contain hundreds, up to tens of thousands of these organelles [9], [67-69]. The great majority of a cell's membrane content is actually attributed to the organelles. The outer plasma membrane only accounts for two to five percent of the cells total membrane content [9], [67]. Half the liquid volume of the cell is comprised of intra organelle fluids [9], [67-69]. A structurally based electrical model based on the totality of the individual contributions will likely show ignoring these organelles will have a significant effect especially when comparing healthy cells from diseased cells. The largest histo-pathological difference in visually identifying healthy cell tissues from diseased cell tissues is the; size, shape, number and distribution of organelles within the cell [11-13], [69-72]. It is therefore recommended that any EIS model comparing the health of cells would include all the membrane bound organelles.

D. Tissue Model Review

This section introduced the empirically based tissue models describing impedance. It introduced the Cole model that could approximate the impedance behavior of cells and tissues. Fricke and Morse explored the subtle connection between structures and function in the electrical network for simple red blood cells. These historical models will form the basis of the "transparent box" tissue model and its development from sub cellular structure.

IV. THE CELL

A. Introduction to the Cell

The cell is the structural and functional unit of all known living organisms. It is the smallest unit of an organism that is classified as living and is sometimes referred to as the building block of life [9]. Humans are multicellular and have approximately 10^{14} or 100 trillion eukaryotic cells; a typical cell size is 10 μm; a typical cell mass is 1 nanogram. All cells possess hereditary material of genes in chains of nucleic acids. The DNA and RNA contain the information necessary to build various proteins such as enzymes, the cell's primary machinery. Eukaryotic cells contain organelles that are analogous to organs in the human body**.** Fig. 4-1 Anatomy of a eukaryotic cell is a cartoon drawing that shows the major organelles within a eukaryotic cell. Organelles are adapted and/or specialized to carry out one or more vital functions for the cell.

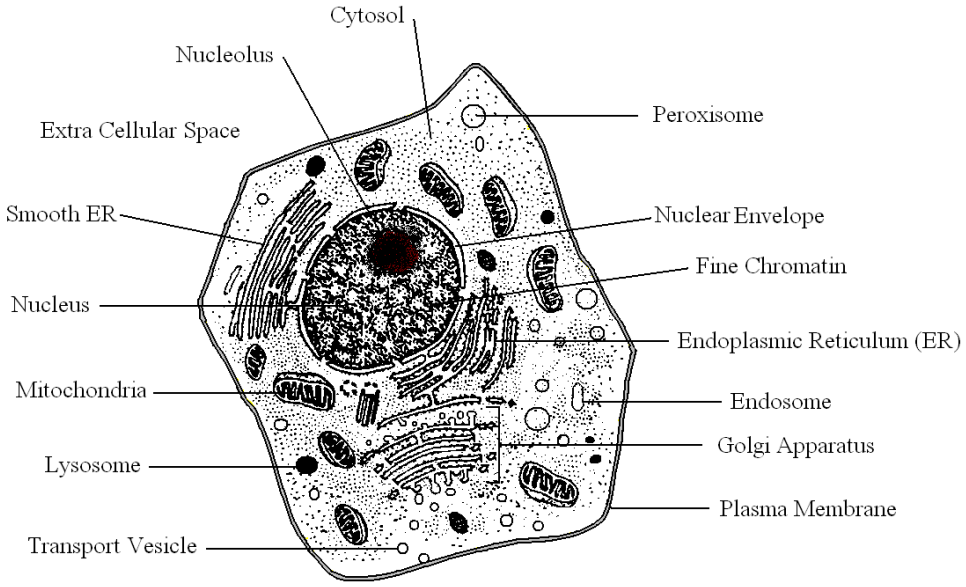

Fig. 4-1Anatomy of a eukaryotic cell

All, eukaryotic cells, have an outer membrane that envelops the cell, separates its interior from its environment, regulates what moves in and out (selectively permeable), and maintains the electric potential of the cell by electrochemical gradients. Inside the membrane, a salty cytoplasm takes up most of the cell volume [9], [68]. All cells possess membrane proteins; in animals that constitutes about 50% of the mass of most membranes, the remainder being lipids and small amounts of carbohydrate. Because lipid molecules are much smaller than protein molecules there are about 50 times more lipid molecules than protein molecules in a given cell membrane [9]. The membrane serves to separate and protect a cell from its surrounding environment. The membranes key structural feature is the double layer of lipids (hydrophobic fat-like molecules) and hydrophilic phosphorus molecules [7], [9]. Hence, the layer is called a phospholipid bilayer, detail of which can be seen in Fig. 4-2 the cell membrane.

Embedded within this membrane are a variety of protein molecules that act as channels and pumps that move different ions and molecules into and out of the cell. The membrane is said to be 'semi-permeable', in that it can either let a substance (molecule or ion) pass through freely, pass through to a limited extent or not pass through at all [7]. The number and type of imbedded proteins largely determine the membranes permeability to particular substances [9]. Cell surface membranes contain receptor proteins that allow cells to detect external signaling molecules such as hormones and antibodies from other cells and/or the environment and relay those signals to the interior of the cell. Other proteins anchor the membrane to macromolecules on either side of the membrane and some proteins act as enzymes to catalyze specific reactions [9]. But it is largely the lipid bilayer that is responsible for making the cell “look” electrically capacitive [43], [44]. The double layer thickness of poorly conducting hydrophobic fatty acids have an approximate dielectric constant range of greater than 2.5 and less than 13.5

[43], [48]. The specific dielectric constant is largely dependent on the content and type of fatty acids that comprise the lipids in the cell membrane [7].

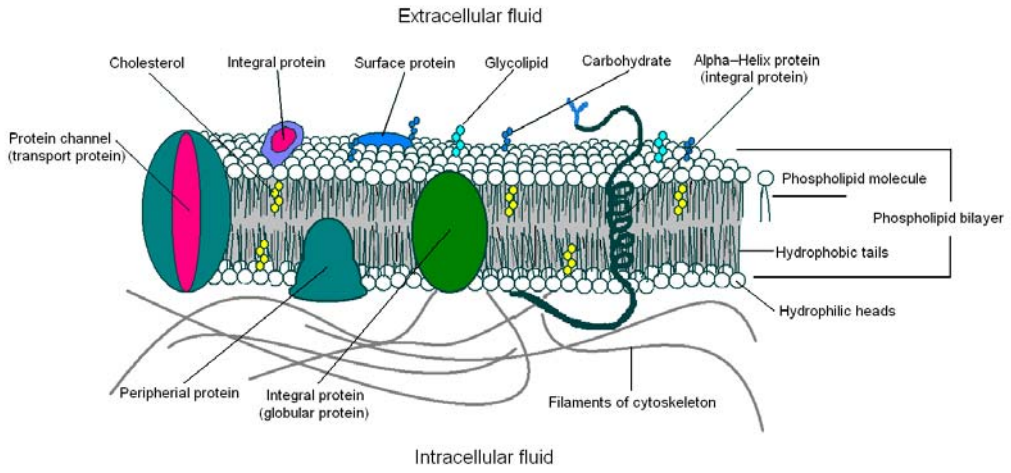

Fig. 4-2 The cell membrane

Some of the more abundant lipids found in bilayers are represented in Fig. 4-3 common membrane lipids. The fatty acids in phospho and glycolipids usually contain an even number of carbon atoms, typically between 14 and 24. The 16- and 18-carbon fatty acids are the most common ones. Fatty acids may be saturated or unsaturated, the length and the degree of unsaturation of fatty acids chains have a profound effect on membranes fluidity and its dielectric properties [7]. The tight spacing between these fatty acid tails provides a hydrophobic barrier to water charged ions and other polar molecules [9]. The polar ends vary in structure and charge giving the membrane specific characteristics for the cells [7]. The polar ends of these molecules form a conductive surface on either side of the lipid bilayer [7]. This structure naturally separates charge between the intracellular space and extra cellular space [9]. This makes the cell look geometrically like a spherical capacitor two conducting layers separated by a dielectric [48].

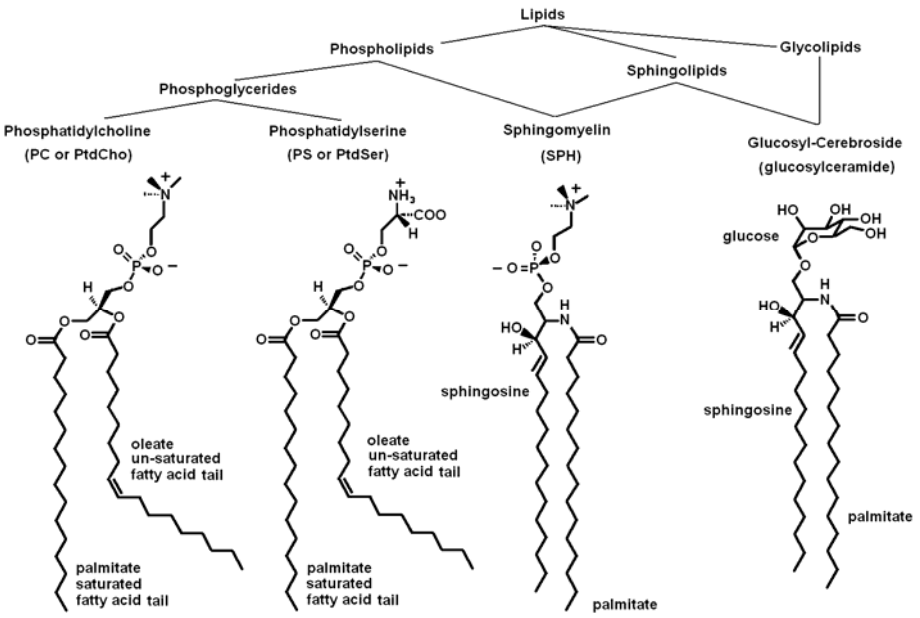

Fig. 4-3 Common membrane lipids

B. Introduction to the Membrane Bound Organelles

The organelles in a cell are analogous to the organs within our body a typical eukaryotic cell will have hundreds or thousands of these smaller membrane bound entities performing specific tasks [9, p. 661]. The organelles have various structural and biochemical differences that affect electrical properties of the cell. These structures certainly affect electrical properties of the cell for given conditions. Each organelle will get a brief introduction which includes its primary function in the cell, its size, shape, number structure and any additional features which will be of interest in building an electrical model.

C. Mitochondria

Mitochondria are rod-shaped organelles that can be considered the power generators of the cell, converting oxygen and nutrients into adenosine triphosphate (ATP). ATP is the chemical energy "currency" of the cell that powers the cell's metabolic activities [9, p.

669]. Mitochondria have elaborate structure important to the functioning of the organelle see Fig 4-4. Mitochondria anatomical crossection.

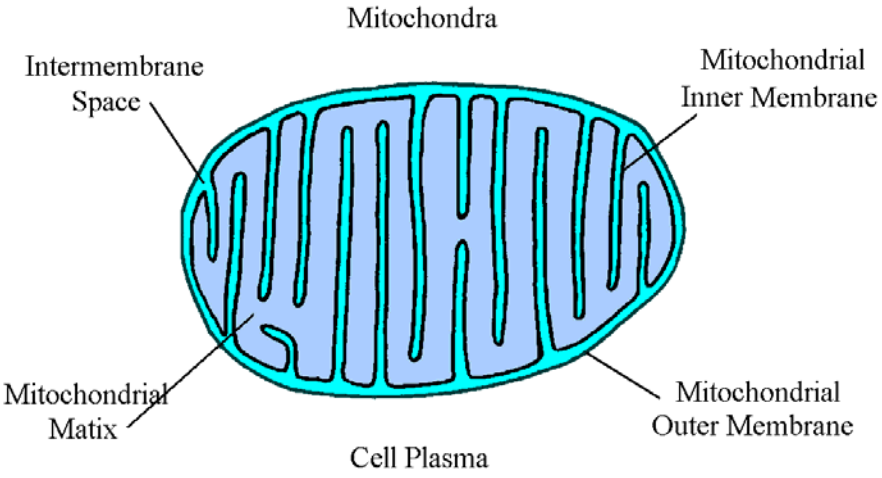

Fig 4-4 Mitochondria anatomical crossection

Two specialized membranes encircle each mitochondrion present in a cell, dividing the organelle into a narrow intermembrane space and a much larger internal matrix, each of which contains highly specialized proteins [9, p. 678], [68, p. 52]. The outer membrane of a mitochondrion contains many channels formed by the protein porin and acts like a sieve, filtering out molecules that are too large [81]. Similarly, the inner membrane, has a much larger surface area which is highly convoluted so that a large number of infoldings called cristae are formed it also allows only certain molecules to pass through but it is much more selective than the outer membrane [9, p. 678]. The larger surface area supports proteins with three types of functions: 1 proteins to facilitate oxidation reactions, 2 ATP synthase to make ATP, and 3 transport proteins for metabolites into and out of the matrix [9, p.660], [68]. Together, the various compartments of a mitochondrion are able to work in harmony to generate ATP in a complex multi-step process [9]. Mitochondria are generally oblong organelles, which range in size between 1 and 10 micrometers in

length, and occur in numbers that directly correlate with the cell's level of metabolic activity [9, p. 771], [68, p. 26]. The organelles are quite flexible, time-lapse studies of living cells have demonstrated that mitochondria change shape rapidly and move about in the cell almost constantly [68]. Movements of the organelles appear to be linked in some way to the microtubules present in the cell, and are probably transported along the network with motor proteins. Consequently, mitochondria may be organized into lengthy traveling chains, packed tightly into relatively stable groups, or appear in many other formations based upon the particular needs of the cell and the characteristics of its micro tubular network [9 p. 769]. On average the density of mitochondria within a cell is uniform [68].

D. The Golgi Apparatus

The Golgi apparatus is an organelle found in most eukaryotic cells [9]. It was identified in 1897 by the Italian physician Camillo Golgi, after whom the Golgi apparatus is named [9]. The Golgi organelle processes and packages macromolecules, such as proteins and lipids, after their synthesis and before they make their way to their destination; it is particularly important in the processing of proteins for secretion. The Golgi is composed of stacks of membrane-bound structures known as cisternae (singular: cisterna). A mammalian cell typically contains 40 to 100 stacks [9, p. 726], [68, p. 26]. Between four and eight cisternae are usually present in a stack Each cisterna comprises a flat, membrane enclosed envelope that includes special Golgi enzymes which modify or help to modify cargo proteins that travel through it [9, p. 731], [82]. The cisternae stack has three functional regions: the cis-Golgi network, medial-Golgi, and trans-Golgi network as can be seen in Fig. 4-5 crossection of a Golgi stack. Vesicles from the endoplasmic reticulum fuse with the network and subsequently progress through the stack to the trans Golgi network, where they are packaged and sent to the required

destination [9]. Each region contains different enzymes which selectively modify the contents depending on where they reside [9], [68]

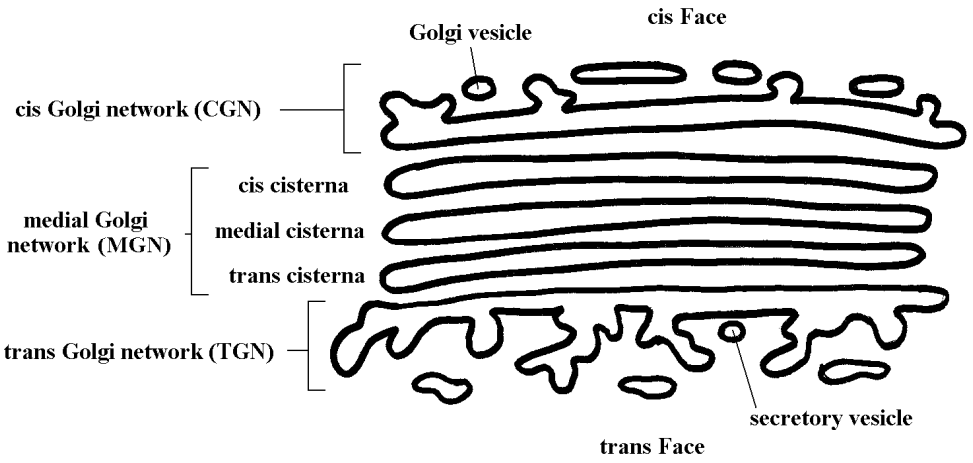

Fig. 4-5 Crossection of a Golgi stack

The cisternae also carry structural proteins important for their maintenance as flattened membranes which stack upon each other [9, pp. 736-737]. Cells synthesize a large number of different macromolecules. The Golgi apparatus is integral in modifying, sorting, and packaging these macromolecules for cell secretion (exocytosis) or use within the cell [9, p.757]. It primarily modifies proteins delivered from the rough endoplasmic reticulum but is also involved in the transport of lipids around the cell, and the creation of lysosomes [9]. In this respect it can be thought of as similar to a "Mail Room;" it packages and labels items which it then sends to different parts of the cell. The Golgi uses vesicular transport. The vesicles that leave the rough endoplasmic reticulum are transported to the cis face of the Golgi apparatus, where they fuse with the Golgi membrane and empty their contents into the lumen. Once inside the lumen, the molecules are modified, sorted and shipped towards their final destination [9]. The Golgi apparatus tends to be larger and more numerous in cells that synthesise and secrete large amounts of substances, for example, the plasma B cells and the antibody-secreting cells of the

immune system have prominent Golgi complexes [9, p. 661]. Those proteins destined for areas of the cell other than either the endoplasmic reticulum or Golgi apparatus are moved towards the trans face, to a complex network of membranes and associated vesicles known as the trans-Golgi network (TGN) [9 p. 731]. This area of the Golgi is the point at which proteins are sorted and shipped to their intended destinations by their placement into one of at least three different types of vesicles, depending upon the molecular marker they carry [9, p. 744].

E. The Endoplasmic Reticulum

The endoplasmic reticulum (ER) is an eukaryotic organelle that forms an interconnected network of tubules, vesicles, and cisternae within cells. Rough endoplasmic reticulua synthesize proteins, while smooth endoplasmic reticulua synthesize lipids and steroids, metabolize carbohydrates and steroids, and regulate calcium concentration, drug detoxification, and attachment of receptors on cell membrane proteins [9, pp. 660-708]. Sarcoplasmic reticulua solely regulate calcium levels. The surface of the rough endoplasmic reticulum (RER) is studded with protein-manufacturing ribosomes giving it a "rough" appearance (hence its name) [9, pp. 689-690]. However, the ribosomes bound to the RER at any one time are not a stable part of this organelle's structure as ribosomes are constantly being bound and released from the membrane. The membrane of the RER is continuous with the outer layer of the nuclear envelope. Although there is no continuous membrane between the RER and the Golgi apparatus, membrane-bound vesicles shuttle proteins between these two compartments using vesicles [9, pp. 726-729]. The ER accounts for between 50 to 60 percent of an average cells total lipid membrane content. The ER has the largest membrane area of any organelle in the cell [9, p.661].

F. The Nucleus

The nucleus is the largest volume membrane enclosed organelle found in eukaryotic cells [9 p. 197]. It contains most of the cell's genetic material, organized as multiple long linear DNA molecules spooled on a complex formed with a large variety of proteins, such as histones, to form chromosomes. The genes within these chromosomes are the cell's nuclear genome [9]. The function of the nucleus is to maintain the integrity of these genes and to control the activities of the cell by regulating gene expression. The main structures making up the nucleus are the nuclear envelope, a double membrane that encloses the entire organelle and separates its contents from the cellular cytoplasm, and the nuclear lamina, a meshwork within the nucleus that adds mechanical support; much like the cytoskeleton supports the cell as a whole [9, p. 670]. Nuclear pores are required to allow movement of molecules across the envelope because the nuclear membrane is impermeable to most molecules [9, pp. 669-671]. These pores cross both of the membranes, providing a channel that allows free movement of small molecules and ions. The movement of larger molecules such as proteins is carefully controlled, and requires active transport regulated by carrier proteins. [9, p. 671] Nuclear transport is crucial to cell function, as movement through the pores is required for both gene expression and chromosomal maintenance. The interior of the nucleus does not contain any membrane-bound sub compartments; it does contain a number of sub nuclear bodies made up of unique proteins, RNA molecules, and particular parts of the chromosomes. The largest of the bodies is the nucleolus, which is mainly involved in the assembly of ribosomes [9, p. 331]. After being produced in the nucleolus, ribosomes are exported to the cytoplasm where they translate mRNA. In mammalian cells, the average diameter of the nucleus is approximately 4 to 6 micrometers (μm), which occupies about 10% of the total cell volume [9, p. 328]. The viscous liquid within it is called nucleoplasm, and is similar in

composition to the cytosol found outside the nucleus. The structure of the nucleus appears as a dense, roughly spherical organelle. The nuclear envelope otherwise known as nuclear membrane consists of two cellular membranes, an inner and an outer membrane, arranged parallel to one another and separated by 10 to 50 nanometers (nm) [9, p. 197]. The nuclear envelope completely encloses the nucleus and separates the cell's genetic material from the surrounding cytoplasm, serving as a barrier. The outer nuclear membrane is continuous with the membrane of the rough endoplasmic reticulum (RER), and is similarly studded with ribosomes as seen in Fig. 4-6 anatomical crossection of the nucleus and the ER. The space between the membranes is called the perinuclear space and is continuous with the ER lumen. The nuclear pores, which provide aqueous channels through the envelope, are composed of multiple proteins, collectively referred to as nucleoporins.

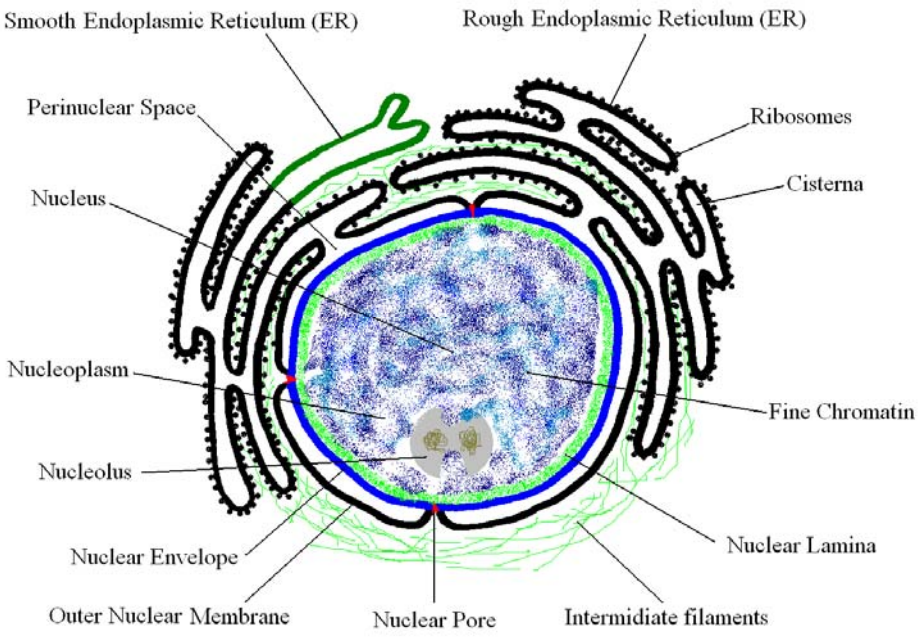

Fig. 4-6 Anatomical crossection of the nucleus and the ER

The pores are 100 nm in total diameter; however, the gap through which molecules can freely diffuse is only about 9 nm wide, due to the presence of regulatory systems

within the pore [9, p. 328]. The small native pore size allows the free passage of ions and other small water-soluble molecules while preventing larger molecules, such as nucleic acids and larger proteins, from inappropriately entering or exiting the nucleus. Large molecules must be actively transported into the nucleus. [9, pp. 839-841]. The nucleus of a typical mammalian cell will have about 3000 to 4000 pores throughout its envelope [9, p. 197], each of which contains a hexagonally donut-shaped ring structure at a position where the inner and outer membranes fuse [9, p. 328]. Attached to the ring is a nuclear basket. The basket shaped structure extends into the nucleoplasm, and a series of filamentous extensions reach out into the cytoplasm. Both these structures serve to mediate binding to nuclear transport proteins [9, p. 672]. The nuclear envelope allows the nucleus to control its contents, and separate them from the rest of the cytoplasm required for controlling processes on either side of the nuclear membrane.

G. *The Peroxisomes*

Peroxisomes are organelles found in virtually all eukaryotic cells. A peroxisome is a membrane-bounded organelle containing catalase an enzyme responsible for degrading hydrogen peroxide, which is toxic to the cell [9, p.661]. In the mammalian "filter organs" liver and kidney, peroxisomes are roughly spherical and relatively large (0.5 to 1.5 um in diameter); in other tissues, they are smaller (0.1 um) and some times called microperoxisomes [68, pp. 26]. The average mammalian cell has approximately 400 peroxisomes that occupy about 1% of the total cell volume [9, p.661]. In most species, peroxisomes have both a dense or granular matrix containing catalase and a crystalline core composed of the enzyme urate oxidase. Peroxisomes get there name because they produce and use hydrogen peroxide for there roll in the catabolic processes [9, pp. 686-681]. A major function of the peroxisome is the breakdown of very long chain fatty acids through beta-oxidation. In animal cells, the very long fatty acids are converted to medium

chain fatty acids, which are subsequently shuttled to the mitochondria where they are eventually broken down into carbon dioxide and water [9, p. 687].

H. The Endosome

The endosome is a membrane bound compartment inside eukaryotic cells. It is a compartment of the endocytic membrane transport pathway from the plasma membrane to the lysosome [68, pp. 36-42]. Molecules internalized from the plasma membrane can follow this pathway all the way to lysosomes for degradation, or they can be recycled back to the plasma membrane [9, pp.751-753]. Molecules are also transported to endosomes from the Golgi and either continue to lysosomes or get recycled back to the Golgi. Furthermore, molecules can be directed into vesicles that bud from the perimeter membrane into the endosome lumen [68, pp. 36-42]. Endosomes therefore represent a major sorting compartment of the endomembrane system in cells. Endosomes are approximately 500 nm in diameter when fully mature [9, p.661]. Endosomes provide an environment for material to be sorted before it reaches the degradative lysosome.

I. The Lysosome

Lysosomes are spherical organelles that contain enzymes (acid hydrolases). They break up food so it is easier to digest. Lysosomes are found in eukariotic cells they digest excess or worn-out organelles, food particles, and engulfed viruses or bacteria [68, p. 36]. The membrane around a lysosome is specially adapted to withstand the low pH environment (4.5 pH) required for the digestive enzymes to work [9, pp. 660-661]. Lysosomes are created by the addition of hydrolytic enzymes to early endosomes from the Golgi apparatus [68, p.36]. The name lysosome derives from the Greek words lyses, which means dissolution or destruction, and soma, which means body. Cell biologists nickname the lysosome "suicide-bags" due to their role in autolysis or programmed cell death. Lysosomes were discovered by the Belgian cytologist Christian de Duve in 1949.

The size of lysosomes varies from 0.1–1.2 μm [9, p.740], [68, p. 26]. At pH 4.8, the interior of the lysosomes is acidic compared to the slightly alkaline cytosol (pH 7.2). The lysosome maintains this pH differential by pumping protons (H+ ions) from the cytosol across the membrane via proton pumps and chloride ion channels [9, p.739]. The lysosomal membrane protects the cytosol, and therefore the rest of the cell, from the degradative enzymes within the lysosome. The cell is additionally protected from any lysosomal acid hydrolases that leak into the cytosol as these enzymes are pH-sensitive and function less well in the alkaline environment of the cytosol.

J. Cell Review

This section briefly introduced the cell and the major membrane bound components of the cell. Emphasis was mainly on the size and structure of each membrane bound organelle since they have the largest effect on impedance. This section introduced the cell and its components such as the mitochondria, the Golgi, the nucleus, the endoplasmic reticulum, the peroxisomes, the endosomes and the lysosomes. It included each organelles major functions, its numbers and locations within the cell as well as other notables. The structural information and shape size and number are important to developing the “transparent box” model.

V. BRIEF INTRODUCTION TO AC CIRCUIT THEORY

A. Introduction

This section is a brief primer for biologists to introduce the electrical relationships used in the development of this model and in the general electrochemical impedance spectroscopy field. It is imperative that other texts be referenced for a more complete understanding of the field. I recommend [37] and [38] as good electrochemical impedance spectroscopy texts.

B. Impedance Definition and Concept of Complex Impedance

The concept of electrical resistance is the ability of a circuit element to resist the flow of electrical current. Ohm's law (5-1) defines resistance in terms of the ratio between voltage and current.

$$R \equiv \frac{E}{I} \tag{5-1}$$

where

E is electromotive force in Volts

I is current in Amperes

R is resistance in Ohms

This well known relationship is limited to the ideal resistor, which has these simplifying properties:

- It follows Ohm's Law at all current and voltage levels
- AC current and voltage signals though a resistor are in phase with each other
- The resistance value is independent of the frequency

Circuit elements exhibit more complex behavior in practice. These non-ideal elements store energy through part of a sinusoidal cycle, which results in a difference in

the current voltage phase. This more complex behavior can be described by impedance, which is more general.

Like resistance, impedance is a measure of the ability of a circuit to resist the flow of electrical current. Unlike resistance, impedance is not limited by the simple ideal properties listed above. If one applies an AC excitation potential to an electrochemical cell containing electrolyte and then measures the current through the electrochemical on can calculate electrochemical impedance. If the AC excitation potential is sinusoidal the current response to this potential will also be a sinusoidal signal. This current signal can be analyzed as a sum of sinusoidal functions. Electrochemical Impedance is normally measured using a small excitation signal in the case of tissue a 1.5 mV excitation signal per mm of electrode spacing is enough to prevent depolarization of excitable tissues. The small signal will also ensure an electrochemical cell's response is pseudo-linear. In a linear or pseudo-linear system, the current response to a sinusoidal potential will be a sinusoid at the same frequency but shifted in phase, see Fig. 5-1 Sinusoidal current response in a linear system.

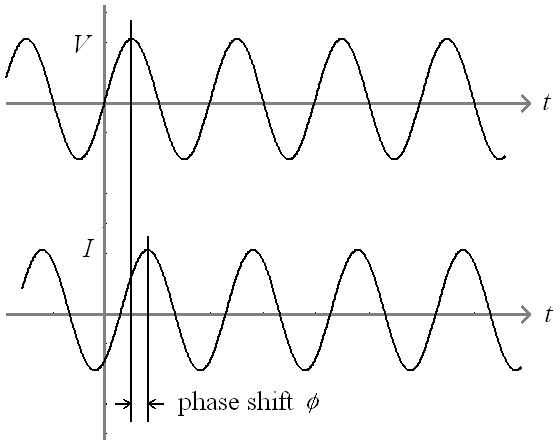

Fig. 5-1 Sinusoidal current response in a linear system

The excitation signal, expressed as a function of time, has the form shown in (5-2)

$$E_t = E_o \cdot \sin(\omega \cdot t) \qquad (5\text{-}2)$$

where

E_t is the potential In Volts at time t

E_0 is amplitude of the signal

ω is the radial frequency

t is the time in seconds

The relationship between radial frequency ω (expressed in radians per second) and frequency f (expressed in hertz cycles per second) is shown in (5-3)

$$\omega = 2 \cdot \pi \cdot f \qquad (5\text{-}3)$$

where

ω is the radial frequency

f is the frequency in Hertz

In a linear system, the response signal, for current through the electrochemical cell or tissue is shown in (5-4) and shifted in phase by some angle ϕ and has different amplitude, I_0.

$$I_t = I_0 \sin(\omega t + \phi) \qquad (5\text{-}4)$$

where

I_t is the current In Amps at time t

I_0 is amplitude of the signal

ω is the radial frequency

t is the time in seconds

ϕ is the phase angle shift

An expression analogous to Ohm's Law allows us to calculate the impedance Z of the system as shown in (5-5)

$$Z = \frac{E_t}{I_t} = \frac{E_0 \sin(\omega t)}{I_0 \sin(\omega t + \phi)} = Z_0 \frac{\sin(\omega t)}{\sin(\omega t + \phi)} \qquad (5\text{-}5)$$

where

Z is the impedance

Z_0 is the impedance magnitude

E_t is the potential In Volts at time t

E_0 is amplitude of the signal

I_t is the current In Amps at time t

I_0 is amplitude of the signal

ω is the radial frequency

t is the time in seconds

ϕ is the phase angle shift

The impedance is therefore expressed in terms of a magnitude, Z_0, and a phase shift, ϕ. If we plot the applied sinusoidal signal *E(t)* on the X-axis of a graph and the sinusoidal response signal *I(t)* on the Y-axis, the result is an oval shaped plot known as a "Lissajous figure" and can be seen in Fig 5-2. Lissajous figure. Analysis of Lissajous

figures on oscilloscope screens was the common method of impedance measurement prior to the availability of modern EIS instrumentation. Perfect symmetrical ovals or circular shapes indicate linearity, whereas tapered, or symmetrically distorted teardrop shaped Lissajous figures would indicate non-linearity [38]

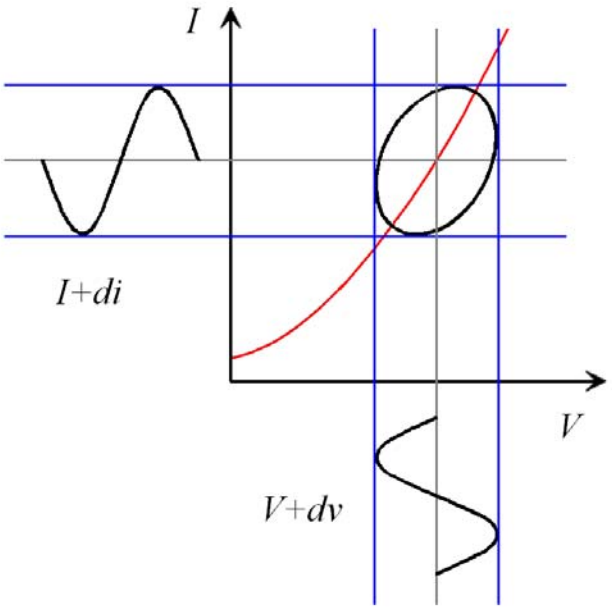

Fig. 5-2 Lissajous figure

Euler's relationship (5-6) is used to express the impedance as a complex function.

$$e^{(j\phi)} = \cos(\phi) + j \cdot \sin(\phi) \qquad (5\text{-}6)$$

where

j is the imaginary number in electrical engineering $\sqrt{-1}$

ϕ is the phase angle

From Euler's relationship potential is described in (5-7)

$$E_t = E_0 \cdot e^{j\omega t} \tag{5-7}$$

where

E_t is the potential in Volts at time t

E_0 is amplitude of the signal

j is the imaginary number in electrical engineering $\sqrt{-1}$

ω is the radial frequency

t is the time in seconds

The current response is expressed in (5-8)

$$I_t = I_0 \cdot e^{(j\omega t - \phi)} \tag{5-8}$$

where

I_t is the current in Amps at time t

I_0 is amplitude of the signal

j is the imaginary number in electrical engineering $\sqrt{-1}$

ω is the radial frequency

t is the time in seconds

The impedance is then represented as a complex number in the frequency domain as either a polar value (magnitude and phase) or as a rectangular representation (real part and imaginary part) this can be seen in (5-9)

$$Z(\omega) = \frac{E}{I} = Z_0 \cdot e^{(j\phi)} = Z_0(\cos(\omega) + j \cdot \sin(\omega)) \qquad (5\text{-}9)$$

where

$Z(\omega)$ is the impedance as a function of radial frequency

Z_0 is the impedance magnitude

E is the potential amplitude in Volts

I is the current amplitude in Amps

ω is the radial frequency

j is the imaginary number $\sqrt{-1}$

ϕ is the phase angle shift

C. Nyquist Plot

Equation (5-9) shows the expression for $Z(\omega)$ is composed of a real and an imaginary part. If the real part is plotted on the X-axis and the imaginary part is plotted on the Y-axis of a chart, then this forms a Nyquist plot as shown in Fig. 5-3 Nyquist plot with impedance vector. Notice that in the Nyquist plot the Y-axis is negative this is because the most common reactance in biological and electrochemical systems is capacitive reactance, which is negative. Each point on the Nyquist plot is the impedance at one frequency Fig 5-4 shows that low frequency data are on the right side of the plot and higher frequencies are on the left. On the Nyquist plot the impedance can be represented as a vector (arrow) of length |Z|. The angle between this vector and the X-axis, the "phase angle", is ϕ (=arg Z). Determining the frequency used to plot a particular point on a Nyquist plot is somewhat difficult since no frequency information is displayed.

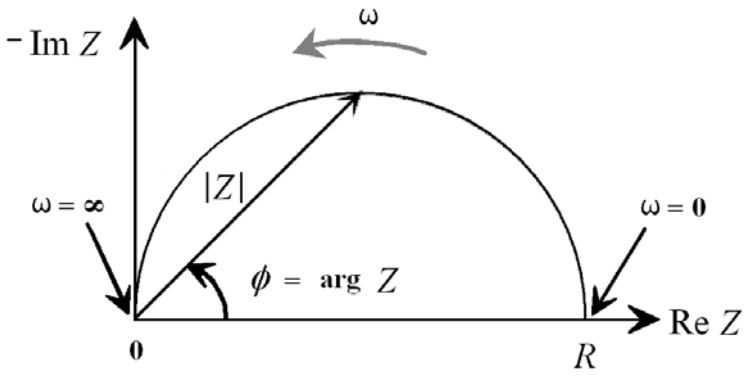

Fig. 5-3 Nyquist Plot with impedance vector

The Nyquist plot in Fig. 5-3 can result from the electrical circuit of Fig. 5-4 Simple equivalent circuit with one time constant.

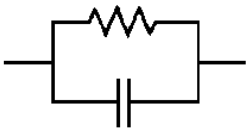

Fig. 5-4 Simple equivalent circuit with one time constant

The semicircle is characteristic of a single "time constant". In this case a single ideal resistor in parallel with a single ideal capacitor. Electrochemical Impedance plots often contain several semicircles. Often only a portion of a semicircle is seen based on frequency bandwidth observed.

D. Bode Plot

The Bode Plot shows impedance information as a function of frequency it is actually two plots magnitude and phase. For the Bode magnitude plot magnitude of the impedance ($|Z|=Z_0$) is plotted on the Y-axis of as a function of the log of the frequency shown on the X-axis. For the Bode phase plot, phase-shift is plotted in the Y-axis as a function of the log of frequency. The Bode plot for the electric circuit of Fig 4-4 is shown in Fig. 5-5.

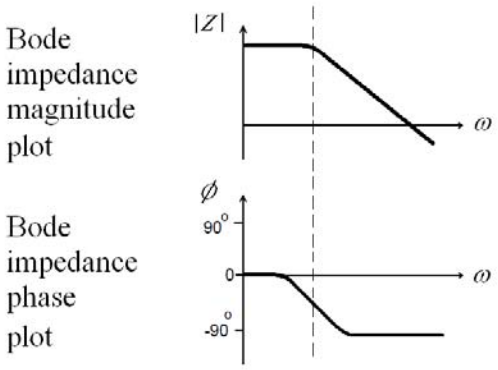

Fig. 5-5 Bode plot

E. Linearity of Electrochemistry Systems

Electrical circuit theory distinguishes between linear and non-linear systems. Impedance analysis of linear circuits is much easier than analysis of non-linear ones. A linear system possesses the property of superposition: If the input consists of the weighted sum of several signals, then the output is simply the superposition, or the weighted sum, of the responses of the system to each of the individual signals [37]. For a potentiostated electrochemical cell, the input is the potential and the output is the current. Electrochemical cells and tissues are not linear care must be exercised. Doubling the voltage will not necessarily double the current. Electrochemical systems can be pseudo-linear the example in Fig. 5-6 Pseudo-linearity of current versus voltage curve details this concept. If you examine a small enough portion of a cell's current versus voltage curve, it appears to be linear. In normal biological impedance measurement practice, a small (1 to 10 mV) AC signal is applied to the cell. With such a small potential signal, the system is pseudo-linear. The cell's large nonlinear response to the DC potential is ignored the measurement is made for the electrochemical cell at the excitation frequency [38].

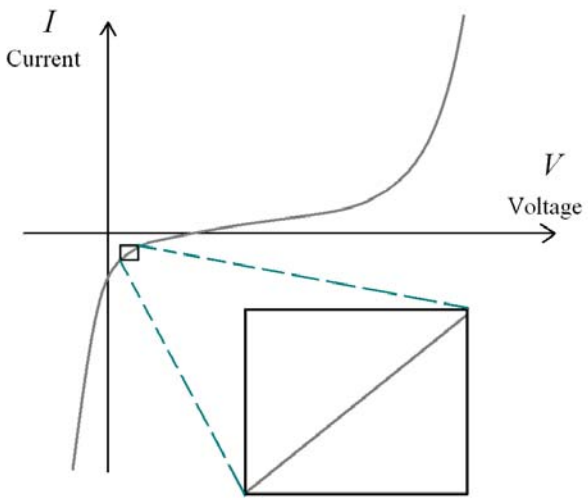

Fig. 5-6 Pseudo-linearity of current versus voltage curve

If the system is non-linear, the current response will contain harmonics of the excitation frequency. A harmonic is a frequency equal to an integer multiplied by the fundamental frequency [38]. For example, the “second harmonic” is a frequency equal to two times the fundamental frequency. Linear systems should not generate harmonics, so the presence or absence of significant harmonic response allows one to determine the systems linearity. As mentioned earlier Lissajous figures on an oscilloscope in the time domain can test for pseudo-linearity but are not as reliable as a spectrum analyzer. If the response is non-linear often a lower excitation voltage may correct the non-linear response condition.

F. Steady State Systems

Measuring an EIS spectrum takes time the system being measured must be at a steady state throughout the time required to measure the spectrum. A common cause of problems in impedance spectroscopy measurements and their analysis is drift in the system being measured. In practice a steady state can be difficult to achieve. The cell can change through a number of factors including; adsorption of solution impurities, growth

of an oxide layer on electrodes, build up of reaction products in solution, coating degradation and temperature changes [37].

G. Electrical Circuit Elements

EIS data is commonly analyzed by fitting it to an equivalent electrical circuit model. Most of the circuit elements in the model are common electrical elements such as ideal resistors, capacitors, and inductors. To be useful, the elements in the model should have a basis in the physical electrochemistry of the system. As an example, most models contain a resistor that models the electrochemical cell's solution resistance. Most models also contain capacitance due to charge separation ether from a thin film or a biological membrane. Some knowledge of the impedance of the standard circuit components is therefore quite useful. And will be important to understand for the development of the biological cell models in later sections. Table 5-1 lists the common circuit elements, the equation for their current versus voltage relationship, and their impedance.

Note that the impedance of an ideal resistor is independent of frequency therefore it has no imaginary component. With only a real impedance component, the current through a resistor stays in phase with the voltage across the resistor. The impedance of an ideal inductor increases as frequency increases. Ideal inductors have purely an imaginary impedance component. As a result, the current through an inductor is phase-shifted -90 degrees with respect to the voltage. The impedance versus frequency behavior of a capacitor is opposite to that of an inductor. A capacitor's impedance decreases as the frequency is raised. Ideal capacitors also have only an imaginary impedance component. The current through a capacitor is phase shifted 90 degrees with respect to the voltage. Actual physical electrical elements are non-ideal and will have some combination of the ideal components. Capacitors and inductors are energy storage components. The

capacitor stores energy in the electric field the inductor stores energy in the magnetic field [97]. Ideal resistors are a purely energy dissipaters and dissipate energy as heat.

Table 5-1
COMMON ELECTRICAL ELEMENTS

Component	Voltage Current Relationship	Impedance
Resistor	$V = I \cdot R$	$Z = R$
Inductor	$V = L \partial i / \partial t$	$Z = L \cdot j\omega$
Capacitor	$I = C \partial v / \partial t$	$Z = 1 / j\omega C$

H. Serial and Parallel Combinations of Circuit Elements

Few electrochemical cells can be modeled using a single equivalent circuit element. Instead, impedance spectroscopy models usually consist of a number of elements in a network. Both serial and parallel combinations of elements occur in both electrochemistry and biological models. There are simple formulas that describe the impedance of circuit elements in both parallel and series combination. Fig. 4-7 Series and parallel combinations show the physical connections and will be used to illustrate relationships.

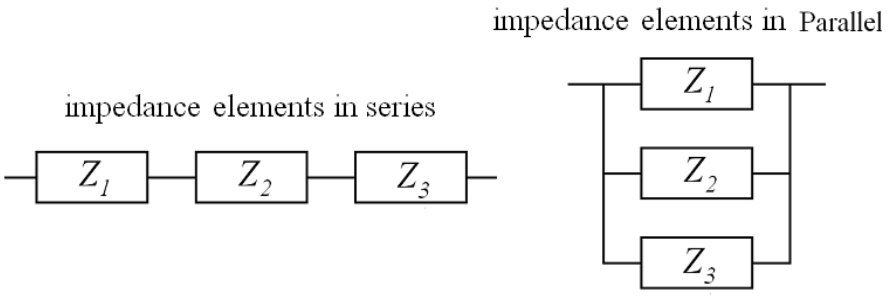

Fig. 5-7 Series and parallel impedance combinations

For linear impedance elements in series you calculate the equivalent impedance from equation 5-10.

$$Z_{equ} = Z_1 + Z_2 + Z_3 + Z_n \tag{5-10}$$

where

Z_{equ} is the impedance of the equivalent circuit

Z_1 is the first impedance in the series

Z_n is the n'th impedance in a series

For linear impedance elements in parallel you calculate the equivalent impedance from equation (5-11)

$$\frac{1}{Z_{equ}} = \frac{1}{Z_1} + \frac{1}{Z_2} + \frac{1}{Z_3} + \frac{1}{Z_n} \tag{5-11}$$

where

Z_{equ} is the impedance of the equivalent circuit

Z_1 is the first impedance in parallel

Z_n is the n'th impedance in parallel

Some observations to highlight are that inductances and resistances simply add in series and increase in value with successive elements added but capacitances decrease when successive capacitors are added in series. In parallel Capacitances add mathematically this is a consequence of the inverse relationship between capacitance and impedance as seen back in Table 5-1. Physically this makes sense in two ways as more capacitors are added in parallel this has the effect of making a parallel plate capacitor with more surface area therefore higher capacitance. As capacitors are added in series this

has the effect of increasing the spacing distance between parallel plates effectively decreasing the electric field strength and decreasing the capacitance [97].

I. AC Circuit Theory Section Review

This section highlighted basic relationships for the electrical elements being used in the model. And how to display those impedance relationships in Nyquist Plots and Bode plots. This section covered the basics of calculating series and parallel impedance elements. Readers interested in employing direct application of electrochemical impedance spectroscopy to tissue will want to read more in-depth about electrode electrolyte interface models [37]. These models were not introduced here since the focus is on developing the underdeveloped tissue models and not the well-developed electrode models.

VI. DEVELOPMENT OF THE "TRANSPARENT BOX" TISSUE MODEL

A. Introduction to the Structure Dependent Model

The concept of producing a structure dependent model is straightforward. Fricke, and Morse set the foundation with the modeling of the red blood cells [52], [53]. Each red blood cell was treated as a spherical capacitor, which isolated a conductive interior from a conductive bath (blood plasma). Each red blood cell was electrically in parallel with its neighbor because they shared the same bath so networks of many individual bed blood cells was simply more membrane resistor capacitor elements in parallel. This distributed network can be simplified into a lumped parameter network. The concept was introduced in Section III and illustrated in Fig. 3-3. The task is to extend this idea by starting with the membrane bound organelles and develop network models for each as parts of the cell. Then develop the organelle networks into the cell. Combine cell networks into cell layers and eventually into a tissue. The distributed elements of many organelle parts get joined into a lumped model of the cell. Many cells get lumped into a tissue layers. The tissue layers get lumped into a whole tissue model this is the model that finally represents the tissue impedance.

B. How to Develop the Ultra-Structurally Based Model

The cell is made up of a number of membrane bound organelles with different shapes, sizes and properties. The structurally based model can be built from the simplest components starting at the lowest level of construction; the organelle membrane. The cell membrane model from [52], [53] will be used to construct all the organelles within the cell. Each organelle will have a specific circuit topology based on its physical structure. Each component value of the organelle network will have a value based on their specific structural and biochemical properties. Each of these organelle circuit topologies will be placed in series or parallel based on their structural relationships within the cell. The

organelle network values will also depend on the numbers of each type. These organelle topologies combine into a cell topology. The cell topology gets repeated to form a tissue layer of like cell types. The tissue layer network topologies of adjacent cell types are combined in parallel to make the tissue network. An electrode interface model can be put in series with the tissue model to complete the model, which then can be used for EIS simulations. This same process is done for healthy and diseased cells; specifically squamous cell carcinomas and benign diseases with similar physical appearances to cancer.

C. Membrane Bound Organelle Network Model Level

The organelle and cell plasma membranes will be constructed based on structure and measurements from electron micrographs [9], [68-72]. Organelle networks will be constructed based on the ideas introduced by Fricke for spheres [52], [53]. The number, structure and shape of the membrane bound organelles within the specific oral mucosal cell types are extracted from electron micrographs (EM) [73-75] and electron tomographs (ET) [76] from histology atlases [67-72]. These important membrane bound organelles include:

Nucleus [9], [67-72], [77-80]

Mitochondria [9], [67-72], [81]

Golgi [9], [67-72], [82]

Endoplasmic reticulum [9], [67-72], [83]

Endosome [9], [67-72]

Peroxisome [9], [67-72]

Lysosome [9], [67-72]

Some membrane bound organelles are simple to calculate membrane surface areas and volumes since they are spherical. Others organelles have more complex shapes but

still can be modeled with polygons or cylinders. There are some organelles, which are too complex in shape so membrane areas need to be approximated by lipid area to volume ratios [9, p. 661]

D. Non-Membrane Bound Organelle and Protein Electrolyte Effects

There are non-membrane organelles and proteins that effect volume displacement of cytoplasm that affects the ionic content of the cell cytoplasm. In the non-membrane bound organelle category are ribosomes and the nucleolus. Connective fibers such as keratin, elastin and myosin also affect the ionic content of the extracellular, intracellular and intra organelle compartments. A difference in ionic content due to protein displacement will change the conductivity therefore the resistance representing these membrane bound electrolytes. More protein causes more electrolyte displacement decreasing conductivity and increasing resistance. Each intra organelle fluid and intracellular fluid conductivity will be determined from organelle and cellular specific sources [1], [3], [9], [67-72], [84].

E. Cell Specific Network Model Level

The cells for each layer in a tissue will be based on the structural characteristics for the cell type and region including cell type, diameter, height, shape and membrane properties [9], [48], [44], [85-88]. These cells will contain a network topology for each organelle type based on the properties of the cell type. The network values will reflect the specific number and sizes of each organelle.

F. Tissue Specific Network Model Level

The tissue layer will be constructed from the series parallel combinations of the cell topology networks for the specific cell type of that layer. The tissue level network will be the parallel combination of all the various tissue layers. The complete network model can have the electrode model put in series with the tissue model. The modeling process will

be repeated for cancer tissue type I, II and III and hyperkeratosis over cancer tissue [11]. Models will be constructed for the commonly misdiagnosed oral tissue conditions of necrotic inflammation and hyperkeratosis [14-20].

G. Foundation of Organelle Construction

Construction of the organelles, cells and tissues starts and ends with a capacitive membrane isolating electrolyte solutions. The basic model construction is based on the ideas introduced by Fricke [52], [53], [89] and Cole [90], [91] for cell suspensions and has been verified for even simpler structures such as liposome suspensions [92]. The expanded ultra structural based model depends on both structure and biochemical properties. The impedance of cell membranes has been accurately measured for several cell types by patch clamp techniques [50], [55], [93], [94]. The simplest representation of a piece of membrane is a simple RC-circuit as shown in Fig. 6-1 the membrane model. The capacitance of a typical membrane, *Cm* arises due to the fact that there are layers of conductive and nonconductive (lipids) media [45]. The capacitance of a typical patch of membrane from patch clamp measurements is C_M = 1uf/cm^2 [50], [52], [53], [55], [85], [95], [105]. That is the membrane capacitance is measured in terms of the area of the membrane, the larger the area, the larger the capacitance [50], [105].

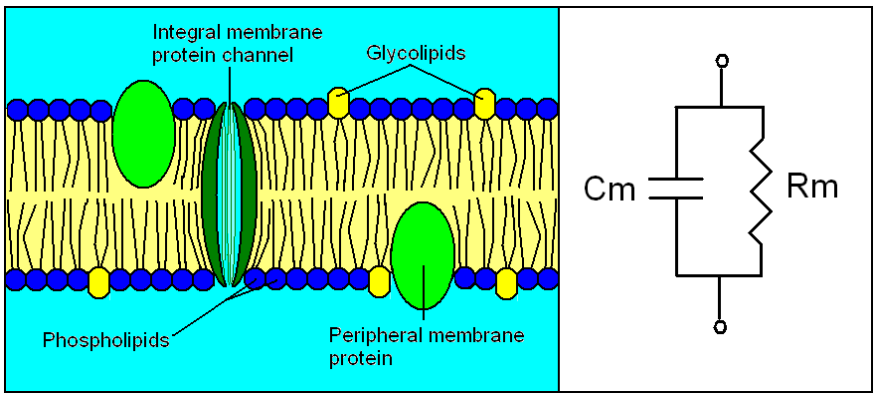

Fig. 6-1 The Membrane Model

Given the approximate value of membrane capacitance per square centimeter (C_M), the capacitor C_m can be calculated for an individual cell or organelle structure by simply multiplying this value by the surface area of the cell or organelle as shown in general in equation (6-1)

$$C_m = C_M \cdot A \tag{6-1}$$

where

C_m is the membrane capacitance value for a single membrane bound volume

C_M is the membrane capacitance per square centimeter

A is the surface area of the membrane for the cell or organelle

For simple spherical shaped organelles such as the endosome, peroxisome and lysosome [9], [67-72] the membrane area can be closely approximated by a sphere so the general equation for membrane capacitance for a spherical entity (cell or organelle) becomes (6-2)

$$C_m = C_M \cdot A = C_M \cdot 4 \cdot \pi \cdot r^2 \tag{6-2}$$

where

C_m is the membrane capacitance value for a single membrane bound volume

C_M is the membrane capacitance per square centimeter

A is the surface area of the membrane for the cell or organelle

r is the radius for a spherical cell or organelle

The membrane also has a resistance associated with it from the integral membrane protein channels. The membrane resistance (R_M) of a typical patch of membrane from

patch clamp measurement experiments, is R_M = 10,000 Ω /cm^2 [50], [55], [65], [66]. In general the higher the protein channel density the lower R_M is [48], [50], [55]. Given the approximate value of membrane resistance per square centimeter, the resistance R_m can be calculated in general for any individual cell or organelle by simply multiplying this value by the surface area (6-3)

$$R_m = R_M \cdot A \tag{6-3}$$

where

R_m is the membrane resistance for a single membrane bound volume

A is the membrane surface area for the cell or organelle

R_M is the membrane resistance per square centimeter of the membrane patch

Assuming a spherical cell or organelle the general equation for the membrane resistor value becomes (6-4)

$$R_m = R_M \cdot 4 \cdot \pi \cdot r^2 \tag{6-4}$$

where

R_m is the membrane resistance for a single membrane bound volume

A is the membrane surface area for the cell or organelle

R_M is the membrane resistance per square centimeter of the membrane patch

r is the radius of a spherical cell or organelle

The smaller the patch of membrane is, the larger its resistance is at low frequencies because there are fewer protein channels to let ions through the membrane to conduct current [50], [85]. There are two main points to emphasize: (i) associated with any

membrane are certain material constants that are independent of the shape of the membrane such as time constants, (ii) the actual electrical properties of a membrane depend on its geometry [53], [85]. To construct a model of a membrane bound entity such as an organelle or cell, the conductivity or the resistivity of the external fluid and internal fluid needs to be determined in order to calculate the lumped parameter resistance for the model. These electrolyte conductivities can be found experimentally or by calculation. Experimental studies by others show cell cytoplasm ranges in resistivity (ρ) from 10Ω-cm to 100Ω-cm [50], [55], [65], [66], [96]. These vary due to the ionic concentration differences and environmental conditions in individual cell and organelle types [50], [55], [85]. Resistivity of a material is defined and expressed as a rod of rectangular cross-section with area A and length L. This necessitates the conversion of an arbitrary liquid volume into a cubic volume with area L^2 and length L. The intra-organelle fluid resistivity is ρ_i so the value for the discrete element of intracellular resistance would be equal to R_i from the definition of resistivity equation (6-5), [97]

$$R_i = \frac{L \cdot \rho_i}{A} \tag{6-5}$$

where

R_i is the interior fluid resistor

A is the cross sectional area of a cubic equivalent volume

L is the length of one side of the cubic equivalent volume

ρ_i intracellular fluid resistivity

For a spherical membrane bound entity with an interior radius (r_i) volume can be calculated. An equivalent length L of a cube with the same volume as the spherical entity

can be calculated and the equation can be reduced from symmetry of a cubic element since for a cubic face A is L^2. So the intracellular resistance becomes (6-6)

$$R_i = \frac{\rho_i}{((4/3)\cdot\pi\cdot r_i^3)^{(1/3)}} = \frac{\rho_i \cdot 0.62035}{r_i} \tag{6-6}$$

where

R_i is the intracellular resistor value of a single cell or organelle entity

r_i is the interior radius of a spherical cell or organelle entity

ρ_i intracellular or intra-organelle fluid resistivity

The interior radius (r_i) from (6-6) is calculated in (6-7) it is the outer radius (r) minus twice the membrane thickness t_m (approximately 5nm [7], [9], [50], [85], [95])

$$r_i = r - 2\cdot t_m = r - (1.0\cdot 10^{-8})m \tag{6-7}$$

where

r_i is the interior radius of a spherical cell or organelle

r is the outer radius of a spherical cell or organelle

t_m is the membrane bilayer thickness (approximately 5nm [7], [9], [50], [85], [95])

The resistivity of the extracellular or extra-organelle electrolyte ρ_e will typically range between 75Ω-cm to 300Ω-cm [43], [50], [55], [66]. The discrete element for the extra cellular and extra-organelle resistance is dependent on the volume of fluid around that entity. The volume of the cell cytoplasm is the volume of the cell minus the sum of the displacement volumes of the organelles in the cell. When modeling the organelle it is

important to calculate the displacement volume of each organelle in order to calculate the amount of cytoplasm. This structural variable in the organelle level of modeling will get exported for use in the cellular model. The cell displacement volume plus other structural variables such as geometric shape and dimensions will get exported with the cell network variables for use in the tissue layer models.

The surrounding fluid or outer fluid for a cell is the extracellular fluid; the fluid surrounding the organelle is the cytoplasm it is external of the intra organelle fluid [9]. The volume of the outer fluid would be the interior volume of the outer containing entity minus the displacement volume of the smaller entity or entities within it. In general the external fluid resistor R_e for the fluid surrounding the inner entity is given by (6-8)

$$R_e = \frac{L \cdot \rho_e}{A} \tag{6-8}$$

where

R_e is the resistor of the fluid volume of the larger containing entity

ρ_e is the resistivity of the extracellular electrolyte

A is the cross sectional area of a cubic equivalent volume

L is the length of one side of the cubic equivalent volume

Calculation of the individual resistance and capacitance values for all the network values for the other organelles follow the same logic as the spherical entity shown in equations (6-1 through 6-8). Simply calculate the membrane area, interior volume and displacement volume for each organelle based on approximate size and structure. Then from the geometric values calculate the network values for each organelle.

H. Notes on Variable Naming Convention

There are seven tissue models developed here: thirty-five network elements per model thirty-five network elements per layer four layers per model for a total of one thousand two hundred twenty-five separate network element variables. This necessitates a standard flexible naming convention for each electrical element. Table 6-1 electrical component variable naming convention provides a key to constructing the variable names.

Table 6-1
ELECTRICAL COMPONENT VARIABLE NAMING CONVENTION

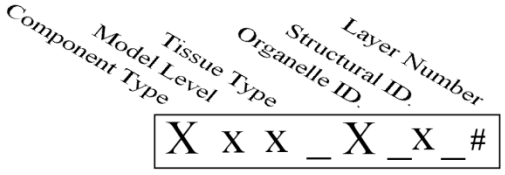

Component Type Abbreviations	
R	Resistor
C	Capacitor

Model Level Abbreviations	
o	Organelle
c	Cell
t	Tissue
ct	Complete Tissue

Tissue Type Abbreviations	
n	Normal
c1	Cancer Type 1
c2	Cancer Type 2
c3	Cancer Type 3
ni	Necrotic Inflammation
hk	Hyperkaratosis
hkc2	Hyperkaratosis With Cancer Type 2

Organelle ID. Abbreviations	
C	Cell
ER	Endoplasmic Reticulum
M	Mitochondria
N	Nucleus
NP	Nuclear Pore
TGN	Trans Golgi Network
MGN	Medial Golgi Network
CGN	Cis Golgi Network
GN	Golgi Network
P	Peroxisome
E	Endosome
L	Lysosome

Structural ID. Abbreviations	
ecf	Extracellular Fluid
cp	Cytoplasm
iof	Intra Organelle Fluid
om	Outer Membrane
im	Inner Membrane
mx	matrix
cp	Cytoplasm
np	nucleoplasm

Each element has three to four parts separated by an underscore. The first letter in the first part of the variable is the element type "*R*" for resistor, "*C*" for capacitor the second group of letters after the element type is the model level and type "*o*" is for organelle level,"*c*" is for cell level, "*t*" is for tissue level and "*ct*" is for complete tissue level. The next letter is for the tissue type "*n*" is for normal, "*hk*" is for hyperkeratosis, "*ni*" is for necrotic inflammation, "*c1*" is for cancer type 1, "*c2*" is for cancer type 2, etc. The second part comes after the first underscore it is the organelle ID. The third part after the

second underscore is the structural abbreviation, this is followed by another underscore and a tissue layer number. For the complete list of abbreviations see Table 6-1 electrical component variable naming convention. An example of a network element name is *Rtn_M_om_*2 it describes the mitochondria outer membrane resistor for the tissue level model second layer. The identification of these elements will become much easier after the cell model is developed.

I. Notes on Geometric Calculations

The electrical parameters depend on many geometric parameters including: the size of organelles, the quantity of each organelle, the volume of cytoplasm displaced by the organelles as well as the volume of cytoplasm displaced by the quantity of large proteins or lipid rafts within the cells. These physical variables are different in diseased cells when compared to normal cells. In the calculations for the geometric parameters that affect the electrical element values the average sizes and shapes of the organelles are estimated from electron micrographs and various references.

The ideas introduced in the K. Cole model earlier in section III lays the foundation for the ideas, rules and methods to construct models for the organelles. Cell model topologies will then be constructed from the organelle topologies. Tissue and cell suspension models can be constructed from the cell model topologies. The structurally simple organelles such as the peroxisomes, endosomes, and lysosomes have the same physical structure and subsequently the same network structure as the basic K. Cole model. Only the size, the properties of the membranes and ionic content (conductivity) of the intra-organelle fluids differ from the K. Cole model. Therefore only the values for the elements are different in these structurally equivalent networks.

J. General Rules and Methods for Network Construction

The rules for constructing all the electrical networks for each organelle are the same. It starts with physical structure of how the membranes and compartments are arranged and what are the properties of the membranes for each structure. The density of porins affect the membrane resistance, more porins per unit area translates to lower resistance. The nature of the electrolyte within the organelle compartment affects the conductivity of the fluid in the compartment and therefore the resistance representing that fluid. Higher ionic content translates to more charge carriers decreasing resistance. Larger volumes contain more ions, which also increases conductivity and therefore decreases resistance. The displacement of the electrolyte volume by large charge neutral proteins or lipid rafts decreases the amount of charged ions within that volume. Those ions displaced no longer contribute as charge carriers lowering the current flow thus increasing the resistance representing that volume. The structure of the organelle will determine the electrical network structure, recall that a patch of membrane behaves as a capacitor in parallel with a resistor as displayed in Fig. 6-2 Development of a network for a membrane bound entity. Using network theory the lower left drawing in Fig. 6-2 the membrane resistances and capacitances can be combined to make a familiar equivalent circuit with fewer components shown in the lower right. To test any network topology created by a physical structure pretend you can follow a hypothetical ion through or around the physical structure to get to the opposite side of a virtual volume containing that structure. In the case of the simple cell shown in the lower left drawing of Fig. 6-2 an ion could take two possible paths, around the cell through the extracellular fluid or through the cell. When one encounters a path choice this translates to a parallel topology [105]. So the resistor representing the electrolyte of the extracellular fluid will be in parallel with the network that represents the membrane bound entity as it shows in the circuit topology of Fig 6-2.

The hypothetical ion can “go through” (transfer charge across) the membrane by either going through the integral transmembrane protein pores which represent a resistance or through the capacitance of the membrane [105].

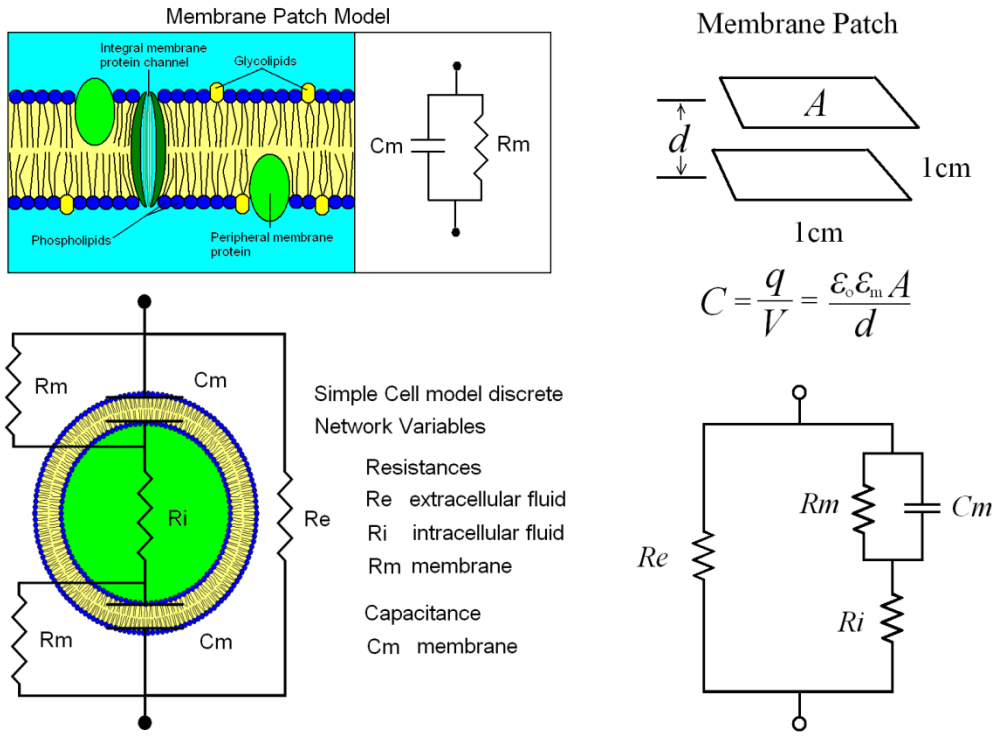

Fig. 6-2 Development of a network for a membrane bound entity

Since this is an “or” situation ether integral transmembrane protein or the membrane itself then these elements representing the path choices are again in parallel. When the hypothetical ion is in the membrane bound entity (cell) it must travel through the intra cellular fluid represented by a resistor so it is in series with the parallel RC network representing the membrane with pores. The hypothetical ion can “go through” (transfer charge across) the membrane on the opposite side of the cell making another parallel RC network in series with the intracellular fluid but it is redundant in terms of topology since we can combine the pair using network theory to reduce the topology to get the

equivalent circuit shown in the bottom right of Fig. 6-2. The construction of all the circuit topology for all organelles cells and tissues follows this same logic pattern [105].

K. Development of the "Transparent Box" Model Construction Review

This section covers the concept of creating a tissue model based on fundamental building blocks. Starting with the organelles and creating networks for individual organelles then constructing a cell with the organelle networks. These cell networks were combined into tissue layer networks and the tissue layer networks are combined with other tissue layers to form a complete tissue layer model network. This section introduced the naming convention for network elements as well as the general rules of network construction for the organelles, cells and tissues.

VII. ORGANELLE LEVEL MODEL DEVELOPMENT

A. The Organelle Level Peroxisome Network Model

We already know the network structure for this simple spherical organelle, now we need to determine the values for each of the 3 elements in the network. The diameter *d* of an average peroxisome in an epithelial cell is 200 nm so the radius *r* is 100 nm [68, p. 26]. From the radius the membrane surface area, displacement volume and electrolyte volume can be calculated. The surface area of an average peroxisome is calculated from (7-1)

$$A_P = 4 \cdot \pi \cdot r_P^{\,2} \tag{7-1}$$

where

A_P is the surface area of the average peroxisome organelle

r_P is the radius of the average peroxisome organelle

The displacement volume of the peroxisome organelle is used for cell level calculations to account for amount of cytoplasm displaced by each peroxisome organelle. The more organelles, the more cytoplasm gets displaced, the fewer charge carriers there are for a given cell volume and the higher the cytoplasm resistor value. The equation for the peroxisome displacing volume is given in (7-2)

$$DVo_p = \frac{4}{3} \cdot \pi \cdot r_P^{\,3} \tag{7-2}$$

where

DVo_P is the organelle level displacement volume of an average peroxisome

r_P is the radius of the average peroxisome organelle

The electrolyte volume of the peroxisome EV_P is the volume of the interior of the peroxisome organelle corrected for the membrane volume. Note it is not so critical to correct this small difference in a large organelle but it becomes important as the organelles get smaller; a 100 nm organelle will have a 12% overestimated volume with out a correction for the membrane and a 50 nm organelle will have a 22% over estimation in volume. The electrolyte volume of the peroxisome calculation is shown with the radius correction for the membrane thickness in (7-3)

$$EV_p = \frac{4}{3} \cdot \pi \cdot \left(r_P - t_m\right)^3 \tag{7-3}$$

where

EV_P is the electrolyte interior volume of the average peroxisome organelle

r_P is the outside radius of the average peroxisome organelle

t_m is the average lipid bilayer thickness ~ 4nm [9], [50], [95]

The radius correction can be seen graphically on the left of Fig. 7-1 Normal peroxisome organelle level network model. The resistance of the inter organelle fluid for a single normal cell peroxisome can be calculated with (7-4

$$Ron\_P\_iof = \frac{\rho_P}{EV_P^{\frac{1}{3}}} \tag{7-4}$$

where

Ron_P_iof is the resistance of a peroxisome intra organelle fluid of a normal cell

EV_P is the electrolyte interior volume of the average peroxisome organelle

ρ_P is the resistivity of the peroxisome intra organelle fluid

The resistance of the peroxisome membrane is inversely proportional to the membrane area and is given by (7-5)

$$Ron\_P\_om = \frac{MR_p}{A_P} \tag{7-5}$$

where

Ron_P_om is the outer membrane resistance of one peroxisome organelle

A_P is the surface area of the average peroxisome organelle membrane

MR_P is the resistance per square centimeter of the peroxisome membrane

The capacitance of the peroxisome is proportional to its surface area and is given by (7-6)

$$Con\_P\_om = A_P \cdot MC \tag{7-6}$$

where

Con_P_om is the capacitor value for one normal peroxisome organelle membrane

A_P is the surface area of the average peroxisome organelle membrane

MC is the capacitance per square centimeter of lipid membrane

Notice how the input variables fit into two categories physical structural variables and biochemical variables. The structural variables are radius, diameter, area, volume and may include other dimensions depending on the geometric shapes. The biochemical variables include capacitance per square centimeter, resistance per square centimeter

(commonly referred to as resistivity). Certain diseases affect both biochemical and structural variables others just biochemical or structural. It becomes handy to separate the variables this way when adjusting the model to replicate diseases. On the right of Fig. 7-1 normal peroxisome organelle level network model is the familiar network topology for a spherical entity.

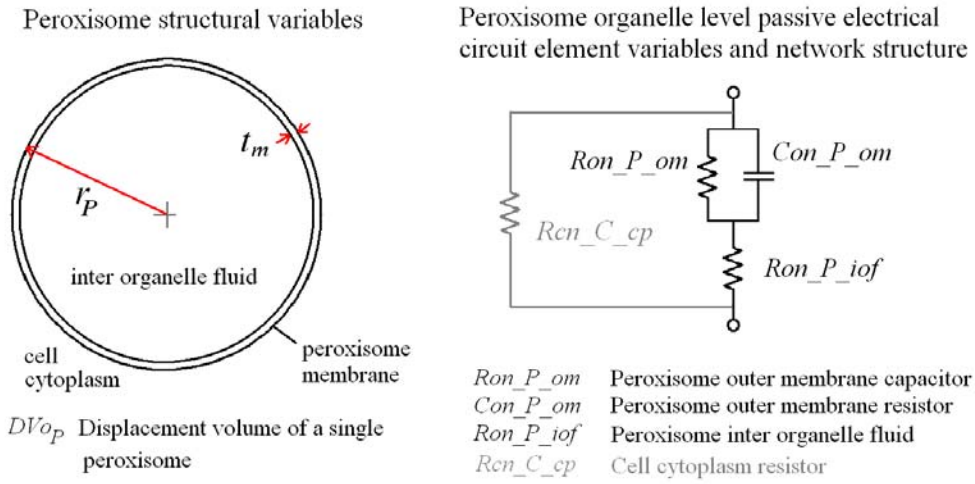

Fig. 7-1 Normal peroxisome organelle level network and export variables

B. The Organelle Level Endosome Network Model

The endosome is a simple spherical organelle with the same structure as the peroxisome only the structural variables and a few of the biochemical variables change. The diameter *d* of an average endosome is 400 nm so the radius *r* is 200 nm [68, p. 26]. From the radius the membrane surface area displacement volume and electrolyte volume can be calculated. The endosome membrane surface area shown in (7-7)

$$A_E = 4 \cdot \pi \cdot r_E^{\,2} \tag{7-7}$$

where

A_E is the surface area of the average endosome organelle

r_E is the radius of the average endosome organelle

The endosome displacement volume is shown in (7-8)

$$DVo_E = \frac{4}{3} \cdot \pi \cdot r_E^{\,3} \tag{7-8}$$

where

DVo_E is the organelle level displacement volume of an average endosome

r_E is the outside radius of the average endosome organelle

The endosome electrolyte volume is shown in (7-9)

$$EV_E = \frac{4}{3} \cdot \pi \cdot \left(r_E - t_m\right)^3 \tag{7-9}$$

where

EV_E is the electrolyte interior volume of the average endosome organelle

r_E is the outside radius of the average endosome organelle

t_m is the average lipid bilayer thickness ~ 4nm [9], [50], [95]

The resistance of the inter organelle fluid for a single normal cell endosome can be calculated with (7-10)

$$Ron\_E\_iof = \frac{\rho_E}{EV_E^{\frac{1}{3}}} \tag{7-10}$$

where

Ron_E_iof is the resistance of an endosomes intra organelle fluid in a normal cell

EV_E is the electrolyte interior volume of the average endosome organelle

ρ_E is the resistivity of the endosome intra organelle fluid

The resistance of the endosome membrane is inversely proportional to the membrane area and is given by (7-11)

$$Ron\_E\_om = \frac{MR_E}{A_E} \tag{7-11}$$

where

Ron_E_om is the outer membrane resistance of one endosome organelle

A_E is the surface area of the average endosome organelle membrane

MR_E is the resistance per square centimeter of the endosome membrane

The capacitance of the endosome is proportional to its surface area and is given by (7-12)

$$Con\_E\_om = A_E \cdot MC \tag{7-12}$$

where

Con_E_om is the capacitor value for one endosome in a normal cell

A_E is the surface area of the average endosome membrane

MC is the capacitance per square centimeter of lipid membrane

C. The Organelle Level Lysosome Network Model

Again this is a simple spherical organelle with the same structure as the peroxisome and endosome; only the structural variables and a few of the biochemical variables change. The diameter *d* of an average lysosome is 1 um so the radius *r* is 500 nm [68, p. 26]. From the radius membrane surface area, displacement volume and electrolyte volume can be calculated. The lysosome membrane surface area is shown in (7-13)

$$A_L = 4 \cdot \pi \cdot r_L^{\,2} \tag{7-13}$$

where

A_L is the surface area of the average lysosome organelle

r_L is the radius of the average lysosome organelle

The average lysosome displacement volume is shown in (7-14)

$$DVo_L = \frac{4}{3} \cdot \pi \cdot r_L^{\,3} \tag{7-14}$$

where

DVo_L is the organelle level displacement volume of an average lysosome

r_L is the outside radius of the average lysosome organelle

The average lysosome electrolyte volume is shown in (7-15)

$$EV_L = \frac{4}{3} \cdot \pi \cdot \left(r_L - t_m\right)^3 \tag{7-15}$$

where

EV_L is the average lysosome organelle electrolyte volume

r_L is the outside radius of the average lysosome organelle

t_m is the average lipid bilayer thickness ~ 4nm

The resistance of the inter organelle fluid for a single normal cell lysosome can be calculated with (7-16)

$$Ron\_L\_iof = \frac{\rho_L}{EV_L^{\frac{1}{3}}} \tag{7-16}$$

where

Ron_L_iof is the resistance of a lysosome intra organelle fluid of a normal cell

EV_L is the average lysosome organelle electrolyte volume

ρ_L is the resistivity of the lysosome intra organelle fluid

The resistance of the lysosome membrane is inversely proportional to the membrane area and is given by (7-17)

$$Ron\_L\_om = \frac{MR_L}{A_L} \tag{7-17}$$

where

A_L is the surface area of the average lysosome organelle membrane

MR_L is the resistance per square centimeter of the lysosome membrane

Ron_L_om is the outer membrane resistance of one lysosome organelle

The capacitance of the lysosome is proportional to its surface area and is given by (7-18)

$$Con\_L\_om = A_L \cdot MC \tag{7-18}$$

where

A_L is the surface area of the lysosome organelle membrane

MC is the capacitance per square centimeter of lipid membrane

Con_L_om is the capacitor value for one normal lysosome organelle membrane

D. The Organelle Level Mitochondria Network Model

The mitochondria have a more complex structure and circuit topology than the previous organelles. The mitochondria have an outer membrane and a pleated inner

membrane. The general shape of the outer membrane is similar to a watermelon see Fig. 7-2 Cross-section of the mitochondria.

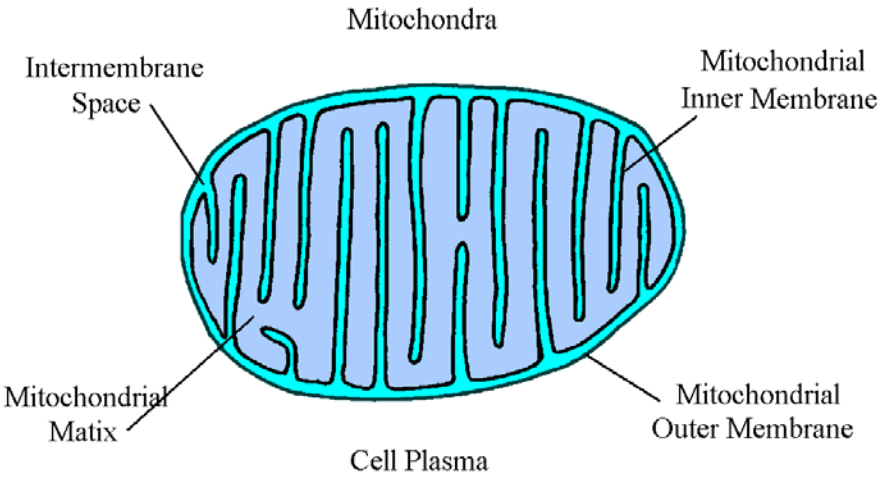

Fig. 7-2 Cross-section of the mitochondria

This shape approximates a cylindrical spheroid; it can be simply and clearly described as a right cylinder with two hemispherical end caps.

The volume of a right cylinder is given by equation (7-19) the volume of a sphere, which is equal to two hemispheres, is shown in equation (7-20) the sum of the volumes is given in equation (7-21)

$$V_{cyl} = \pi \cdot r^2 \cdot l \qquad (7\text{-}19)$$

where

V_{cyl} is the volume of a cylinder

r is the radius of the cylinder

l is the cylinder length it is approximately equal to r in a mitochondrion

Volume of two hemispheres is equal to a sphere shown in (7-20)

$$V_{sph} = \frac{4}{3} \cdot \pi \cdot r^3 \qquad (6\text{-}20)$$

where

V_{sph} is the volume of a sphere

r is the radius of the sphere

So the total volume of the hemispherical end capped right cylinder or cylindrical spheroid with length r and an over all length of $3r$ is the sum of equations (7-19) and (7-20) making the total volume of the cylindrical spheroid equal to (7-21)

$$V_{cyl\_sph} = V_{cyl} + V_{sph} = \pi \cdot r^2 \cdot r + \frac{4}{3} \cdot \pi \cdot r^3 = \frac{7}{3} \cdot \pi \cdot r^3 \qquad (7\text{-}21)$$

where

V_{cyl_sph} is the displacement volume for a cylindrical spheroid

r is the cylindrical spheroid outer membrane radius

Note in these equations the radius of the hemispheres, the cylinder and the length of the cylinder are all the same. The surface area of the combination of the cylinder and the hemispheres is the sum of the surface area of the curved section of the cylinder plus the surface area of a sphere with the same radius. The surface area of a sphere, equal to two hemispheres and is given in (7-22)

$$A_{sph} = 4 \cdot \pi \cdot r^2 \quad (7\text{-}22)$$

where

A_{sph} is the area of a sphere

r is the radius of the sphere

The lateral surface area of a right cylinder is given in equation (7-23)

$$A_{cyl} = 2 \cdot \pi \cdot r \cdot l \quad (7\text{-}23)$$

where

A_{cyl} is the area of the lateral surface of a cylinder

r is the radius of the cylinder

l is the length of the cylinder

Equation (6-24) is the combined sum of the surface areas for a cylinder with length r_{Mom} and radius r_{Mom} it representing the outer membrane surface area of a mitochondria

$$A_{M\_om} = 6 \cdot \pi \cdot r_{Mom}^{\ 2} \quad (7\text{-}24)$$

where

A_{M_om} area of the mitochondria outer membrane surface

r_{Mom} is the mitochondria outside membrane radius

The inner membrane in the mitochondria is pleated to increase surface area for the membrane bound proteins. This inner membrane forms two separate compartments each

with a separate volume as shown in Fig. 7-2 and Fig. 7-3. The one for the inter-membrane space is shown in light blue and the matrix fluid is shown in the lavender. The inner membrane radius r_{Mim} can be calculated using equation (7-25) it will be used to calculate the mitochondria intra-organelle structures, surface areas and volumes. An exaggerated view of membrane structure with variable names is shown in the right of Fig. 7-3 Geometric model of the mitochondria.

$$r_{Mim} = r_{Mom} - t_{Mims} \tag{7-25}$$

where

r_{Mim} is the mitochondria inner membrane radius

r_{Mom} is the mitochondria outside membrane radius

t_{Mims} is the average thickness of the mitochondria inter-membrane space

The average thickness of the inter-membrane space of the mitochondria can be approximated from cell electron micrographs it is approximately 25nm [9, p. 678]

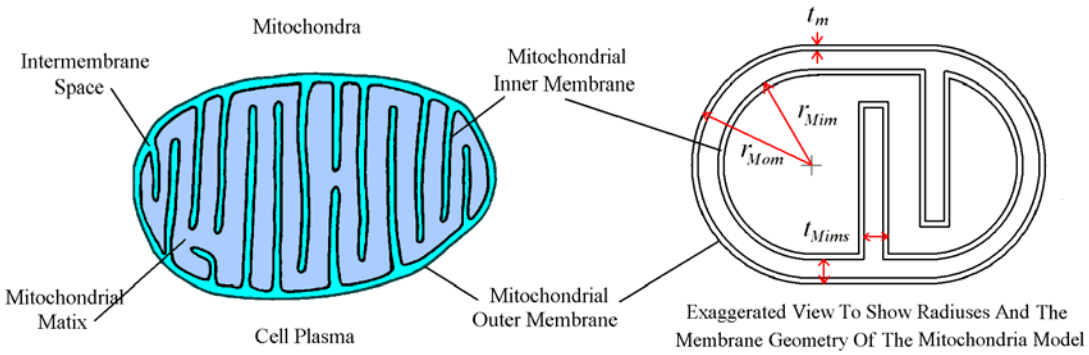

Fig. 7-3 Geometric model of the mitochondria

The inner membrane surface area of one face of one pleat can be approximated by the surface area of a disk with average inner radius $r_{Mim,}$ shown in (7-26)

$$A_{disk} = \pi \cdot r_{Mim}{}^2 \tag{7-26}$$

where

A_{disk} is the surface area of one disk

r_{Mim} is the inner membrane radius

The approximate surface area of the entire inner membrane can be calculated as approximately 10 circular disks with average inner radius r_{Mim}-t_m times two to account for both sides of the pleat plus the surface area combination of the cylinder and the hemispheres has a radius r_{Mim} and accounts for the inner membrane parts closest to the borders and nearest to the outer membrane. The total inner membrane structure area calculation is shown in (7-27)

$$A_{Mim} = 20 \cdot \pi \cdot r_{Mim}{}^2 + 6 \cdot \pi \cdot r_{Mim}{}^2 = 26 \cdot \pi \cdot r_{Mim}{}^2 \tag{7-27}$$

where

A_{Mim} is the mitochondria inner membrane surface area

r_{Mim} is the mitochondria inner membrane radius

To correct for the lipid bilayer thickness in the calculations of volume (more critical for smaller organelles or organelles with complex pleated structures where membrane thickness displaces a relatively larger portion of the organelles volume) there are two distinct volumes; the displacement volume labeled (*DV*) or and the electrolyte volume (*EV*). Note: the displacement volume is used for export to the cell level modeling so displacement volumes will further labeled as *DVo* for organelle level and *DVc* for cell level. The *DVo* pertains to a single organelle displacement where as *DVc* pertains to the

displacement by all of the organelles in a cell. The displacement volume of an organelle or structure includes the space taken up by the membranes. The *EV* or electrolyte volume is an interior liquid volume in other words the volume without the membrane contribution. The *EV* deals with just the volume that has soluble charge carriers within an organelle or sub structure it is important for calculating the resistance of the introrganelle fluid. From equation (7-21) the organelle level displacement volume of a single mitochondria organelle is given by (7-28)

$$DVo_M = \frac{7}{3} \cdot \pi \cdot r_{Mom}{}^3 \tag{7-28}$$

where

DVo_M is the organelle level mitochondria displacement volume

r_{Mom} is the mitochondria outside membrane radius

To calculate the electrolyte volumes *EV*s for the mitochondria it is instructive to refer to the organelle structure diagram and calculate simpler sub volumes of a complex structure then sum them together. Notice the inter-membrane space in Fig. 7-3 the first simple geometric structure we can easily calculate is the inter-membrane shell it can be calculated by subtracting the outer cylindrical spheroid from the inner cylindrical spheroid notice that for the electrolyte volume we will want to omit the membrane volume contribution by subtracting the membrane thickness from the radii. The outer inter-membrane shell electrolyte volume is calculated in (7-29)

$$EV_{Moim} = \frac{7}{3} \cdot \pi \cdot \left(r_{Mom} - t_m\right)^3 - \frac{7}{3} \cdot \pi \cdot r_{Mim}{}^3 \tag{7-29}$$

where

EV_{Moim} is the mitochondria outer inter-membrane volume

r_{Mom} is the mitochondria outer radius of the outer membrane

t_m is the average lipid bilayer membrane thickness

r_{Mim} is the mitochondria outer radius of the inner membrane

The inter-membrane space electrolyte volume in the pleated areas extending from the outer inter membrane volume can be approximated as the volume of 10 cylindrical disks with thickness equal to the average thickness of the mitochondria inter-membrane space corrected for membrane thickness this calculation is shown in (7-30)

$$EV_{Miim} = \left(10 \cdot \pi \cdot \left(r_{Mim} - t_m\right)^2 \cdot t_{Mims} - t_m\right) \tag{7-30}$$

where

EV_{Miim} is the mitochondria inner inter-membrane volume (pleat fluid volume)

r_{Mim} is the mitochondria inner membrane radius

t_{Mims} is the pleat thickness in the inter-membrane space of the mitochondria

t_m is the average lipid bilayer membrane thickness

The total inter-membrane fluid volume shown in light blue in Fig. 7-2 is the sum of the inner and outer inter-membrane volumes and is given by (7-31)

$$EV_{Min} = EV_{Moim} + EV_{Mimm} \tag{7-31}$$

where

EV_{Min} is the mitochondria inter-membrane volume

EV_{Moim} is the mitochondria outer shell inter-membrane volume

EV_{Miim} is the mitochondria inner inter-membrane volume (pleat fluid volume)

Note, to calculate the electrolyte volume of the matrix the displacement volume of the inter-membrane space must be calculated then subtracted from the equivalent electrolyte volume of the whole mitochondrion (ie. the entire outer cylindrical spheroid corrected for the outer membrane thickness). The displacement volume for the inter-membrane shell can be calculated by subtracting the outer cylindrical spheroid from the inner cylindrical spheroid including the membrane volume contribution of the inner membrane. The displacement volume of the inter-membrane outer shell space including the inner membrane is shown in equation (7-32).

$$DV_{Moim} = \left[\frac{7}{3} \cdot \pi \cdot \left(r_{Mom} - t_m \right)^3 - \frac{7}{3} \cdot \pi \cdot \left(r_{Mim} - t_m \right)^3 \right] \tag{7-32}$$

where

DV_{Moim} is the mitochondria outer inter-membrane displacement volume

r_{Mom} is the mitochondria outer radius of the outer membrane

t_m is the average lipid bilayer membrane thickness

r_{Mim} is the mitochondria outer radius of the inner membrane

The displacement volume of the inner inter-membrane space (pleat disks space volume) including membrane volume is shown in (7-33).

$$DV_{Miim} = \left(10 \cdot \pi \cdot \left(r_{Mim} - t_m \right)^2 \cdot t_{Mims} \right) \tag{7-33}$$

where

DV_{Miim} is the mitochondria inner inter-membrane volume including membrane

r_{Mim} is the mitochondria inner membrane radius

t_{Mims} is the pleat thickness in the inter-membrane space of the mitochondria

t_m is the average lipid bilayer membrane thickness

The total inter-membrane displacement volume is given in (7-34).

$$DV_{Min} = DV_{Moim} + DV_{Mimm} \tag{7-34}$$

where

DV_{Min} is the mitochondria intermembrane displacement volume

DV_{Moim} is the mitochondria outer shell inter-membrane displacement volume

DV_{Miim} is the mitochondria inner inter-membrane displacement volume (pleats)

The entire interior volume of the mitochondria corrected for the outer membrane is shown in equation (7-35) and can be called the electrolytic volume of the entire mitochondria.

$$EV_M = \frac{7}{3} \cdot \pi \cdot \left(r_{Mom} - t_m\right)^3 \tag{7-35}$$

where

EV_M is the mitochondria equivalent electrolytic volume

r_{Mom} is the mitochondria outer radius of the outer membrane

t_m is the average lipid bilayer membrane thickness

The calculation for the matrix volume is simply the electrolytic volume of the entire mitochondria subtracted by the displacement volume of the entire inter-membrane space as shown in equation (7-36)

$$EV_{Mmx} = EV_M - DV_{Min} \tag{7-36}$$

where

EV_{mx} is the mitochondria matrix electrolyte volume.

EV_M is the mitochondria equivalent electrolytic volume

DV_{Min} is the mitochondria inter-membrane displacement volume

The normal cell mitochondrion electrical network topology and variable identification is shown in Fig. 7-4 Mitochondrion organelle level network and export variables.

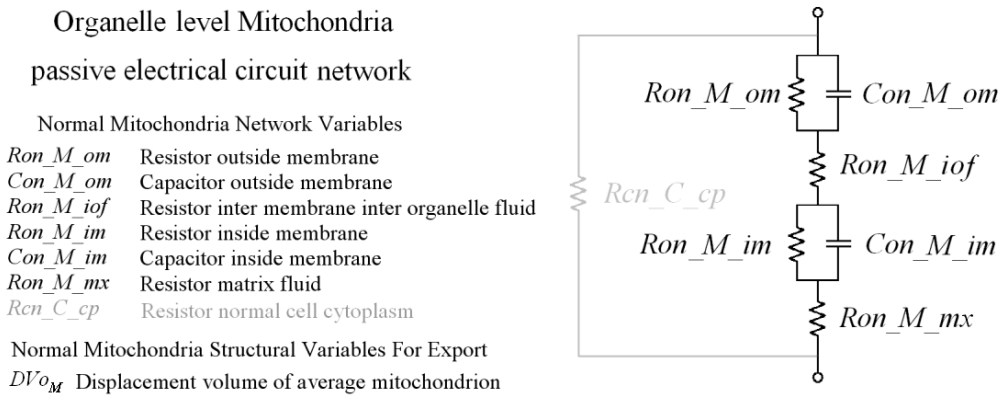

Fig. 7-4 Mitochondrion organelle level network and export variables

Note the presence of the resistor for the cytoplasm *Rcn_C_cp,* it is a cell level component shown in the organelle level topology. It is only shown for completeness it illustrates the relationship with the surrounding electrolyte. Its value depends on the number of organelles displacing cytoplasm in the model. The organelle level

displacement volume of an average mitochondrion (DVo_M) gets multiplied by the number of mitochondria in the cell level model. Displacement volumes in the organelle model are an export parameter to the cell level model; this will account for the mitochondria specific electrolyte volume correction. The same displacement volume correction gets performed for each organelle type and number to adjust the cytoplasm resistance at the cell model level. The equation for this will be introduced later in section VIII The Cell Level Model.

The resistance of the mitochondria inter-membrane fluid can be calculated with equation (7-37)

$$Ron\_M\_iof = \frac{\rho_{Min}}{EV_M^{\frac{1}{3}}} \tag{7-37}$$

where

Ron_M_iof is the resistance of a mitochondria inter-membrane fluid in a normal cell

EV_M is the electrolyte interior volume of the mitochondria inter-membrane space

ρ_{Min} is the resistivity of the mitochondria inter-membrane space electrolyte

The resistance of the mitochondria outer membrane is inversely proportional to the membrane area and is given by equation (7-38)

$$Ron\_M\_om = \frac{MR_{Mom}}{A_{Mom}} \tag{7-38}$$

where

Ron_E_om is the outer membrane resistance of one mitochondria organelle

A_{Mom} is the surface area of the average mitochondria's outer membrane

MR_{Mom} is the resistance per cm^2 of the mitochondria's outer membrane

The capacitance of the mitochondria outer membrane is proportional to its surface area and is given by equation (7-39)

$$Con\_M\_om = A_M \cdot MC \tag{7-39}$$

where

Con_M_om is a single mitochondria's outer membrane capacitor value in a normal cell

A_{Mom} is the surface area of the average mitochondria's outer membrane

MC is the capacitance per square centimeter of lipid membrane

The resistance of the mitochondria matrix fluid can be calculated with equation (7-40)

$$Ron\_M\_mx = \frac{\rho_{Mmx}}{EV_{Mmx}^{\frac{1}{3}}} \tag{7-40}$$

where

Ron_M_mx is the resistance of a mitochondria matrix fluid in a normal cell

EV_{Mmx} is the interior electrolyte volume of the mitochondria matrix fluid space

ρ_{Mmx} is the resistivity of the mitochondria matrix electrolyte

The resistance of the mitochondria inner membrane is inversely proportional to the membrane area and is given by equation (7-41)

$$Ron\_M\_im = \frac{MR_{Mim}}{A_{Mim}} \tag{7-41}$$

where

Ron_M_im is the inner membrane resistance of one mitochondria organelle

A_{Mim} is the surface area of the average mitochondria's inner membrane

MR_{Mim} is the resistance per cm^2 of the mitochondria's inner membrane

The capacitance of the mitochondria inner membrane is proportional to its surface area and is given by equation (7-42)

$$Con\_M\_im = A_{Mim} \cdot MC \tag{7-42}$$

where

Con_M_im is a single mitochondria's inner membrane capacitor value in a normal cell

A_{Mim} is the surface area of the average mitochondria's inner membrane

MC is the capacitance per square centimeter of lipid membrane

E. The Organelle Level Golgi Apparatus Network Model

The Golgi apparatus is made of a stack of cisterna with three distinct regions as shown in Fig. 7-5 The Golgi apparatus cross-section. A cis. Golgi network faces the endoplasmic reticulum. The medial Golgi network typically composed of three cisterna is in the center and the trans Golgi network facing out toward the outer membrane region is the last cisterna network. Each membrane bound cisterna envelope has different proteins imbedded in them for different functions. The electrolyte within the intra-organelle fluid

for each compartment is different. The physical structures that comprise the Golgi stack can be approximated by three-dimensional rectangular structures.

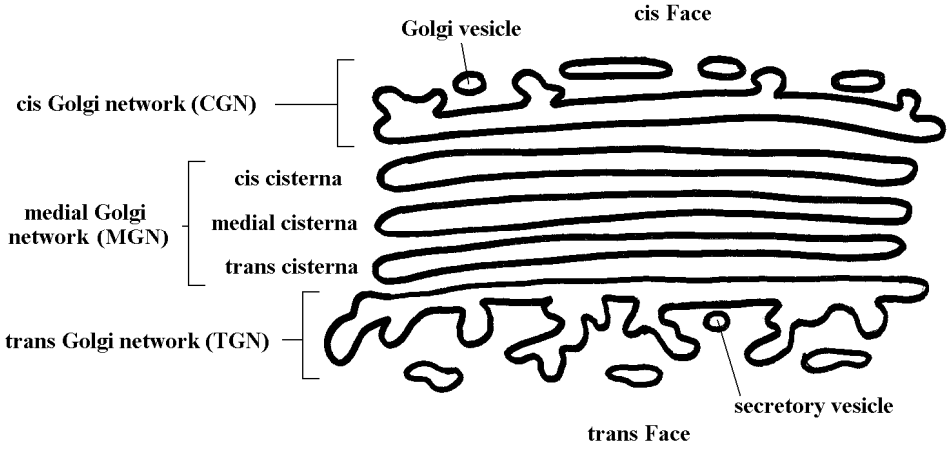

Fig. 7-5 The Golgi apparatus cross-section

From electron micrographs of Golgi apparatus a simple estimate of the dimensions of the cisterna can be made for a specific cell type. To model the structure electrically an approximate membrane surface area and volume must be calculated. For the medial Golgi network a simple approximation is found by calculating the volume and surface area of a simple three-dimensional rectangular box with dimensions of an average cisterna. The membrane surface area for an average Golgi medial cisterna is given by the sum of the individual surface areas of each side of a representative rectangular box shown in (7-43)

$$A_{GMCom} = 2 \cdot \left(l_{GMC} \cdot w_{GMC}\right) + 2 \cdot \left(l_{GMC} \cdot d_{GMC}\right) + 2 \cdot \left(d_{GMC} \cdot w_{GMC}\right) \qquad (7\text{-}43)$$

where

A_{GMCom} is the surface area of an average Golgi medial cisterna outer membrane

l_{GMC} is the length of the average Golgi medial cisterna

d_{GMC} is the depth of the average Golgi medial cisterna

w_{GMC} is the width of the average Golgi medial cisterna

The displacement volume of an average Golgi medial cisterna is given by (7-44)

$$DV_{GMC} = l_{GMC} \cdot w_{GMC} \cdot d_{GMC} \tag{7-44}$$

where

DV_{GMC} is the displacement volume of an average Golgi medial cisterna

l_{GMC} is the length of the average Golgi medial cisterna

d_{GMC} is the depth of the average Golgi medial cisterna

w_{GMC} is the width of the average Golgi medial cisterna

The electrolyte volume of the average Golgi medial cisterna is given by (7-45) this equation compensates for the lipid membrane volume by reducing the overall dimensions by twice the membrane thickness.

$$EV_{GMC} = \left(l_{GMC} - 2 \cdot t_m\right) \cdot \left(w_{GMC} - 2 \cdot t_m\right) \cdot \left(d_{GMC} - 2 \cdot t_m\right) \tag{7-45}$$

where

EV_{GMC} is the electrolyte volume of an average Golgi medial cisterna

l_{GMC} is the length of the average Golgi medial cisterna

d_{GMC} is the depth of the average Golgi medial cisterna

w_{GMC} is the width of the average Golgi medial cisterna

t_m is the average lipid bilayer thickness ~ 4nm [9], [50], [95]

For flexibility and generality the Golgi structure is modeled in three sections since a particular disease may only affect one section of the Golgi. The section names and relationships can be seen in Fig. 7-5 The Golgi apparatus cross-section. for simplicity in modeling, each of these sections has geometric properties proportional to the average Golgi medial cisterna. The medial Golgi network (MGN) is comprised of the three middle cisterna they have a total surface area and volume that is three times the average Golgi medial cisterna values calculated in equations (7-43, 7-44, 7-45). The medial Golgi network membrane surface area is given by (7-46).

$$A_{MGNom} = 3 \cdot A_{GMCom} = 6 \cdot \left(l_{GMC} \cdot w_{GMC} \right) + 6 \cdot \left(l_{GMC} \cdot d_{GMC} \right) + 6 \cdot \left(d_{GMC} \cdot w_{GMC} \right) \quad (7\text{-}46)$$

where

A_{MGNom} is the surface area of the medial Golgi network membranes

A_{GMCom} is the surface area of an average Golgi medial cisterna outer membrane

l_{GMC} is the length of the average Golgi medial cisterna

d_{GMC} is the depth of the average Golgi medial cisterna

w_{GMC} is the width of the average Golgi medial cisterna

The medial Golgi network displacement volume is given by (7-47).

$$DVo_{MGN} = 3 \cdot DV_{GMC} = 3 \cdot l_{GMC} \cdot w_{GMC} \cdot d_{GMC} \quad (7\text{-}47)$$

where

DVo_{MGN} is the organelle level displacement volume of the medial Golgi network

DV_{GMC} is the displacement volume of an average Golgi medial cisterna

l_{GMC} is the length of the average Golgi medial cisterna

d_{GMC} is the depth of the average Golgi medial cisterna

w_{GMC} is the width of the average Golgi medial cisterna

The medial Golgi network electrolyte volume is given by (7-48).

$$EV_{MGN} = 3 \cdot EV_{GMC} = 3 \cdot \left(l_{GMC} - 2 \cdot t_m\right) \cdot \left(w_{GMC} - 2 \cdot t_m\right) \cdot \left(d_{GMC} - 2 \cdot t_m\right) \qquad (7\text{-}48)$$

where

EV_{MGN} is the electrolyte volume of the medial Golgi network

EV_{GMC} is the electrolyte volume of an average Golgi medial cisterna

l_{GMC} is the length of the average Golgi medial cisterna

d_{GMC} is the depth of the average Golgi medial cisterna

w_{GMC} is the width of the average Golgi medial cisterna

t_m is the average lipid bilayer thickness ~ 4nm [9], [50], [95]

It would be impractical to create a geometric analog for the complex structure of the cis and trans Golgi networks. For convenience a volume and surface area multiplier are used to estimate both the trans Golgi network and cis Golgi network average geometric properties. The multipliers act on the average Golgi medial cisterna (AGMC) and are based on the approximate geometric ratios between the TGN and the AGMC and the CGN and the AGMC. The membrane surface area for the cis Golgi network is given in (7-49)

$$A_{CGN} = AxCGN \cdot A_{GMCom} \qquad (7\text{-}49)$$

where

A_{CGN} is the membrane surface area of the cis Golgi network

A_{GMCom} is the surface area of an average Golgi medial cisterna outer membrane

$AxCGN$ is the CGN membrane area multiplier

The displacement volume for the cis Golgi Network is given in (7-50)

$$DVo_{CGN} = VxCGN \cdot DV_{GMC} \tag{7-50}$$

where

DVo_{CGN} is the organelle level displacement volume of the CGN

DV_{GMC} is the displacement volume of an average Golgi medial cisterna

$VxCGN$ is the CGN membrane volume multiplier

The electrolyte volume for the cis Golgi Network is given in (7-51)

$$EV_{CGN} = VxCGN \cdot EV_{GMC} \tag{7-51}$$

where

EV_{CGN} is the electrolyte volume of the CGN

EV_{GMC} is the electrolyte volume of an average Golgi medial cisterna

$VxCGN$ is the CGN membrane volume multiplier

The membrane surface area for the trans Golgi Network is given in (7-52)

$$A_{TGN} = AxTGN \cdot A_{GMCom} \tag{7-52}$$

where

A_{TGN} is the membrane surface area of the TGN

A_{GMCom} is the surface area of an average Golgi medial cisterna outer membrane

$AxTGN$ is the TGN membrane area multiplier

The displacement volume for the trans Golgi Network is given in (7-53)

$$DVo_{TGN} = VxTGN \cdot DV_{GMC} \tag{7-53}$$

where

DVo_{TGN} is the organelle level displacement volume of the TGN

DVo_{GMC} is the displacement volume of an average Golgi medial cisterna

$VxTGN$ is the TGN membrane volume multiplier

The electrolyte volume for the trans Golgi Network is given in (7-54)

$$EV_{TGN} = VxTGN \cdot EV_{GMC} \tag{7-54}$$

where

EV_{TGN} is the electrolyte volume of the TGN

EV_{GMC} is the electrolyte volume of an average Golgi medial cisterna

$VxTGN$ is the TGN membrane volume multiplier

The normal cell Golgi electrical network topology and variable identification is shown in Fig. 7-6 Golgi organelle level network and export variables. Notice how the cisterna networks are electrically in parallel. Each of the three Golgi cisterna networks

has the same circuit topology as the simple spherical organelles but of course the circuit element values are different since the electrolyte volumes and membrane areas and chemical properties are much different. Note the presence of the resistor for the cytoplasm *Rcn_C_cp;* it is a cell level component shown in the organelle topology for completeness. Its value will change depending on the number of organelles displacing cytoplasm in the model. The displacement volume of an average Golgi network represented by the variable DVo_G; it gets multiplied by the number of Golgi in the cell level model. An important note on the Golgi displacement volume for one Golgi network: it is the sum of the sub networks (cis, trans and medial) and is given by equation (7-55)

$$DVo_G = DVo_{CGN} + DVo_{MGCN} + DVo_{TGN} \tag{7-55}$$

where

DVo_G is the organelle level displacement volume of a single Golgi apparatus

DVo_{CGN} is the organelle level displacement volume of the CGN

DVo_{MGN} is the organelle level displacement volume of an MGN

DVo_{TGN} is the organelle level displacement volume of the TGN

Displacement volumes in the organelle model are an export parameter to the cell level model this will account for the Golgi specific electrolyte volume correction. Use the geometric values from the previous calculations to calculate the individual component values in the network as before.

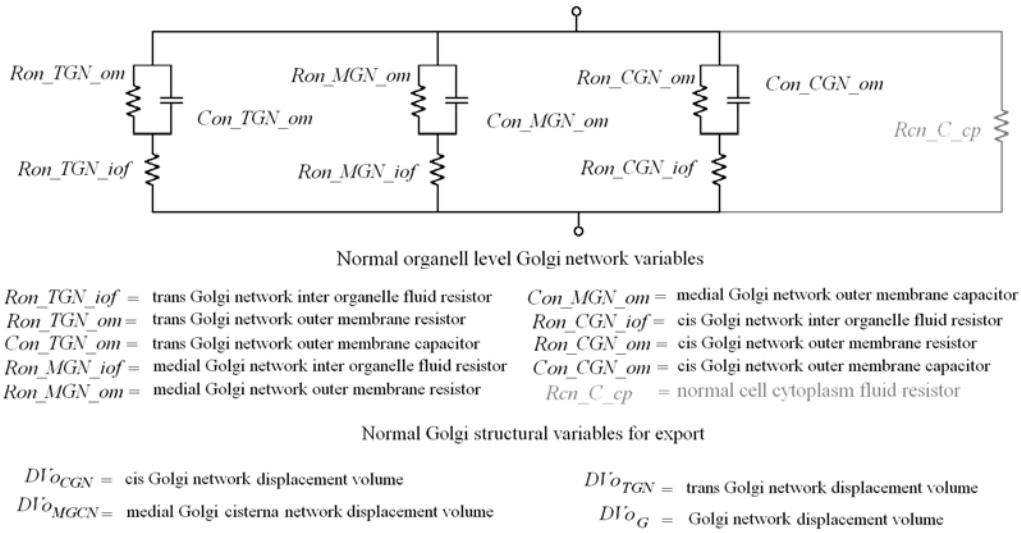

Fig. 7-6 Golgi organelle level network and export variables

The Resistor value for the organelle level model representing the outer membrane of the trans Golgi network is inversely proportional to the membrane area and is given by (7-56)

$$Ron\_TGN\_om = \frac{MR_{TGN}}{A_{TGN}} \tag{7-56}$$

where

Ron_TGN_om	is the outer membrane resistance of a single TGN
A_{TGN}	is the surface area of the TGN membrane
MR_{TGN}	is the resistance per square centimeter of the TGN membrane

The capacitance of the trans Golgi network membrane is proportional to its surface area and is given by (7-57)

$$Con\_TGN\_om = A_{TGN} \cdot MC \tag{7-57}$$

where

Con_TGN_om is the capacitor value for one normal TGN membrane

A_{TGN} is the surface area of the average TGN membrane

MC is the capacitance per square centimeter of lipid membrane

The resistance of the inter organelle fluid for a single normal cell TGN can be calculated with (7-58)

$$Ron\_TGN\_iof = \frac{\rho_{TGN}}{EV_{TGN}^{\frac{1}{3}}} \tag{7-58}$$

where

Ron_TGN_iof is the resistance of a normal cell TGN intra organelle fluid

EV_{TGN} is the electrolyte interior volume of the TGN

ρ_{TGN} is the resistivity of the TGN intra organelle fluid

The Resistor value for the organelle level model representing the outer membrane of the medial Golgi network is inversely proportional to the membrane area and is given by (7-59)

$$Ron\_MGN\_om = \frac{MR_{MGN}}{A_{MGN}} \tag{7-59}$$

where

Ron_MGN_om is the outer membrane resistance of a MGN

A_{MGN} is the surface area of the MGN membrane

MR_{MGN} is the resistance per square centimeter of the MGN membrane

The capacitance of the trans Golgi network membrane is proportional to its surface area and is given by equation (7-60)

$$Con\_MGN\_om = A_{MGN} \cdot MC \tag{7-60}$$

where

Con_MGN_om is the capacitor value for the MGN membrane of a normal Golgi

A_{MGN} is the surface area of the average MGN membrane

MC is the capacitance per square centimeter of lipid membrane

The resistance of the inter organelle fluid for a single normal cell TGN can be calculated with (7-61)

$$Ron\_MGN\_iof = \frac{\rho_{MGN}}{EV_{MGN}^{\frac{1}{3}}} \tag{7-61}$$

where

Ron_MGN_iof is the resistance of a normal cell MGN intra organelle fluid

EV_{MGN} is the electrolyte interior volume of the MGN

ρ_{MGN} is the resistivity of the MGN intra organelle fluid

The Resistor value for the organelle level model representing the outer membrane of the cis Golgi network is inversely proportional to the membrane area and is given by (7-62)

$$Ron\_CGN\_om = \frac{MR_{CGN}}{A_{CGN}} \tag{7-62}$$

where

Ron_CGN_om is the outer membrane resistance of a CGN

A_{CGN} is the surface area of the CGN membrane

MR_{CGN} is the resistance per square centimeter of the CGN membrane

The capacitance of the cis Golgi network membrane is proportional to its surface area and is given by equation (7-63)

$$Con\_CGN\_om = A_{CGN} \cdot MC \tag{7-63}$$

where

Con_CGN_om is the capacitor value for the CGN membrane of a normal Golgi

A_{CGN} is the surface area of the average CGN membrane

MC is the capacitance per square centimeter of lipid membrane

The resistance of the inter organelle fluid for a single normal cell CGN can be calculated with equation (7-64)

$$Ron\_CGN\_iof = \frac{\rho_{CGN}}{EV_{CGN}^{\frac{1}{3}}} \tag{7-64}$$

where

Ron_CGN_iof is the resistance of a normal cell CGN intra organelle fluid

EV_{CGN} is the electrolyte interior volume of the CGN

ρ_{CGN} is the resistivity of the MGN intra organelle fluid

F. The Organelle Level Nucleus & Endoplasmic Reticulm Network Model

The network model for the nucleus and the endoplasmic reticulum organelles are combined because they share the same membranes [9, p. 660]. The outer membrane of

the nucleus is the outer membrane of the endoplasmic reticulm. The nucleus is roughly spherical in shape so calculating the inner membrane surface area is elementary. The outer membrane is surface area is more dificult to calculate with simple geometry. Fortunately studies measuring the relative amounts of lipid by weight according to organelle have provided ratios that can be used to calculate the ER membrane surface area. Studies also have shown relative intracellular compartment volumes. The volume of both the smooth and rough ER is two and a half times larger than the nuclear volume [9, p. 661]. The diameter of a normal healthy cell nucleus is four to six micro-meters. The spacing between the inner and outer membranes of the nucleus is ten to fifty nano-meters. This is the same dimension range for the width of the ER cisterna [9, p. 670], [68, p. 26]. A healthy mature differentiated cell will have a nuclear inner membrane surface area to outer plasma membrane ratio of greater than eight and typically less than thirty [9, p. 661]. A typical ER surface area will be one hundred to two hundered times larger than the nuclear inner membrane area [9, p. 662]. These relationships allow for the simplified aproximation of the ER geometric parameters for the calculation of the electrical network values. The nuclear inner membrane surface area is calculated using (7-65)

$$A_{Nim} = 4 \cdot \pi \cdot r_{Nim}{}^{2} \tag{7-65}$$

where

A_{Nim} is the nuclear inner membrane surface area

r_{Nim} is the Nuclear inner membrane radius

The nucleoplasm electrolyte volume calculation is shown in (7-66)

$$EV_N = \frac{4}{3} \cdot \pi \cdot \left(r_{Nim} - t_m\right)^3 \tag{6-66}$$

where

EV_N is the average nucleus electrolyte volume or nucleoplasm

r_{Nim} is the outside radius of the nucleus inner membrane

t_m is the average lipid bilayer thickness ~ 4nm [9], [50], [95]

The calculation for the electrolyte volume of the endoplasmic reticulum is based on relative organelle volume ratios determined from experiments and electron micrographs [9], [68-72]. The ER electrolyte volume is shown in (7-67)

$$EV_{ER} = KV_{NER} \cdot EV_N \tag{7-67}$$

where

EV_{ER} is the endoplasmic electrolyte volume

EV_N is the average nucleus electrolyte volume or nucleoplasm

KV_{NER} is the Nuclear to ER volume ratio multiplier ~ 2.5 [9]

The average ER membrane area is given by equation (7-68).

$$A_{ERom} = KA_{NER} \cdot A_{Nim} \tag{7-68}$$

where

A_{ERom} is the ER outer membrane surface area

A_{Nim} is the nuclear inner membrane surface area

KA_{NER} is the nuclear to ER membrane area multiplier ~ 150 [9]

The nuclear membrane volume calculation is shown in equation (7-69)

$$V_{Nm} = \frac{4}{3} \cdot \pi \cdot r_{Nim}{}^{3} - EV_N \qquad (7\text{-}69)$$

where

V_{Nm} is the nuclear membrane volume

r_{Nim} is the outside radius to the inner nuclear membrane

The ER membrane volume calculation is shown in (7-70). It follows that the lipid membrane volume for the ER will be proportional to the area of the nuclear membrane times the nuclear to ER membrane area multiplier

$$V_{ERm} = KA_{NER} \cdot V_{Nm} \qquad (7\text{-}70)$$

where

V_{ERm} is the endoplasmic reticulum outer lipid membrane volume

V_{Nm} is the volume of the nuclear membrane

KA_{NER} is the nuclear to ER membrane area multiplier ~ 150

The displacement volume for the nucleus and the ER is the sum of the electrolyte volumes and the lipid membrane volumes for both the nucleus and endoplasmic reticulum shown in equation (7-71)

$$DVo_{NER} = EV_N + EV_{ER} + V_{Nm} + V_{ERm} \qquad (7\text{-}71)$$

where

DVo_{NER} is the nuclear and endoplasmic reticulum displacement volume

EV_{ER} is the endoplasmic electrolyte volume

EV_N is the average nucleus electrolyte volume or nucleoplasm

V_{ERm} is the endoplasmic reticulum outer lipid membrane volume

V_{Nm} is the volume of the nuclear membrane

The passive electrical network structure of the combination of nucleus and ER is shown in Fig. 7-7 Nucleus and endoplasmic reticulum organelle level structure and network. Note how the nucleopore resistance is in parallel with the outer endoplasmic reticulum and inner nuclear membranes. That is because the nucleopore has direct access from the cell cytoplasm to the nucleoplasm by way of the nucleopores. Current conducting ions can take either a path through the ER membrane into the perinuclear space by way of the ER intra organelle fluid and through the nuclear membrane or through the nucleopore before conducting through the nucleoplasm. Of course current conduction can bypass the ER and nucleus and simply flow through the cytoplasm represented in Fig. 7-7 as a resistor in light gray since it is actually a cell level model component and not an organelle model level component.

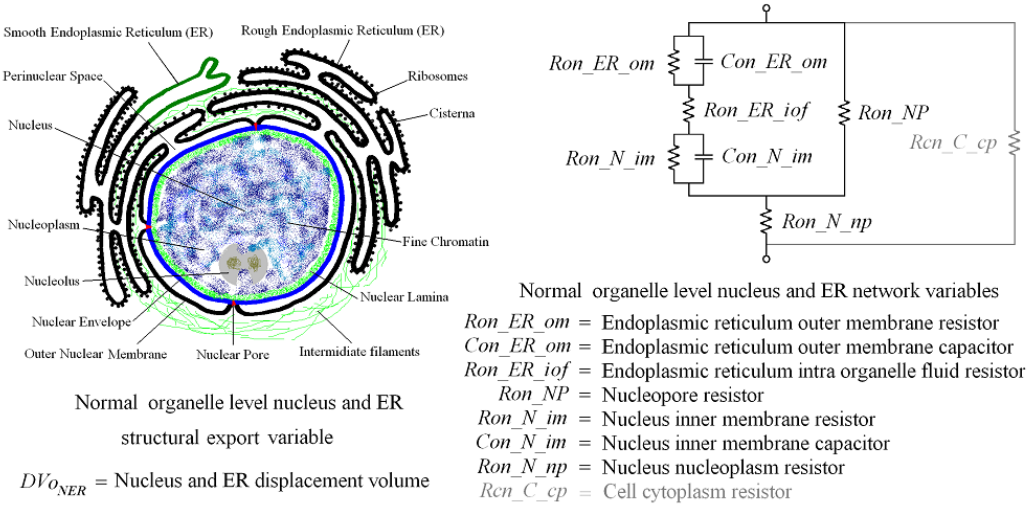

Fig. 7-7 Nucleus & endoplasmic reticulum organelle level structure and network

The calculation for the normal cell organelle level endoplasmic reticulum outer membrane resistor is inversely proportional to the membrane area and is given by (7-72)

$$Ron\_ER\_om = \frac{MR_{ERom}}{A_{ERom}} \tag{7-72}$$

where

Ron_ER_om is the outer membrane resistance of ER organelle

A_{ERom} is the ER outer membrane surface area

MR_{ERom} is the resistance per cm^2 of the ER's outer membrane

The capacitance of the endoplasmic reticulum membrane is proportional to its surface area and is given by (7-73)

$$Con\_ER\_om = A_{ERom} \cdot MC \tag{7-73}$$

where

Con_ER_om is the capacitor value for a normal ER membrane

A_{ER} is the surface area of the average ER membrane

MC is the capacitance per square centimeter of lipid membrane

The resistance of the endoplasmic reticulum inter-organelle fluid within the perinuclear space can be calculated with equation (7-74)

$$Ron\_ER\_iof = \frac{\rho_{ER}}{EV_{ER}^{\frac{1}{3}}} \tag{7-74}$$

where

Ron_ER_iof is the normal cell inter organelle resistance of the ER organelle

EV_{ER} is the endoplasmic reticulum electrolyte volume

ρ_{ER} is the resistivity of the endoplasmic reticulum electrolyte

The calculation for the normal cell organelle level nuclear inner membrane resistor is inversely proportional to the inner membrane area and is given by (7-75)

$$Ron\_N\_om = \frac{MR_{Nim}}{A_{Nim}} \tag{7-75}$$

where

Ron_N_im is the normal cell organelle level resistance of the nuclear inner membrane

A_{ERom} is the nucleus inner membrane surface area

MR_{Nim} is the resistance per cm^2 of the nucleus's inner membrane

The capacitance of the nuclear inner membrane is proportional to its surface area and is given by equation (7-76)

$$Con\_N\_im = A_{Nim} \cdot MC \tag{7-76}$$

where

Con_N_im is the capacitor value for a normal nuclear membrane

A_{Nim} is the surface area of the inner nuclear membrane

MC is the capacitance per square centimeter of lipid membrane

The resistance of the nucleoplasm or inter-organelle fluid within the nuclear space can be calculated with equation (7-77)

$$Ron\_N\_np = \frac{\rho_N}{EV_N^{\frac{1}{3}}} \qquad (7\text{-}77)$$

where

Ron_N_np is the normal cell nucleoplasm resistance

EV_N is the nuclear electrolyte volume

ρ_N is the resistivity of the nuclear electrolyte

The resistance of the nucleopore is proportional to the pore density and the area of the nuclear membrane and is given by equation (7-78).

$$Ron\_NP = G_{pore} \cdot npd \cdot A_{Nim} \qquad (7\text{-}78)$$

where

Ron_NP is the organelle level resistance of the nuclear pores in a normal cell

G_{pore} is the conductance of a single nuclear pore complex or nucleopore

npd is the nuclear pore density

G. The Organelle Level Model Development Review

The organelle level model is the first level of model to be developed in the multi level "Transparent Box" tissue model. In this section the membrane bound organelle networks were developed for use as sub components in the cell level model. The organelle models also include the displacement value for an individual organelle to be

exported to the cell level model for the calculation of cell cytoplasm volume. The modular level design of the “Transparent Box” tissue model makes it ideal for implementation in a spreadsheet program. Each cell type in a tissue can have separate organelle level worksheets to give different cells in different layers properties unique to that individual cell layer. Next section details the development of the next higher layer in the “Transparent Box” tissue model, the cell level model.

VIII. CELL LEVEL MODEL DEVELOPMENT

A. Combining the Organelle Elements Together to Construct the Cell

The organelle level circuit network elements can be combined with a cells outer membrane and cytoplasm network to create a complete geometrically based passive circuit element network that will provide the most realistic impedance response for the comparison of healthy and diseased tissues. The cell level model is constructed using the same guidelines as the organelles. The organelle networks are all electrically in parallel with each other and in series with the outer cell membrane network, together they are all parallel to the extracellular fluid resistance. This is shown in Fig. 8-1 the whole cell passive element "Transparent Box" model circuit topology. The values for the individual electrical elements representing the organelles in the cell level model depend on the number of organelles of each type in the cell being modeled.

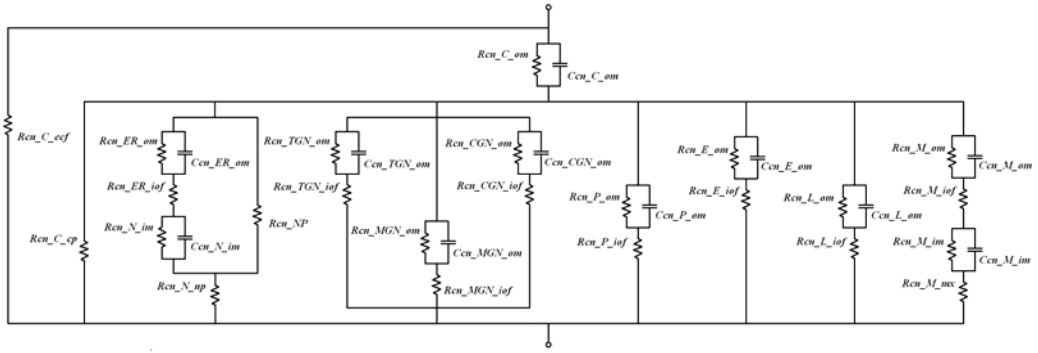

Fig. 8-1 The whole cell passive element "Transparent Box" model circuit topology

The value of each electrical element representing the nucleus and the endoplasmic reticulum in a normal healthy cell is equal to the value at the organelle level since the number of nuclei and ER is only one. Cancer cells may have multiple nuclei and ER's therefore the equation for calculating the cell level values will be shown. Each additional organelle included in the cell model will be in parallel. Recall from network theory

capacitances in parallel simply add. The general formula for parallel capacitances is given in equation (8-1)

$$C_{par} = C_1 + C_2 + C_3 + ...C_{np};\ \text{since}\ C_1 = C_2 = C_3 = C_{np}\ \text{then}\ C_{par} = C_1 \cdot np \qquad (8\text{-}1)$$

where

C_{par} is the parallel equivalent capacitance

C_1 is a capacitor element

np is the number of capacitor elements in parallel

The general formula for resistors in parallel is R_1 divided by the number of elements in parallel (np) as seen in (8-2)

$$\frac{1}{R_{par}} = \frac{1}{R_1} + \frac{1}{R_2} + \frac{1}{R_3} + ...\frac{1}{R_{np}};\ \text{since}\ R_1 = R_2 = R_3 = R_{np}\ \text{then}\ R_{par} = \frac{R_1}{np} \qquad (8\text{-}2)$$

where

R_{par} is the parallel equivalent resistor value

R_1 is a resistor element in parallel

np is the number of resistor elements in parallel

So it follows the cell level resistor value for the endoplasmic reticulum outer membrane can be calculated by (8-3)

$$Rcn\_ER\_om = \frac{Ron\_ER\_om}{ER_{num}} \qquad (8\text{-}3)$$

where

Rcn_ER_om is the cell level outer membrane resistor for the ER in a normal cell

Ron_ER_om is the organelle level outer membrane resistor for a single ER in a normal cell

ER_{num} is the number of ER organelles in the cell level model

It also follows from equation (8-1) that the cell level outer membrane capacitor for the endoplasmic reticulum can be calculated using (8-4)

$$Ccn\_ER\_om = Con\_ER\_om \cdot ER_{num} \tag{8-4}$$

where

Ccn_ER_om is the cell level outer membrane resistor for the ER in a normal cell

Con_ER_om is the organelle level outer membrane resistor for a single ER in a normal cell

ER_{num} is the number of ER organelles in the cell level model

The cell level resistor value for the endoplasmic reticulum inter organelle fluid can be calculated by using equation (8-5)

$$Rcn\_ER\_iof = \frac{Ron\_ER\_iof}{ER_{num}} \tag{8-5}$$

where

Rcn_ER_iof is the cell level inter organelle fluid resistor for the ER in a normal cell

Ron_ER_iof is the organelle level inter organelle fluid resistor for a single ER in a normal cell

ER_{num} is the number of ER organelles in the cell level model

The cell level resistor value for the nucleus inner membrane can be calculated by (8-6)

$$Rcn\_N\_im = \frac{Ron\_N\_im}{N_{num}} \tag{8-6}$$

where

Rcn_ER_im is the cell level inner membrane resistor for the nucleus in a normal cell

Ron_ER_im is the organelle inner membrane resistor for a single nucleus in a normal cell

N_{num} is the number of nucleus organelles in the cell level model

The cell level inner membrane capacitor for the nucleus can be calculated by (8-7)

$$Ccn\_N\_im = Con\_N\_im \cdot N_{num} \tag{8-7}$$

where

Ccn_N_im is the cell level outer membrane capacitor for the nucleus in a normal cell

Con_N_im is the organelle level outer membrane capacitor for one nucleus in a normal cell

N_{num} is the number of nucleus organelles in the cell level model normally one

The cell level resistor value for the nucleoplasm can be calculated by (8-8)

$$Rcn\_N\_np = \frac{Ron\_N\_np}{N_{num}} \tag{8-8}$$

where

Rcn_N_np is the cell level nucleoplasm resistor for normal cell

Ron_N_np is the organelle level inter nucleoplasm resistor for a single normal cell

N_{num} is the number of nucleus organelles in the cell level model, normally one

The cell level resistor value for the nuclear pore resistor can be calculated by (8-9).

$$Rcn\_NP = \frac{Ron\_NP}{N_{num}} \tag{8-9}$$

where

Rcn_NP is the cell level nuclear pore resistor for normal cell

Ron_N_np is the organelle level nuclear pore resistor for a single normal cell

N_{num} is the number of nucleus organelles in the cell level model, normally one

The displacement volume of the nucleus and ER must be calculated to adjust the value of the cell cytoplasm resistance. The displacement volume calculation is shown in (8-10)

$$DVc_{NER} = DVo_{NER} \cdot N_{num} \tag{8-10}$$

where

DVc_{NER} is the nuclear and ER total displacement volume at cell level

DVo_{NER} is the nuclear and ER single organelle displacement volume

N_{num} is the number of nucleus organelles in the cell level model, normally one

The cell level resistor value for the trans Golgi network outer membrane can be calculated by using equation (8-11)

$$Rcn\_TGN\_om = \frac{Ron\_TGN\_om}{G_{num}} \tag{8-11}$$

where

Rcn_TGN_om is the cell level outer membrane resistor for the TGN in a normal cell

Ron_TGN_om is the organelle level outer membrane resistor for a TGN in a normal cell

G_{num} is the number of Golgi organelles in the cell level model

The cell level outer membrane capacitor for the trans Golgi network can be calculated by equation (8-12)

$$Ccn\_TGN\_om = Con\_TGN\_om \cdot G_{num} \tag{8-12}$$

where

Ccn_TGN_om is the cell level outer membrane capacitor for the TGN in a normal cell

Con_TGN_om is the organelle level outer membrane capacitor for a single TGN in a normal cell

G_{num} is the number of Golgi organelles in the cell level model

The cell level resistor value for the trans Golgi network inter organelle fluid can be calculated by equation (8-13)

$$Rcn\_TGN\_iof = \frac{Ron\_TGN\_iof}{G_{num}} \tag{8-13}$$

where

Rcn_TGN_iof is the cell level inter organelle fluid resistor for the TGN in a normal cell

Ron_TGN_iof is the organelle level inter organelle fluid resistor for a TGN in a normal cell

G_{num} is the number of Golgi organelles in the cell level model

The displacement volume of the trans Golgi network must be calculated to adjust the value of the cell cytoplasm resistance. The displacement volume calculation is shown in (8-14)

$$DVc_{TGN} = DVo_{TGN} \cdot G_{num} \tag{8-14}$$

where

DVc_{TGN} is the total displacement volume of all TGN at cell level

DVo_{TGN} is the TGN single organelle displacement volume

G_{num} is the number of Golgi organelles in the cell level model

The cell level resistor value for the medial Golgi network outer membrane can be calculated by using equation (8-15)

$$Rcn\_MGN\_om = \frac{Ron\_MGN\_om}{G_{num}} \tag{8-15}$$

where

Rcn_MGN_om is the cell level outer membrane resistor for the MGN in a normal cell

Ron_MGN_om is the organelle outer membrane resistor for a single MGN in a normal cell

G_{num} is the number of Golgi organelles in the cell level model

The cell level inner membrane capacitor for the medial Golgi network can be calculated by equation (8-16)

$$Ccn\_MGN\_om = Con\_MGN\_om \cdot G_{num} \tag{8-16}$$

where

Ccn_MGN_om is the cell level outer membrane capacitor for the MGN in a normal cell

Con_MGN_om is the organelle level outer membrane capacitor for one MGN in a normal cell

G_{num} is the number of Golgi organelles in the cell level model

The cell level resistor value for the inter organelle fluid for all the medial Golgi networks in the cell can be calculated by (8-17)

$$Rcn\_MGN\_iof = \frac{Ron\_MGN\_iof}{G_{num}} \tag{8-17}$$

where

Rcn_MGN_iof	is the cell level inter organelle fluid resistor for all MGN in a normal cell
Ron_MGN_iof	is the organelle level inter organelle fluid resistor for one MGN in a normal cell
G_{num}	is the number of Golgi organelles in the cell level model

The displacement volume of the medial Golgi networks used to adjust the value of the cell cytoplasm resistance is shown in equation (8-18)

$$DVc_{MGN} = DVo_{MGN} \cdot G_{num} \tag{8-18}$$

where

DVc_{MGN}	is the total displacement volume of all medial Golgi networks at cell level
DVo_{MGN}	is the medial Golgi networks single organelle displacement volume
G_{num}	is the number of Golgi organelles in the cell level model

The cell level resistor value for the cis Golgi network outer membrane can be calculated by using equation (8-19)

$$Rcn\_CGN\_om = \frac{Ron\_CGN\_om}{G_{num}} \tag{8-19}$$

where

Rcn_CGN_om is the cell level outer membrane resistor for the CGN in a normal cell

Ron_CGN_om is the organelle outer membrane resistor for a single CGN in a normal cell

G_{num} is the number of Golgi organelles in the cell level model

The cell level outer membrane capacitor for the cis Golgi network can be calculated by equation (8-20)

$$Ccn\_CGN\_om = Con\_CGN\_om \cdot G_{num} \tag{8-20}$$

where

Ccn_CGN_om is the cell level outer membrane capacitor for the CGN in a normal cell

Con_CGN_om is the organelle level outer membrane capacitor for one CGN in a normal cell

G_{num} is the number of Golgi organelles in the cell level model

The cell level resistor value for the inter organelle fluid for all the medial Golgi networks in the cell can be calculated by equation (8-21)

$$Rcn\_CGN\_iof = \frac{Ron\_CGN\_iof}{G_{num}} \tag{8-21}$$

where

Rcn_CGN_iof is the cell level inter organelle fluid resistor for all CGN in a normal cell

Ron_CGN_iof is the organelle level inter organelle fluid resistor for one CGN in a normal cell

G_{num} is the number of Golgi organelles in the cell level model

The displacement volume of the cis Golgi networks used to adjust the value of the cell cytoplasm resistance is shown in equation (8-22)

$$DVc_{CGN} = DVo_{CGN} \cdot G_{num} \tag{8-22}$$

where

DVc_{CGN} is the total displacement volume of all cis Golgi networks at cell level

DVo_{CGN} is the cis Golgi networks single organelle displacement volume

G_{num} is the number of Golgi organelles in the cell level model

The cell level resistor value for the peroxisome outer membrane can be calculated by (8-23)

$$Rcn\_P\_om = \frac{Ron\_P\_om}{P_{num}} \tag{8-23}$$

where

Rcn_P_om is the cell level outer membrane resistor for the peroxisome in a normal cell

Ron_P_om is the organelle outer membrane resistor for a single peroxisome in a normal cell

P_{num} is the number of peroxisome organelles in the cell level model

The cell level outer membrane capacitor for the peroxisome can be calculated by equation (8-24)

$$Ccn\_P\_om = Con\_P\_om \cdot P_{num} \tag{8-24}$$

where

Ccn_P_om is the cell level outer membrane capacitor for all peroxisomes in a normal cell

Con_P_om is the organelle level outer membrane capacitor for one peroxisome

P_{num} is the number of peroxisome organelles in the cell level model

The cell level resistor value for the inter organelle fluid for all of the peroxisome in a cell can be calculated by equation (8-25)

$$Rcn\_P\_iof = \frac{Ron\_P\_iof}{P_{num}} \tag{8-25}$$

where

Rcn_P_iof is the cell level inter organelle fluid resistor for all peroxisomes in a normal cell

Ron_P_iof is the organelle level inter organelle fluid resistor of a single peroxisome

P_{num} is the number of peroxisome organelles in the cell level model

The displacement volume of all the peroxisomes in the cell is shown in equation (8-26). It is used to adjust the value of the cell cytoplasm resistance.

$$DVc_P = DVo_P \cdot P_{num} \tag{8-26}$$

where

DVc_P is the total displacement volume of all the peroxisomes at the cell level

DVo_P is the peroxisome displacement volume for a single organelle

P_{num} is the number of peroxisome organelles in the cell level model

The cell level resistor value for the endosome outer membrane can be calculated by (8-27)

$$Rcn\_E\_om = \frac{Ron\_E\_om}{E_{num}} \tag{8-27}$$

where

Rcn_E_om is the cell level outer membrane resistor for the endosome in a normal cell

Ron_E_om is the organelle outer membrane resistor for a single endosome in a normal cell

E_{num} is the number of endosome organelles in the cell level model

The cell level outer membrane capacitor for the endosome can be calculated by equation (8-28)

$$Ccn\_E\_om = Con\_E\_om \cdot E_{num} \tag{8-28}$$

where

Ccn_E_om is the cell level outer membrane capacitor for all endosome in a normal cell

Con_E_om is the organelle level outer membrane capacitor for one endosome

E_{num} is the number of endosome organelles in the cell level model

The cell level resistor value for the inter organelle fluid for all of the endosome in a cell can be calculated by equation (8-29)

$$Rcn\_E\_iof = \frac{Ron\_E\_iof}{E_{num}} \tag{8-29}$$

where

Rcn_E_iof is the cell level inter organelle fluid resistor for all endosome in a normal cell

Ron_E_iof is the organelle level inter organelle fluid resistor of a single endosome

E_{num} is the number of endosome organelles in the cell level model

The displacement volume of all the endosome in the cell is shown in equation (8-30). It is used to adjust the value of the cell cytoplasm resistance.

$$DVc_E = DVo_E \cdot E_{num} \tag{8-30}$$

where

DVc_E is the total displacement volume of all the endosome at the cell level

DVo_E is the endosome displacement volume for a single organelle

E_{num} is the number of endosome organelles in the cell level model

The cell level resistor value for the lysosome outer membrane can be calculated by (8-31)

$$Rcn\_L\_om = \frac{Ron\_L\_om}{L_{num}} \tag{8-31}$$

where

Rcn_L_om is the cell level outer membrane resistor for the lysosome in a normal cell

Ron_L_om is the organelle outer membrane resistor for a single lysosome in a normal cell

L_{num} is the number of lysosome organelles in the cell level model

The cell level outer membrane capacitor for the lysosome can be calculated by (8-32)

$$Ccn\_L\_om = Con\_L\_om \cdot L_{num} \tag{8-32}$$

where

Ccn_L_om is the cell level outer membrane capacitor for all lysosome in a normal cell

Con_L_om is the organelle level outer membrane capacitor for one lysosome

L_{num} is the number of lysosome organelles in the cell level model

The cell level resistor value for the inter organelle fluid for all of the lysosome in a cell can be calculated by (8-33)

$$Rcn\_L\_iof = \frac{Ron\_L\_iof}{L_{num}} \tag{8-33}$$

where

Rcn_L_iof is the cell level inter organelle fluid resistor for all lysosome in a normal cell

Ron_L_iof is the organelle level inter organelle fluid resistor of a single lysosome

L_{num} is the number of lysosome organelles in the cell level model

The displacement volume of all the lysosome in the cell is shown in equation (8-34). It is used to adjust the value of the cell cytoplasm resistance.

$$DVc_L = DVo_L \cdot L_{num} \tag{8-34}$$

where

DVc_L is the total displacement volume of all the lysosome at the cell level

DVo_L is the lysosome displacement volume for a single organelle

L_{num} is the number of lysosome organelles in the cell level model

The cell level resistor value for the mitochondria outer membrane can be calculated by equation (8-35)

$$Rcn\_M\_om = \frac{Ron\_M\_om}{M_{num}} \tag{8-35}$$

where

Rcn_M_om is the cell level outer membrane resistor for the mitochondria in a normal cell

Ron_M_om is the organelle outer membrane resistor for a mitochondrion in a normal cell

M_{num} is the number of mitochondria organelles in the cell level model

The cell level outer membrane capacitor for the mitochondria can be calculated by equation (8-36)

$$Ccn\_M\_om = Con\_M\_om \cdot M_{num} \tag{8-36}$$

where

Ccn_M_om is the cell level outer membrane capacitor for all mitochondria in a normal cell

Con_M_om is the organelle level outer membrane capacitor for one mitochondrion

M_{num} is the number of mitochondria organelles in the cell level model

The cell level resistor value for the inter organelle fluid for all of the mitochondria in a cell can be calculated by equation (8-37)

$$Rcn\_M\_iof = \frac{Ron\_M\_iof}{M_{num}} \tag{8-37}$$

where

Rcn_M_iof is the cell level inter organelle fluid resistor for all mitochondria in a normal cell

Ron_M_iof is the organelle level inter organelle fluid resistor of a single mitochondrion

M_{num} is the number of mitochondria organelles in the cell level model

The cell level resistor value for the mitochondria inner membrane can be calculated by equation (8-38)

$$Rcn\_M\_im = \frac{Ron\_M\_im}{M_{num}} \tag{8-38}$$

where

Rcn_M_im is the cell level inner membrane resistor for the mitochondria in a normal cell

Ron_M_im is the organelle inner membrane resistor for a mitochondrion in a normal cell

M_{num} is the number of mitochondria organelles in the cell level model

The cell level inner membrane capacitor for the mitochondria can be calculated by (8-39)

$$Ccn\_M\_im = Con\_M\_im \cdot M_{num} \tag{8-39}$$

where

Ccn_M_im is the cell level inner membrane capacitor for all mitochondria in a normal cell

Con_M_im is the organelle level inner membrane capacitor for one mitochondrion

M_{num} is the number of mitochondria organelles in the cell level model

The cell level resistor value for the matrix fluid for all of the mitochondria in a cell can be calculated by equation (8-40)

$$Rcn\_M\_mx = \frac{Ron\_M\_mx}{M_{num}} \tag{8-40}$$

where

Rcn_M_mx is the cell level matrix fluid resistor for all mitochondria in a normal cell

Ron_M_mx is the organelle level matrix fluid resistor of a single mitochondrion

M_{num} is the number of mitochondria organelles in the cell level model

The displacement volume of all the mitochondria in the cell is shown in equation (8-41). It is used to adjust the value of the cell cytoplasm resistance.

$$DVc_M = DVo_M \cdot M_{num} \tag{8-41}$$

where

DVc_M is the total displacement volume of all the mitochondria at the cell level

DVo_M is the displacement volume for a mitochondrion organelle

M_{num} is the number of mitochondria organelles in the cell level model

B. Construct the Cell Geometry Plasma Membrane

The cell outer plasma membrane can be modeled as a sphere (suitable for cell suspensions of yeast and other roughly spherical cells) but a cube or a trapezoidal polygon is more appropriate for cells of the oral mucosa. A tissue can be modeled with various shapes and sizes of cells depending on the layer within the tissue. So a general cell model treating the cell shape as a polygon with height, width and depth geometry independent of each other will allow for a more flexible cell model than a fixed cube would. There is a requirement that the shapes fit together perfectly in a single layer without voids described as a geometric tessellation. Fig 8-2 Geometric shapes for the outer cell membrane model shows how the various shapes can tessellate in each cell layer.

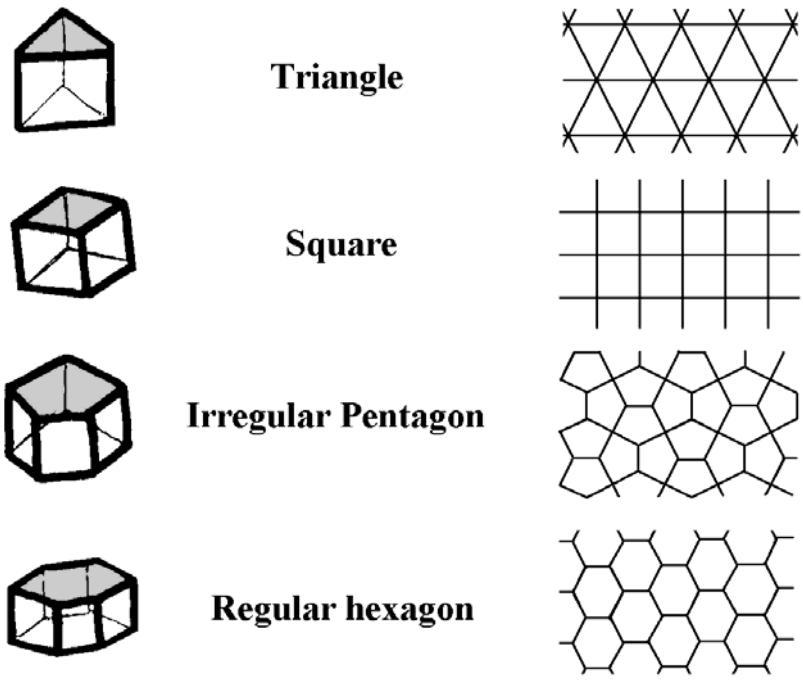

Fig. 8-2 Geometric shapes for the outer cell membrane model

The choice for a certain cell shape model is based on closest mach to the cross section of cells and tissues being modeled. There are two suitable shapes that will tessellate and can be used to approximate healthy epithelial cells they are the irregular pentagon or the regular hexagon. The cross section shape that more closely approximates epithelial cancer cells is either the square or the irregular pentagon. The irregular pentagon is the most flexible choice it can represent both the healthy and diseased cells. The irregular pentagon can approximate the three main cell types found in the epithelial tissue by simply changing the dimensions of the sides and height for each type as shown in Fig. 8-3 Irregular pentagon cell shapes.

To calculate the membrane resistance and capacitance the membrane surface area must be found. To calculate the exracellular fluid resistance the extracellular fluid volume around the cell perimeter must be found. To calculate the cytoplamic resistance the volume of the cell electrolyte must be calculated. All of these elements are geometrically dependent. The formulas used to calculate them are based on the tessellating geometric figure of choice in this case the irregular pentagon.

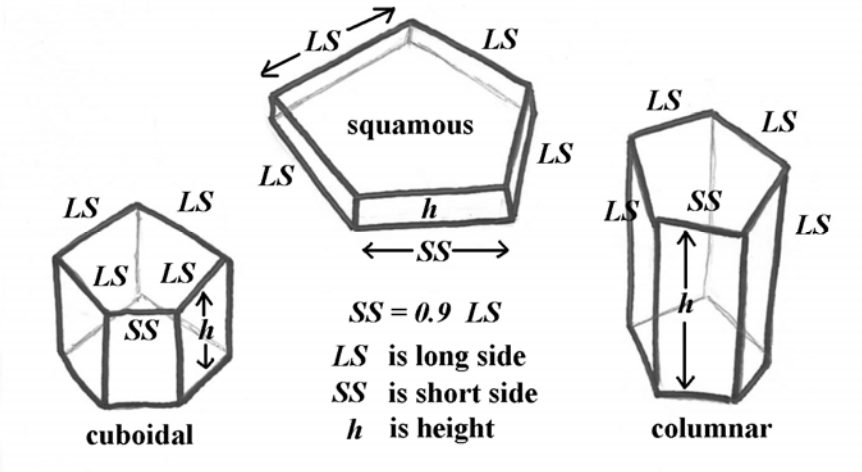

Fig. 8-3 Irregular pentagon cell shapes

The total surface area of the cell includes the surface areas of the five side faces and surface area of the top and bottom of the irregular pentagon. The volume is the cross section of the irregular pentagon multiplied by the height. To calculate the surface area of the irregular pentagon it is convenient to split it up into four right triangles and solve for the area of each triangle, Fig. 8-4 Irregular pentagon geometry illustrates this split. The sum of the triangle surface areas then gives the surface area of the irregular pentagon.

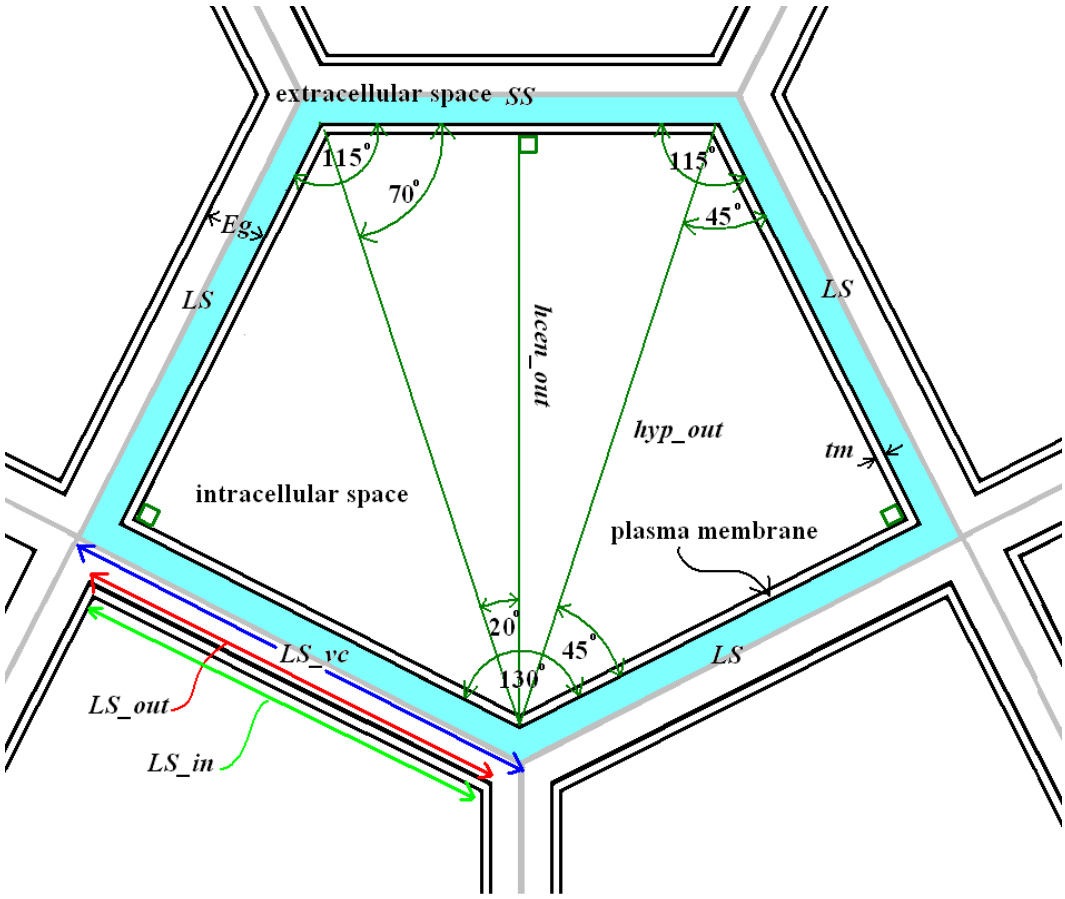

Fig. 8-4 Irregular pentagon geometry

Notice there are actually three irregular pentagons stacked one within each other. The outermost pentagon dimension in gray represents the cell diameter including the extracellular fluid. The outermost pentagon dimensions are used to calculate the

displacement volume of a cell and the extracellular fluid for calculating the number of cells in a volume of tissue. The next smaller pentagon is the outer cell dimension. It includes the outer membrane and it is used to calculate the cell membrane surface area. The innermost pentagon is used to calculate the cell cytoplasm volume. These three irregular pentagons share the same angles and proportion. An illustration of how to calculate one is an illustration of how to calculate them all. Simple plane geometry and the equation of the area of a triangle (one half base times height) is all that is required. Using the irregular pentagon in Fig 8-4 the surface area of one face of the outer membrane is calculated using the appropriate outer dimensions. First calculate the surface area of the two larger right triangles, shown in equation (8-42) and then sum with the area of the two smaller right triangles to get the total area of one face of the irregular pentagon.

$$SA_{LRT} = LS\_out^2 \tag{8-42}$$

where

SA_{LRT} is the surface area of the two outer large right triangles

LS_out is the long side outer dimension of the irregular pentagon

To calculate the smaller right triangles the height of the center *hcent_out* needs to be calculated and is given by (8-43)

$$hcent\_out = hyp\_out \cdot \cos(20°) = \sqrt{2} \cdot Ls\_out \cdot \cos(20°) \tag{8-43}$$

where

hcent_out is the center height of the smaller triangles

hyp_out is the hypotenuse of the triangles within the outer irregular pentagon

LS_out is the long side outer dimension of the irregular pentagon

The Surface area of the two smaller triangles is calculated by equation (8-44)

$$SA_{SRT} = \frac{9 \cdot \sqrt{2}}{10} LS\_out^2 \cdot \cos(20°) \quad (8\text{-}44)$$

where

SA_{SRT} is the surface area of the two outer smaller right triangles

LS_out is the long side outer dimension of the irregular pentagon

The sum of these areas of the component triangles provides the total area of one face of the irregular pentagon given in equation (8-45)

$$SA\_out\_face_{IP} = SA_{LRT} + SA_{SRT} = LS\_out^2 \cdot (1 + \frac{9 \cdot \sqrt{2}}{10} \cdot \cos(20°)) \quad (8\text{-}45)$$

where

$SA\_out\_face_{IP}$ is the surface area of one face of the irregular pentagon

SA_{LRT} is the surface area of the two outer large right triangles

SA_{SRT} is the surface area of the two outer smaller right triangles

LS_out is the long side outer dimension of the irregular pentagon

The cell outer membrane surface area is made up of the five rectangular sides and the top and bottom irregular pentagon surfaces it is given by equation (8-46)

$$A_{ipc} = 2 \cdot (LS\_out^2 \cdot (1 + \frac{9 \cdot \sqrt{2}}{10} \cdot \cos(20°))) + \frac{49}{10} \cdot LS\_out \cdot h\_cell \quad (8\text{-}46)$$

where

A_{ipc} is the surface area of one irregular pentagon cylinder cell

LS_out is the long side outer dimension of the irregular pentagon

h_cell is the height of the irregular pentagon cylinder

The interior cell volume is the volume inside the irregular pentagonal cylinder with dimensions reduced by the membrane thickness. The long side dimension for the interior of the irregular pentagon is given by equation (8-47)

$$LS\_in = LS\_out - 2 \cdot tm \quad (8\text{-}47)$$

where

LS_in is the long side inner dimension of the irregular pentagon

LS_out is the long side outer dimension of the irregular pentagon

tm is the plasma membrane thickness ~ 5nm

The interior volume is calculated with equation (8-48).

$$CIV = LS\_in^2 \cdot (1 + \frac{9 \cdot \sqrt{2}}{10} \cdot \cos(20°)) \cdot (h\_cell - 2 \cdot tm) \quad (8\text{-}48)$$

where

CIV is the cell interior volume

LS_in is the long side inner dimension of the irregular pentagon

H_cell is the height of the irregular pentagon cylinder

The displacement volume of the irregular pentagonal cylinder or virtual cell displacement volume includes the cell volume and extra cellular fluid volume. The dimension long side virtual cell (*LS_vc*) is used to calculate the virtual cell displacement volume it is calculated using equation (8-49)

$$LS\_vc = LS\_out + Eg \tag{8-49}$$

where

LS_vc is the long side dimension of the irregular pentagon which includes the extracellular fluid

LS_out is the long side outer dimension of the irregular pentagon

Eg is the extracellular fluid gap between adjacent cells ~15 to 50nm

The displacement volume of the virtual cell is given in equation (8-50)

$$DV\_vc = LS\_vc^2 \cdot (1 + \frac{9 \cdot \sqrt{2}}{10} \cdot \cos(20°)) \cdot (h\_cell + Eg) \tag{8-50}$$

where

DV_vc is the displacement volume of the virtual cell (includes the extracellular fluid volume)

LS_vc is the long side dimension of the irregular pentagon plus extracellular fluid

h_cell is the height of the irregular pentagon cylinder

Eg is the extracellular fluid gap between adjacent cells ~15 to 50nm

The displacement volume of the cell is given in equation (8-51)

$$DV\_c = LS\_out^2 \cdot (1 + \frac{9 \cdot \sqrt{2}}{10} \cdot \cos(20°)) \cdot h\_cell \qquad (8\text{-}51)$$

where

DV_c is the displacement volume of cell

LS_out is the long side outer dimension of the irregular pentagon

h_cell is the height of the irregular pentagon cylinder

The extracellular fluid volume is calculated by subtracting the cell volume from the virtual cell volume it is given by equation (8-52)

$$EV\_ef = (DV\_vc - DV\_c) - PECV(DV\_vc - DV\_c) \qquad (8\text{-}52)$$

where

EV_ef is the electrolyte volume of the extracellular fluid surrounding the cell

DV_c is the displacement volume of cell

DV_vc is the displacement volume of the virtual cell (includes extracellular fluid volume)

PECV is the percent of extracellular cell protein volume

There is one more geometric parameter important in calculating the intracellular fluid volume or cytoplasm electrolyte volume. It is based on the expression of a protein within a cell; specifically the displacement volume of large proteins in the cell. This displacement volume is a function of the protein size and quantity expressed. This is based on the cell type, the level of cell differentiation and the health of the cells. An example is squamous epithelial cells at the surface of the skin, they produce ~22% more keratin protein than cuboidal epithelial cells in the middle layers [9]. This keratin protein will act as a tough protective abrasion resistant layer. It will also decrease the space available electrolyte making the outer layers relatively more resistive. There are various proteins that are expressed in the cell that are too small to matter, only larger proteins that are expressed in quantities greater than what is found normally in the stem cells or undifferentiated daughter cells of the tissue are considered in this model. The calculation for the protein displacement is approximated by equation (8-53) where the connective proteins of interest are keratin, elastin, myosin, actin and collagen.

$$DVc_{pro} = PCV \cdot CIV \tag{8-53}$$

where

DVc_{PRO} is the displacement volume of cell protein

PCV is the percentage of cell volume that is connective protein

CIV is the cell interior volume

The electrolyte volume of the cell cytoplasm is the total interior volume of the cell minus the displacement by the organelles and proteins. The equation for the displacement volume of all the membrane bound organelles is given by equation (8-54)

$$DVc_{TO} = DVc_M + DVc_L + DVc_E + DVc_P + DVc_{NER} + DVc_{CGN} + DVc_{CGN} + DVc_{TGN}$$

(8-54)

where

DVc_{TO} is the total displacement volume of all the membrane bound organelles

DVc_M is the total displacement volume of all the mitochondria at the cell level

DVc_L is the total displacement volume of all the lysosome at the cell level

DVc_E is the total displacement volume of all the endosome at the cell level

DVc_P is the total displacement volume of all the peroxisomes at the cell level

DVc_{NER} is the nuclear and ER total displacement volume at cell level

DVc_{CGN} is the total displacement volume of all cis Golgi networks at cell level

DVc_{MGN} is the total displacement volume of all medial Golgi networks at cell level

DVc_{TGN} is the total displacement volume of all TGN at cell level

The electrolyte volume of the cell cytoplasm is given by (8-55)

$$EVc = CIV - (DVc_{TO} + DVc_{PRO}) \qquad (8\text{-}55)$$

where

EVc is the volume of electrolyte in the cell

CIV is the cell interior volume

DVc_{TO} is the total displacement volume of all the membrane bound organelles

DVc_{PRO} is the displacement volume of cell proteins within the cell

The cell level electrical network model parameters can be calculated for a single cell with all the geometric displacement parameters from the organelles known and calculated. The calculation for finding the resistor value representing the conductive ions in the cytoplasm is given in equation (8-56)

$$Rcn\_C\_cp = \frac{\rho_{CP}}{EV_C^{\frac{1}{3}}} \tag{8-56}$$

where

Rcn_P_cp is the resistance of the cytoplasm of a normal cell

EV_C is the electrolyte interior volume of the average cell

ρ_{CP} is the resistivity of the cytoplasm

In general the resistance of the cells plasma membrane is inversely proportional to the membrane area and is given by equation (8-57)

$$Rcn\_C\_om = \frac{MR_{PM}}{A_{PM}} \tag{8-57}$$

where

Rcn_C_om is the outer membrane resistance of one cell

A_{PM} is the surface area of the average cell plasma membrane

MR_{PM} is the resistance per square centimeter of the plasma membrane

For this case the cell model is the irregular pentagon so the plasma membrane area A_{PM} is the area of the irregular pentagon A_{ipc} so equation (8-57) can be written as equation (7-58)

$$Rcn\_C\_om = \frac{MR_{PM}}{A_{ipc}} \tag{8-58}$$

where

Rcn_C_om is the outer membrane resistance of one cell

A_{ipc} is the surface area of the irregular pentagonal cylinder cell

MR_{PM} is the resistance per square centimeter of the plasma membrane

The general capacitance of the cell plasma membrane is proportional to its surface area and is given by equation (8-59)

$$Ccn\_C\_om = A_{PM} \cdot MC \tag{8-59}$$

where

Ccn_C_om is the capacitor value for one normal cell plasma membrane

A_{PM} is the surface area of the average cell plasma membrane

MC is the capacitance per square centimeter of lipid membrane

The capacitance of the irregular pentagonal cell plasma membrane is proportional to its surface area and is given by equation (8-60)

$$Ccn\_C\_om = A_{ipc} \cdot MC \tag{8-60}$$

where

Ccn_C_om is the capacitor value for one normal cell plasma membrane

A_{ipc} is the surface area of the irregular pentagonal cylinder cell

MC is the capacitance per square centimeter of lipid membrane

The calculation for the resistor value representing the conductive ions in the extracellular fluid of a single cell is shown in equation (8-61)

$$Rcn\_C\_ecf = \frac{\rho_{ef}}{EV\_ef^{\frac{1}{3}}} \tag{8-61}$$

where

Rcn_C_ecf is the resistance of the extracellular fluid around a normal cell

EV_ef is the extracellular fluid volume of a single average cell

ρ_{ef} is the resistivity of the extracellular fluid

The cell level model has geometric export parameters to the tissue level models just as the organelle level model has geometric export parameters to the cell level. These export parameters include the displacement volume of a single cell; the virtual cell height as well as the virtual length. The height and length are important for determining the electrode spacing and modeling the effective measurement depth of a particular probe spacing. The virtual equivalent length is the length of a side of a square with equivalent area to any arbitrary cells cross sectional shape in this case the irregular pentagon. And as its name implies (virtual) it includes the cell length and the associated extracellular fluid around the cell. The formula for calculating the export parameter of the displacement

volume of a single cell and its associated extra cellular fluid is provided in equation (8-62)

$$DV\_vc = (LS\_out + Eg)^2 \cdot (1 + \frac{9 \cdot \sqrt{2}}{10} \cdot \cos(20°)) \cdot (h\_cell + Eg) \quad (8\text{-}62)$$

where

DV_vc is the displacement volume of cell including associated extracellular fluid volume

LS_out is the long side outer dimension of the irregular pentagon

h_cell is the height of the irregular pentagon cylinder

Eg is the extracellular fluid gap between adjacent cells ~15 to 50nm

The equivalent length of a cube with the same cross sectional area as the cell is calculated in equation (8-63) as simply the square root of the area of the virtual cell cross section.

$$EL\_vc = \sqrt{(LS\_out + Eg)^2 \cdot (1 + \frac{9 \cdot \sqrt{2}}{10} \cdot \cos(20°))} \quad (8\text{-}63)$$

where

EL_vc is the equivalent length of the virtual cell

LS_out is the long side outer dimension of the irregular pentagon

Eg is the extracellular fluid gap between adjacent cells ~15 to 50nm

The virtual cell height is the height of the cell including the extracellular fluid gap shown in equation (8-64)

$$h\_vc = h\_cell + Eg \tag{8-64}$$

where

h_vc is the overall height of the virtual cell

h_cell is the height of the irregular pentagon cylinder cell

The list of variables that will get exported to the tissue model will include both electrical and geometric variables for the cell and can be seen Fig. 8-5 Cell level schematic with variables for export. The tissue layer and tissue schematics share the same topology, as the cell level schematic in Fig. 8-5 only the component values will change.

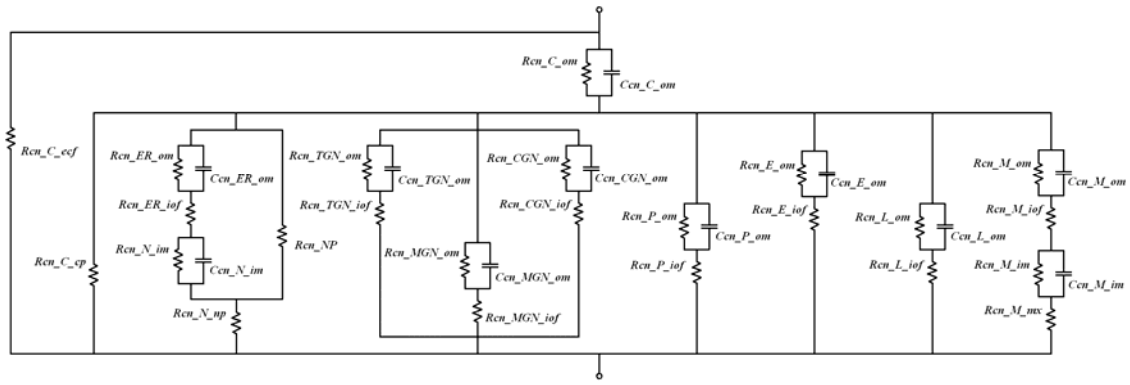

Normal Cell, cell level variables for export

Network element variables

Rcn_C_ecf	*Ccn_ER_om*	*Rcn_NP*	*Ccn_MGN_om*	*Rcn_P_om*	*Rcn_E_iof*	*Ccn_M_om*
Rcn_C_cp	*Rcn_ER_iof*	*Rcn_TGN_om*	*Rcn_MGN_iof*	*Ccn_P_om*	*Rcn_L_om*	*Rcn_M_iof*
Rcn_C_om	*Rcn_N_im*	*Ccn_TGN_om*	*Rcn_CGN_om*	*Rcn_P_iof*	*Ccn_L_om*	*Rcn_M_im*
Ccn_C_om	*Ccn_N_im*	*Rcn_TGN_iof*	*Ccn_CGN_om*	*Rcn_E_om*	*Rcn_L_iof*	*Ccn_M_im*
Rcn_ER_om	*Rcn_N_np*	*Rcn_MGN_om*	*Rcn_CGN_iof*	*Ccn_E_om*	*Rcn_M_om*	*Rcn_M_mx*

Geometric variables

DI_vc *EL_vc* *h_vc*

Fig. 8-5 Cell level schematic with variables for export

C. The Cell Level Model Development Review

To calculate the values for the cell level model it required the organelle level network elements be imported. The cell outer dimensions and shape had to be determined. The model is flexible and could be adapted for other tissues since the size and shape of the cell can be different from the irregular pentagonal cylinder. The total displacement volume of all entities within the cell had to be calculated. This displacement volume includes the membrane bound organelles and the structural proteins. Here again the cell level model can be calculated in a worksheet within a spreadsheet for each cell type in a tissue. Each tissue type can gave unique cell dimensions, protein content, organelle numbers and properties. The network element values can be exported to the tissue level model along with associated geometrical information like displacement volume and height. The next section will be the tissue layer model where the cells will be combined in series parallel networks of cells to combine into a tissue type.

IX. TISSUE LEVEL MODEL DEVELOPMENT

A. Introduction to the Tissue Model Construction

The tissue level model takes the cell level model and combines them into series parallel arrangements of length, width and depth; all dependent on the particular electrode spacing and arrangement. Naturally, a tissue sample will be larger for larger electrode spacing. With epithelial cell tissue there are at least three distinct layers of cell types each with different shapes and properties for each layer see Fig. 9-1 Condensed view of the epithelial cell tissue of the oral mucosa. The reason this drawing is the condensed view of epithelial tissue is that the number of cells in a layer of actual tissue may be 30 or 40 cells high and a drawing of that size would not allow for the easy observation of cell size changes. In order to make a more realistic model the tissue will need to be comprised from layers of cells of differing shape and properties to match each major layer of the tissue being modeled.

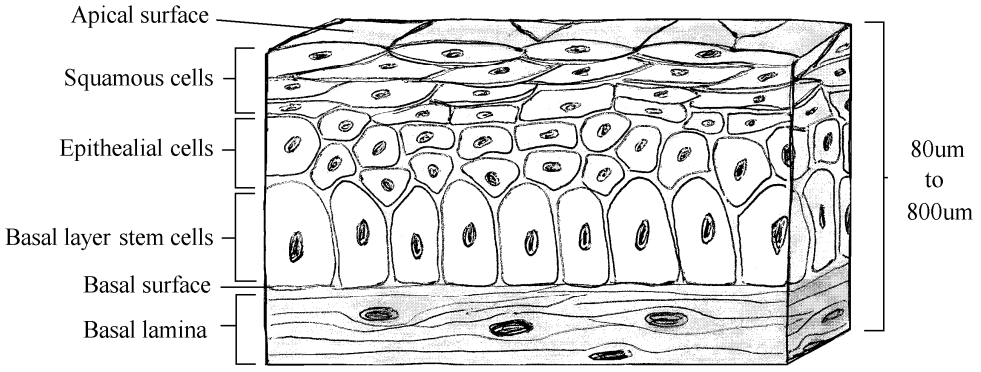

Fig. 9-1 Condensed view of the epithelial cell tissue of the oral mucosa

B. Cell Model Shapes for the Layers in the Tissue Model

The Basal layer stem cells are typically a single cell layer high. The stem cell shape is columnar and can be approximated using a tall irregular pentagonal cylinder. The next

layer is the epithelial cell layer they have a cuboidal shape. An irregular pentagon cylinder with approximate height equal to their width can approximate the cuboidal cells. The typical cuboidal epithelial cell layer has as height of approximately five to fifteen cells high depending on the tissue location [68 pp. 98-145]. Cells closer to the bottom of this epithelial layer slightly resemble the poorly differentiated stem and daughter cells and as the cells progress to the squamous layer they get slightly flatter and wider. The uppermost layer is the squamous epithelial cell layer these flat cells can still be approximated by the irregular pentagon with a height approximately one-tenth the side length. The squamous cell layer is about five to thirty cell heights tall [20], [68 p. 101].

C. Cell Model Properties for the Layers in the Tissue Model

Each individual cell carries with it the network that was developed in section VII the cell level model. The network values will be affected by the cell properties for the cells specific to that layer. For example the squamous cell layer will have cells with more connective proteins especially keratin. This will make it displace more electrolyte as compared to a cell from the basal stem cell layer. With all other parameters being equal (generally they are not, these cell types have different surface areas, volumes and other organelle differences) the reduced volume of conductive ions in the squamous due to protein volume will cause the cells to be relatively more resistive. It is generally not this simple to predict the effects of multiple changes between cell types, shapes and properties and this illustrates is why the model is required.

D. Tissue Level Model Diseased Cell Shapes and Properties

The diseased tissues often don’t have cells and cell layers with the same shape and size as healthy normal cells. The abnormal cells may have different numbers and sizes of organelles depending on the disease and the level of progression. The cells of cancer may be indistinguishable from layer to layer. All the cells may appear as undifferentiated stem

and daughter cells because cell division is not restricted to the basal layer. A tissue model for cancer may look like a single layer of cells of the same type so there might not be a reason to model multiple geometries and multiple layers making the model easier in this regard.

E. General Tissue Model with Multiple Cell Layer Construction

The general tissue model approximating tissue that has multiple distinct cell layers requires a cell level model network be calculated for each distinct cell type. For the normal healthy tissue this requires at least three network models, one for the columnar basal layer stem cells and daughter cells, one for the cuboidal epithelial cells and one for the squamous cells. The height of each layer in the tissue will determine the number of individual cells that fit vertically in each layer. The electrode geometry and spacing will determine the number of cells in the length and width dimensions for the layer. The number of cells in the vertical (height) and horizontal (width) determines the number of cell networks in parallel; the number of cells in length (with current flow) determines the number of cell networks in series. The basic individual cell topology will remain the same only the values representing the individual elements within the network will change. These series parallel calculations are done for each layer. The final tissue model is then the parallel combination of these networks. In general a tissue can have *n* layers of distinct cells; in this case one would have *n* parallel networks. The healthy normal tissue will have an n = 3 for illustration purposes the model can include a layer for the basal cells in this case n = 4. The parallel combination of these *n* network layers comprises the tissue model. This concept is illustrated with a simple square cross section cell shape instead of a more complex shape in Fig. 9-2 series parallel tissue layer construction. Each of the cubes (cells) in Fig. 9-2 represents the cell and the network for that cell. Each of the components within the cell network topology has the same component values from

cell to cell in the same layer. This makes the series parallel combination of multi cell networks shown in Fig. 9-3 cell network topology trivial to calculate.

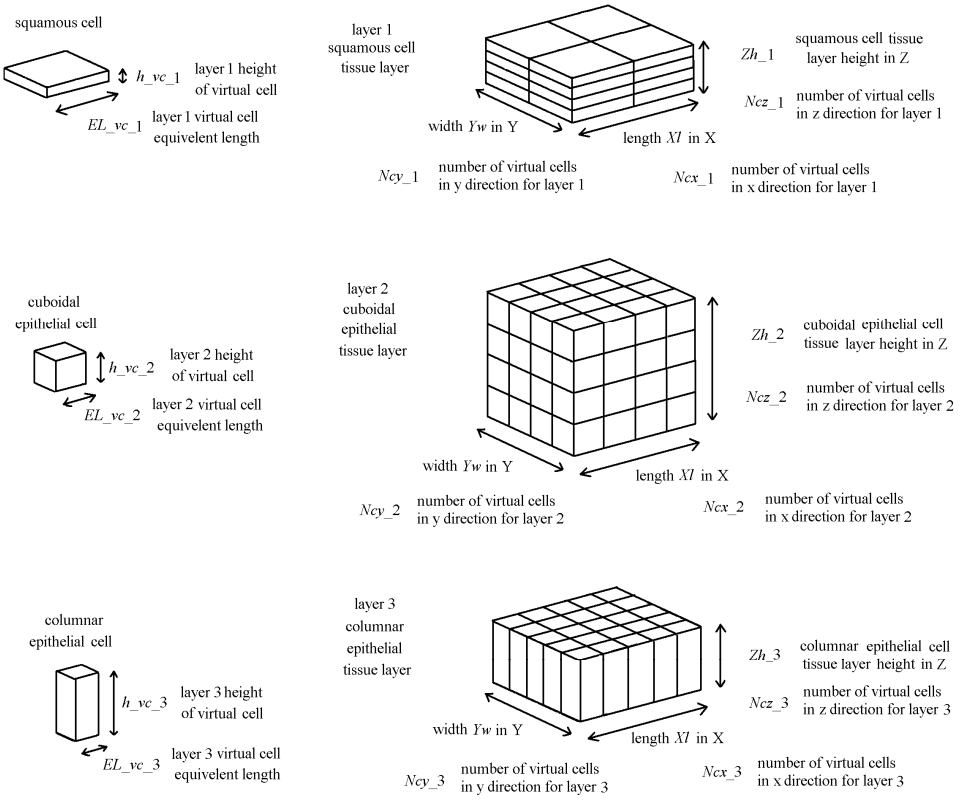

Fig. 9-2 Series parallel tissue layer construction

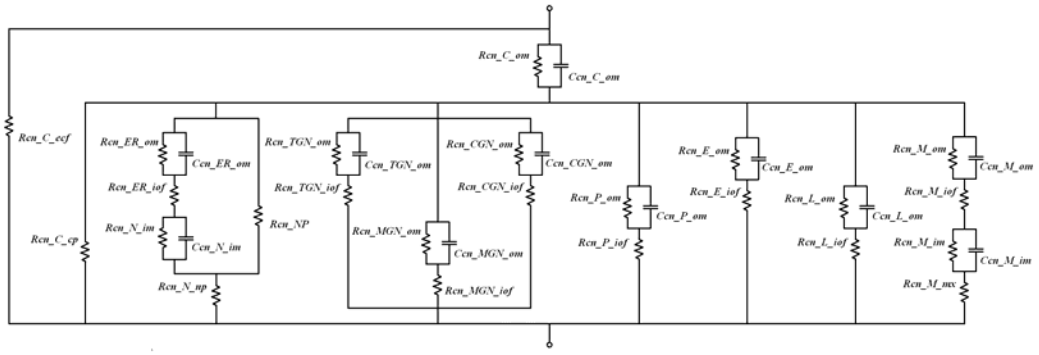

Fig. 9-3 Cell network topology

When the expanded “Transparent Box” cell model was constructed in section VII, equivalent geometric output parameters for export were calculated these parameters are used to calculate the number of cells in the three orthogonal directions X,Y and Z. The equivalent length of the virtual cell (*EL_vc*) is the length of the sides of a square that has the same cross sectional area as the cell shape being modeled. The equivalent length of the virtual cell export variable name does not identify the tissue layer it belongs to so an additional placeholder in the variable is added to designate the specific layer within a tissue for tissues with multiple layers. The equivalent length of the virtual cell (*EL_vc*) becomes (*EL_vc_n*) where *n* is a number designating a specific layer in a tissue. The equivalent length of the virtual cell for the squamous cell layer in FIG. 8.2 is (*EL_vc*_1). Notice it is twice as long as the equivalent length of the virtual cell for the cuboidal epithelial cell layer (*EL_vc*_2). Because the equivalent length is equal to the side length of a square it is both the length dimension and the width dimension of the cell. For determining the number of cells in a tissue sample in the length X and width Y dimension simply divide the sample length or width by the equivalent length cell of the cell for that layer. The number of virtual squamous cells in the Y direction for layer one of a tissue is given by equation (9-1)

$$Ncy\_1 = \frac{Yw}{EL\_vc\_1} \tag{9-1}$$

where

*Ncy*_1 is the number of virtual cell elements in Y for the first tissue layer

Yw is the width of the sample tissue calculated from probe dimensions

*EL_vc*_1 is the equivalent length of a virtual cell in the first tissue layer

The number of virtual squamous cells in the length direction for layer one of a tissue is given by (9-2)

$$Ncx\_1 = \frac{Xl}{EL\_vc\_1} \tag{9-2}$$

where

*Ncl*_1 is the number of virtual cell elements in the length of the first tissue layer

Xl is the length of the tissue cell sample calculated from probe dimensions

*EL_vc*_1 is the equivalent length of a virtual cell in the first tissue layer

The number of virtual squamous cells high in the vertical direction for layer one of a tissue is given by (9-3)

$$Ncz\_1 = \frac{Zh\_1}{h\_vc\_1} \tag{9-3}$$

where

*Nch*_1 is the number of virtual cell elements high in the first tissue layer

*Zh*_1 is the height of the tissue cell sample layer

*h_vc*_1 is the equivalent height of a virtual cell in the first tissue layer

In the first tissue layer shown in Fig. 9-2 the number of virtual cell elements long and wide is two, the number of virtual elements tall is four. For the second tissue layer the virtual cuboidal epithelial cells the number of cells in the width direction is given by equation (9-4)

$$Ncw\_2 = \frac{Yw}{EL\_vc\_2} \tag{9-4}$$

where

*Ncw*_2 is the number of virtual cell elements in the width of the second layer

Yw is the width of the cell tissue sample calculated from probe dimensions

*EL_vc*_2 is the equivalent length of a virtual cell in the second tissue layer

The number of virtual cuboidal epithelial cells in the length direction for second layer of a tissue is given by (9-5)

$$Ncl\_2 = \frac{Xl}{EL\_vc\_2} \tag{9-5}$$

where

*Ncl*_2 is the number of virtual cell elements in the length of the second layer

Xl is the length of the cell tissue sample calculated from probe dimensions

*EL_vc*_2 is the equivalent length of a virtual cell in the second tissue layer

The number of virtual cuboidal epithelial cells high in the vertical direction for second layer of a tissue is given by equation (9-6)

$$Nch\_2 = \frac{Zh\_2}{h\_vc\_2} \tag{9-6}$$

where

*Nch*_2 is the number of virtual cell elements high in the second tissue layer

*Zh*_2 is the height of the cuboidal cell layer in the tissue sample

*h_vc*_2 is the equivalent height of a virtual cell in the second tissue layer

The second tissue layer in Fig. 9-2 shows four virtual cell elements in all three directions: length, width and height. The number of virtual columnar cells in the width direction for third layer of a tissue is given by equation (9-7)

$$Ncw\_3 = \frac{Yw}{EL\_vc\_3} \tag{9-7}$$

where

*Ncw*_3 is the number of virtual cell elements in the width of the third layer

Yw is the width of the cell tissue sample calculated from probe dimensions

*EL_vc*_3 is the equivalent length of a virtual cell in the third tissue layer

The number of virtual columnar epithelial cells in the length direction for third layer of a tissue is given by equation (9-8)

$$Ncl\_3 = \frac{Xl}{EL\_vc\_3} \tag{9-8}$$

where

*Ncl*_3 is the number of virtual cell elements in the length of the third layer

Xl is the length of the cell tissue sample calculated from probe dimensions

*EL_vc*_3 is the equivalent length of a virtual cell in the third tissue layer

The number of virtual columnar epithelial cells high in the vertical direction for third layer of a tissue is given by equation (9-9)

$$Ncz\_3 = \frac{Zh\_3}{h\_vc\_3} \tag{9-9}$$

where

*Nch*_3 is the number of virtual cell elements high in the third tissue layer

*Zh*_3 is the height of the columnar cell tissue layer in the sample

*h_vc*_3 is the equivalent height of a virtual cell in the third tissue layer

In Fig. 9-2 the third tissue layer shows five virtual cell elements in length and width but height is only one virtual cell element tall. These same calculations can be done for more or less cell layers in a tissue. Some cells in a layer may have the same dimensions as cells in adjacent cell layers but require this calculation because the network values for the elements are different due to biochemical or organelle differences. For level three cancers all the cells have uniform defects throughout the tissue and can be modeled as one thick layer of cells that are equal in size and shape. In this case, for a level three cancer one would only need to find the number of cells spanning the entire sample in all three directions and not be concerned with multiple layers of different cells.

F. Calculating the Network Elements for the Tissue Layers

With the number of cells in each direction in a layer of a sample known and the values known for the network elements of a typical cell in that layer, the network values can be calculated for that layer. The network topology remains the same; the individual values of resistor and capacitor are different depending on the numbers of cells (networks) in series or parallel. Recall the general formula for resistances in series is the sum of the resistances (9-10)

$$R_{ser} = R_1 + R_2 + R_3 + ...R_{ns};\ \text{since}\ R_1 = R_2 = R_3 = R_{ns}\ \text{then}\ R_{ser} = R_1 \cdot ns \qquad (9\text{-}10)$$

where

R_{ser} is the series equivalent resistance

R_1 is a resistor element in series

ns is the number of resistors in series

The formula for resistors in parallel also reduces down see (9-11) it becomes R_1 divided by the number of elements in parallel (*np*).

$$\frac{1}{R_{par}} = \frac{1}{R_1} + \frac{1}{R_2} + \frac{1}{R_3} + ... \frac{1}{R_{np}}; \text{ since } R_1 = R_2 = R_3 = R_{np} \text{ then } R_{par} = \frac{R_1}{np} \qquad (9\text{-}11)$$

where

R_{par} is the parallel equivalent resistor value

R_1 is a resistor element in parallel

np is the number of resistor elements in parallel

Capacitors in series do not simply add they behave like resistors in parallel. The formula for capacitors in series and parallel are shown in (9-12) and (9-13) respectively.

$$\frac{1}{C_{ser}} = \frac{1}{C_1} + \frac{1}{C_2} + \frac{1}{C_3} + ... \frac{1}{C_{ns}}; \text{ since } C_1 = C_2 = C_3 = C_{ns} \text{ then } C_{ser} = \frac{C_1}{ns} \qquad (8\text{-}12)$$

where

C_{ns} is the series equivalent capacitance

C_1 is a capacitor element

ns is the number of capacitor elements in series

Capacitors in parallel add

$$C_{par} = C_1 + C_2 + C_3 + ...C_{np};\ \text{since}\ C_1 = C_2 = C_3 = C_{np}\ \text{then}\ C_{par} = C_1 \cdot np \qquad (9\text{-}13)$$

where

C_{par} is the parallel equivalent capacitance

C_1 is a capacitor element

np is the number of capacitor elements in parallel

The number of elements in series is the number of cells in the lengthwise direction. The number of cells in parallel is the product of the number of cells in the width direction times the number of cells that are in the vertical direction height. The general equation for resistance for any resistor element at the tissue level in a layer *n* is the resistance element at the cell level times the number of cells in series divided by the number of cells in parallel for that layer of tissue this is given in (9-14)

$$Rt\_n = Rc\_n \cdot \frac{Ncx\_n}{Ncz\_n \cdot Ncy\_n} \qquad (9\text{-}14)$$

where

Rt_n is a resistor element at the tissue level in layer *n*

Rc_n is the resistor element at the cellular level in layer *n*

Ncx_n is the number of virtual cells in series the X direction in layer *n*

Ncw_n is the number of virtual cells in the Y direction layer *n*

Nch_n is the number of virtual cells in the Z direction (height of layer *n*)

The general equation for capacitance for any capacitor element at the tissue level in a layer *n* is the capacitance element at the cell level times the number of cells in parallel divided by the number of cells in series for that layer of tissue this is given in (9-15)

$$Ct\_n = Cc\_n \cdot \frac{Ncy\_n \cdot Ncz\_n}{Ncx\_n} \tag{9-15}$$

where

Ct_n is the capacitor element at the tissue level in layer *n*

Cc_n is the capacitor element at the cellular level in layer *n*

Ncx_n is the number of virtual cells in series the X direction in layer *n*

Ncw_n is the number of virtual cells in the Y direction layer *n*

Nch_n is the number of virtual cells in the Z direction (height of layer *n*)

With equations (9-14) and (9-15) all of the circuit elements for each layer can be calculated. Each variable representing the electrical element value will have a number to distinguish the layer it represents. In general, the outer membrane resistor for a normal cell in the tissue level model will be identified as *Rtn_C_om* but this variable name does not identify the tissue layer it belongs to so an additional placeholder in the variable is added to designate the layer within a tissue that the electrical element represents. The variable *Rtn_C_om* thus becomes *Rtn_C_om_n* where *n* is any number representing a specific layer. The cell outer membrane resistance value at the tissue level for the first squamous epithelial layer is given by (9-16)

$$Rtn\_C\_om\_1 = Rcn\_C\_om\_1 \cdot \frac{Ncx\_1}{Ncz\_1 \cdot Ncy\_1} \tag{9-16}$$

where

*Rtn_C_om*_1 is the outer membrane resistor at the tissue level for layer 1

*Rcn_C_om*_1 is the outer membrane resistor at the cell level for layer 1

*Ncx*_1 is the number of virtual cells in X for tissue layer 1

*Ncy*_1 is the number of virtual cells in Y for tissue layer 1

*Ncz*_1 is the number of virtual cells in Z (height of tissue layer 1)

The virtual cell extra cellular fluid resistance value at the tissue level for the squamous epithelial layer is given by (9-17)

$$Rtn\_C\_ecf\_1 = Rcn\_C\_ecf\_1 \cdot \frac{Ncx\_1}{Ncz\_1 \cdot Ncy\_1} \qquad (9\text{-}17)$$

where

*Rtn_C_ecf*_1 is the extra cellular fluid resistor at the tissue level for layer 1

*Rcn_C_ecf*_1 is the extra cellular fluid resistor at the cell level for layer 1

*Ncx*_1 is the number of virtual cells in X for tissue layer 1

*Ncy*_1 is the number of virtual cells in Y for tissue layer 1

*Ncz*_1 is the number of virtual cells in Z (height of tissue layer 1)

The virtual cell cytoplasm resistance value at the tissue level for the squamous epithelial layer is given by (9-18)

$$Rtn\_C\_cp\_1 = Rcn\_C\_cp\_1 \cdot \frac{Ncx\_1}{Ncy\_1 \cdot Ncz\_1} \qquad (9\text{-}18)$$

where

*Rtn_C_cp*_1	is the cytoplasm fluid resistor at the tissue level for layer 1
*Rcn_C_cp*_1	is the extra cellular fluid resistor at the cell level for layer 1
*Ncx*_1	is the number of virtual cells in X for tissue layer 1
*Ncy*_1	is the number of virtual cells in Y for tissue layer 1
*Ncz*_1	is the number of virtual cells in Z (height of tissue layer 1)

The virtual cell plasma outer membrane capacitor value at the tissue level for the squamous epithelial layer is given by (9-19)

$$Ctn\_C\_om\_1 = Ccn\_C\_om\_1 \cdot \frac{Ncy\_1 \cdot Ncz\_1}{Ncx\_1} \qquad (9\text{-}19)$$

where

*Ctn_C_om*_1	is the tissue level outer plasma membrane capacitor for layer 1
Ccn_C_om-1	is the cell level outer plasma membrane capacitor for layer 1
*Ncx*_1	is the number of virtual cells in X for tissue layer 1
*Ncy*_1	is the number of virtual cells in Y for tissue layer 1
*Ncz*_1	is the number of virtual cells in Z (height of tissue layer 1)

The virtual cell endoplasmic reticulum outer membrane capacitor value at the tissue level for the squamous epithelial layer is given by (9-20)

$$Ctn\_ER\_om\_1 = Ccn\_ER\_om\_1 \cdot \frac{Ncy\_1 \cdot Ncz\_1}{Ncx\_1} \qquad (9\text{-}20)$$

where

*Ctn_ER_om*_1	is the tissue level ER outer membrane capacitor for layer 1
Ccn_ER_om-1	is the cell level ER outer membrane capacitor for layer 1
*Ncx*_1	is the number of virtual cells in X for tissue layer 1
*Ncy*_1	is the number of virtual cells in Y for tissue layer 1
*Ncz*_1	is the number of virtual cells in Z (height of tissue layer 1)

The endoplasmic reticulum outer membrane resistor value at the tissue level for the squamous epithelial layer is given by (9-21)

$$Rtn\_ER\_om\_1 = Rcn\_ER\_om\_1 \cdot \frac{Ncx\_1}{Ncz\_1 \cdot Ncy\_1} \qquad (9\text{-}21)$$

where

*Rtn_ER_om*_1	is the tissue level ER outer membrane resistor for layer 1
*Rcn_ER_om*_1	is the cell level ER outer membrane resistor for layer 1
*Ncx*_1	is the number of virtual cells in X for tissue layer 1
*Ncy*_1	is the number of virtual cells in Y for tissue layer 1
*Ncz*_1	is the number of virtual cells in the Z (height of tissue layer 1)

The endoplasmic reticulum inter organelle fluid resistor value at the tissue level for the squamous epithelial layer is given by (9-22)

$$Rtn\_ER\_iof\_1 = Rcn\_ER\_iof\_1 \cdot \frac{Ncx\_1}{Ncz\_1 \cdot Ncy\_1} \qquad (9\text{-}22)$$

where

*Rtn_ER_iof*_1	is the tissue level ER inter organelle fluid resistor for layer 1
*Rcn_ER_iof*_1	is the cell level ER inter organelle fluid resistor for layer 1
*Ncx*_1	is the number of virtual cells in series X for tissue layer 1
*Ncy*_1	is the number of virtual cells in Y for tissue layer 1
*Ncz*_1	is the number of virtual cells in Z (height of tissue layer 1)

The nucleus inner membrane resistor value at the tissue level for the squamous epithelial layer is given by (9-22)

$$Rtn\_N\_im\_1 = Rcn\_N\_im\_1 \cdot \frac{Ncx\_1}{Ncz\_1 \cdot Ncy\_1} \tag{9-22}$$

where

*Rtn_N_im*_1	is the tissue level nucleus inter membrane resistor for layer 1
*Rcn_N_im*_1	is the cell level nucleus inter membrane element for layer 1
*Ncx*_1	is the number of virtual cells in X for tissue layer 1
*Ncy*_1	is the number of virtual cells in Y for tissue layer 1
*Ncz*_1	is the number of virtual cells in Z (height of tissue layer 1)

The virtual cell nucleus inner membrane capacitor value at the tissue level for the squamous epithelial layer is given by (9-23)

$$Ctn\_N\_im\_1 = Ccn\_N\_im\_1 \cdot \frac{Ncy\_1 \cdot Ncz\_1}{Ncx\_1} \tag{9-23}$$

where

*Ctn_N_im*_1 is the tissue level nucleus inner membrane capacitor for layer 1

Ccn_N_im-1 is the cell level nucleus inner membrane capacitor for layer 1

*Ncx*_1 is the number of virtual cells in X for tissue layer 1

*Ncy*_1 is the number of virtual cells in Y for tissue layer 1

*Ncz*_1 is the number of virtual cells in Z (height of tissue layer 1)

The nucleus nucleoplasm resistor value at the tissue level for the squamous epithelial layer is given by (9-24)

$$Rtn\_N\_np\_1 = Rcn\_N\_np\_1 \cdot \frac{Ncx\_1}{Ncz\_1 \cdot Ncy\_1} \qquad (9\text{-}24)$$

where

*Rtn_N_np*_1 is the tissue level nucleoplasm resistor element for layer 1

*Rcn_N_np*_1 is the cell level nucleoplasm resistor element for layer 1

*Ncx*_1 is the number of virtual cells in X for tissue layer 1

*Ncy*_1 is the number of virtual cells in Y for tissue layer 1

*Ncz*_1 is the number of virtual cells in Z (height of tissue layer 1)

The nucleopore resistor value at the tissue level for the squamous epithelial layer is given by (9-24)

$$Rtn\_NP\_1 = Rcn\_NP\_1 \cdot \frac{Ncx\_1}{Ncz\_1 \cdot Ncy\_1} \qquad (9\text{-}24)$$

where

*Rtn_NP*_1	is the tissue level nucleopore resistor element for layer 1
*Rcn_NP*_1	is the cell level nucleopore resistor element for layer 1
*Ncx*_1	is the number of virtual cells in X for tissue layer 1
*Ncy*_1	is the number of virtual cells in Y for tissue layer 1
*Ncz*_1	is the number of virtual cells in Z (height of tissue layer 1)

The trans Golgi network outer membrane resistor value at the tissue level for the squamous epithelial layer is given by (9-25)

$$Rtn\_TGN\_om\_1 = Rcn\_TGN\_om\_1 \cdot \frac{Ncx\_1}{Ncz\_1 \cdot Ncy\_1} \qquad (9\text{-}25)$$

where

*Rtn_TGN_om*_1	is the tissue level TGN outer membrane resistor for layer 1
*Rcn_TGN_om*_1	is the cell level TGN outer membrane resistor for layer 1
*Ncx*_1	is the number of virtual cells in X for tissue layer 1
*Ncy*_1	is the number of virtual cells in Y for tissue layer 1
*Ncz*_1	is the number of virtual cells in Z (height of tissue layer 1)

The virtual cell trans Golgi network outer membrane capacitor value at the tissue level for the squamous epithelial layer is given by (9-26)

$$Ctn\_TGN\_om\_1 = Ccn\_TGN\_om\_1 \cdot \frac{Ncy\_1 \cdot Ncz\_1}{Ncx\_1} \qquad (9\text{-}26)$$

where

*Ctn_TGN_om*_1 is the tissue level TGN outer membrane capacitor for layer 1

Ccn_TGN_om-1 is the cell level TGN outer membrane capacitor for layer 1

*Ncx*_1 is the number of virtual cells in X for tissue layer 1

*Ncy*_1 is the number of virtual cells in Y for tissue layer 1

*Ncz*_1 is the number of virtual cells in Z (height of tissue layer 1)

The virtual cell trans Golgi network inter organelle fluid resistor value at the tissue level for the squamous epithelial layer is given by (9-27)

$$Rtn\_TGN\_iof\_1 = Rcn\_TGN\_iof\_1 \cdot \frac{Ncx\_1}{Ncz\_1 \cdot Ncy\_1} \tag{9-27}$$

where

*Rtn_TGN_iof*_1 is the tissue level TGN inter organelle fluid resistor for layer 1

*Rcn_TGN_iof*_1 is the cell level TGN inter organelle fluid resistor for layer 1

*Ncx*_1 is the number of virtual cells in X for tissue layer 1

*Ncy*_1 is the number of virtual cells Y for tissue layer 1

*Ncz*_1 is the number of virtual cells in Z (height of tissue layer 1)

The medial Golgi network outer membrane resistor value at the tissue level for the squamous epithelial layer is given by (9-28)

$$Rtn\_MGN\_om\_1 = Rcn\_MGN\_om\_1 \cdot \frac{Ncx\_1}{Ncz\_1 \cdot Ncy\_1} \tag{9-28}$$

where

*Rtn_MGN_om*_1	is the tissue level MGN outer membrane resistor for layer 1
*Rcn_MGN_om*_1	is the cell level MGN outer membrane resistor for layer 1
*Ncx*_1	is the number of virtual cells in X for tissue layer 1
*Ncy*_1	is the number of virtual cells Y for tissue layer 1
*Ncz*_1	is the number of virtual cells in Z (height of tissue layer 1)

The virtual cell medial Golgi network outer membrane capacitor value at the tissue level for the squamous epithelial layer is given by (9-29)

$$Ctn\_MGN\_om\_1 = Ccn\_MGN\_om\_1 \cdot \frac{Ncy\_1 \cdot Ncz\_1}{Ncx\_1} \qquad (9\text{-}29)$$

where

*Ctn_MGN_om*_1	is the tissue level MGN outer membrane capacitor for layer 1
Ccn_MGN_om-1	is the cell level MGN outer membrane capacitor for layer 1
*Ncx*_1	is the number of virtual cells in X for tissue layer 1
*Ncy*_1	is the number of virtual cells Y for tissue layer 1
*Ncz*_1	is the number of virtual cells in Z (height of tissue layer 1)

The virtual cell medial Golgi network inter organelle fluid resistor value at the tissue level for the squamous epithelial layer is given by (9-30)

$$Rtn\_MGN\_iof\_1 = Rcn\_MGN\_iof\_1 \cdot \frac{Ncx\_1}{Ncz\_1 \cdot Ncy\_1} \qquad (9\text{-}30)$$

where

*Rtn_MGN_iof*_1	is the tissue level MGN inter organelle fluid resistor in layer 1
*Rcn_MGN_iof*_1	is the cell level MGN inter organelle fluid resistor for layer 1
*Ncx*_1	is the number of virtual cells in X for tissue layer 1
*Ncy*_1	is the number of virtual cells Y for tissue layer 1
*Ncz*_1	is the number of virtual cells in Z (height of tissue layer 1)

The cis Golgi network outer membrane resistor value at the tissue level for the squamous epithelial layer is given by (9-31)

$$Rtn\_CGN\_om\_1 = Rcn\_CGN\_om\_1 \cdot \frac{Ncx\_1}{Ncz\_1 \cdot Ncy\_1} \tag{9-31}$$

where

*Rtn_CGN_om*_1	is the tissue level CGN outer membrane resistor for layer 1
*Rcn_CGN_om*_1	is the cell level CGN outer membrane resistor for layer 1
*Ncx*_1	is the number of virtual cells in X for tissue layer 1
*Ncy*_1	is the number of virtual cells Y for tissue layer 1
*Ncz*_1	is the number of virtual cells in Z (height of tissue layer 1)

The virtual cell cis Golgi network outer membrane capacitor value at the tissue level for the squamous epithelial layer is given by (9-32)

$$Ctn\_CGN\_om\_1 = Ccn\_CGN\_om\_1 \cdot \frac{Ncy\_1 \cdot Ncz\_1}{Ncx\_1} \tag{9-32}$$

where

*Ctn_CGN_om*_1 is the tissue level CGN outer membrane capacitor for layer 1

Ccn_CGN_om-1 is the cell level CGN outer membrane capacitor for layer 1

*Ncx*_1 is the number of virtual cells in X for tissue layer 1

*Ncy*_1 is the number of virtual cells Y for tissue layer 1

*Ncz*_1 is the number of virtual cells in Z (height of tissue layer 1)

The virtual cell cis Golgi network inter organelle fluid resistor value at the tissue level for the squamous epithelial layer is given by (9-33)

$$Rtn\_CGN\_iof\_1 = Rcn\_CGN\_iof\_1 \cdot \frac{Ncx\_1}{Ncz\_1 \cdot Ncy\_1} \tag{9-33}$$

where

*Rtn_CGN_iof*_1is the tissue level CGN inter organelle fluid resistor for layer 1

*Rcn_CGN_iof*_1 is the cell level CGN inter organelle fluid resistor for layer 1

*Ncx*_1 is the number of virtual cells in X for tissue layer 1

*Ncy*_1 is the number of virtual cells Y for tissue layer 1

*Ncz*_1 is the number of virtual cells in Z (height of tissue layer 1)

The peroxisome outer membrane resistor value at the tissue level for the squamous epithelial layer is given by (9-34)

$$Rtn\_P\_om\_1 = Rcn\_P\_om\_1 \cdot \frac{Ncx\_1}{Ncz\_1 \cdot Ncy\_1} \tag{9-34}$$

where

*Rtn_P_om*_1 is the tissue level peroxisome outer membrane resistor for layer 1

*Rcn_P_om*_1 is the cell level peroxisome outer membrane resistor for layer 1

*Ncx*_1 is the number of virtual cells in X for tissue layer 1

*Ncy*_1 is the number of virtual cells Y for tissue layer 1

*Ncz*_1 is the number of virtual cells in Z (height of tissue layer 1)

The virtual cell peroxisome outer membrane capacitor value at the tissue level for the squamous epithelial layer is given by (9-35)

$$Ctn\_P\_om\_1 = Ccn\_P\_om\_1 \cdot \frac{Ncy\_1 \cdot Ncz\_1}{Ncx\_1} \qquad (9\text{-}35)$$

where

*Ctn_P_om*_1 is the tissue level peroxisome outer membrane capacitor for tissue layer 1

Ccn_P_om-1 is the cell level peroxisome outer membrane capacitor for layer 1

*Ncx*_1 is the number of virtual cells in X for tissue layer 1

*Ncy*_1 is the number of virtual cells Y for tissue layer 1

*Ncz*_1 is the number of virtual cells in Z (height of tissue layer 1)

The virtual cell peroxisome inter organelle fluid resistor value at the tissue level for the squamous epithelial layer is given by (9-36)

$$Rtn\_P\_iof\_1 = Rcn\_P\_iof\_1 \cdot \frac{Ncx\_1}{Ncz\_1 \cdot Ncy\_1} \qquad (9\text{-}36)$$

where

*Rtn_P_iof*_1	is the peroxisome inter organelle fluid resistor of the first layer
*Rcn_P_iof*_1	is the cell level peroxisome inter organelle fluid resistor in tissue layer 1
*Ncx*_1	is the number of virtual cells in X for tissue layer 1
*Ncy*_1	is the number of virtual cells Y for tissue layer 1
*Ncz*_1	is the number of virtual cells in Z (height of tissue layer 1)

The endosome outer membrane resistor value at the tissue level for the squamous epithelial layer is given by (9-37)

$$Rtn\_E\_om\_1 = Rcn\_E\_om\_1 \cdot \frac{Ncx\_1}{Ncz\_1 \cdot Ncy\_1} \tag{9-37}$$

where

*Rtn_E_om*_1	is the tissue level endosome outer membrane resistor for layer 1
*Rcn_E_om*_1	is the cell level endosome outer membrane resistor for layer 1
*Ncx*_1	is the number of virtual cells in X for tissue layer 1
*Ncy*_1	is the number of virtual cells Y for tissue layer 1
*Ncz*_1	is the number of virtual cells in Z (height of tissue layer 1)

The virtual cell endosome outer membrane capacitor value at the tissue level for the squamous epithelial layer is given by (9-38)

$$Ctn\_E\_om\_1 = Ccn\_E\_om\_1 \cdot \frac{Ncy\_1 \cdot Ncz\_1}{Ncx\_1} \tag{9-38}$$

where

*Ctn_E_om*_1	is the tissue level endosome outer membrane capacitor in layer 1
Ccn_E_om-1	is the cell level endosome outer membrane capacitor for layer 1
*Ncx*_1	is the number of virtual cells in X for tissue layer 1
*Ncy*_1	is the number of virtual cells Y for tissue layer 1
*Ncz*_1	is the number of virtual cells in Z (height of tissue layer 1)

The virtual cell endosome inter organelle fluid resistor value at the tissue level for the squamous epithelial layer is given by (9-39)

$$Rtn\_E\_iof\_1 = Rcn\_E\_iof\_1 \cdot \frac{Ncx\_1}{Ncz\_1 \cdot Ncy\_1} \tag{9-39}$$

where

*Rtn_E_iof*_1	is the endosome inter organelle fluid resistor for tissue layer 1
*Rcn_E_iof_*	is the cell level endosome inter organelle fluid resistor for layer 1
*Ncx*_1	is the number of virtual cells in X for tissue layer 1
*Ncy*_1	is the number of virtual cells Y for tissue layer 1
*Ncz*_1	is the number of virtual cells in Z (height of tissue layer 1)

The lysosome outer membrane resistor value at the tissue level for the squamous epithelial layer is given by (9-40)

$$Rtn\_L\_om\_1 = Rcn\_L\_om\_1 \cdot \frac{Ncx\_1}{Ncz\_1 \cdot Ncy\_1} \tag{9-40}$$

where

*Rtn_L_om*_1	is the tissue level lysosome outer membrane resistor for layer 1
*Rcn_L_om*_1	is the cell level lysosome outer membrane resistor for layer 1
*Ncx*_1	is the number of virtual cells in X for tissue layer 1
*Ncy*_1	is the number of virtual cells Y for tissue layer 1
*Ncz*_1	is the number of virtual cells in Z (height of tissue layer 1)

The virtual cell lysosome outer membrane capacitor value at the tissue level for the squamous epithelial layer is given by (9-41)

$$Ctn\_L\_om\_1 = Ccn\_L\_om\_1 \cdot \frac{Ncz\_1 \cdot Ncy\_1}{Ncx\_1} \quad (9\text{-}41)$$

where

*Ctn_L_om*_1	is the tissue level lysosome outer membrane capacitor for layer 1
Ccn_L_om-1	is the cell level lysosome outer membrane capacitor for layer 1
*Ncx*_1	is the number of virtual cells in X for tissue layer 1
*Ncy*_1	is the number of virtual cells Y for tissue layer 1
*Ncz*_1	is the number of virtual cells in Z (height of tissue layer 1)

The virtual cell lysosome inter organelle fluid resistor value at the tissue level for the squamous epithelial layer is given by (9-42)

$$Rtn\_L\_iof\_1 = Rcn\_L\_iof\_1 \cdot \frac{Ncx\_1}{Ncz\_1 \cdot Ncy\_1} \quad (9\text{-}42)$$

where

*Rtn_L_iof*_1	is the tissue level lysosome inter organelle fluid resistor for tissue layer 1
*Rcn_L_iof*_1	is the cell level lysosome inter organelle fluid resistor for layer 1
*Ncx*_1	is the number of virtual cells in X for tissue layer 1
*Ncy*_1	is the number of virtual cells Y for tissue layer 1
*Ncz*_1	is the number of virtual cells in Z (height of tissue layer 1)

The mitochondria outer membrane resistor value at the tissue level for the squamous epithelial layer is given by (9-43)

$$Rtn\_M\_om\_1 = Rcn\_M\_om\_1 \cdot \frac{Ncx\_1}{Ncz\_1 \cdot Ncy\_1} \qquad (9\text{-}43)$$

where

*Rtn_M_om*_1	is the mitochondria outer membrane resistor for tissue layer 1
*Rcn_M_om*_1	is the cell level mitochondria outer membrane resistor for layer 1
*Ncx*_1	is the number of virtual cells in X for tissue layer 1
*Ncy*_1	is the number of virtual cells Y for tissue layer 1
*Ncz*_1	is the number of virtual cells in Z (height of tissue layer 1)

The virtual cell mitochondria outer membrane capacitor value at the tissue level for the squamous epithelial layer is given by (9-44)

$$Ctn\_M\_om\_1 = Ccn\_M\_om\_1 \cdot \frac{Ncy\_1 \cdot Ncz\_1}{Ncx\_1} \qquad (9\text{-}44)$$

where

*Ctn_M_om*_1 is the mitochondria outer membrane capacitor for tissue layer 1

Ccn_M_om-1 is the cell level mitochondria outer membrane capacitor for tissue layer 1

*Ncx*_1 is the number of virtual cells in X for tissue layer 1

*Ncy*_1 is the number of virtual cells Y for tissue layer 1

*Ncz*_1 is the number of virtual cells in Z (height of tissue layer 1)

The virtual cell mitochondria inter organelle fluid resistor value at the tissue level for the squamous epithelial layer is given by (9-45)

$$Rtn\_M\_iof\_1 = Rcn\_M\_iof\_1 \cdot \frac{Ncx\_1}{Ncz\_1 \cdot Ncy\_1} \qquad (9\text{-}45)$$

where

*Rtn_M_iof*_1 is the mitochondria inter organelle fluid resistor for tissue layer 1

*Rcn_M_iof*_1 is the layer 1 cell level mitochondria inter organelle fluid resistor

*Ncx*_1 is the number of virtual cells in X for tissue layer 1

*Ncy*_1 is the number of virtual cells Y for tissue layer 1

*Ncz*_1 is the number of virtual cells in Z (height of tissue layer 1)

The mitochondria inner membrane resistor value at the tissue level for the squamous epithelial layer is given by (9-46)

$$Rtn\_M\_im\_1 = Rcn\_M\_im\_1 \cdot \frac{Ncx\_1}{Ncz\_1 \cdot Ncy\_1} \qquad (9\text{-}46)$$

where

*Rtn_M_im*_1 is the tissue level mitochondria inner membrane resistor for tissue layer 1

*Rcn_M_im*_1 is the cell level mitochondria inner membrane resistor for layer 1

*Ncx*_1 is the number of virtual cells in X for tissue layer 1

*Ncy*_1 is the number of virtual cells Y for tissue layer 1

*Ncz*_1 is the number of virtual cells in Z (height of tissue layer 1)

The virtual cell mitochondria inner membrane capacitor value at the tissue level for the squamous epithelial layer is given by (9-47)

$$Ctn\_M\_im\_1 = Ccn\_M\_im\_1 \cdot \frac{Ncy\_1 \cdot Ncz\_1}{Ncx\_1} \qquad (9\text{-}47)$$

where

*Ctn_M_im*_1 is the mitochondria inner membrane capacitor for tissue layer 1

Ccn_M_im-1 is the cell level mitochondria inner membrane capacitor for tissue layer 1

*Ncx*_1 is the number of virtual cells in X for tissue layer 1

*Ncy*_1 is the number of virtual cells Y for tissue layer 1

*Ncz*_1 is the number of virtual cells in Z (height of tissue layer 1)

The virtual cell mitochondria matrix fluid resistor value at the tissue level for the squamous epithelial layer is given by (9-48)

$$Rtn\_M\_mx\_1 = Rcn\_M\_mx\_1 \cdot \frac{Ncx\_1}{Ncz\_1 \cdot Ncy\_1} \qquad (9\text{-}48)$$

where

*Rtn_M_mx*_1	is the tissue level mitochondria matrix fluid resistor for layer 1
*Rcn_M_mx*_1	is the cell level mitochondria matrix fluid resistor for layer 1
*Ncx*_1	is the number of virtual cells in X for tissue layer 1
*Ncy*_1	is the number of virtual cells Y for tissue layer 1
*Ncz*_1	is the number of virtual cells in Z (height of tissue layer 1)

For tissue models that have multiple layers the calculations follow the same logic as used for layer one. The calculations for the circuit elements at the tissue level for the *n*th layer would use the same equations as layer 1 except the number of virtual cells in each direction will be specific to the *n*th layer. After the network values are calculated for each layer of tissue the network for the tissue as a whole can be calculated.

G. Calculating the Network Elements for the Whole Tissue

The network for the tissue as a whole can be calculated after finding the network values for each layer comprising the tissue. If the sample has three layers like the normal healthy epithelial cell tissue shown in Fig. 9-1 then the network values would be the parallel combination of each element from each of the three layers as illustrated in Fig. 9-4 Combining tissue layers into whole epithelial cell tissue. The network topology for tissue again remains the same as the cell topology it is just the individual network element values that change due to the combinations of the cell and tissue networks. In general, one can create a model with *n* layers of tissue each with a different cell model. The individual electrical elements representing parts of the cell for each layer will be combined in parallel.

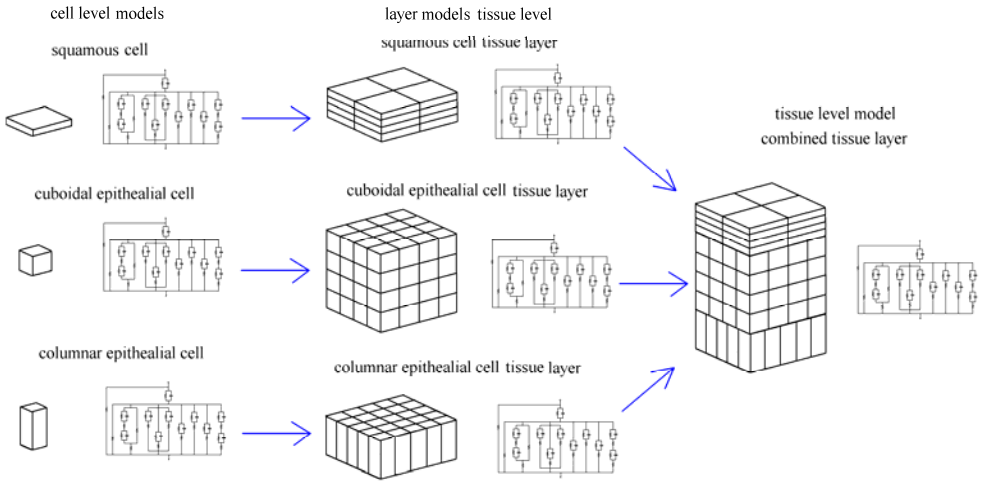

Fig. 9-4 Combining tissue layers into whole epithelial cell tissue

The equivalent resistance for resistor elements in parallel with *n* layers is given by (9-49)

$$\frac{1}{Rt\_eqv} = \frac{1}{Rt\_1} + \frac{1}{Rt\_2} + \frac{1}{Rt\_3} + ... \frac{1}{Rt\_n} \qquad (9\text{-}49)$$

where

Rt_eqv is the parallel equivalent resistor value for *n* tissue layers

*Rt*_1 is a resistor element in parallel from tissue layer 1

*Rt*_2 is a resistor element in parallel from tissue layer 2

*Rt*_3 is a resistor element in parallel from tissue layer 3

Rt_n is a resistor element in parallel from *n*th tissue layer

n is the number of resistor elements in parallel for the tissue

The capacitor elements in parallel are the sum of the individual capacitor elements from layer to layer and is shown in (9-50)

$$Ct\_eqv = Ct\_1 + Ct\_2 + Ct\_3 + ...Ct\_n \qquad (9\text{-}50)$$

where

Ct_eqv is the parallel equivalent capacitor value for *n* tissue layers

*Ct*_1 is a capacitor element in parallel from tissue layer 1

*Ct*_2 is a capacitor element in parallel from tissue layer 2

*Ct*_3 is a capacitor element in parallel from tissue layer 3

Ct_n is a capacitor element in parallel from *n*th tissue layer

n is the number of capacitor elements (tissue layers) in parallel

The combined tissue calculation for each element for the three layers of the normal epithelial cell tissue of Fig. 9-4 uses equations (9-49) and (9-50). The variable names have been slightly abbreviated to make the equations fit the page. The abbreviated variable names reference the longer more descriptive variable names after each respective equation. The combined tissue model calculation for the cell outer membrane resistance is given by (9-51)

$$Rctn\_C\_om = \frac{Rcom1 \cdot Rcom2 \cdot Rcom3}{Rcom1 \cdot Rcom2 + Rcom2 \cdot Rcom3 + Rcom3 \cdot Rcom1} \qquad (9\text{-}51)$$

where

Rctn_C_om is the outer membrane resistor element for the combined tissue

*Rcom*1 is the 1st layer outer membrane resistor, abbreviation of *Rtn_C_om*_1

*Rcom*2 is the 2nd layer outer membrane resistor, abbreviation of *Rtn_C_om*_2

*Rcom*3 is the 3rd layer outer membrane resistor, abbreviation of *Rtn_C_om*_3

The combined tissue model calculation for the extra cellular fluid resistance is given by (9-52)

$$Rctn\_C\_ecf = \frac{Rcecf1 \cdot Rcecf2 \cdot Rcecf3}{Rcecf1 \cdot Rcecf2 + Rcecf2 \cdot Rcecf3 + Rcecf3 \cdot Rcecf1} \quad (9\text{-}52)$$

where

Rctn_C_ecf is the extra cellular fluid resistor element for the combined tissue

*Rcecf*1 is the 1st layer extra cellular fluid resistor, abbreviation of *Rtn_C_ecf_*1

*Rcecf*2 is the 2nd layer extra cellular fluid resistor, abbreviation of *Rtn_C_ecf_*2

*Rcecf*3 is the 3rd layer extra cellular fluid resistor, abbreviation of *Rtn_C_ecf_*3

The combined tissue model calculation for the cell cytoplasm resistance value is given by (9-53)

$$Rctn\_C\_cp = \frac{Rccp1 \cdot Rccp2 \cdot Rccp3}{Rccp1 \cdot Rccp2 + Rccp2 \cdot Rccp3 + Rccp3 \cdot Rccp1} \quad (9\text{-}53)$$

where

Rctn_C_cp is the cell cytoplasm resistor element for the combined tissue

*Rccp*1 is the 1st layer cell cytoplasm resistor, abbreviation of *Rtn_C_cp_*1

*Rccp*2 is the 2nd layer cell cytoplasm resistor, abbreviation of *Rtn_C_cp_*2

*Rccp*3 is the 3rd layer cell cytoplasm resistor, abbreviation of *Rtn_C_cp_*3

The combined tissue model calculation for the cell outer membrane capacitor is given by (9-54)

$$Cctn\_C\_om = Ccom1 + Ccom2 + Ccom3 \quad (9\text{-}54)$$

where

Cctn_C_om is the outer membrane capacitor element for the combined tissue

*Ccom*1 is the 1st layer outer membrane capacitor, abbreviation of *Ctn_C_om*_1

*Rcom*2 is the 2nd layer outer membrane capacitor, abbreviation of *Ctn_C_om*_2

*Rcom*3 is the 3rd layer outer membrane capacitor, abbreviation of *Ctn_C_om*_3

The combined tissue model calculation for the endoplasmic reticulum outer membrane resistance is given by (9-55)

$$Rctn\_ER\_om = \frac{Roerm1 \cdot Roerm2 \cdot Roerm3}{Roerm1 \cdot Roerm2 + Roerm2 \cdot Roerm3 + Roerm3 \cdot Roerm1} \quad (9\text{-}55)$$

where

Rctn_ER_om is the ER outer membrane resistor element for the combined tissue

*Roerm*1 is the 1st layer ER membrane resistor, abbreviation of *Rcn_ER_om*_1

*Roerm*2 is the 2nd layer ER membrane resistor, abbreviation of *Rcn_ER_om*_2

*Roerm*3 is the 3rd layer ER membrane resistor, abbreviation of *Rcn_ER_om*_3

The combined tissue model calculation for the endoplasmic reticulum outer membrane capacitor is given by (9-56)

$$Cctn\_ER\_om = Coerm1 + Coerm2 + Coerm3 \tag{9-56}$$

where

Cctn_ER_om is the ER outer membrane capacitor element for the combined tissue

*Coerm*1 is the 1st layer outer membrane capacitor, abbreviation of C*tn_ER_om*_1

*Coerm*2 is the 2nd layer outer membrane capacitor, abbreviation of *Ctn_ER_om*_2

*Coerm*3 is the 3rd layer outer membrane capacitor, abbreviation of *Ctn_ER_om*_3

The combined tissue model calculation for the endoplasmic reticulum inter-organelle fluid resistor is given by (9-57)

$$Rctn\_ER\_iof = \frac{Roerf1 \cdot Roerf2 \cdot Roerf3}{Roerf1 \cdot Roerf2 + Roerf2 \cdot Roerf3 + Roerf3 \cdot Roerf1} \tag{9-57}$$

where

Rctn_ER_iof is the ER inter organelle fluid resistor element for the combined tissue

*Roerf*1 is the 1st layer ER organelle fluid resistor, abbreviation of *Rtn_ER_iof*_1

*Roerf*2 is the 2nd layer ER organelle fluid resistor, abbreviation of *Rtn_ER_iof*_2

*Roerf*3 is the 3rd layer ER organelle fluid resistor, abbreviation of *Rtn_ER_iof*_3

The combined tissue model calculation for the nuclear inner membrane resistor is given by (9-58)

$$Rctn\_N\_im = \frac{Ronm1 \cdot Ronm2 \cdot Ronm3}{Ronm1 \cdot Ronm2 + Ronm2 \cdot Ronm3 + Ronm3 \cdot Ronm1} \tag{9-58}$$

where

Rctn_N_im is the nucleus inner membrane resistor element for the combined tissue

*Ronm*1 is the 1st layer nuclear membrane resistor, abbreviation of *Rcn_N_om*_1

*Ronm*2 is the 2nd layer nuclear membrane resistor, abbreviation of *Rcn_N_om*_2

*Ronm*3 is the 3rd layer nuclear membrane resistor, abbreviation of *Rcn_N_om*_3

The combined tissue model calculation for the nuclear inner membrane capacitor is given by (9-59)

$$Cctn\_N\_im = Conm1 + Conm2 + Conm3 \tag{9-59}$$

where

Cctn_N_im is the inner nuclear membrane capacitor element for the combined tissue

*Conm*1 is the 1st layer outer membrane capacitor, abbreviation of C*tn_ER_om*_1

*Conm*2 is the 2nd layer outer membrane capacitor, abbreviation of *Ctn_ER_om*_2

*Conm*3 is the 3rd layer outer membrane capacitor, abbreviation of *Ctn_ER_om*_3

The combined tissue model calculation for the nucleoplasm resistor is given by (9-60)

$$Rctn\_N\_np = \frac{Ronp1 \cdot Ronp2 \cdot Ronp3}{Ronp1 \cdot Ronp2 + Ronp2 \cdot Ronp3 + Ronp3 \cdot Ronp1} \tag{9-60}$$

where

Rctn_N_np is the nucleoplasm resistor element for the combined tissue

*Ronp*1 is the 1st tissue layer nucleoplasm resistor, abbreviation of *Rcn_N_om*_1

*Ronp*2 is the 2nd tissue layer nucleoplasm resistor, abbreviation of *Rcn_N_om*_2

*Ronp*3 is the 3rd tissue layer nucleoplasm resistor, abbreviation of *Rcn_N_om*_3

The combined tissue model calculation for the nuclearpore resistor component value is given by (9-61)

$$Rctn\_NP = \frac{Rnp1 \cdot Rnp2 \cdot Rnp3}{Rnp1 \cdot Rnp2 + Rnp2 \cdot Rnp3 + Rnp3 \cdot Rnp1} \qquad (9\text{-}61)$$

where

Rctn_NP is the nucleopore resistor element for the combined tissue

*Ronp*1 is the 1st tissue layer nucleopore resistor, abbreviation of *Rcn_N_om*_1

*Ronp*2 is the 2nd tissue layer nucleopore resistor, abbreviation of *Rcn_N_om*_2

*Ronp*3 is the 3rd tissue layer nucleopore resistor, abbreviation of *Rcn_N_om*_3

The combined tissue model calculation for the trans Golgi network outer membrane resistor is given by (9-62)

$$Rctn\_TGN\_om = \frac{Rotgm1 \cdot Rotgm2 \cdot Rotgm3}{Rotgm1 \cdot Rotgm2 + Rotgm2 \cdot Rotgm3 + Rotgm3 \cdot Rotgm1} \qquad (9\text{-}62)$$

where

Rctn_TGN_om is the combined tissue trans Golgi network outer membrane resistor

*Rotgm*1 is the 1st tissue layer TGN resistor, abbreviation of *Rcn_TGN_om*_1

*Rotgm*2 is the 2nd tissue layer TGN resistor, abbreviation of *Rcn_TGN_om*_2

*Rotgm*3 is the 3rd tissue layer TGN resistor, abbreviation of *Rcn_TGN_om*_3

The combined tissue model calculation for the trans Golgi network outer membrane capacitor is given by (9-63)

$$Cctn\_TGN\_om = Cotgm1 + Cotgm2 + Cotgm3 \qquad (9\text{-}63)$$

where

Cctn_TGN_om is the TGN capacitor element for the combined tissue

*Cotgm*1 is the 1st tissue layer abbreviation of TGN membrane capacitor C*tn_TGN_om*_1

*Cotgm*2 is the 2nd layer abbreviation of TGN membrane capacitor *Ctn_TGN_om*_2

*Cotgm*3 is the 3rd layer abbreviation of TGN membrane capacitor *Ctn_TGN_om*_3

The combined tissue model calculation for the trans Golgi network inter organelle fluid is given by (9-64)

$$Rctn\_TGN\_iof = \frac{Rotgf1 \cdot Rotgf2 \cdot Rotgf3}{Rotgf1 \cdot Rotgf2 + Rotgf2 \cdot Rotgf3 + Rotgf3 \cdot Rotgf1} \qquad (9\text{-}64)$$

where

Rctn_TGN_iof is the combined tissue trans Golgi network inter organelle fluid resistor

*Rotgf*1 is the 1st layer TGN fluid resistor, abbreviation of *Rcn_TGN_iof_*1

*Rotgf*2 is the 2nd layer TGN fluid resistor, abbreviation of *Rcn_TGN_iof_*2

*Rotgf*3 is the 3rd layer TGN fluid resistor, abbreviation of *Rcn_TGN_iof_*3

The combined tissue model calculation for the medial Golgi network outer membrane resistor is given by (9-65)

$$Rctn\_MGN\_om = \frac{Romgm1 \cdot Romgm2 \cdot Romgm3}{Romgm1 \cdot Romgm2 + Romgm2 \cdot Romgm3 + Romgm3 \cdot Romgm1} \quad (9\text{-}65)$$

where

*Rctn_MGN_*om is the combined tissue medial Golgi network outer membrane resistor

*Romgm*1 is the 1st tissue layer MGN resistor, abbreviation of *Rcn_MGN_om_*1

*Romgm*2 is the 2nd tissue layer MGN resistor, abbreviation of *Rcn_MGN_om_*2

*Romgm*3 is the 3rd tissue layer MGN resistor, abbreviation of *Rcn_MGN_om_*3

The combined tissue model calculation for the medial Golgi network outer membrane capacitor is given by (9-66)

$$Cctn\_MGN\_om = Comgm1 + Comgm2 + Comgm3 \quad (9\text{-}66)$$

where

Cctn_MGN_om is the MGN capacitor element for the combined tissue

*Comgm*1 is the 1st layer abbreviation of MGN membrane capacitor Ctn_*MGN_om*_1

*Comgm*2 is the 2nd layer abbreviation of MGN membrane cap capacitor *Ctn_MGN_om*_2

*Comgm*3 is the he 3rd layer abbreviation of MGN membrane capacitor *Ctn_MGN_om*_3

The combined tissue model calculation for the medial Golgi network inter organelle fluid is given by (9-67)

$$Rctn\_MGN\_iof = \frac{Romgf1 \cdot Romgf2 \cdot Romgf3}{Romgf1 \cdot Romgf2 + Romgf2 \cdot Romgf3 + Romgf3 \cdot Romgf1} \quad (9\text{-}67)$$

where

Rctn_MGN_iof is the combined tissue MGN inter organelle fluid resistor

*Romgf*1 is the 1st layer MGN fluid resistor, abbreviation of *Rcn_MGN_iof*_1

*Romgf*2 is the 2nd layer MGN fluid resistor, abbreviation of *Rcn_MGN_iof*_2

*Romgf*3 is the 3rd layer MGN fluid resistor, abbreviation of *Rcn_MGN_iof_*3

The combined tissue model calculation for the cis Golgi network outer membrane resistor is given by (9-68)

$$Rctn\_CGN\_om = \frac{Rocgm1 \cdot Rocgm2 \cdot Rocgm3}{Rocgm1 \cdot Rocgm2 + Rocgm2 \cdot Rocgm3 + Rocgm3 \cdot Rocgm1} \quad (9\text{-}68)$$

where

Rctn_CGN_om is the combined tissue cis Golgi network outer membrane resistor

*Rocgm*1 is the 1st tissue layer CGN resistor, abbreviation of *Rcn_CGN_om_*1

*Rocgm*2 is the 2nd tissue layer CGN resistor, abbreviation of *Rcn_CGN_om_*2

*Rocgm*3 is the 3rd tissue layer CGN resistor, abbreviation of *Rcn_CGN_om_*3

The combined tissue model calculation for the cis Golgi network outer membrane capacitor is given by (9-69)

$$Cctn\_CGN\_om = Cocgm1 + Cocgm2 + Cocgm3 \quad (9\text{-}69)$$

where

Cctn_CGN_om is the CGN capacitor element for the combined tissue

*Cocgm*1 is the 1st layer abbreviation of CGN membrane cap C*tn_CGN_om*_1

*Cocgm*2 is the 2nd layer abbreviation of CGN membrane cap *Ctn_CGN_om*_2

*Cocgm*3 is the 3rd layer abbreviation of CGN membrane cap *Ctn_CGN_om*_3

The combined tissue model calculation for the cis Golgi network inter organelle fluid is given by (9-70)

$$Rctn\_CGN\_iof = \frac{Rocgf1 \cdot Rocgf2 \cdot Rocgf3}{Rocgf1 \cdot Rocgf2 + Rocgf2 \cdot Rocgf3 + Rocgf3 \cdot Rocgf1} \quad (9\text{-}70)$$

where

Rctn_CGN_iof is the combined tissue cis Golgi network inter organelle fluid resistor

*Rocgf*1 is the 1st layer CGN fluid resistor, abbreviation of *Rcn_CGN_iof*_1

*Rocgf*2 is the 2nd layer CGN fluid resistor, abbreviation of *Rcn_CGN_iof*_2

*Rocgf*3 is the 3rd layer CGN fluid resistor, abbreviation of *Rcn_CGN_iof*_3

The combined tissue model calculation for the peroxisome outer membrane resistor is given by (9-62)

$$Rctn\_P\_om = \frac{Ropm1 \cdot Ropm2 \cdot Ropm3}{Ropm1 \cdot Ropm2 + Ropm2 \cdot Ropm3 + Ropm3 \cdot Ropm1} \qquad (9\text{-}62)$$

where

Rctn_P_om is the peroxisome outer membrane resistor for the combined tissue

*Ropm*1 is the 1st tissue layer peroxisome resistor, abbreviation of *Rcn_P_om*_1

*Ropm*2 is the 2nd tissue layer peroxisome resistor, abbreviation of *Rcn_P_om*_2

*Ropm*3 is the 3rd tissue layer peroxisome resistor, abbreviation of *Rcn_P_om*_3

The combined tissue model calculation for the peroxisome outer membrane capacitor is given by (9-63)

$$Cctn\_P\_om = Copm1 + Copm2 + Copm3 \qquad (9\text{-}63)$$

where

Cctn_P_om is the peroxisome membrane capacitor element for the combined tissue

*Copm*1 is the 1st layer abbreviation of peroxisome membrane cap C*tn_P_om*_1

*Copm*2 is the 2nd layer abbreviation of peroxisome membrane cap *Ctn_P_om*_2

*Copm*3 is the 3rd layer abbreviation of peroxisome membrane cap *Ctn_P_om*_3

The combined tissue model calculation for the peroxisome inter organelle fluid is given by (9-64)

$$Rctn\_P\_iof = \frac{Ropf1 \cdot Ropf2 \cdot Ropf3}{Ropf1 \cdot Ropf2 + Ropf2 \cdot Ropf3 + Ropf3 \cdot Ropf1} \quad (9\text{-}64)$$

where

Rctn_P_iof is the combined tissue peroxisome inter organelle fluid resistor

*Ropf*1 is the 1st layer peroxisome fluid resistor, abbreviation of *Rcn_P_iof*_1

*Ropf*2 is the 2nd layer peroxisome fluid resistor, abbreviation of *Rcn_P_iof*_2

*Ropf*3 is the 3rd layer peroxisome fluid resistor, abbreviation of *Rcn_P_iof*_3

The combined tissue model calculation for the endosome outer membrane resistor is given by (9-65)

$$Rctn\_E\_om = \frac{Roem1 \cdot Roem2 \cdot Roem3}{Roem1 \cdot Roem2 + Roem2 \cdot Roem3 + Roem3 \cdot Roem1} \quad (9\text{-}65)$$

where

Rctn_E_om is the endosome outer membrane resistor for the combined tissue

*Roem*1 is the 1st tissue layer endosome resistor, abbreviation of *Rcn_E_om*_1

*Roem*2 is the 2nd tissue layer endosome resistor, abbreviation of *Rcn_E_om*_2

*Roem*3 is the 3rd tissue layer endosome resistor, abbreviation of *Rcn_E_om*_3

The combined tissue model calculation for the endosome outer membrane capacitor is given by (9-66)

$$Cctn\_E\_om = Coem1 + Coem2 + Coem3 \quad (9\text{-}66)$$

where

Cctn_E_om is the endosome membrane capacitor element for the combined tissue

*Copm*1 is the 1st layer abbreviation of endosome membrane cap C*tn_E_om*_1

*Copm*2 is the 2nd layer abbreviation of endosome membrane cap *Ctn_E_om*_2

*Copm*3 is the 3rd layer abbreviation of endosome membrane cap *Ctn_E_om*_3

The combined tissue model calculation for the endosome inter organelle fluid is given by (9-67)

$$Rctn\_E\_iof = \frac{Roef1 \cdot Roef2 \cdot Roef3}{Roef1 \cdot Roef2 + Roef2 \cdot Roef3 + Roef3 \cdot Roef1} \quad (9\text{-}67)$$

where

Rctn_P_iof is the combined tissue endosome inter organelle fluid resistor

*Roef*1 is the 1st layer endosome fluid resistor, abbreviation of *Rcn_E_iof*_1

*Roef*2 is the 2nd layer endosome fluid resistor, abbreviation of *Rcn_E_iof*_2

*Roef*3 is the 3rd layer endosome fluid resistor, abbreviation of *Rcn_E_iof*_3

The combined tissue model calculation for the lysosome outer membrane resistor is given by (9-68)

$$Rctn\_L\_om = \frac{Rolm1 \cdot Rolm2 \cdot Rolm3}{Rolm1 \cdot Rolm2 + Rolm2 \cdot Rolm3 + Rolm3 \cdot Rolm1} \quad (9\text{-}68)$$

where

Rctn_L_om is the lysosome outer membrane resistor for the combined tissue

*Rolm*1 is the 1st tissue layer lysosome resistor, abbreviation of *Rcn_L_om*_1

*Rolm*2 is the 2nd tissue layer lysosome resistor, abbreviation of *Rcn_L_om*_2

*Rolm*3 is the 3rd tissue layer lysosome resistor, abbreviation of *Rcn_L_om*_3

The combined tissue model calculation for the lysosome outer membrane capacitor is given by (9-69)

$$Cctn\_L\_om = Colm1 + Colm2 + Colm3 \tag{9-69}$$

where

Cctn_L_om is the lysosome membrane capacitor element for the combined tissue

*Colm*1 is the 1st layer abbreviation of lysosome membrane cap C*tn_L_om*_1

*Colm*2 is the 2nd layer abbreviation of lysosome membrane cap *Ctn_L_om*_2

*Colm*3 is the 3rd layer abbreviation of lysosome membrane cap *Ctn_L_om*_3

The combined tissue model calculation for the lysosome inter organelle fluid is given by (9-70)

$$Rctn\_L\_iof = \frac{Rolf1 \cdot Rolf2 \cdot Rolf3}{Rolf1 \cdot Rolf2 + Rolf2 \cdot Rolf3 + Rolf3 \cdot Rolf1} \tag{9-70}$$

where

Rctn_L_iof is the combined tissue lysosome inter organelle fluid resistor

*Rolf*1 is the 1st layer lysosome fluid resistor, abbreviation of *Rcn_L_iof*_1

*Rolf*2 is the 2nd layer lysosome fluid resistor, abbreviation of *Rcn_L_iof*_2

*Rolf*3 is the 3rd layer lysosome fluid resistor, abbreviation of *Rcn_L_iof*_3

The combined tissue model calculation for the mitochondria outer membrane resistor is given by (9-71)

$$Rctn\_M\_om = \frac{Romom1 \cdot Romom2 \cdot Romom3}{Romom1 \cdot Romom2 + Romom2 \cdot Romom3 + Romom3 \cdot Romom1} \quad (9\text{-}71)$$

where

Rctn_P_om is the mitochondria outer membrane resistor for the combined tissue

*Romom*1 is the 1st tissue layer mitochondria resistor, abbreviation of *Rcn_M_om*_1

*Romom*2 is the 2nd tissue layer mitochondria resistor, abbreviation of *Rcn_M_om*_2

Romom 3 is the 3rd tissue layer mitochondria resistor, abbreviation of *Rcn_M_om*_3

The combined tissue model calculation for the mitochondria outer membrane capacitor is given by (9-72)

$$Cctn\_M\_om = Comom1 + Comom2 + Comom3 \quad (9\text{-}72)$$

where

Cctn_M_om is the mitochondria outer membrane capacitor for the combined tissue

*Comom*1 is the 1st layer abbreviation of mitochondria membrane cap C*tn_M_om*_1

*Comom*2 is the 2nd layer abbreviation of mitochondria membrane cap *Ctn_M_om_*2

*Comom*3 is the 3rd layer abbreviation of mitochondria membrane cap *Ctn_M_om_*3

The combined tissue model calculation for the mitochondria inner membrane resistor is given by (9-73)

$$Rctn\_M\_im = \frac{Romim1 \cdot Romim2 \cdot Romim3}{Romim1 \cdot Romim2 + Romim2 \cdot Romim3 + Romim3 \cdot Romim1} \quad (9\text{-}73)$$

where

Rctn_M_im is the mitochondria inner membrane resistor for the combined tissue

*Romim*1 is the 1st tissue layer mitochondria resistor, abbreviation of *Rcn_M_im_*1

*Romim*2 is the 2nd tissue layer mitochondria resistor, abbreviation of *Rcn_M_im_*2

*Romim*3 is the 3rd tissue layer mitochondria resistor, abbreviation of *Rcn_M_im_*3

The combined tissue model calculation for the mitochondria inner membrane capacitor is given by (9-74)

$$Cctn\_M\_im = Comim1 + Comim2 + Comim3 \quad (9\text{-}74)$$

where

Cctn_M_im is the mitochondria inner membrane capacitor for the combined tissue

*Comim*1 is the 1st layer abbreviation of mitochondria membrane cap C*tn_M_om_*1

*Comim*2 is the 2nd layer abbreviation of mitochondria membrane cap *Ctn_M_om_*2

*Comim*3 is the 3rd layer abbreviation of mitochondria membrane cap *Ctn_M_om_*3

The combined tissue model calculation for the mitochondria matrix fluid is given by (9-75)

$$Rctn\_M\_mx = \frac{Romx1 \cdot Romx2 \cdot Romx3}{Romx1 \cdot Romx2 + Romx2 \cdot Romx3 + Romx3 \cdot Romx1} \quad (9\text{-}75)$$

where

Rctn_M_mx is the combined tissue mitochondria matrix fluid resistor

*Romx*1 is the 1st layer mitochondria fluid resistor, abbreviation of *Rcn_M_mx_*1

*Romx*2 is the 2nd layer mitochondria fluid resistor, abbreviation of *Rcn_M_mx_*2

*Romx*3 is the 3rd layer mitochondria fluid resistor, abbreviation of *Rcn_M_mx_*3

The final circuit topology is familiar shown with the appropriate variable names in Fig. 9-5 circuit topology of the combined tissue network. This topology can now be reduced using circuit theory without adversely affecting the shape and behavior of the EIS output. All of the biological meaning of this model is captured in the lower more fundamental elements of the model including the organelle sizes numbers and other cell properties.

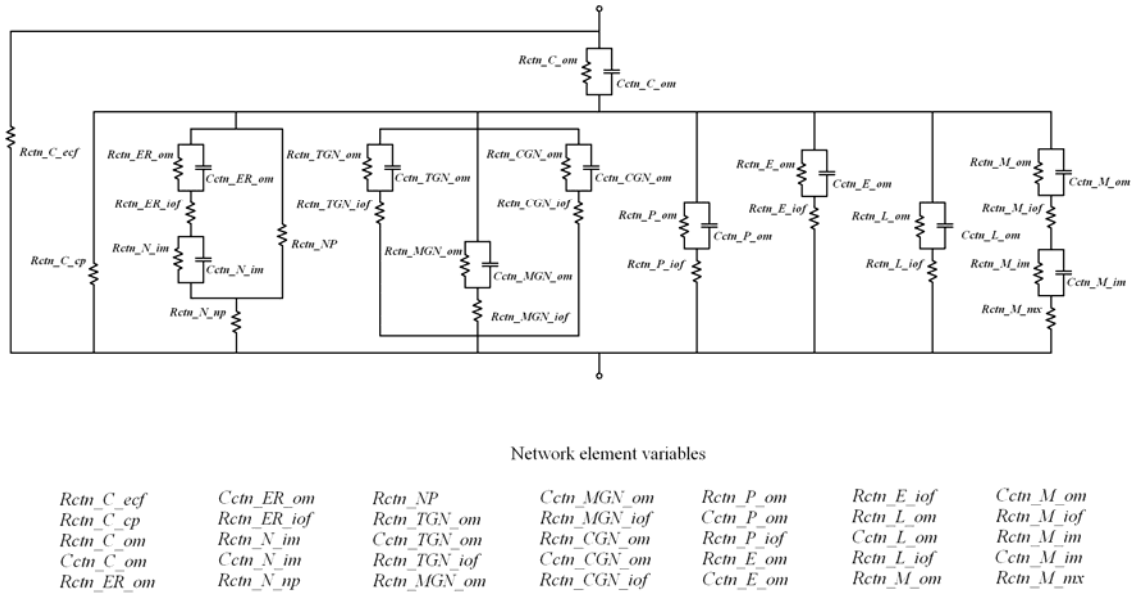

Network element variables

Rctn_C_ecf	*Cctn_ER_om*	*Rctn_NP*	*Cctn_MGN_om*	*Rctn_P_om*	*Rctn_E_iof*	*Cctn_M_om*
Rctn_C_cp	*Rctn_ER_iof*	*Rctn_TGN_om*	*Rctn_MGN_iof*	*Cctn_P_om*	*Rctn_L_om*	*Rctn_M_iof*
Rctn_C_om	*Rctn_N_im*	*Cctn_TGN_om*	*Rctn_CGN_om*	*Rctn_P_iof*	*Cctn_L_om*	*Rctn_M_im*
Cctn_C_om	*Cctn_N_im*	*Rctn_TGN_iof*	*Cctn_CGN_om*	*Rctn_E_om*	*Rctn_L_iof*	*Cctn_M_im*
Rctn_ER_om	*Rctn_N_np*	*Rctn_MGN_om*	*Rctn_CGN_iof*	*Cctn_E_om*	*Rctn_M_om*	*Rctn_M_mx*

Fig. 9-5 Circuit topology of the combined tissue network

Reducing the cell network in the lower levels of the model would come at the expense of biological meaning. Retaining this cumbersome architecture this far makes this model more powerful because one can see the effects of changing individual parameters. This detailed model can be used to predict the effects of disease when the model and real EIS measurement frequency responses are compared.

H. Tissue Network Model Development Review

In this section we combined the cell model into a matrix of repeating series and parallel cell networks to form a tissue layer of a specific cell type. Those tissue networks of specific cell types were stacked together to form a tissue resulting in parallel networks. This combined tissue model is the “Transparent Box” tissue model the model can be modified by changing the primary geometric and biochemical parameters. The network elements of the tissue model can be calculated on a worksheet referencing the required network variables from the cell model worksheet. The model has been developed fairly general and can be modified for various tissues cells and diseases. The next section will

provide the network element results and the overall frequency response of a four-layer tissue model for normal healthy oral mucosa.

X. MODEL DEVELOPMENT WITH THE MONTE CARLO METHOD

A. The Reason for Randomness

Employing the Monte Carlo method into the “Transparent Box” model more closely mimics the uncertainty of real tissue responses. The randomness of the inputs produces less deterministic outputs. The elevated uncertainty demands that the methods developed to identify the diseased tissue from healthy tissue using the impedance model be more robust. The integration of random variables will start at the most fundamental levels of the “Transparent Box” model from the simplest structural and chemical components at the organelle level through the cell level for each of the tissue layers. This section will describe the modifications to produce random values for each primary variable that were developed in prior sections.

B. Introduction to the Monte Carlo Method

Monte Carlo method is a class of computational algorithms that rely on repeated random sampling to compute their results. Monte Carlo methods are especially useful for simulating systems with many coupled degrees of freedom such as cellular structures and complex interdependent networks [102]. Monte Carlo methods are often used in computer simulations of physical and mathematical systems. These methods are most suited to calculation by a computer and tend to be used when it is infeasible to compute an exact result with a deterministic algorithm [103]. The Monte Carlo method is “less expensive” to use compared to a minimum and maximum analysis. An “expensive” analysis would be to determine the largest possible inputs that will produce the largest possible outputs. Or the smallest possible inputs that result in the smallest possible outputs. Some inputs may have inverse effects on outputs. Each of the primary variables would have to be investigated sweeping the values to find the maximum output. The max-min analysis is unpractical for several reasons and the possibility that the system

would be at these extremes is very rare [103]. In most cases systems tend to run between these extremes close to the average because of the numerous natural random processes. Designing a system based on the extremes in your model is expensive because you will have to over build your system for the extremely rare event. It is like building your home under ground out of steel and concrete to survive a direct hit from a F5 tornado (200+mph wind speed) in Arizona. An F5 tornado may touch down in Arizona in our lifetime but it is just not very probable. It's best to save money and build a home above ground to survive the more probable maximum wind speeds. In the same respect the Monte Carlo method allows for the evaluation of probable impedance responses from the "Transparent Box" model. This uncertainty demands the algorithms and procedures used to identify a disease are robust enough to predict the disease accurately for the majority of possibilities.

C. Random Generation of the Primary Variables

Each primary variable in the "Transparent Box" model will have a random value generated between a range of possible maximum and minimum values. This model was built in Microsoft Excel® but can be built in any suitable spreadsheet or mathematical software. For Microsoft Excel® the random number generator function = RAND() returns an evenly distributed random number greater than or equal to 0 and less than 1 [104]. A new random number is returned every time the worksheet is calculated. In order to calculate a random number between two arbitrary values in Excel® use the equation (10-1)

$$rand\_var = \text{RAND}()*(high\_value - low\_value) + low\_value \qquad (10\text{-}1)$$

where

rand_var is a uniform random value between highest and lowest values

high_value is the largest possible value for the random variable

low_value is the smallest possible value for the random variable

Fig. 10-1 Excel® screen shot of perioxosome radius calculation of shows how this is done in the “Transparent Box” model.

J11 = = RAND()*(J8-J9)+J9

	J	K	L	M	N
4					
5	perioxosome	perioxosome	perioxosome	perioxosome	perioxosome
6	**radius**	radius	surface	displacement	electrolyte
7	**in nm**	in M	area in M^2	vol. in M^3	vol in M^3
8	**250**	2.50E-07	7.8540E-13	6.5450E-20	6.1601E-20
9	**100**	1.00E-07	1.2566E-13	4.1888E-21	3.7060E-21
10	175.00	1.75E-07	4.56E-13	3.48E-20	3.27E-20
11	168.82	1.69E-07	3.5816E-13	2.0156E-20	1.8697E-20

Fig. 10-1 Excel® screen shot of perioxosome radius calculation

There are 256 primary variables for each tissue model; each will have a random number generating a value between the maximum and minimum values. The calculation for these others is just like this example in Fig. 10-1.

D. Complications with Randomly Generated Values

Problems may arise where a random value sequence in the model causes meaningless results. In this model there are many interconnected primary variables that determine the network values in the model. Some variables have a direct proportionality effect on output, some are inversely proportional and others have more complex relationships. For real cells there are mutually exclusive relationships between many of these variables. There are certain scenarios that will cause problems that may show up in the random

calculations that never show up in real life. One such problem is in the calculation of random variables for the mitochondria. If the random variables generator produces both large numbers for the quantity and the radius of the mitochondria then the total mitochondria displacement volume could be larger than the total volume of the cell. This scenario becomes more apparent if the random size of the cell is on the smaller size of the normal range. In real cells if you had large mitochondria there would be fewer of them required to produce the energy needs for the cell. In real cells with small mitochondria there are usually many more of them to satisfy the energy requirements. With the unrealistic result of large numbers of large sized mitochondria it produces negative electrolyte volumes and as a result negative resistances. To remedy these problems of mutual exclusivity in the model there are at least three solutions available. The first and easiest solution is to delete the results of a randomly generated solution that contains negative resistances. The more elaborate solution is to have conditional controls to prevent nonsensical answers by restricting the number or size range of random variables based on previously calculated interdependent values but this can be difficult to implement in Excel®. The third solution is to limit the ranges of the maximum and minimum allowable ranges for the random variables so that the displacement values can't be larger than the cell volume. The most effective way to fix this situation has been to use a combination of the first and third solution. It is desirable to have the largest possible allowable range for each variable especially when it comes to the diseased tissue models so reduction of the range of such variables must be tempered. Any results that do not make sense can be eliminated or ignored but it provides the best range of possibilities when the acceptable min-max variable ranges are large. For the healthy tissue model more restrictions on the normal operating range of each of the primary variables can be accepted. It can be effectively argued that the range of these variables should be tighter

(smaller) because healthy cells are supreme regulators despite inefficiencies even under non ideal conditions. Unhealthy cells on the other hand struggle to regulate under normal conditions therefore the range of allowable primary variables should be relaxed or larger than the healthy normal cells.

E. Monitoring Complications of Random Generated Values

Monitoring the results of the random variables can be done using comparative analysis as this helps troubleshoot problems. A few ways to monitor this is by using percent calculations and comparisons with the average. The cell numbers being evaluated can be mind bogglingly large or small. Relative comparisons are easier to relate too and understand so throughout the model there are comparative areas and volumes normalized by the total cell membrane area and the total volume of the cell. This way it is clear to see what percentage of the cell volume is comprised of a specific organelle or what percentage of a of a cells total membrane area is from a specific organelle.

F. Review of Model Development with the Monte Carlo Method

This section introduced the inclusion of randomness into the "Transparent Box" model with the Monte Carlo method. The Monte Carlo method provides a more realistic output compared to maximum and minimum analysis. The randomness introduced to all the primary variables is a more practical way of analysis since there are so many coupled degrees of freedom in the model where minimum and maximum events are extremely rare. This section showed how to implement the Monte Carlo method in Excel® using the RAND() function and ended with a discussion on potential errors and complications that can arise and how to avoid them.

XI. THE “TRANSPARENT BOX” MODEL

A. Normal Tissue Model Primary Variables Values

The passive element “Transparent Box” model for normal healthy oral tissue was developed in the previous sections; the formulas can be integrated into a spreadsheet or other mathematical program. The primary variable values for the normal cell model are shown in Table 11-1 and continued on Table 11-3. The primary variable name is listed on the left column. Each tissue layer has its own column pair one on the left for a maximum value and on the right for a minimum value. The random value used in the calculations will be between these two max min values. One will notice that for normal healthy cells most values are identical for each layer. The separation of layers like this becomes important for modeling diseases where only certain cell layers are affected. The units are shown following the variable name. The references for the values in the table are in the far right hand column. One may notice the primary variables that represent the organelle membrane resistance and electrolyte resistivity are uniformly the same for all types of organelles. This is for two reasons. First the primary goal of this research was to evaluate the structural effects on tissue impedance rather than biochemical and two, specific organelle membrane and intra organelle fluid resistivity for epithelial tissue have not been researched or published yet. These values can be modified in the future for the small organelle specific differences. There are over two hundred and fifty individual primary input variables in the model. This may seem redundant in the normal healthy tissue model because of the multiple cell layers but this flexibility will be required when modeling various diseased tissues. Some diseases affect the structures of only certain cell layers or a subset of certain organelles within the cells. This is the primary reason for the complexity of the model related to the multiple primary variables.

Table 11-1
PRIMARY VARIABLE VALUES FOR THE NORMAL CELL MODEL PART I

Name of Variable	Units	Tissue Layer 1 Squamous Cell		Tissue Layer 2 Cuboidal Cell		Tissue Layer 3 Columinar Cell		Tissue Layer 4 Basal Cell		Variable Value References
		Max	Min	Max	Min	Max	Min	Max	Min	
t_m	nm	5	4	5	4	5	4	5	4	[7], [9], [50], [55], [95]
MC	uF/cm^2	1.15	0.85	1.15	0.85	1.15	0.85	1.15	0.85	[48], [50], [55], [89]
r_P	nm	250	100	250	100	250	100	250	100	[9], [68], [69], [99]
ρ_P	Ohm*cm	90	75	90	75	90	75	90	75	[1], [84], [85], [99]
MR_P	MOhm/cm^2	110	90	110	90	110	90	110	90	[48], [50], [55], [89]
P_{num}		300	240	500	400	500	400	500	400	[9], [68], [69], [71], [93]
r_E	nm	100	20	100	20	100	20	100	20	[9], [68], [69], [99]
ρ_E	Ohm*cm	90	75	90	75	90	75	90	75	[1], [84], [85], [99]
MR_E	MOhm/cm^2	110	90	110	90	110	90	110	90	[48], [50], [55], [89]
E_{num}		278	240	464	400	464	400	464	400	[9], [68], [69], [71], [93]
r_L	nm	400	100	400	100	400	100	400	100	[9], [68], [69], [99]
ρ_L	Ohm*cm	90	75	90	75	90	75	90	75	[1], [84], [85], [99]
MR_L	MOhm/cm^2	110	90	110	90	110	90	110	90	[48], [50], [55], [89]
L_{num}		36	23	45	29	45	29	45	29	[9], [68], [69], [71], [93]
r_{Mim}	nm	565	180	565	180	565	180	565	180	[9], [68], [69], [81], [99]
r_{Mom}	nm	600	200	600	200	600	200	600	200	[9], [68], [69], [81], [99]
t_{Mims}	nm	35	20	35	20	35	20	35	20	[9], [68], [69], [81], [99]
ρ_{Min}	Ohm*cm	90	75	90	75	90	75	90	75	[1], [84], [85], [99]
ρ_{Mmx}	Ohm*cm	30	10	30	10	30	10	30	10	[1], [84], [85], [99]
MR_{Mom}	MOhm/cm^2	110	90	110	90	110	90	110	90	[48], [50], [55], [89]
MR_{Mim}	MOhm/cm^2	110	90	110	90	110	90	110	90	[48], [50], [55], [89]
M_{num}		200	150	400	300	400	300	400	300	[9], [68], [69], [71], [93]
l_{GMC}	um	1.10	0.90	1.10	0.90	1.10	0.90	1.10	0.90	[9], [68], [69], [99]
d_{GMC}	um	0.80	0.70	0.80	0.70	0.80	0.70	0.80	0.70	[9], [68], [69], [99]
w_{GMC}	um	0.08	0.07	0.08	0.07	0.08	0.07	0.08	0.07	[9], [68], [69], [99]
$VxCGN$		1.7	1.5	1.7	1.5	1.7	1.5	1.7	1.5	[9], [68], [69], [99]
$VxTGN$		2.2	2	2.2	2	2.2	2	2.2	2	[9], [68], [69], [99]
$AxCGN$		1.9	1.7	1.9	1.7	1.9	1.7	1.9	1.7	[9], [68], [69], [99]
$AxTGN$		2.4	2.2	2.4	2.2	2.4	2.2	2.4	2.2	[9], [68], [69], [99]
MR_{MGN}	MOhm/cm^2	110	90	110	90	110	90	110	90	[48], [50], [55], [89]
MR_{CGN}	MOhm/cm^2	110	90	110	90	110	90	110	90	[48], [50], [55], [89]
MR_{TGN}	MOhm/cm^2	110	90	110	90	110	90	110	90	[48], [50], [55], [89]

The system for naming the variables strived for clarity and brevity but with so many primary variable names there are two tables of definitions provided. The definitions for the variables in Table 11-1 are provided in Table 11-2 Primary variable definitions for the normal cell model part 1 and are listed in the same order for convenience.

Table 11-2
PRIMARY VARIABLE DEFINITIONS FOR THE NORMAL CELL MODEL PART I

t_m	is the average lipid bilayer thickness ~ 4nm
MC	is the capacitance per square centimeter of lipid membrane
r_P	is the radius of the average peroxisome organelle
ρ_P	is the resistivity of the peroxisome intra organelle fluid
MR_P	is the resistance per square centimeter of the peroxisome membrane
P_{num}	is the number of peroxisome organelles in the cell level model
r_E	is the outside radius of the average endosome organelle
ρ_E	is the resistivity of the endosome intra organelle fluid
MR_E	is the resistance per square centimeter of the endosome membrane
E_{num}	is the number of endosome organelles in the cell level model
r_L	is the radius of the average lysosome organelle
ρ_L	is the resistivity of the lysosome intra organelle fluid
MR_L	is the resistance per square centimeter of the lysosome membrane
L_{num}	is the number of lysosome organelles in the cell level model
r_{Mim}	is the mitochondria inner membrane radius
r_{Mom}	is the mitochondria outside membrane radius
t_{Mims}	is the average thickness of the mitochondria inter-membrane space
ρ_{Min}	is the resistivity of the mitochondria inter-membrane space electrolyte
ρ_{Mmx}	is the resistivity of the mitochondria matrix electrolyte
MR_{Mom}	is the resistance per cm^2 of the mitochondria's outer membrane
MR_{Mim}	is the resistance per cm^2 of the mitochondria's inner membrane
M_{num}	is the number of mitochondria organelles in the cell level model
l_{GMC}	is the length of the average Golgi medial cisterna
d_{GMC}	is the depth of the average Golgi medial cisterna
w_{GMC}	is the width of the average Golgi medial cisterna
$VxCGN$	is the CGN membrane volume multiplier
$VxTGN$	is the TGN membrane volume multiplier
$AxCGN$	is the CGN membrane surface area multiplier
$AxTGN$	is the TGN membrane surface area multiplier
MR_{MGN}	is the resistance per square centimeter of the MGN membrane
MR_{CGN}	is the resistance per square centimeter of the CGN membrane
MR_{TGN}	is the resistance per square centimeter of the TGN membrane

Table 11-3
PRIMARY VARIABLE VALUES FOR THE NORMAL CELL MODEL PART II

Name of Variable	Units	Tissue Layer 1 Squamous Cell		Tissue Layer 2 Cuboidal Cell		Tissue Layer 3 Columnar Cell		Tissue Layer 4 Basal Cell		Variable Value References
		Max	Min	Max	Min	Max	Min	Max	Min	
ρ_{MGN}	Ohm*cm	90	75	90	75	90	75	90	75	[1], [84], [85], [99]
ρ_{CGN}	Ohm*cm	90	75	90	75	90	75	90	75	[1], [84], [85], [99]
ρ_{TGN}	Ohm*cm	90	75	90	75	90	75	90	75	[1], [84], [85], [99]
G_{num}		50	24	50	24	50	24	50	24	[9], [68], [69], [71], [93]
r_{nim}	um	1.40	0.80	1.80	1.30	2.50	1.70	1.80	1.40	[9], [68], [69], [81], [99]
KV_{NER}		0.5	0.4	0.5	0.4	0.5	0.4	0.5	0.4	[9], [71], [83], [93], [94]
KA_{NER}		190	170	190	170	190	170	190	170	[9], [71], [83], [93], [94]
Mr_{erom}	MOhm/cm^2	110	90	110	90	110	90	110	90	[48], [50], [55], [89]
ρ_{er}	Ohm*cm	90	75	90	75	90	75	90	75	[9], [68], [69], [71], [93]
Mr_{nim}	MOhm/cm^2	110	90	110	90	110	90	110	90	[48], [50], [55], [77], [89]
ρ_{n}	Ohm*cm	90	75	90	75	90	75	90	75	[1], [84], [85], [99]
G_{pore}	pS	1000	750	1000	750	1000	750	1000	750	[84], [85], [78]
Npd	pores/um^2	50	40	50	40	50	40	50	40	[9], [68], [71], [83], [94]
ER_{num}		1	1	1	1	1	1	1	1	[9], [68], [71], [83], [94]
N_{num}		1	1	1	1	1	1	1	1	[9], [68], [71], [83], [94]
LS_out	um	18.00	14.00	7.00	5.60	7.00	5.60	7.00	5.60	[9], [68], [69], [71]
H_cell	um	2.80	2.20	14.00	18.00	28.00	18.00	12.00	10.00	[9], [68], [69], [71]
Eg	nm	120	50	120	50	120	50	120	50	[9], [68], [69], [71]
PCV	percent	35%	15%	15%	10%	15%	10%	15%	10%	[9], [98], [99]
$PECV$	percent	45%	18%	15%	10%	15%	10%	25%	15%	[9], [69], [71], [101]
ρ_{CP}	Ohm*cm	85	60	85	60	85	60	85	60	[1], [84], [85], [96], [99]
MR_{PM}	MOhm/cm^2	115	85	115	85	115	85	115	85	[48], [50], [55], [89]
ρ_{ef}	Ohm*cm	80	55	80	55	80	55	80	55	[1], [84], [85], [99]
Yw	cm	0.2	0.2	0.2	0.2	0.2	0.2	0.2	0.2	[50], [55], [65]
Xl	cm	0.3	0.3	0.3	0.3	0.3	0.3	0.3	0.3	[50], [55], [65]
Ncz_n		55	55	20	20	4	4	20	20	[9], [98], [99]
Zh_n	um | percent	161	20%	282	35%	112	14%	242	30%	[9], [98], [99]
$ANAm\_n$		1.00	1.00	1.00	1.00	1.00	1.00	1.00	1.00	[9], [68]
$Mimpm\_n$		1.00	1.00	1.00	1.00	1.00	1.00	1.00	1.00	[9], [68], [69], [71], [93]
$Mimrm\_n$		1.00	1.00	1.00	1.00	1.00	1.00	1.00	1.00	[9], [68], [69], [71], [93]
Nrm_n		1.00	1.00	1.00	1.00	1.00	1.00	1.00	1.00	[9], [68], [69], [71], [93]
Orm_n		1.00	1.00	1.00	1.00	1.00	1.00	1.00	1.00	[9], [68], [69], [71], [93]

The definitions for the variables in Table 11-3 are provided in Table 11-4 Primary variable definitions for the normal cell model part 2 and are listed in the same order for convenience.

Table 11-4
PRIMARY VARIABLE DEFINITIONS FOR THE NORMAL CELL MODEL PART II

ρ_{MGN}	is the resistivity of the MGN intra organelle fluid
ρ_{CGN}	is the resistivity of the CGN intra organelle fluid
ρ_{TGN}	is the resistivity of the TGN intra organelle fluid
G_{num}	is the number of Golgi organelles in the cell level model
R_{nim}	is the nuclear inner membrane radius
KV_{NER}	is the nuclear to ER volume ratio multiplier ~ 2.5
KA_{NER}	is the nuclear to ER membrane area multiplier ~ 150
Mr_{erom}	is the resistance per cm^2 of the ER's outer membrane
P_{er}	is the resistivity of the endoplasmic reticulm electrolyte
Mr_{nim}	is the resistance per cm^2 of the nucleus's inner membrane
P_n	is the resistivity of the nuclear electrolyte
G_{pore}	is the conductance of a single nuclear pore complex or nucleopore
Npd	is the nuclear pore density
ER_{num}	is the number of ER organelles in the cell level model
N_{num}	is the number of nucleus organelles in the cell level model
LS_out	is the long side outer dimension of the irregular pentagon (~ cell side)
H_cell	is the height of the irregular pentagon cylinder (~ cell height)
Eg	is the extracellular fluid gap between adjacent cells ~15 to 50nm
PCV	is the percentage of cell volume that is connective protein
$PECV$	is the percentage of extracellular volume that is connective protein
ρ_{CP}	is the resistivity of the cytoplasm
MR_{PM}	is the resistance per square centimeter of the plasma membrane
ρ_{ef}	is the resistivity of the extracellular fluid
Yw	is the width of the sample tissue calculated from probe dimensions.
Xl	is the length of the tissue cell sample calculated from probe dimensions
Ncz_n	is the number of vertical cells in the cell sample layer n
Zh_n	is the height of the tissue cell sample layer n and the percent of total tissue comprising the layer
$ANAm\_n$	is the anaplastic multiplier for cell layer n for an atrophied cell it is less than 1, for a normal cell it is 1 for a swollen cell it is greater than 1
$Mimpm\_n$	is the mitochondria inner membrane pleat multiplier for cell layer n
$Mimrm\_n$	is the mitochondria inner membrane radius multiplier for cell layer n
Nrm_n	is the nuclear inner membrane radius multiplier
Orm_n	is the organelle radius reduction multiplier it acts on all except nucleus

B. Normal Tissue Model Network Element Values

The network element values' corresponding to the primary variable values of Tables 11-1 and 11-3 is shown in Table 11-5 Resistor and capacitor network values. It's difficult to get a feel for the differences in the network elements when they are listed in table form. The data is easier to evaluate quickly when displayed in graphical form. The resistances are shown in two plots; the small resistances of the membranes and the larger resistances of the electrolytes. Fig. 11-1 Membrane resistor value element ranges for normal tissue displays the resistance of each membrane element for comparison.

Table 11-5
RESISTOR AND CAPACITOR NETWORK VALUES FOR NORMAL TISSUE

Element	value	variance +-	units	Element	value	variance +-	units	Element	value	variance +-	units
Rctn_C_om	1.342E+01	4.366E+00	Ohms	*Rctn_C_ecf*	7.186E+03	7.516E+01	Ohms	*Cctn_C_om*	6.955E-10	2.475E-10	Farads
Rcn_ER_om	6.594E+01	1.206E+01	Ohms	*Rctn_C_cp*	1.210E+03	2.298E+02	Ohms	*Cctn_ER_om*	2.884E-09	6.676E-10	Farads
Rctn_N_im	3.301E-01	1.750E-01	Ohms	*Rctn_ER_iof*	7.348E+03	2.922E+02	Ohms	*Cctn_N_im*	1.690E-11	8.376E-12	Farads
Rctn_NP	2.116E+04	1.206E+04	Ohms	*Rctn_N_np*	5.984E+03	7.005E+02	Ohms	*Cctn_TGN_om*	1.160E-10	7.202E-11	Farads
Rctn_TGN_om	1.753E-03	1.019E-04	Ohms	*Rctn_TGN_iof*	8.250E+02	2.902E+02	Ohms	*Cctn_MGN_om*	1.475E-10	8.752E-11	Farads
Rctn_MGN_om	2.297E-03	2.328E-04	Ohms	*Rctn_MGN_iof*	7.282E+02	2.902E+02	Ohms	*Cctn_CGN_om*	9.140E-11	5.743E-11	Farads
Rctn_CGN_om	1.370E-03	6.310E-05	Ohms	*Rctn_CGN_iof*	9.051E+02	3.223E+02	Ohms	*Cctn_P_om*	1.269E-10	1.049E-10	Farads
Rctn_P_om	2.154E-05	1.603E-05	Ohms	*Rctn_P_iof*	1.263E+02	5.726E+01	Ohms	*Cctn_E_om*	1.765E-11	1.677E-11	Farads
Rctn_E_om	3.012E-06	2.792E-06	Ohms	*Rctn_E_iof*	8.315E+02	5.847E+02	Ohms	*Cctn_L_om*	3.143E-11	2.961E-11	Farads
Rctn_L_om	4.521E-04	3.856E-04	Ohms	*Rctn_L_iof*	1.692E+03	1.157E+03	Ohms	*Cctn_M_om*	7.898E-10	6.981E-10	Farads
Rctn_M_om	2.195E-04	1.720E-04	Ohms	*Rctn_M_iof*	1.193E+02	5.931E+01	Ohms	*Cctn_M_im*	3.020E-09	2.698E-09	Farads
Rctn_M_im	1.258E-03	1.007E-03	Ohms	*Rctn_M_mx*	2.080E+01	4.752E+00	Ohms				

Fig. 11-2 Fluid and pore resistor value ranges for normal tissue compares the larger resistances. Fig. 11-3 shows the relative membrane capacitance value ranges for normal tissue. All of these figures have log scales because of the wide-ranging values.

The first striking observation when examining Fig. 11-1 is that many of the organelle membrane element resistors at the tissue level are on the order of milli-Ohms. Resistances this small can be practically considered short circuits relative to the other elements. A tiny resistance in series has little effect on the overall network. But a tiny resistance in parallel can have a huge effect.

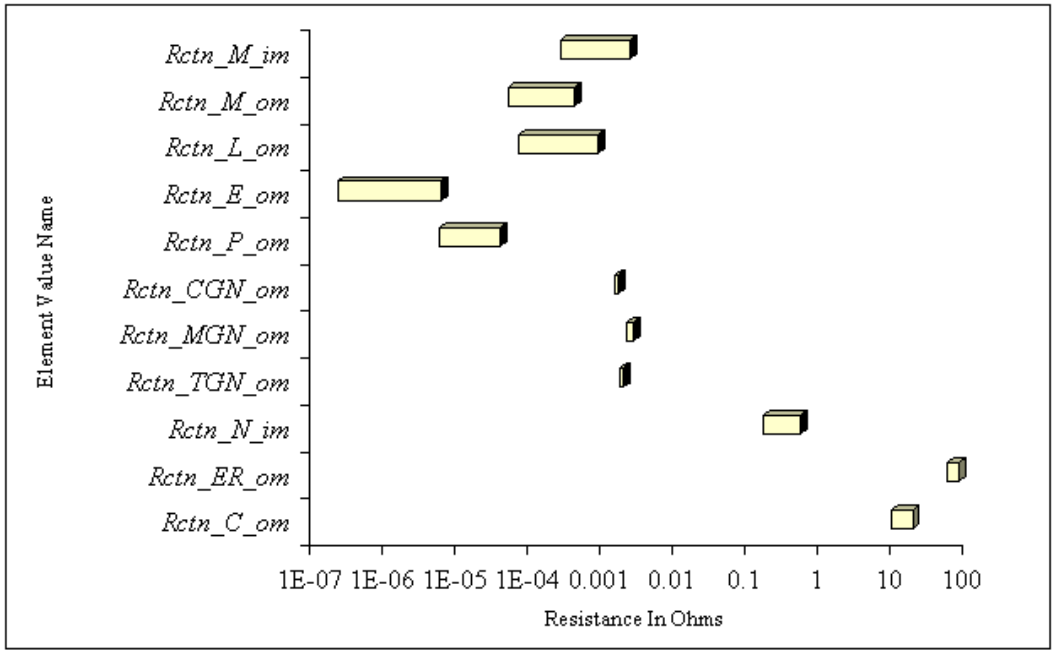

Fig. 11-1 Membrane resistor value element ranges for normal tissue

This is because elements in parallel no mater how large, become inconsequential since virtually all the current will flow into the tiny resistor. These small membrane resistances are a result of having large numbers of organelles in parallel.

Membrane resistances that are significant contributors to the network impedance are associated with organelles or parts of the cell that have fewer of them, such as the nucleus and the endoplasmic reticulum. The resistances of the intra organelle fluids are larger on the order of kilo-Ohms and will have an effect on the overall network impedance but because the organelles are in parallel with each other the overall resistance representing the cell interior will be on the order of tens of Ohms. Examining the capacitor network elements one can see the capacitances range a couple of orders of magnitude. The largest capacitance value belongs to the mitochondria inner membrane. The second largest capacitance belongs to the endoplasmic reticulum membrane.

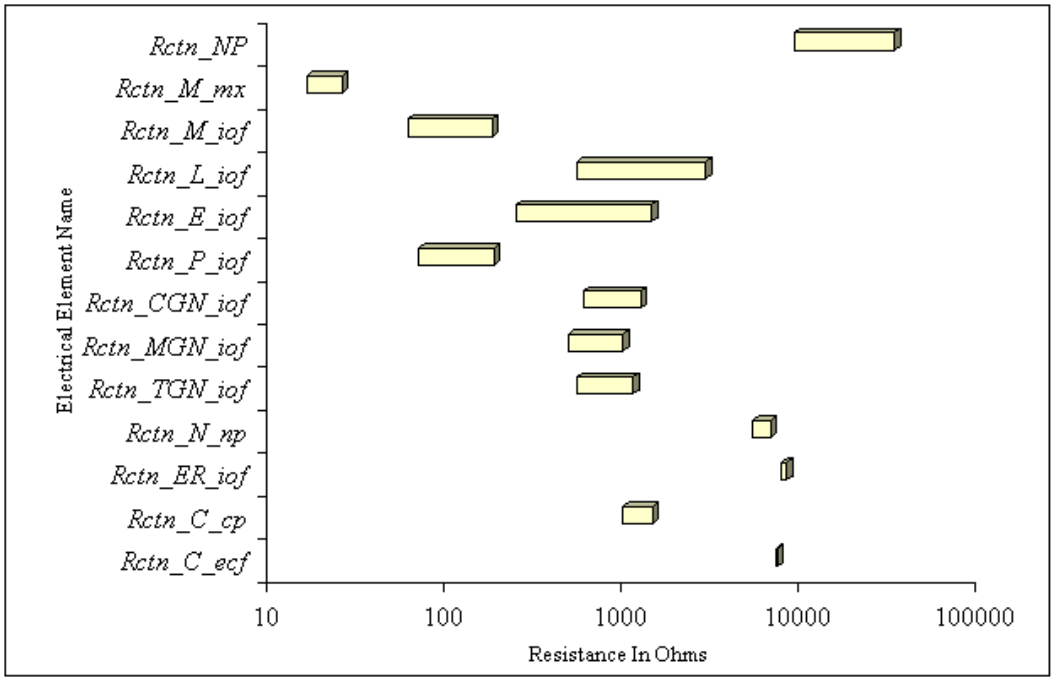

Fig. 11-2 Fluid and pore resistor value ranges for normal tissue

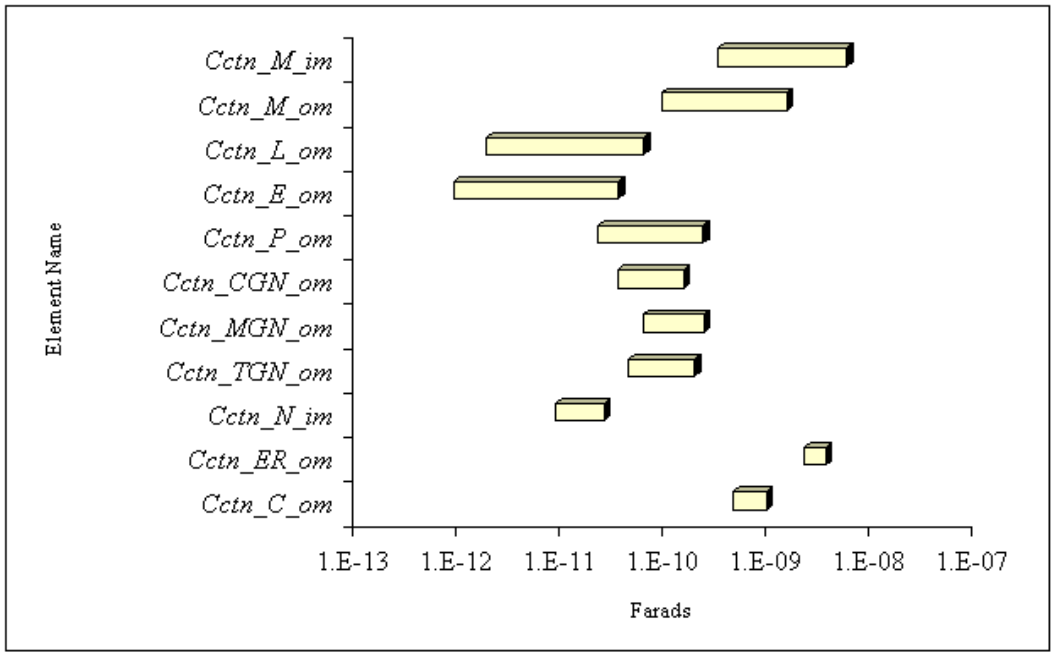

Fig. 11-3 Membrane capacitor value ranges for normal tissue

The third largest capacitance is from the mitochondria outer membrane. The fourth largest capacitance belongs to the cell outer plasma membrane.

The nuclear membrane capacitance value is tied for last with that of the peroxisome and the endosome membranes. The magnitudes of these capacitance values are deceiving. They do not determine their relative effect on the impedance. The position of the capacitances in the network has a greater effect than the relative component value. Take the mitochondria outer membrane and inner membrane capacitors; they are twice as large and ten times as large respectively as the cell outer membrane capacitor values. Yet because the mitochondria capacitors are in series as can be seen in Fig. 11-4 the overall capacitance due to the influence of the mitochondria is only 1.5 times that of the outer membrane. But the real dominating effect is from the small mitochondria membrane resistances that are in parallel with the membrane capacitance. These tiny resistances virtually short the mitochondria capacitance negating its reactive effect to the overall model.

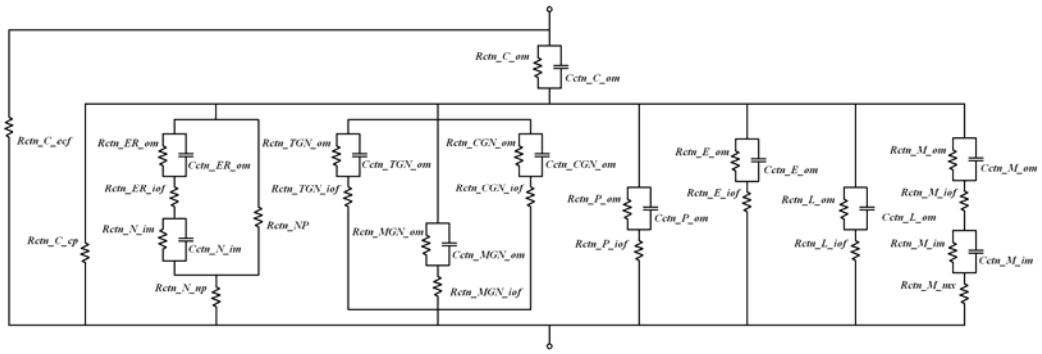

Network element variables

Rctn_C_ecf	*Cctn_ER_om*	*Rctn_NP*	*Cctn_MGN_om*	*Rctn_P_om*	*Rctn_E_iof*	*Cctn_M_om*
Rctn_C_cp	*Rctn_ER_iof*	*Rctn_TGN_om*	*Rctn_MGN_iof*	*Cctn_P_om*	*Rctn_L_om*	*Rctn_M_iof*
Rctn_C_om	*Rctn_N_im*	*Cctn_TGN_om*	*Rctn_CGN_om*	*Rctn_P_iof*	*Cctn_L_om*	*Rctn_M_im*
Cctn_C_om	*Cctn_N_im*	*Rctn_TGN_iof*	*Cctn_CGN_om*	*Rctn_E_om*	*Rctn_L_iof*	*Cctn_M_im*
Rctn_ER_om	*Rctn_N_np*	*Rctn_MGN_om*	*Rctn_CGN_iof*	*Cctn_E_om*	*Rctn_M_om*	*Rctn_M_mx*

Fig. 11-4 Normal cell tissue model network topology

It turns out the small membrane capacitance of the nucleus has a more dominant effect on the overall impedance than the large capacitances of the more numerous organelles like the mitochondria because it is not shorted by a tiny parallel resistance. The combination of the network, the variable, its location in the network and its relation to the other elements in the network determines its overall impact on the impedance of the model. Looking at relative magnitudes of elements alone will not provide a reliable indicator of elements overall effect on impedance; this is why the circuit models are evaluated as a whole.

C. Frequency Response of the Normal Tissue Model Network

The traditional plot to show tissue impedance is the Nyquist plot where the imaginary part of the impedance is plotted in the Y-axis and the real part is plotted in the X-axis. This plot is often referred to as a Cole-Cole plot after the pioneers of bio-impedance [50]. This plot is convenient for examining the ranges of the real and complex parts of the impedance. The impedance response of the network model is shown in Fig. 11-5 The Nyquist plot of the normal tissue model.

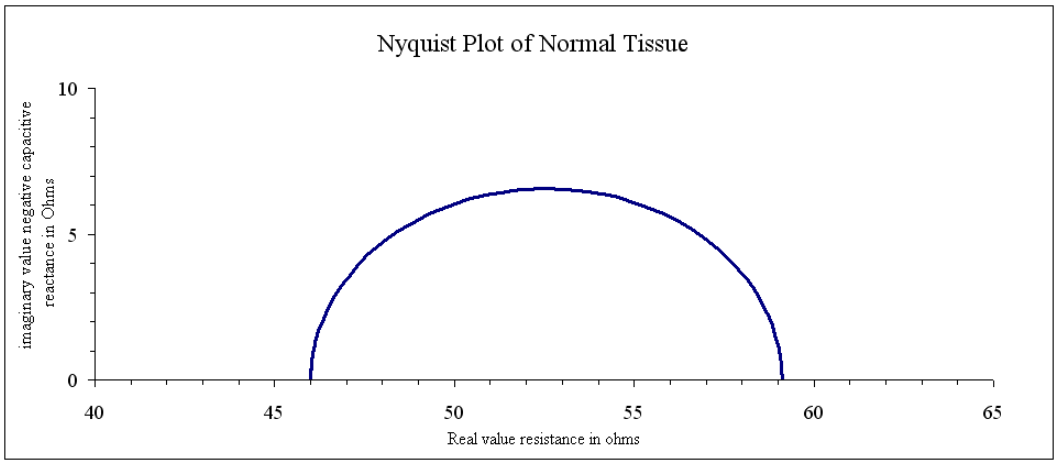

Fig. 11-5 The Nyquist plot of the normal tissue model

The impedance at low frequencies is on the farthest right of the curve and moves counter clockwise as frequency increases. Note the ranges of values for the real part (resistance in ohms) goes from a maximum of 59 Ohms to a minimum of 46 Ohms.

The frequency response of the tissue can also be shown in a Bode magnitude plot and Bode phase plot. The Bode magnitude plot provides the magnitude of the impedance as a function of frequency it's shown in Fig. 11-6 Bode magnitude plot of the normal tissue model.

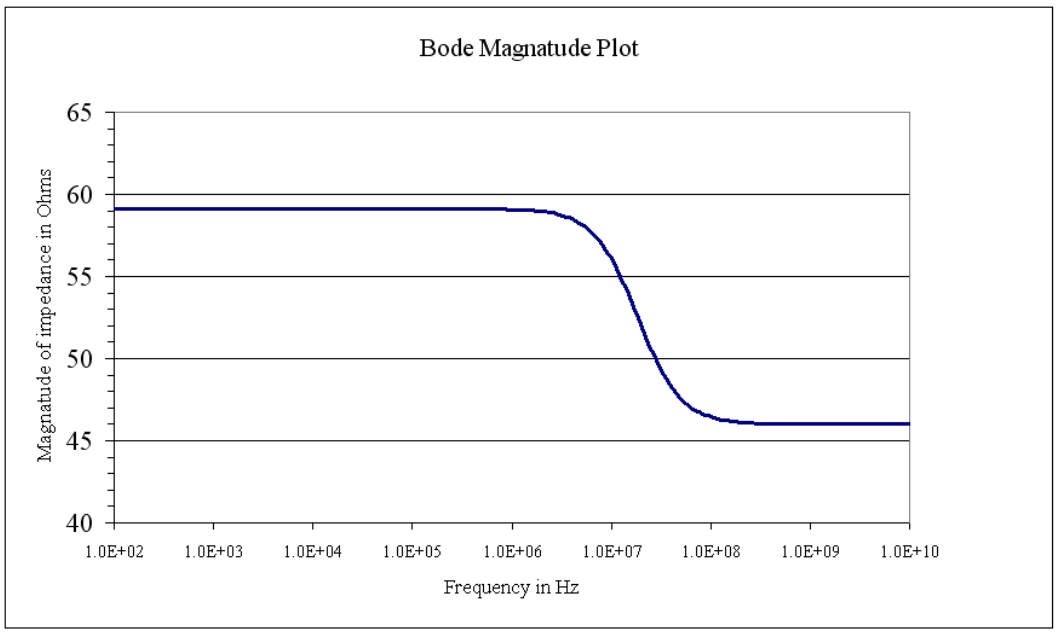

Fig. 11-6 Bode magnitude plot of the normal tissue model

The Bode phase plot provides the phase shift as a function of frequency. It is shown in Fig. 11-7 Bode phase plot of the normal tissue model. For simplicity of display the average primary variables were used to produce all three of these plots, a range of random plots would result in wider thicker looking lines where data points would overlap. Notice how it appears there is only a single dispersion this system. A single RC time constant model like the Cole model with three elements can approximate this

frequency response. The problem of course for a single RC circuit model is there is no method to examine ultra structural changes within the model so it has little biological value in this regard.

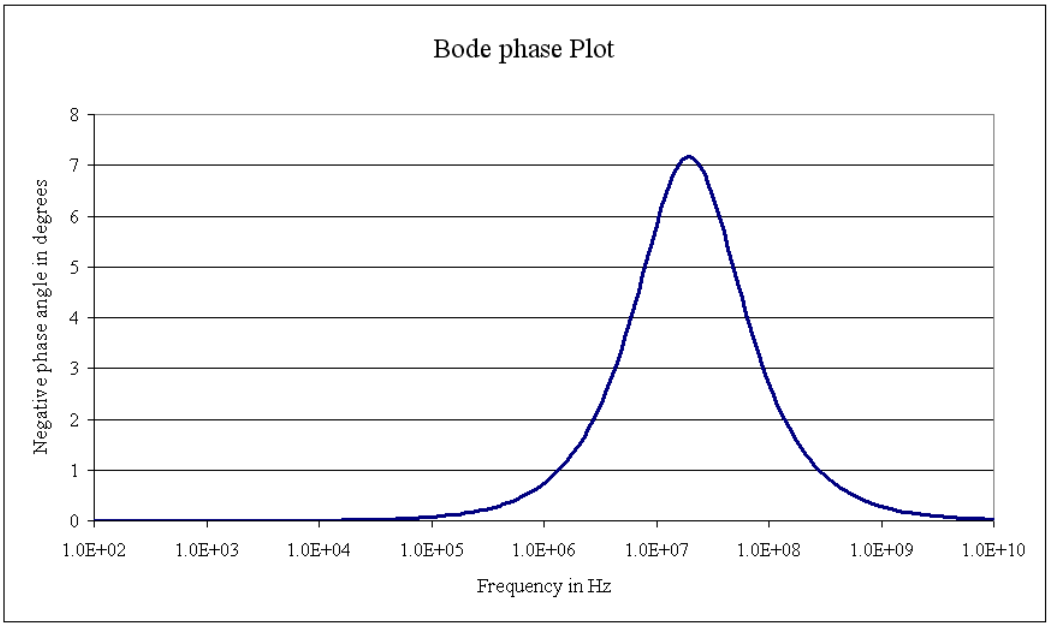

Fig. 11-7 Bode phase plot of the normal tissue model

D. The Normal Tissue "Transparent Box" Model Review

This section compiled the primary input variables and the resulting electrical network elements for the normal oral mucosa tissue impedance network model that consists of four cell layers. The layers comprise the squamous cells, cuboidal epithelial cells, columnar epithelial stem cells and the basal cells. The relative network element value ranges were examined. The frequency response output of the network was also examined in Nyquist and Bode plots. The output data from the model provides a comparative baseline for other diseased tissues. But close examination shows the model may be reduced for simplification. From an electrical engineering perspective it would be very attractive to eliminate some of the circuit elements that do not contribute to the overall

response of the circuit. This type of circuit element removal for network simplification must be done carefully. Just because a circuit element is insignificant in the normal cell model does not mean it will be true for other tissues. The power of this model is the detail available to evaluate diseased tissues and not the simplicity of evaluating and plotting the data. The next task is to modify the normal oral mucosa tissue impedance network model for diseased oral mucosal tissues such as cancer.

XII. THE "TRANSPARENT BOX" MODEL FOR DISEASED TISSUE

A. Normal Tissue Model Modifications to Model Disease

The "Transparent Box" passive element normal healthy tissue model can be easily be modified to model diseases. Most diseases affect the sub cellular structure and biochemistry of the cells and tissue. To model disease all that is needed is to modify the primary variables in the "Transparent Box" model for a normal tissue to reflect the effects of the specific disease. A convenient way to do this is to have multipliers for all the primary structural variables that may get modified in a disease. The multiplier variables were introduced in section 11 in Fig. 11-3 and are shown in Table 12-1 Tissue model modification multipliers.

Table 12-1
TISSUE MODEL MODIFICATION MULTIPLIERS

Name of Variable	Units	Tissue Layer 1 Squamous Cell		Tissue Layer 2 Cuboidal Cell		Tissue Layer 3 Columinar Cell		Tissue Layer 4 Basal Cell		Variable Value References
		Max	Min	Max	Min	Max	Min	Max	Min	
ANAm_n		1.00	1.00	1.00	1.00	1.00	1.00	1.00	1.00	[9], [69], [71]
Mimpm_n		1.00	1.00	1.00	1.00	1.00	1.00	1.00	1.00	[9], [68], [69], [71], [93]
Mimrm_n		1.00	1.00	1.00	1.00	1.00	1.00	1.00	1.00	[9], [68], [69], [71], [93]
Nrm_n		1.00	1.00	1.00	1.00	1.00	1.00	1.00	1.00	[9], [68], [69], [71], [93]
Orm_n		1.00	1.00	1.00	1.00	1.00	1.00	1.00	1.00	[9], [68], [69], [71], [93]

The multiplier will be 1 for healthy normal cell tissues and will be larger or smaller than 1 for diseased tissues. For example the nuclear radius multiplier (*Nrm_n*) will be larger than 1 typically, 2.5 to 3 for cancer cells since cancer cells have an enlarged nucleus whereas *Nrm_n* for hyperkeratosis tissue will be about 0.7 making the nucleus smaller. There is a multiplier assigned to the max value and the min value for each

variable this makes the multiplier more flexible for asymmetrical manipulation of the allowable range. Each multiplier variable will have a layer designation number *n* following the multiplier variable name. Each variable ends with a max or min designation. The max or maximum designator is the multiplier for the uppermost random variable range used in the Monte Carlo simulation. The min or minimum is the multiplier for the lowest range used in the Monte Carlo simulation. So the nuclear radius multiplier acting on the max value for tissue layer 1 will be *Nrm_1_max* to avoid confusion from layer to layer and to add flexibility in modifying the model for diseases.

The anaplasia or de-differentiation multiplier (*ANAm_n*) acts on the cell dimensional variables *LS_out* and *h_cell* in the cell level model since cancer and other diseases commonly affect the overall shape and size of a cell. There are two mitochondria multipliers since many diseases affect separate structural parts within the mitochondria. One multiplier acts on the number of inner pleats or crista in the mitochondria at the organelle level model; it is called the mitochondria inter-membrane pleat multiplier (*Mimpm_n*). The other multiplier acts on the size or length of the mitochondria crista; it is called the mitochondria inner membrane radius multiplier (*Mimrm_n*). It acts on the maximum and minimum range of the mitochondria inner membrane radius r_{Mim}. The organelle radius reduction multiplier (*Orm_n*) is a convenient way to affect the size of all the organelles at once; some diseases like cancer can shrink all the organelles in a cell. Orm_*n* acts on the all the organelle radii in the organelle level model. These multipliers make it convenient to modify primary cell values globally. A more targeted approach is to change each individual parameter for each layer and highlight the change in the spreadsheet or in the notes.

B. Cancer Type 1 Tissue Model

Cancer type 1 is a subjective level of cancer development used by pathologists to grade tumors it describes a well-differentiated squamous cell carcinoma [11, p. 6]. Cancer type 1 is the lowest grade of cancer. It features almost normal keratin and it contains cells that undergo mitoses away from the basal membrane [11 p. 9]. The primary variable values for the cancer type 1 cell model are shown in Table 12-2 Part I and are continued in Table 12-3 Part II. The primary variable name is listed on the left column. Each tissue layer has its own column thus its own unique pair of values: a maximum and a minimum value. In the calculation of the network element values a random primary value is computed for the variable between the maximum and minimum values. One will notice that most values are the same for each layer. The values that are highlighted in yellow are different from the normal healthy tissue model. In the cancer type 1 model there is an increase in the numbers of peroxisomes, endosomes and mitochondria for the first three layers of tissue [70, p.51]. The radius of each of these organelles has decreased slightly in the affected cells for the second and third tissue layers. The numbers of lysosomes has decreased in the cancer affected cell layers [70, p. 59]. The nucleus radius is larger in the affected cell layers because the DNA can no longer condense on the histones, the chromosomes have mismatches, multiple copies and are damaged resulting in the failure of the nucleus to return to normal post mitotic size [9, p. 1316], [69, pp. 14-17]. One out of ten cuboidal cells has multiple nuclei from defective mitosis [12] hence the maximum range of N_{num} is 1.1 in cell layers one through three. The endoplasmic reticulum membrane area decreases as the nucleus membrane increases [100], [101] this is shown in the model by a smaller nuclear to endoplasmic reticulum area multiplier KA_{NER}.

Table 12-2
CANCER TYPE 1 PRIMARY VARIABLE VALUES PART I

Name of Variable	Units	Tissue Layer 1 Squamous Cell		Tissue Layer 2 Cuboidal Cell		Tissue Layer 3 Columnar Cell		Tissue Layer 4 Basal Cell		Variable Value References
		Max	Min	Max	Min	Max	Min	Max	Min	
t_m	nm	5	4	5	4	5	4	5	4	[7], [9], [50], [55], [95]
MC	uF/cm^2	1.15	0.85	1.15	0.85	1.15	0.85	1.15	0.85	[48], [50], [55], [89]
r_P	nm	250	100	225	90	225	90	250	100	[9], [68], [69], [99]
ρ_P	Ohm*cm	90	75	90	75	90	75	90	75	[1], [84], [85], [99]
MR_P	MOhm/cm^2	110	90	110	90	110	90	110	90	[48], [50], [55], [89]
P_{num}		360	288	600	480	600	480	500	400	[9], [68], [69], [71], [93]
r_E	nm	100	20	90	18	90	18	100	20	[9], [68], [69], [99]
ρ_E	Ohm*cm	90	75	90	75	90	75	90	75	[1], [84], [85], [99]
MR_E	MOhm/cm^2	110	90	110	90	110	90	110	90	[48], [50], [55], [89]
E_{num}		334	288	557	480	557	480	464	400	[9], [68], [69], [71], [93]
r_L	nm	400	100	360	90	360	90	400	100	[9], [68], [69], [99]
ρ_L	Ohm*cm	90	75	90	75	90	75	90	75	[1], [84], [85], [99]
MR_L	MOhm/cm^2	110	90	110	90	110	90	110	90	[48], [50], [55], [89]
L_{num}		32	21	36	23	41	26	45	29	[9], [68], [69], [71], [93]
r_{Mim}	nm	500	144	500	336	524	304	565	180	[9], [68], [69], [81], [99]
r_{Mom}	nm	660	200	660	440	690	400	600	200	[9], [68], [69], [81], [99]
t_{Mims}	nm	35	20	35	20	35	20	35	20	[9], [68], [69], [81], [99]
ρ_{Min}	Ohm*cm	90	75	90	75	90	75	90	75	[1], [84], [85], [99]
ρ_{Mmx}	Ohm*cm	30	10	30	10	30	10	30	10	[1], [84], [85], [99]
MR_{Mom}	MOhm/cm^2	110	90	110	90	110	90	110	90	[48], [50], [55], [89]
MR_{Mim}	MOhm/cm^2	110	90	110	90	110	90	110	90	[48], [50], [55], [89]
M_{num}		260	195	480	360	480	360	400	300	[9], [68], [69], [71], [93]
l_{GMC}	um	1.10	0.90	1.10	0.90	1.10	0.90	1.10	0.90	[9], [68], [69], [99]
d_{GMC}	um	0.80	0.70	0.80	0.70	0.80	0.70	0.80	0.70	[9], [68], [69], [99]
w_{GMC}	um	0.08	0.07	0.08	0.07	0.08	0.07	0.08	0.07	[9], [68], [69], [99]
$VxCGN$		1.7	1.5	1.7	1.5	1.7	1.5	1.7	1.5	[9], [68], [69], [99]
$VxTGN$		2.2	2	2.2	2	2.2	2	2.2	2	[9], [68], [69], [99]
$AxCGN$		1.9	1.7	1.9	1.7	1.9	1.7	1.9	1.7	[9], [68], [69], [99]
$AxTGN$		2.4	2.2	2.4	2.2	2.4	2.2	2.4	2.2	[9], [68], [69], [99]
MR_{MGN}	MOhm/cm^2	110	90	110	90	110	90	110	90	[48], [50], [55], [89]
MR_{CGN}	MOhm/cm^2	110	90	110	90	110	90	110	90	[48], [50], [55], [89]
MR_{TGN}	MOhm/cm^2	110	90	110	90	110	90	110	90	[48], [50], [55], [89]

Table 12-3
CANCER TYPE 1 PRIMARY VARIABLE VALUES PART II

Name of Variable	Units	Tissue Layer 1 Squamous Cell		Tissue Layer 2 Cuboidal Cell		Tissue Layer 3 Columinar Cell		Tissue Layer 4 Basal Cell		Variable Value References
		Max	Min	Max	Min	Max	Min	Max	Min	
ρ_{MGN}	Ohm*cm	90	75	90	75	90	75	90	75	[1], [84], [85], [99]
ρ_{CGN}	Ohm*cm	90	75	90	75	90	75	90	75	[1], [84], [85], [99]
ρ_{TGN}	Ohm*cm	90	75	90	75	90	75	90	75	[1], [84], [85], [99]
G_{num}		50	24	50	24	50	24	50	24	[9], [68], [69], [71], [93]
r_{nim}	um	1.23	1.06	2.34	2.03	3.25	2.21	1.80	1.40	[9], [68], [69], [81], [99]
KV_{NER}		0.5	0.4	0.5	0.4	0.5	0.4	0.5	0.4	[9], [71], [83], [93], [94]
KA_{NER}		195	175	127	114	127	114	190	170	[9], [71], [83], [93], [94]
Mr_{erom}	MOhm/cm^2	110	90	110	90	110	90	110	90	[48], [50], [55], [89]
ρ_{er}	Ohm*cm	90	75	90	75	90	75	90	75	[9], [68], [69], [71], [93]
Mr_{nim}	MOhm/cm^2	110	90	110	90	110	90	110	90	[48], [50], [55], [77], [89]
ρ_{n}	Ohm*cm	90	75	90	75	90	75	90	75	[1], [84], [85], [99]
G_{pore}	pS	1000	750	2000	1000	2000	1000	1000	750	[84], [85], [78]
Npd	pores/um^2	50	40	50	40	50	40	50	40	[9], [68], [71], [83], [94]
ER_{num}		1	1	1.05	1	1	1	1	1	[9], [68], [71], [83], [94]
N_{num}		1.1	1.01	1.1	1.05	1.1	1.01	1	1	[9], [68], [71], [83], [94]
LS_out	um	18.00	14.00	7.00	5.60	7.00	5.60	7.00	5.60	[9], [68], [69], [71]
H_cell	um	2.80	2.20	14.00	18.00	28.00	18.00	12.00	10.00	[9], [68], [69], [71]
Eg	nm	120	50	120	50	120	50	120	50	[9], [68], [69], [71]
PCV	percent	30%	10%	12%	8%	15%	10%	15%	10%	[9], [98], [99]
$PECV$	percent	40%	18%	12%	8%	15%	10%	25%	15%	[9], [69], [71], [101]
ρ_{CP}	Ohm*cm	85	60	85	60	85	60	85	60	[1], [84], [85], [96], [99]
MR_{PM}	MOhm/cm^2	110	90	110	90	110	90	110	90	[48], [50], [55], [89]
ρ_{ef}	Ohm*cm	80	55	80	55	80	55	80	55	[1], [84], [85], [99]
Yw	cm	0.2	0.2	0.2	0.2	0.2	0.2	0.2	0.2	[50], [55], [65]
Xl	cm	0.3	0.3	0.3	0.3	0.3	0.3	0.3	0.3	[50], [55], [65]
Ncz_n		45	45	30	30	4	4	20	20	[9], [98], [99]
Zh_n	um | percent	131	14%	424	47%	112	12%	242	27%	[9], [98], [99]
$ANAm\_n$		1.00	1.00	1.00	1.00	1.00	1.00	1.00	1.00	[9], [68]
$Mimpm\_n$		0.80	0.80	0.80	0.80	0.80	0.80	1.00	1.00	[9], [68], [69], [71], [93]
$Mimrm\_n$		0.80	0.80	0.80	0.80	0.80	0.80	1.00	1.00	[9], [68], [69], [71], [93]
Nrm_n		1.10	1.10	1.30	1.30	1.30	1.30	1.00	1.00	[9], [68], [69], [71], [93]
Orm_n		1.00	1.00	0.90	0.90	0.90	0.90	1.00	1.00	[9], [68], [69], [71], [93]

The protein volume in the cell decreases as large keratin fiber production is decreased and replaced by the ramped up expression of smaller fibers such as actin and myosin [69, p. 7], [70, p.152]. This change in connective protein affects the displacement of cytoplasm. The primary variable reflecting the change in displacement is the protein cell volume variable *PCV,* note it is 15% lower than the *PCV* of normal squamous and cuboidal cells. There is a reduction in the extracellular connective proteins too; this is shown in the model by a lower *PECV* in the first three layers of the model. The decrease in keratin makes the tissue feel softer. Pathologists report tumors are said to be noticeably more elastic from the keratin replacement by actin [12]. The number of cells making up the squamous cell layer decreases while the number of cuboidal shaped cells increases over normal [9, p. 1319-1320]. In the model the height of each layer or relative thickness of each layer changes with progression of the disease. This cancer type 1 model shows that the squamous cell layer has shrunk by 10 cells while the cuboidal epithelial cells have increased by 10 cells. This changes the relative heights for each layer *Zh_n.* The cells at the squamous layer still show terminal differentiation from the cuboidal cells [11, p. 9] so the overall dimensions of the cells still remain the same. The conductance of the nuclear pores for the affected cancer cells increases due to structural damage caused by the disease [77-78]. This can be seen in layer two and three with a G_{pore} twice as large as a healthy normal cell. The maximum number of endoplasmic reticulum organelles increases to a value of 1.05 in the second tissue layer. This translates to one out of twenty cells has an additional endoplasmic reticulum. The cells with multiple endoplasmic reticulum are a result of malfunctioning mitosis in cells with multiple nuclei.

In the cancer affected cell layers the mitochondria have reduced number and size of crista [69, p. 12]. This is implemented in the model by reduced mitochondria inner membrane pleat multiplier *Mimpm_n* and a reduced mitochondria inner membrane radius

multiplier *Mimrm_n.* The cancer cells have an increase in organelle numbers but the size of those organelles is smaller and is controlled in the model by a smaller organelle radius multiplier *Orm_n* for the affected tissue layers.

This cancer has not developed past the basal membrane so the basal cell layer organelle numbers remain the same as that of the normal tissue. The absence of highlighting in the forth column of Table 12-2 and 12-3 also shows that the cancer is contained.

The resulting resistor and capacitor network element values for cancer type 1 corresponding to the primary element variables in Tables 12-2 and 12-3 are shown in Table 12-4 Cancer type 1 network element values. It is difficult to compare the relative magnitudes of these network values in a table so Fig. 12-1 through Fig. 12-3 provides a graphical method to compare the magnitude and range of possible network values for the model.

Table 12-4
CANCER TYPE 1 NETWORK ELEMENT VALUES

Element	value	variance +-	units	Element	value	variance +-	units	Element	value	variance +-	units
Rctn_C_om	1.242E+01	3.230E+00	Ohms	*Rctn_C_ecf*	5.772E+03	8.835E+01	Ohms	*Cctn_C_om*	6.473E-10	2.209E-10	Farads
Rcn_ER_om	3.217E+01	4.933E+00	Ohms	*Rctn_C_cp*	1.321E+03	3.351E+02	Ohms	*Cctn_ER_om*	1.490E-09	3.237E-10	Farads
Rctn_N_im	3.719E-01	8.653E-02	Ohms	*Rctn_ER_iof*	9.641E+03	4.059E+02	Ohms	*Cctn_N_im*	2.620E-11	9.168E-12	Farads
Rctn_NP	8.894E+03	4.877E+03	Ohms	*Rctn_N_np*	4.579E+03	1.237E+02	Ohms	*Cctn_TGN_om*	1.160E-10	7.202E-11	Farads
Rctn_TGN_om	1.753E-03	1.019E-04	Ohms	*Rctn_TGN_iof*	8.250E+02	2.902E+02	Ohms	*Cctn_MGN_om*	1.475E-10	8.752E-11	Farads
Rctn_MGN_om	2.297E-03	2.328E-04	Ohms	*Rctn_MGN_iof*	7.282E+02	2.902E+02	Ohms	*Cctn_CGN_om*	9.140E-11	5.743E-11	Farads
Rctn_CGN_om	1.370E-03	6.310E-05	Ohms	*Rctn_CGN_iof*	9.051E+02	3.223E+02	Ohms	*Cctn_P_om*	1.408E-10	1.165E-10	Farads
Rctn_P_om	1.828E-05	1.415E-05	Ohms	*Rctn_P_iof*	1.131E+02	5.130E+01	Ohms	*Cctn_E_om*	1.959E-11	1.861E-11	Farads
Rctn_E_om	2.257E-06	2.092E-06	Ohms	*Rctn_E_iof*	7.257E+02	5.120E+02	Ohms	*Cctn_L_om*	2.670E-11	2.516E-11	Farads
Rctn_L_om	4.601E-04	3.924E-04	Ohms	*Rctn_L_iof*	1.930E+03	1.320E+03	Ohms	*Cctn_M_om*	1.251E-09	9.401E-10	Farads
Rctn_M_om	2.098E-04	1.512E-04	Ohms	*Rctn_M_iof*	5.956E+01	2.340E+01	Ohms	*Cctn_M_im*	2.895E-09	2.237E-09	Farads
Rctn_M_im	6.014E-04	4.314E-04	Ohms	*Rctn_M_mx*	1.426E+01	1.150E-01	Ohms				

Each graphic shows a logarithmic x-axis because the wide ranging values. Fig. 12-1 Membrane resistor value ranges for cancer type 1 shows how small the organelle membranes are and how they relate to each other.

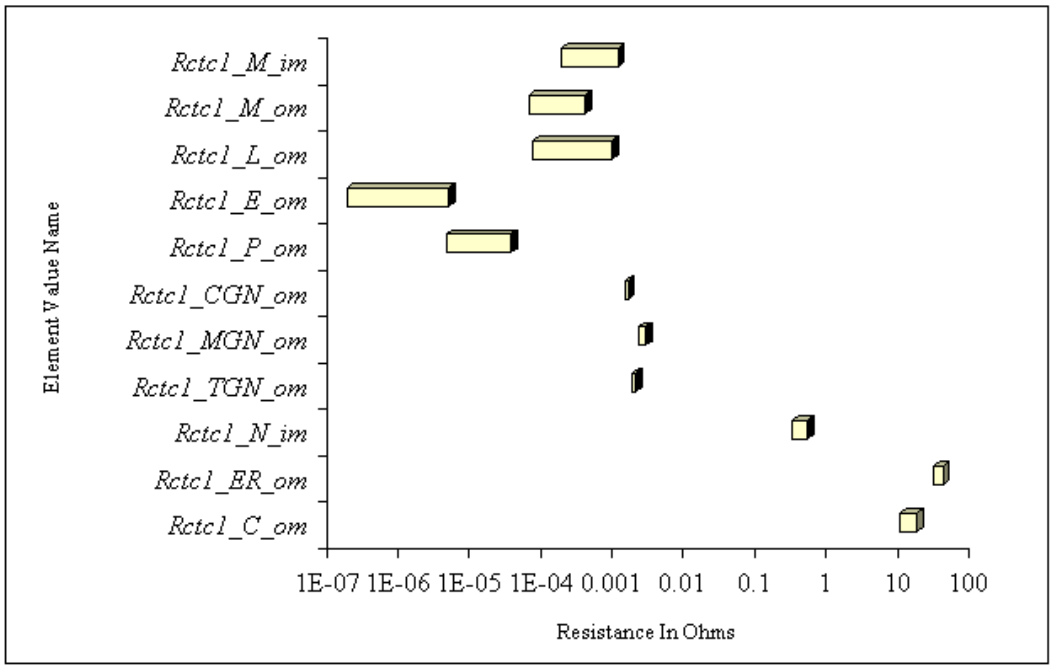

Fig. 12-1 Membrane resistor value ranges for cancer type 1

Fig. 12-2 Fluid and pore resistor value ranges for cancer type 1 shows they are much larger relative to the membrane resistors but range over three decades verses eight decades for the membranes. Fig. 12-3 Membrane capacitor value ranges for cancer type 1 shows the ranges vary within three decades.

The absolute value and range of a network element does not in itself demonstrate the effect it has on the “Transparent Box” model. A large value for a resistor or capacitor does not mean that it will dominate the output. The location of the element in the electrical network and its value will determine the relative dominance or importance of an element in the output of the model.

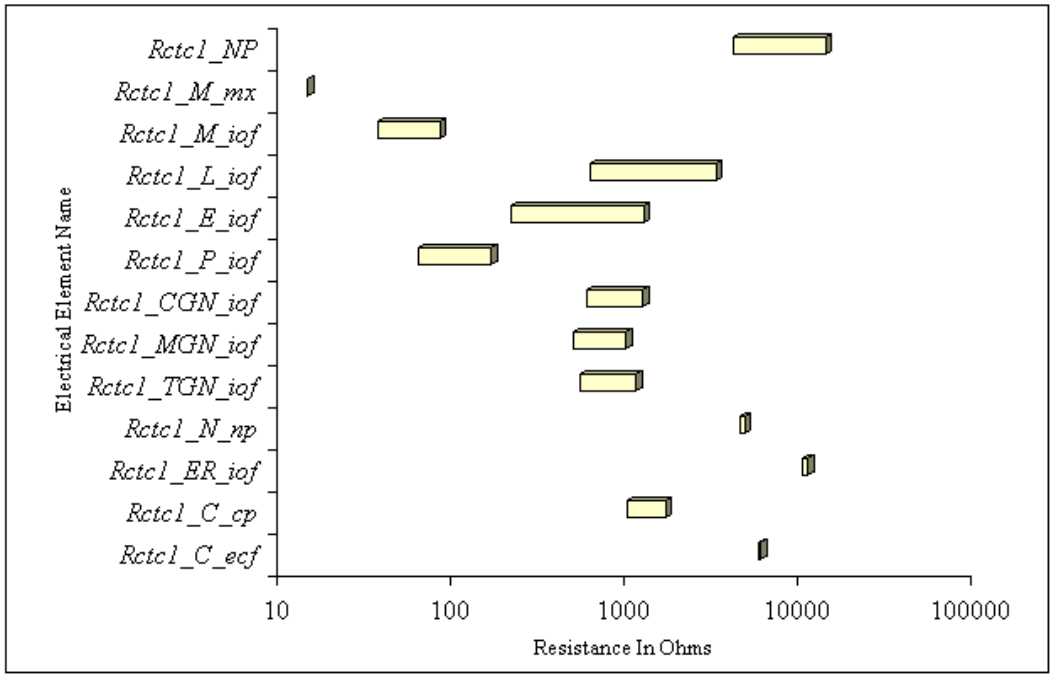

Fig. 12-2 Fluid and pore resistor value ranges for cancer type 1

A more meaningful comparison of individual network element values will be seen in the next chapter where a direct comparison of network elements from each tissue model will be compared side by side.

The impedance response or frequency response of the cancer type 1 model will be investigated after introducing the primary variable changes and network element values for the rest of the diseases. The impedance response will be plotted on a common Nyquist, Bode magnitude and Bode phase plot for comparison with normal tissue and all the other diseases modeled in this research. There will be other graphical comparisons and tools introduced used to help identify the differences in the various diseases. These other diseases include cancer types 2 and 3, hyperkeratosis, inflammation, and hyperkeratosis combined with cancer type 2.

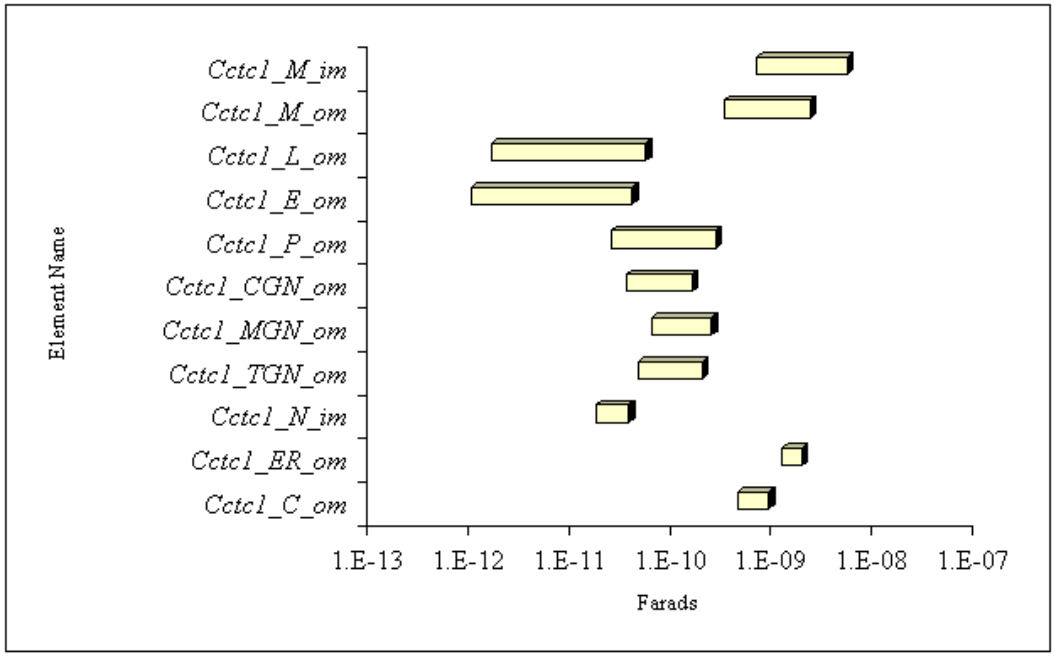

Fig. 12-3 Membrane capacitor value ranges for cancer type 1

C. Cancer Type 2 Tissue Model

Cancer type 2 is also a subjective level of cancer development used by pathologists to grade tumors as it describes moderately differentiated squamous cell carcinoma [11, p. 6]. Cancer type 2 is the medium grade of cancer because it features considerable pleomorphism, less squamous differentiation and it contains moderate mitoses distributed throughout the tissue and away from the basal membrane [11 p. 9]. The cancer type 2 primary variable values are shown in Table 12-5 Part I and are continued on Table 12-6 Part II. Again the highlighted values are different from normal healthy tissue values. One may notice like cancer type 1 there is an increase in the numbers of peroxisomes, endosomes and mitochondria for the first three layers of tissue [70, p.51]. While the number of lysosomes in the cancer affected cell layers has decreased [70, p. 59]. Like cancer type 1 the nucleus radius is on average larger in the affected cell layers because the DNA in the nucleus can no longer condense on the histones, the chromosomes

themselves have mismatches, multiple copies and are damaged resulting in the failure of the nucleus to return to normal pre mitotic and pre cancer size, number and shape [9, p. 1316], [69, pp. 14-17]. Approximately one out of ten cuboidal cells will have multiple nuclei [12] hence N_{num} is 1.1 in cell layer two. The endoplasmic reticulum membrane area decreases as the nucleus membrane increases [100], [101]. This is shown in the model by a smaller nuclear to endoplasmic reticulum area multiplier $KA_{NER.}$ The protein volume in the cell is lower than in cancer type 1 as large keratin fiber production is further replaced by smaller fibers of actin and myosin [69, p. 7], [70, p.152]. This change in protein affects the displacement of cytoplasm. The primary variable reflecting the change in displacement is the protein cell volume variable *PCV*. There is a reduction in the extracellular connective proteins too; this is shown in the model by a lower *PECV* in the first three layers of the model. The decrease in keratin makes the tissue feel softer as pathologists report tumors are said to be noticeably more elastic from the keratin replacement by actin [12]. The drastic decrease in structural protein makes the tissue easy to rupture with moderate sheer forces. This makes the tissue tend to look red, tender and easy to bleed [12]. The electrical effect of a decrease in structural protein volume is an increase in electrolyte volume increasing charge carrier availability. The number of cells making up the squamous cell layer decreases even more than cancer type 1, thinning this layer while the number of cuboidal shaped cells increases [9, p. 1319-1320]. The cells at the squamous layer show only moderate differentiation from the cuboidal cells [11, p. 9]. The mitochondria have reduced number and size of crista like cancer type 1 in the affected cell layers [69, p. 12].

Table 12-5
CANCER TYPE 2 PRIMARY VARIABLE VALUES PART I

Name of Variable	Units	Tissue Layer 1 Squamous Cell		Tissue Layer 2 Cuboidal Cell		Tissue Layer 3 Columinar Cell		Tissue Layer 4 Basal Cell		Variable Value References
		Max	Min	Max	Min	Max	Min	Max	Min	
t_m	nm	5	4	5	4	5	4	5	4	[7], [9], [50], [55], [95]
MC	uF/cm^2	1.15	0.85	1.15	0.85	1.15	0.85	1.15	0.85	[48], [50], [55], [89]
r_P	nm	225	85	213	80	213	80	250	100	[9], [68], [69], [99]
ρ_P	Ohm*cm	90	75	90	75	90	75	90	75	[1], [84], [85], [99]
MR_P	MOhm/cm^2	110	90	110	90	110	90	110	90	[48], [50], [55], [89]
P_{num}		360	288	650	520	550	440	500	400	[9], [68], [69], [71], [93]
r_E	nm	90	17	85	16	85	16	100	20	[9], [68], [69], [99]
ρ_E	Ohm*cm	90	75	90	75	90	75	90	75	[1], [84], [85], [99]
MR_E	MOhm/cm^2	110	90	110	90	110	90	110	90	[48], [50], [55], [89]
E_{num}		334	288	603	520	510	440	464	400	[9], [68], [69], [71], [93]
r_L	nm	360	85	340	80	340	80	400	100	[9], [68], [69], [99]
ρ_L	Ohm*cm	90	75	90	75	90	75	90	75	[1], [84], [85], [99]
MR_L	MOhm/cm^2	110	90	110	90	110	90	110	90	[48], [50], [55], [89]
L_{num}		32	21	32	20	41	26	45	29	[9], [68], [69], [71], [93]
r_{Mim}	nm	452	144	491	273	491	273	565	180	[9], [68], [69], [81], [99]
r_{Mom}	nm	600	200	690	440	690	440	600	200	[9], [68], [69], [81], [99]
t_{Mims}	nm	35	20	35	20	35	20	35	20	[9], [68], [69], [81], [99]
ρ_{Min}	Ohm*cm	90	75	90	75	90	75	90	75	[1], [84], [85], [99]
ρ_{Mmx}	Ohm*cm	30	10	30	10	30	10	30	10	[1], [84], [85], [99]
MR_{Mom}	MOhm/cm^2	110	90	110	90	110	90	110	90	[48], [50], [55], [89]
MR_{Mim}	MOhm/cm^2	110	90	110	90	110	90	110	90	[48], [50], [55], [89]
M_{num}		260	195	500	375	440	330	400	300	[9], [68], [69], [71], [93]
l_{GMC}	um	1.10	0.90	1.10	0.90	1.10	0.90	1.10	0.90	[9], [68], [69], [99]
d_{GMC}	um	0.80	0.70	0.80	0.70	0.80	0.70	0.80	0.70	[9], [68], [69], [99]
w_{GMC}	um	0.07	0.06	0.08	0.07	0.08	0.07	0.08	0.07	[9], [68], [69], [99]
$VxCGN$		1.7	1.5	1.7	1.5	1.7	1.5	1.7	1.5	[9], [68], [69], [99]
$VxTGN$		2.2	2	2.2	2	2.2	2	2.2	2	[9], [68], [69], [99]
$AxCGN$		1.9	1.7	1.9	1.7	1.9	1.7	1.9	1.7	[9], [68], [69], [99]
$AxTGN$		2.4	2.2	2.4	2.2	2.4	2.2	2.4	2.2	[9], [68], [69], [99]
MR_{MGN}	MOhm/cm^2	110	90	110	90	110	90	110	90	[48], [50], [55], [89]
MR_{CGN}	MOhm/cm^2	110	90	110	90	110	90	110	90	[48], [50], [55], [89]
MR_{TGN}	MOhm/cm^2	110	90	110	90	110	90	110	90	[48], [50], [55], [89]

Table 12-6
CANCER TYPE 2 PRIMARY VARIABLE VALUES PART II

Name of Variable	Units	Tissue Layer 1 Squamous Cell		Tissue Layer 2 Cuboidal Cell		Tissue Layer 3 Columinar Cell		Tissue Layer 4 Basal Cell		Variable Value References
		Max	Min	Max	Min	Max	Min	Max	Min	
ρ_{MGN}	Ohm*cm	90	75	90	75	90	75	90	75	[1], [84], [85], [99]
ρ_{CGN}	Ohm*cm	90	75	90	75	90	75	90	75	[1], [84], [85], [99]
ρ_{TGN}	Ohm*cm	90	75	90	75	90	75	90	75	[1], [84], [85], [99]
G_{num}		50	24	50	24	50	24	50	24	[9], [68], [69], [71], [93]
r_{nim}	um	1.23	1.06	2.59	2.18	3.60	2.38	1.80	1.40	[9], [68], [69], [81], [99]
KV_{NER}		0.5	0.4	0.5	0.4	0.5	0.4	0.5	0.4	[9], [71], [83], [93], [94]
KA_{NER}		190	170	85.5	76.5	85.5	76.5	190	170	[9], [71], [83], [93], [94]
Mr_{erom}	MOhm/cm^2	110	90	110	90	110	90	110	90	[48], [50], [55], [89]
ρ_{er}	Ohm*cm	90	75	90	75	90	75	90	75	[9], [68], [69], [71], [93]
Mr_{nim}	MOhm/cm^2	110	90	110	90	110	90	110	90	[48], [50], [55], [77], [89]
ρ_{n}	Ohm*cm	90	75	90	75	90	75	90	75	[1], [84], [85], [99]
G_{pore}	pS	1000	750	3000	1000	3000	1000	1000	750	[84], [85], [78]
Npd	pores/um^2	50	40	50	40	50	40	50	40	[9], [68], [71], [83], [94]
ER_{num}		1	1	1.08	1	1	1	1	1	[9], [68], [71], [83], [94]
N_{num}		1.1	1.01	1.1	1.08	1.1	1.01	1	1	[9], [68], [71], [83], [94]
LS_out	um	18.00	14.00	7.00	5.60	7.00	5.60	7.00	5.60	[9], [68], [69], [71]
H_cell	um	2.80	2.20	14.00	18.00	28.00	18.00	12.00	10.00	[9], [68], [69], [71]
Eg	nm	120	50	120	50	120	50	120	50	[9], [68], [69], [71]
PCV	percent	30%	10%	10%	6%	12%	8%	15%	10%	[9], [98], [99]
$PECV$	percent	40%	18%	10%	6%	12%	10%	25%	15%	[9], [69], [71], [101]
ρ_{CP}	Ohm*cm	85	60	85	60	85	60	85	60	[1], [84], [85], [96], [99]
MR_{PM}	MOhm/cm^2	110	90	110	90	110	90	110	90	[48], [50], [55], [89]
ρ_{ef}	Ohm*cm	80	55	80	55	80	55	80	55	[1], [84], [85], [99]
Yw	cm	0.2	0.2	0.2	0.2	0.2	0.2	0.2	0.2	[50], [55], [65]
Xl	cm	0.3	0.3	0.3	0.3	0.3	0.3	0.3	0.3	[50], [55], [65]
Ncz_n		35	35	42	42	3	3	20	20	[9], [98], [99]
Zh_n	um | percent	102	10%	593	58%	84	8%	242	24%	[9], [98], [99]
$ANAm\_n$		1.00	1.00	1.00	1.00	1.00	1.00	1.00	1.00	[9], [68]
$Mimpm\_n$		0.80	0.80	0.75	0.65	0.75	0.65	1.00	1.00	[9], [68], [69], [71], [93]
$Mimrm\_n$		0.80	0.80	0.75	0.65	0.75	0.65	1.00	1.00	[9], [68], [69], [71], [93]
Nrm_n		1.10	1.10	1.80	1.40	1.80	1.40	1.00	1.00	[9], [68], [69], [71], [93]
Orm_n		0.90	0.85	0.85	0.80	0.85	0.80	1.00	1.00	[9], [68], [69], [71], [93]

The deformed mitochondria crista is implemented in the model with a reduced mitochondria inner membrane pleat multiplier *Mimpm_n* and a reduced mitochondria inner membrane radius multiplier *Mimrm_n.* Like cancer type 1 this cancer has not developed past the basal membrane yet but the growing cancer cells crowd out the basal layer and this is reflected in the model by a lower number of cells comprising the fourth layer. The organelle numbers in the forth layer still remain the same as that of the normal cell model. The network element values for cancer type 2 corresponding to the primary element variables in Tables 12-5 and 12-6 are shown in Table 12-7 Cancer type 2 resistor and capacitor network element values.

Table 12-7
CANCER 2 NETWORK ELEMENT VALUES

Element	value	variance +-	units	Element	value	variance +-	units	Element	value	variance +-	units
Rctn_C_om	1.242E+01	3.230E+00	Ohms	*Rctn_C_ecf*	5.772E+03	8.835E+01	Ohms	*Cctn_C_om*	6.473E-10	2.209E-10	Farads
Rcn_ER_om	3.217E+01	4.933E+00	Ohms	*Rctn_C_cp*	1.321E+03	3.351E+02	Ohms	*Cctn_ER_om*	1.490E-09	3.237E-10	Farads
Rctn_N_im	3.719E-01	8.653E-02	Ohms	*Rctn_ER_iof*	9.641E+03	4.059E+02	Ohms	*Cctn_N_im*	2.620E-11	9.168E-12	Farads
Rctn_NP	8.894E+03	4.877E+03	Ohms	*Rctn_N_np*	4.579E+03	1.237E+02	Ohms	*Cctn_TGN_om*	1.160E-10	7.202E-11	Farads
Rctn_TGN_om	1.753E-03	1.019E-04	Ohms	*Rctn_TGN_iof*	8.250E+02	2.902E+02	Ohms	*Cctn_MGN_om*	1.475E-10	8.752E-11	Farads
Rctn_MGN_om	2.297E-03	2.328E-04	Ohms	*Rctn_MGN_iof*	7.282E+02	2.902E+02	Ohms	*Cctn_CGN_om*	9.140E-11	5.743E-11	Farads
Rctn_CGN_om	1.370E-03	6.310E-05	Ohms	*Rctn_CGN_iof*	9.051E+02	3.223E+02	Ohms	*Cctn_P_om*	1.408E-10	1.165E-10	Farads
Rctn_P_om	1.828E-05	1.415E-05	Ohms	*Rctn_P_iof*	1.131E+02	5.130E+01	Ohms	*Cctn_E_om*	1.959E-11	1.861E-11	Farads
Rctn_E_om	2.257E-06	2.092E-06	Ohms	*Rctn_E_iof*	7.257E+02	5.120E+02	Ohms	*Cctn_L_om*	2.670E-11	2.516E-11	Farads
Rctn_L_om	4.601E-04	3.924E-04	Ohms	*Rctn_L_iof*	1.930E+03	1.320E+03	Ohms	*Cctn_M_om*	1.251E-09	9.401E-10	Farads
Rctn_M_om	2.098E-04	1.512E-04	Ohms	*Rctn_M_iof*	5.956E+01	2.340E+01	Ohms	*Cctn_M_im*	2.895E-09	2.237E-09	Farads
Rctn_M_im	6.014E-04	4.314E-04	Ohms	*Rctn_M_mx*	1.426E+01	1.150E-01	Ohms				

It is difficult to compare the relative magnitudes of these network values in a table so Fig. 12-4 through Fig. 12-6 provides a graphical method to compare the magnitude and range of possible network values for the model. Each graphic shows a logarithmic x-axis because the wide ranging values. Fig. 12-4 Membrane resistor value ranges for cancer type 2 shows how small the organelle membranes are and how they relate to each other. Fig. 12-5 Fluid and pore resistor value ranges for cancer type 2 shows they are much larger relative to the membrane resistors but range over four decades verses nine decades for the membranes.

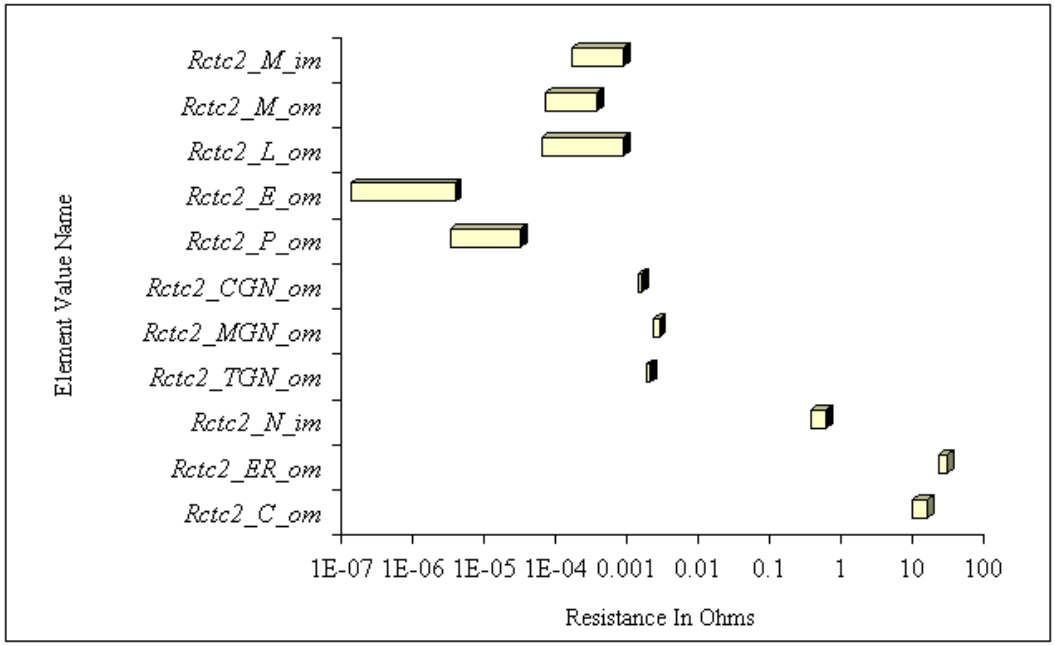

Fig. 12-4 Membrane resistor value ranges for cancer type 2

Fig 12-6 Membrane capacitor value ranges for cancer type 2 shows the ranges vary within four decades. The absolute value and range of a network element does not in itself demonstrate the effect it has on the "Transparent Box" model. A large value for a resistor or capacitor does not mean that it will dominate the output.

The location of the element in the electrical network and its value will determine the relative dominance or importance of an element in the output of the model. Again the impedance response corresponding to cancer type 2 will be plotted on a common Nyquist, Bode magnitude and Bode phase plot with the rest of the diseased tissues.

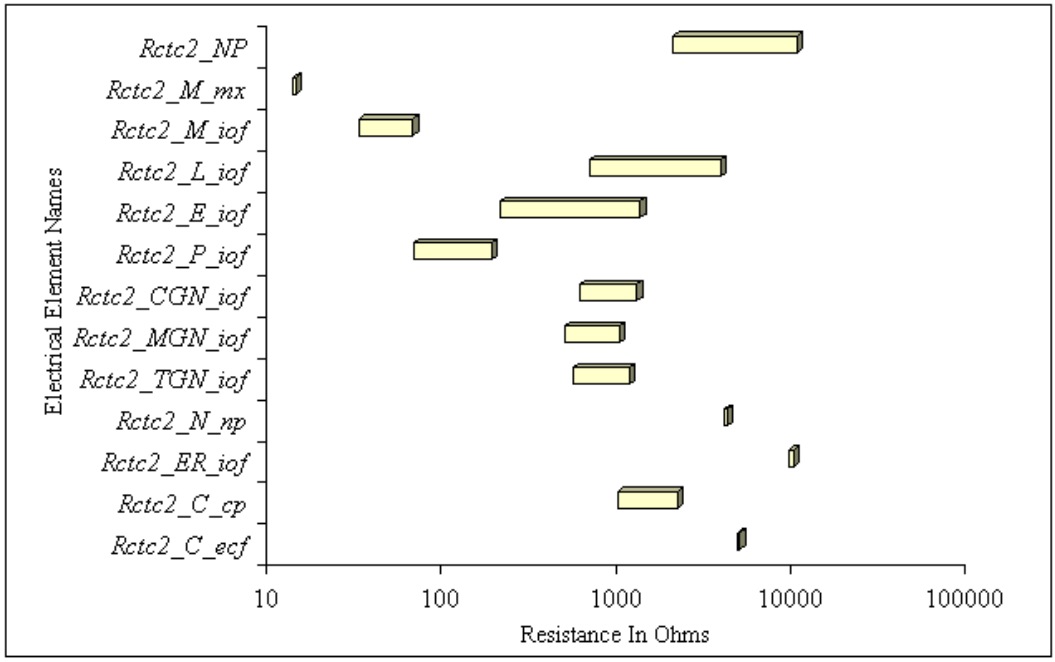

Fig. 12-5 Fluid and pore resistor value ranges for cancer type 2

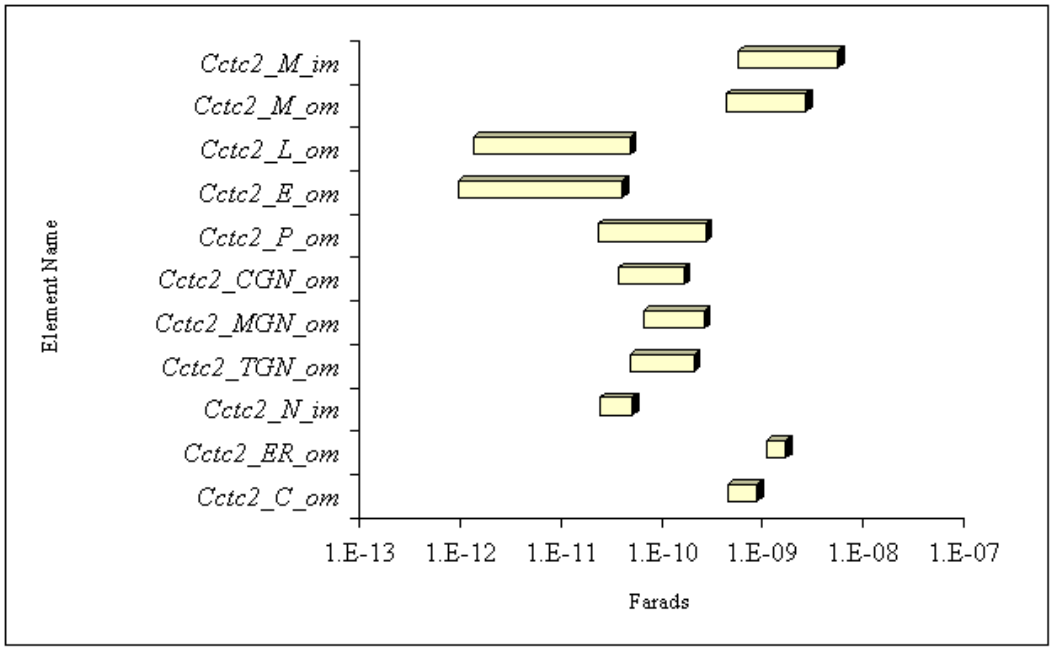

Fig 12-6 Membrane capacitor value ranges for cancer type 2

D. Cancer Type 3 Tissue Model

Cancer type 3 is the most severe type of cancer grade used by pathologists. It describes poorly differentiated squamous cell carcinoma [11, p. 6]. Cancer type 3 has sheets of anaplastic cells showing considerable pleomorphism. Cells invade into stroma mitoses, are prominent tumor borders and are usually ragged indicating breaches in the basal membrane [11, p. 6]. Cancer type 3 is a "true cancer" in that the cells have become invasive [9, pp. 1320-1326]. The values for the primary variables in the cancer type 3 model are shown in Table 12-8 and are continued on Table 12-9. Again the highlighted values are different from normal healthy tissue values. One may notice like in cancers type 1 and 2 there is an increase in the numbers of peroxisomes, endosomes and mitochondria for the first three layers of tissue [70, p.51]. Mitochondria numbers increase to keep up with the large energy demand required by aggressive cell growth. The numbers of lysosomes in the cancer affected cell layers decreases from normal [70, p. 59]. Like cancer types 1 and 2 the nucleus radius is on average is even larger in the affected cell layers because the DNA in the nucleus can no longer condense on the histones, the chromosomes themselves have mismatches, multiple copies and are damaged resulting in the failure of the nucleus to return to normal pre mitotic and pre cancer size and shape [9, p. 1316], [69, pp. 14-17]. Approximately one out of ten cuboidal cells will have multiple nuclei [12] hence N_{num} is 1.1 in cell layer two. The protein volume in the cell is lower than in cancers types 1 and 2 as keratin fiber production has halted and replaced by smaller fibers of actin and myosin which aid in cell movement [69, p. 7], [70, p.152]. This change helps the cells to change shape, move and invade other tissues. The change in protein still affects the displacement of cytoplasm like previously shown in cancers types 1 and 2. The primary variable reflecting the change in displacement is the protein cell volume variable *PCV*. Pathologists report tumors of

cancer 3 are said to be even more elastic than cancer 1 and 2 [12]. Cancer type 3 has lower amounts of extracellular structural proteins and can be identified in the model by comparatively lower *PECV* values. These cancer cells express agents that destroy the extracellular structural proteins providing detachment and an easy path for movement into new locations. The drastic decrease in structural protein makes the tissue easy to rupture with moderate sheer forces. This makes the tissue tend to look inflamed, tender and easy to bleed [12]. The electrical effect of a decrease in structural protein volume is an increase in electrolyte volume increasing charge carrier availability. The number of cells making up the squamous cell layer decreases even more than cancer 1 and 2 thinning this layer while the number of cuboidal shaped cells increases [9, p. 1319-1320]. The cells at the squamous layer show very little differentiation from the cuboidal cells [11, p. 9]. Because of the pleomorphism and dedifferentiation, all the affected cells loose their normal structural shape. In the cancer type 3 model this is accounted for by increasing the structural variables *LS_out*, *H_cell* and the anaplastic multiplier *ANAm_2.*

The crista in the mitochondria of cancer type 3 has reduced number and size as energy production swings from aerobic to mostly anaerobic activity more so than cancer types 1 and 2 [69, p. 12]. The deformed mitochondria crista is implemented in the model with a reduced mitochondria inner membrane pleat multiplier *Mimpm_n* and a reduced Mitochondria inner membrane radius multiplier *Mimrm_n.* Unlike cancer types 1 and 2 this cancer has invaded past the basal membrane. The growing cancer cells crowd out the basal layer; this is reflected in the model by a much lower number of cells comprising the fourth layer.

Table 12-8
CANCER TYPE 3 PRIMARY VARIABLE VALUES PART I

Name of Variable	Units	Tissue Layer 1 Squamous Cell		Tissue Layer 2 Cuboidal Cell		Tissue Layer 3 Columinar Cell		Tissue Layer 4 Basal Cell		Variable Value References
		Max	Min	Max	Min	Max	Min	Max	Min	
t_m	nm	5	4	5	4	5	4	5	4	[7], [9], [50], [55], [95]
MC	uF/cm^2	1.15	0.85	1.15	0.85	1.15	0.85	1.15	0.85	[48], [50], [55], [89]
r_P	nm	225	85	213	80	213	80	250	100	[9], [68], [69], [99]
ρ_P	Ohm*cm	90	75	90	75	90	75	90	75	[1], [84], [85], [99]
MR_P	MOhm/cm^2	110	90	110	90	110	90	110	90	[48], [50], [55], [89]
P_{num}		420	336	675	540	600	480	500	400	[9], [68], [69], [71], [93]
r_E	nm	90	17	85	16	85	16	100	20	[9], [68], [69], [99]
ρ_E	Ohm*cm	90	75	90	75	90	75	90	75	[1], [84], [85], [99]
MR_E	MOhm/cm^2	110	90	110	90	110	90	110	90	[48], [50], [55], [89]
E_{num}		390	336	626	540	557	480	464	400	[9], [68], [69], [71], [93]
r_L	nm	400	100	340	80	340	80	400	100	[9], [68], [69], [99]
ρ_L	Ohm*cm	90	75	90	75	90	75	90	75	[1], [84], [85], [99]
MR_L	MOhm/cm^2	110	90	110	90	110	90	110	90	[48], [50], [55], [89]
L_{num}		32	21	29	19	41	26	45	29	[9], [68], [69], [71], [93]
r_{Mim}	nm	404	120	426	292	649	156	565	180	[9], [68], [69], [81], [99]
r_{Mom}	nm	540	170	690	550	900	260	600	200	[9], [68], [69], [81], [99]
t_{Mims}	nm	35	20	35	20	35	20	35	20	[9], [68], [69], [81], [99]
ρ_{Min}	Ohm*cm	90	75	90	75	90	75	90	75	[1], [84], [85], [99]
ρ_{Mmx}	Ohm*cm	30	10	30	10	30	10	30	10	[1], [84], [85], [99]
MR_{Mom}	MOhm/cm^2	110	90	110	90	110	90	110	90	[48], [50], [55], [89]
MR_{Mim}	MOhm/cm^2	110	90	110	90	110	90	110	90	[48], [50], [55], [89]
M_{num}		300	225	472	448	460	345	400	300	[9], [68], [69], [71], [93]
l_{GMC}	um	1.10	0.90	1.10	0.90	1.10	0.90	1.10	0.90	[9], [68], [69], [99]
d_{GMC}	um	0.80	0.70	0.80	0.70	0.80	0.70	0.80	0.70	[9], [68], [69], [99]
w_{GMC}	um	0.07	0.06	0.08	0.07	0.08	0.07	0.08	0.07	[9], [68], [69], [99]
$VxCGN$		1.7	1.5	1.7	1.5	1.7	1.5	1.7	1.5	[9], [68], [69], [99]
$VxTGN$		2.2	2	2.2	2	2.2	2	2.2	2	[9], [68], [69], [99]
$AxCGN$		1.9	1.7	1.9	1.7	1.9	1.7	1.9	1.7	[9], [68], [69], [99]
$AxTGN$		2.4	2.2	2.4	2.2	2.4	2.2	2.4	2.2	[9], [68], [69], [99]
MR_{MGN}	MOhm/cm^2	110	90	110	90	110	90	110	90	[48], [50], [55], [89]
MR_{CGN}	MOhm/cm^2	110	90	110	90	110	90	110	90	[48], [50], [55], [89]
MR_{TGN}	MOhm/cm^2	110	90	110	90	110	90	110	90	[48], [50], [55], [89]

Table 12-9
CANCER TYPE 3 PRIMARY VARIABLE VALUES PART II

Name of Variable	Units	Tissue Layer 1 Squamous Cell		Tissue Layer 2 Cuboidal Cell		Tissue Layer 3 Columinar Cell		Tissue Layer 4 Basal Cell		Variable Value References
		Max	Min	Max	Min	Max	Min	Max	Min	
ρ_{MGN}	Ohm*cm	90	75	90	75	90	75	90	75	[1], [84], [85], [99]
ρ_{CGN}	Ohm*cm	90	75	90	75	90	75	90	75	[1], [84], [85], [99]
ρ_{TGN}	Ohm*cm	90	75	90	75	90	75	90	75	[1], [84], [85], [99]
G_{num}		50	24	45	21.6	50	24	50	24	[9], [68], [69], [71], [93]
r_{nim}	um	1.23	1.06	4.90	3.12	3.60	2.38	1.80	1.40	[9], [68], [69], [81], [99]
KV_{NER}		0.5	0.4	0.5	0.4	0.5	0.4	0.5	0.4	[9], [71], [83], [93], [94]
KA_{NER}		190	160	47.5	40	47.5	40	190	160	[9], [71], [83], [93], [94]
Mr_{erom}	MOhm/cm^2	110	90	110	90	110	90	110	90	[48], [50], [55], [89]
ρ_{er}	Ohm*cm	90	75	90	75	90	75	90	75	[9], [68], [69], [71], [93]
Mr_{nim}	MOhm/cm^2	110	90	110	90	110	90	110	90	[48], [50], [55], [77], [89]
ρ_{n}	Ohm*cm	90	75	90	75	90	75	90	75	[1], [84], [85], [99]
G_{pore}	pS	1000	750	1000	1000	3000	1000	1000	750	[84], [85], [78]
Npd	pores/um^2	60	50	60	50	60	50	50	40	[9], [68], [71], [83], [94]
ER_{num}		1	1	1.5	1	1	1	1	1	[9], [68], [71], [83], [94]
N_{num}		1.1	1.01	1.1	1.08	1.1	1.01	1	1	[9], [68], [71], [83], [94]
LS_out	um	18.00	14.00	7.70	6.16	7.00	5.60	7.00	5.60	[9], [68], [69], [71]
H_cell	um	2.80	2.20	15.40	19.80	28.00	18.00	12.00	10.00	[9], [68], [69], [71]
Eg	nm	120	50	120	50	120	50	120	50	[9], [68], [69], [71]
PCV	percent	30%	10%	5%	1%	9%	7%	12%	10%	[9], [98], [99]
$PECV$	percent	40%	18%	8%	5%	9%	5%	20%	10%	[9], [69], [71], [101]
ρ_{CP}	Ohm*cm	85	60	85	60	85	60	85	60	[1], [84], [85], [96], [99]
MR_{PM}	MOhm/cm^2	110	90	110	90	110	90	110	90	[48], [50], [55], [89]
ρ_{ef}	Ohm*cm	80	55	80	55	80	55	80	55	[1], [84], [85], [99]
Yw	cm	0.2	0.2	0.2	0.2	0.2	0.2	0.2	0.2	[50], [55], [65]
Xl	cm	0.3	0.3	0.3	0.3	0.3	0.3	0.3	0.3	[50], [55], [65]
Ncz_n		20	20	67	67	3	3	10	10	[9], [98], [99]
Zh_n	um | percent	58	4%	1040	80%	84	6%	121	9%	[9], [98], [99]
$ANAm\_n$		1.00	1.00	1.10	1.10	1.00	1.00	1.00	1.00	[9], [68]
$Mimpm\_n$		0.80	0.80	0.65	0.55	0.75	0.65	1.00	1.00	[9], [68], [69], [71], [93]
$Mimrm\_n$		0.80	0.80	0.65	0.55	0.75	0.65	1.00	1.00	[9], [68], [69], [71], [93]
Nrm_n		1.10	1.10	3.40	2.00	1.80	1.40	1.00	1.00	[9], [68], [69], [71], [93]
Orm_n		0.90	0.85	0.85	0.80	0.85	0.80	1.00	1.00	[9], [68], [69], [71], [93]

The network element values for cancer type 3 corresponding to the primary element variables in Tables 12-8 and 12-9 are shown in Table 12-10 Cancer type 3 resistor and capacitor network values.

Table 12-10
CANCER TYPE 3 NETWORK ELEMENT VALUES

Element	value	variance +-	units	Element	value	variance +-	units	Element	value	variance +-	units
Rctn_C_om	1.244E+01	2.546E+00	Ohms	*Rctn_C_ecf*	3.536E+03	1.011E+02	Ohms	*Cctn_C_om*	6.012E-10	1.622E-10	Farads
Rcn_ER_om	1.030E+01	8.299E-01	Ohms	*Rctn_C_cp*	1.463E+03	5.225E+02	Ohms	*Cctn_ER_om*	9.342E-10	3.488E-10	Farads
Rctn_N_im	7.678E-01	2.238E-01	Ohms	*Rctn_ER_iof*	8.116E+03	1.027E+03	Ohms	*Cctn_N_im*	1.175E-10	6.314E-11	Farads
Rctn_NP	1.772E+03	1.410E+03	Ohms	*Rctn_N_np*	2.306E+03	2.991E+02	Ohms	*Cctn_TGN_om*	1.089E-10	6.769E-11	Farads
Rctn_TGN_om	1.853E-03	1.061E-04	Ohms	*Rctn_TGN_iof*	8.855E+02	3.132E+02	Ohms	*Cctn_MGN_om*	1.385E-10	8.227E-11	Farads
Rctn_MGN_om	2.427E-03	2.439E-04	Ohms	*Rctn_MGN_iof*	7.817E+02	3.132E+02	Ohms	*Cctn_CGN_om*	8.583E-11	5.398E-11	Farads
Rctn_CGN_om	1.448E-03	6.542E-05	Ohms	*Rctn_CGN_iof*	9.715E+02	3.478E+02	Ohms	*Cctn_P_om*	1.496E-10	1.261E-10	Farads
Rctn_P_om	1.349E-05	1.114E-05	Ohms	*Rctn_P_iof*	1.175E+02	5.605E+01	Ohms	*Cctn_E_om*	2.093E-11	2.000E-11	Farads
Rctn_E_om	1.436E-06	1.341E-06	Ohms	*Rctn_E_iof*	6.700E+02	4.877E+02	Ohms	*Cctn_L_om*	2.061E-11	1.949E-11	Farads
Rctn_L_om	4.472E-04	3.867E-04	Ohms	*Rctn_L_iof*	2.425E+03	1.684E+03	Ohms	*Cctn_M_om*	1.902E-09	8.967E-10	Farads
Rctn_M_om	1.926E-04	1.190E-04	Ohms	*Rctn_M_iof*	3.039E+01	3.474E+00	Ohms	*Cctn_M_im*	2.311E-09	1.585E-09	Farads
Rctn_M_im	2.677E-04	1.610E-04	Ohms	*Rctn_M_mx*	1.159E+01	2.563E+00	Ohms				

The relative magnitudes and ranges of possible network values of the network values for the model contained in table 12-9 are shown in Fig. 12-7 through Fig. 12-9 Each graphic uses a logarithmic x-axis scale because the wide ranging values. Fig. 12-7 Membrane resistor value ranges for cancer type 3 shows how small the organelle membranes are and how they relate to each other. Fig. 12-8 Fluid and pore resistor value ranges for cancer type 3 shows they are much larger relative to the membrane resistors but range over three decades verses nine for the membranes.

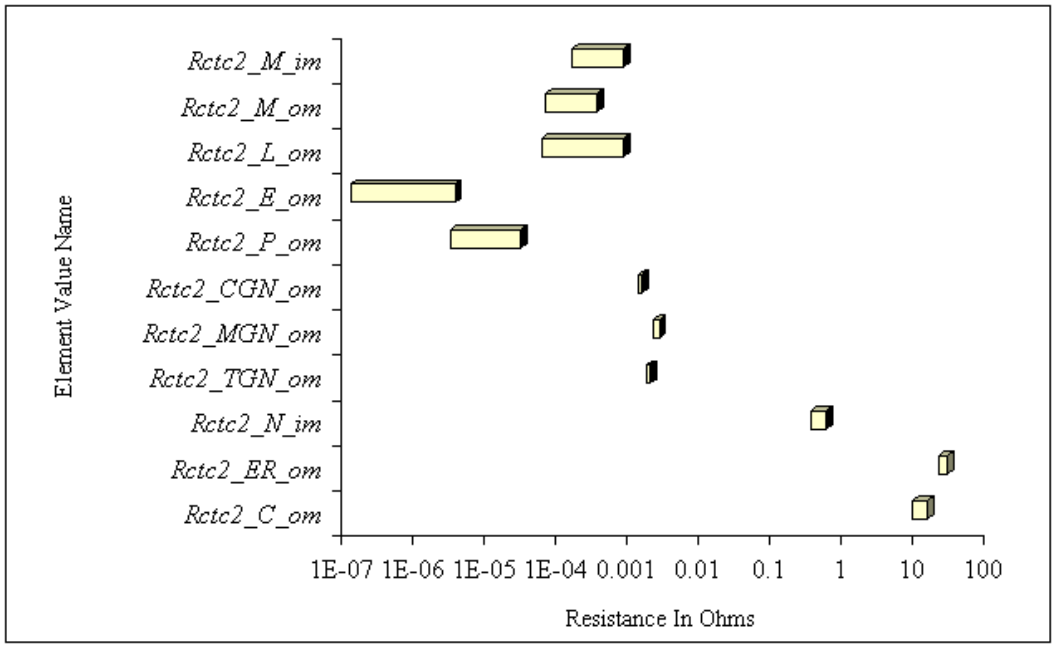

Fig. 12-7 Membrane resistor value ranges for cancer type 3

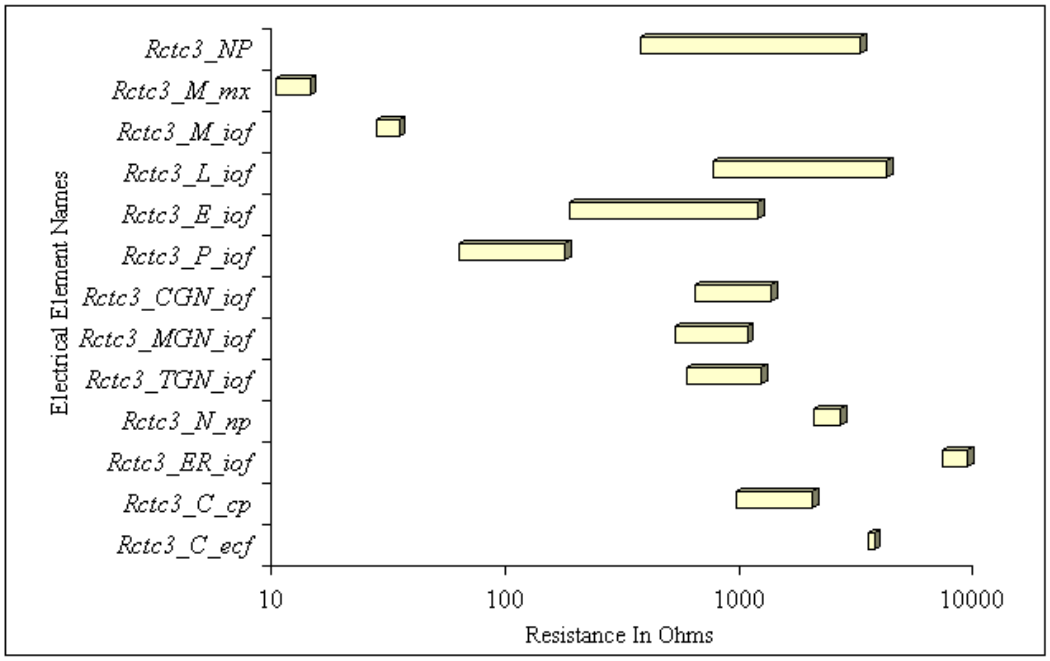

Fig. 12-8 Fluid and pore resistor value ranges for cancer type 3

Fig. 12-9 Membrane capacitor value ranges for cancer type 3 shows the ranges vary within four decades.

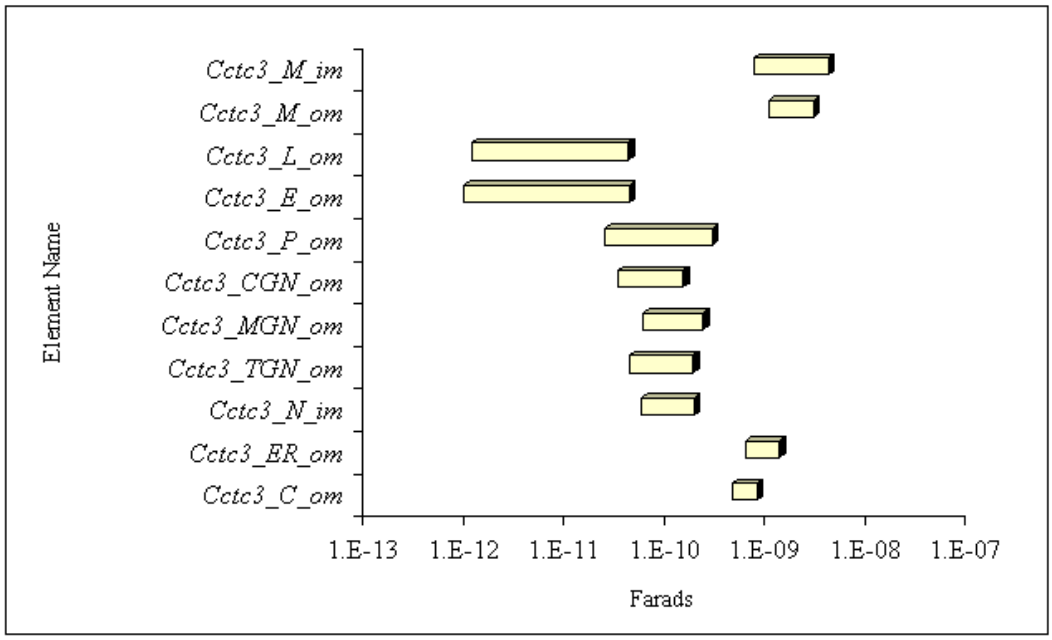

Fig. 12-9 Membrane capacitor value ranges for cancer type 3

The impedance response corresponding to cancer type 3 will also be plotted on a common Nyquist, Bode magnitude and Bode phase plot to help highlight impedance response differences between the disease models.

E. Hyperkeratosis Tissue Model

Hyperkeratosis is a benign oral disease that manifests itself as white painless thickened oral mucosal tissue; it is often mistaken for oral cancer during a routine oral examination. Hyperkeratosis is a result of the over expression of keratin in the squamous cells. One of the cells response to a chronic irritant is the over expression of keratin. Poorly fitting dentures or the long-term use of tobacco products irritates the oral mucosa and often leads to hyperkeratosis. The values for the primary variables in the hyperkeratosis model are shown in Table 12-11 and are continued on Table 12-12. Again the highlighted values are different from normal healthy tissue values. Unlike cancer there is a decrease in the numbers of peroxisomes, endosomes, lysosomes and mitochondria for the first two layers of tissue [68, p. 447].

Table 12-11
HYPERKERATOSIS PRIMARY VARIABLE VALUES PART I

Name of Variable	Units	Tissue Layer 1 Squamous Cell		Tissue Layer 2 Cuboidal Cell		Tissue Layer 3 Columinar Cell		Tissue Layer 4 Basal Cell		Variable Value References
		Max	Min	Max	Min	Max	Min	Max	Min	
t_m	nm	5	4	5	4	5	4	5	4	[7], [9], [50], [55], [95]
MC	uF/cm^2	1.15	0.85	1.15	0.85	1.15	0.85	1.15	0.85	[48], [50], [55], [89]
r_P	nm	250	100	250	100	250	100	250	100	[9], [68], [69], [99]
ρ_P	Ohm*cm	90	75	90	75	90	75	90	75	[1], [84], [85], [99]
MR_P	MOhm/cm^2	110	90	110	90	110	90	110	90	[48], [50], [55], [89]
P_{num}		300	240	500	400	500	400	500	400	[9], [68], [69], [71], [93]
r_E	nm	100	20	100	20	100	20	100	20	[9], [68], [69], [99]
ρ_E	Ohm*cm	90	75	90	75	90	75	90	75	[1], [84], [85], [99]
MR_E	MOhm/cm^2	110	90	110	90	110	90	110	90	[48], [50], [55], [89]
E_{num}		278	240	464	400	464	400	464	400	[9], [68], [69], [71], [93]
r_L	nm	400	100	400	100	400	100	400	100	[9], [68], [69], [99]
ρ_L	Ohm*cm	90	75	90	75	90	75	90	75	[1], [84], [85], [99]
MR_L	MOhm/cm^2	110	90	110	90	110	90	110	90	[48], [50], [55], [89]
L_{num}		36	23	45	29	45	29	45	29	[9], [68], [69], [71], [93]
r_{Mim}	nm	565	180	565	180	565	180	565	180	[9], [68], [69], [81], [99]
r_{Mom}	nm	600	200	600	200	600	200	600	200	[9], [68], [69], [81], [99]
t_{Mims}	nm	35	20	35	20	35	20	35	20	[9], [68], [69], [81], [99]
ρ_{Min}	Ohm*cm	90	75	90	75	90	75	90	75	[1], [84], [85], [99]
ρ_{Mmx}	Ohm*cm	30	10	30	10	30	10	30	10	[1], [84], [85], [99]
MR_{Mom}	MOhm/cm^2	110	90	110	90	110	90	110	90	[48], [50], [55], [89]
MR_{Mim}	MOhm/cm^2	110	90	110	90	110	90	110	90	[48], [50], [55], [89]
M_{num}		200	150	400	300	400	300	400	300	[9], [68], [69], [71], [93]
l_{GMC}	um	1.10	0.90	1.10	0.90	1.10	0.90	1.10	0.90	[9], [68], [69], [99]
d_{GMC}	um	0.80	0.70	0.80	0.70	0.80	0.70	0.80	0.70	[9], [68], [69], [99]
w_{GMC}	um	0.08	0.07	0.08	0.07	0.08	0.07	0.08	0.07	[9], [68], [69], [99]
$VxCGN$		1.7	1.5	1.7	1.5	1.7	1.5	1.7	1.5	[9], [68], [69], [99]
$VxTGN$		2.2	2	2.2	2	2.2	2	2.2	2	[9], [68], [69], [99]
$AxCGN$		1.9	1.7	1.9	1.7	1.9	1.7	1.9	1.7	[9], [68], [69], [99]
$AxTGN$		2.4	2.2	2.4	2.2	2.4	2.2	2.4	2.2	[9], [68], [69], [99]
MR_{MGN}	MOhm/cm^2	110	90	110	90	110	90	110	90	[48], [50], [55], [89]
MR_{CGN}	MOhm/cm^2	110	90	110	90	110	90	110	90	[48], [50], [55], [89]
MR_{TGN}	MOhm/cm^2	110	90	110	90	110	90	110	90	[48], [50], [55], [89]

Table 12-12
HYPERKERATOSIS PRIMARY VARIABLE VALUES PART II

Name of Variable	Units	Tissue Layer 1 Squamous Cell		Tissue Layer 2 Cuboidal Cell		Tissue Layer 3 Columinar Cell		Tissue Layer 4 Basal Cell		Variable Value References
		Max	Min	Max	Min	Max	Min	Max	Min	
ρ_{MGN}	Ohm*cm	90	75	90	75	90	75	90	75	[1], [84], [85], [99]
ρ_{CGN}	Ohm*cm	90	75	90	75	90	75	90	75	[1], [84], [85], [99]
ρ_{TGN}	Ohm*cm	90	75	90	75	90	75	90	75	[1], [84], [85], [99]
G_{num}		50	24	50	24	50	24	50	24	[9], [68], [69], [71], [93]
r_{nim}	um	1.12	0.96	1.44	1.56	2.00	2.04	1.80	1.40	[9], [68], [69], [81], [99]
KV_{NER}		0.5	0.4	0.5	0.4	0.5	0.4	0.5	0.4	[9], [71], [83], [93], [94]
KA_{NER}		200	180	200	180	200	180	200	180	[9], [71], [83], [93], [94]
Mr_{erom}	MOhm/cm^2	110	90	110	90	110	90	110	90	[48], [50], [55], [89]
ρ_{er}	Ohm*cm	90	75	90	75	90	75	90	75	[9], [68], [69], [71], [93]
Mr_{nim}	MOhm/cm^2	110	90	110	90	110	90	110	90	[48], [50], [55], [77], [89]
ρ_{n}	Ohm*cm	90	75	90	75	90	75	90	75	[1], [84], [85], [99]
G_{pore}	pS	1000	750	1000	750	1000	750	1000	750	[84], [85], [78]
Npd	pores/um^2	50	40	50	40	50	40	50	40	[9], [68], [71], [83], [94]
ER_{num}		1	1	1	1	1	1	1	1	[9], [68], [71], [83], [94]
N_{num}		1	1	1	1	1	1	1	1	[9], [68], [71], [83], [94]
LS_out	um	18.00	14.00	7.00	5.60	7.00	5.60	7.00	5.60	[9], [68], [69], [71]
H_cell	um	2.80	2.20	14.00	18.00	28.00	18.00	12.00	10.00	[9], [68], [69], [71]
Eg	nm	120	50	120	50	120	50	120	50	[9], [68], [69], [71]
PCV	percent	80%	65%	30%	20%	15%	10%	15%	10%	[9], [98], [99]
PECV	percent	55%	45%	25%	15%	15%	10%	25%	15%	[9], [69], [71], [101]
ρ_{CP}	Ohm*cm	85	60	85	60	85	60	85	60	[1], [84], [85], [96], [99]
MR_{PM}	MOhm/cm^2	110	90	110	90	110	90	110	90	[48], [50], [55], [89]
ρ_{ef}	Ohm*cm	80	55	80	55	80	55	80	55	[1], [84], [85], [99]
Yw	cm	0.2	0.2	0.2	0.2	0.2	0.2	0.2	0.2	[50], [55], [65]
Xl	cm	0.3	0.3	0.3	0.3	0.3	0.3	0.3	0.3	[50], [55], [65]
Ncz_n		65	65	10	10	5	5	20	20	[9], [98], [99]
Zh_n	um | percent	190	27%	141	20%	141	20%	242	34%	[9], [98], [99]
ANAm_n		1.00	1.00	1.00	1.00	1.00	1.00	1.00	1.00	[9], [68]
Mimpm_n		1.00	1.00	1.00	1.00	1.00	1.00	1.00	1.00	[9], [68], [69], [71], [93]
Mimrm_n		1.00	1.00	1.00	1.00	1.00	1.00	1.00	1.00	[9], [68], [69], [71], [93]
Nrm_n		1.00	1.00	1.00	1.00	1.00	1.00	1.00	1.00	[9], [68], [69], [71], [93]
Orm_n		1.00	1.00	1.00	1.00	1.00	1.00	1.00	1.00	[9], [68], [69], [71], [93]

Mitochondria numbers decrease as cells ascend to the surface due to lower energy demand. The nucleus condenses to its smallest size as cells are fully differentiated [68, p. 446]. The protein volume in the cell is higher than in normal tissue as keratin fiber production has increased to protect the underlying tissue from chronic irritation [68, pp. 446-448]. The increase in protein displaces cytoplasm and organelles. The primary variable reflecting the change in displacement of the intracellular fluid is the protein cell volume variable *PCV*. Pathologists report the surface of hyperkeratosis tissue is tough and inelastic than normal oral mucosa [17]. The increase in structural protein makes the tissue surface appear translucent white sometimes granular and tough [17]. An increase in connective filaments between dead squamous cells prevents the normal sloughing off of individual dead cells at the surface of the oral mucosa. The extracellular protein cell volume variable *PCEV* displaces the volume of the extra cellular fluid resulting in increased resistance between cells. This dead skin cell layer gets tougher and thicker as more dead cells from lower layers get pushed up to replace old ones producing a callous thick layer of poorly conductive skin [44]. This manifests in the model as a 35% thicker layer of squamous cells compared to normal. This model of hyperkeratosis tissue is fairly average with a *PCV* of 80% for the first layer of cells in extreme cases protein cell volume at the surface can be over 90%.

In more extreme cases organelles disappear as tough connective proteins increase. The dead cells also build up to form an extremely thick dense calloused hide.

The network element values for hyperkeratosis tissue corresponding to the primary element variables in Tables 12-11 and 12-12 are shown in Table 12-13 hyperkeratosis tissue resistor and capacitor network values.

Table 12-13
HYPERKERATOSIS TISSUE NETWORK ELEMENT VALUES

Element	value	variance +-	units	Element	value	variance +-	units	Element	value	variance +-	units
Rctn_C_om	1.417E+01	4.277E+00	Ohms	*Rctn_C_ecf*	9.202E+03	1.721E+01	Ohms	*Cctn_C_om*	7.499E-10	2.768E-10	Farads
Rcn_ER_om	4.252E+01	9.495E+00	Ohms	*Rctn_C_cp*	2.036E+03	8.430E+02	Ohms	*Cctn_ER_om*	1.902E-09	5.153E-10	Farads
Rctn_N_im	2.604E-01	6.325E-02	Ohms	*Rctn_ER_iof*	9.303E+03	1.602E+02	Ohms	*Cctn_N_im*	1.415E-11	3.876E-12	Farads
Rctn_NP	2.017E+04	7.411E+03	Ohms	*Rctn_N_np*	6.169E+03	1.422E+02	Ohms	*Cctn_TGN_om*	1.171E-10	7.274E-11	Farads
Rctn_TGN_om	1.736E-03	1.009E-04	Ohms	*Rctn_TGN_iof*	8.167E+02	2.873E+02	Ohms	*Cctn_MGN_om*	1.490E-10	8.841E-11	Farads
Rctn_MGN_om	2.274E-03	2.304E-04	Ohms	*Rctn_MGN_iof*	7.210E+02	2.873E+02	Ohms	*Cctn_CGN_om*	9.232E-11	5.801E-11	Farads
Rctn_CGN_om	1.357E-03	6.247E-05	Ohms	*Rctn_CGN_iof*	8.961E+02	3.191E+02	Ohms	*Cctn_P_om*	1.219E-10	1.009E-10	Farads
Rctn_P_om	2.138E-05	1.565E-05	Ohms	*Rctn_P_iof*	1.251E+02	5.669E+01	Ohms	*Cctn_E_om*	1.696E-11	1.612E-11	Farads
Rctn_E_om	3.134E-06	2.905E-06	Ohms	*Rctn_E_iof*	8.652E+02	6.084E+02	Ohms	*Cctn_L_om*	3.107E-11	2.928E-11	Farads
Rctn_L_om	4.573E-04	3.901E-04	Ohms	*Rctn_L_iof*	1.711E+03	1.170E+03	Ohms	*Cctn_M_om*	7.456E-10	6.591E-10	Farads
Rctn_M_om	2.325E-04	1.822E-04	Ohms	*Rctn_M_iof*	1.264E+02	6.283E+01	Ohms	*Cctn_M_im*	2.851E-09	2.547E-09	Farads
Rctn_M_im	1.405E-03	1.125E-03	Ohms	*Rctn_M_mx*	2.203E+01	5.033E+00	Ohms				

The relative magnitudes and ranges of possible network values for the model contained in Table 12-13 are shown in Fig. 12-10 through Fig. 12-12 Each graphic uses a logarithmic x-axis scale because the wide ranging values. Fig. 12-10 Membrane resistor value ranges for hyperkeratosis tissue shows how small the organelle membranes values are and how they relate to each other. Fig. 12-11 Fluid and pore resistor value ranges for hyperkeratosis tissue shows they are much larger relative to the membrane resistors. Fig. 12-12 Membrane capacitor value ranges for hyperkeratosis tissue shows the values is very similar to the other models. An element-by-element comparison must be done in order to see any meaningful differences. The impedance response corresponding to the hyperkeratosis tissue will be plotted on a common Nyquist, Bode magnitude and Bode phase plot with the other diseases for comparison.

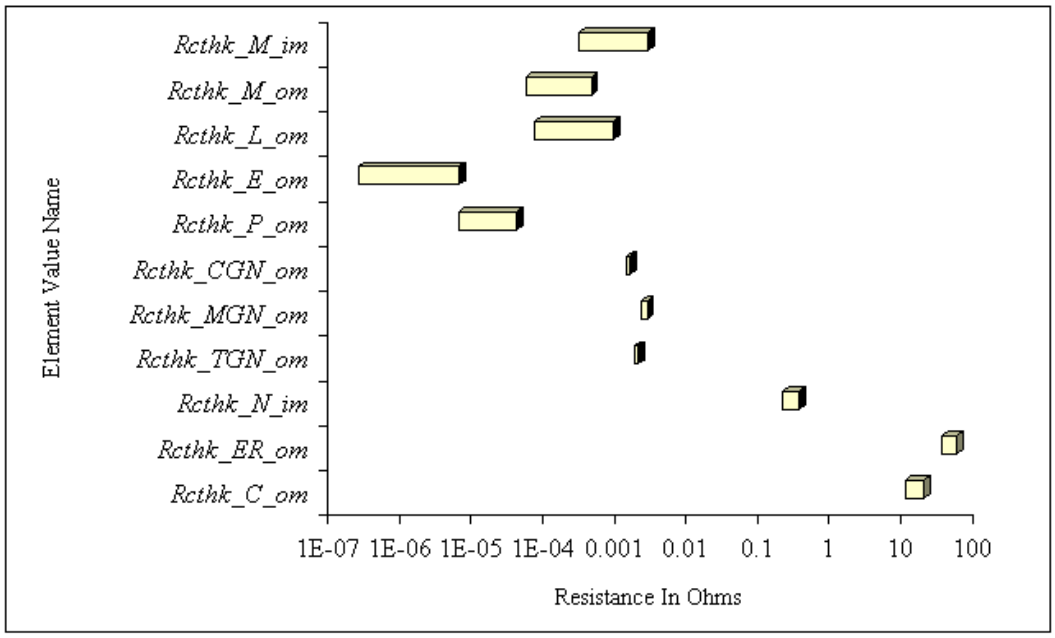

Fig. 12-10 Membrane resistor value ranges for hyperkeratosis tissue

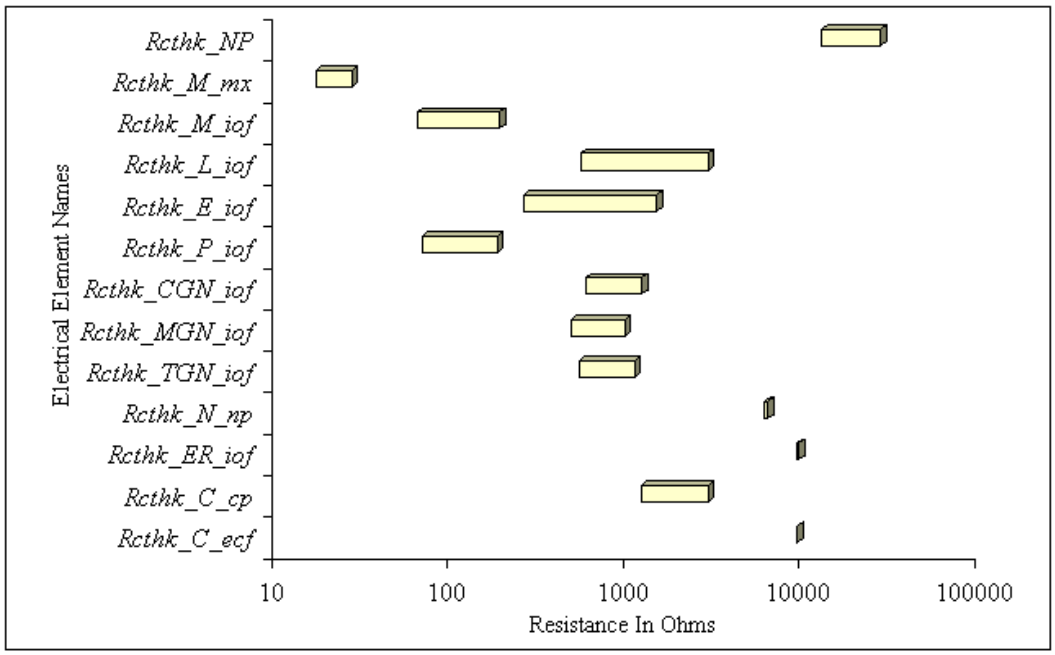

Fig. 12-11 Fluid and pore resistor value ranges for hyperkeratosis tissue

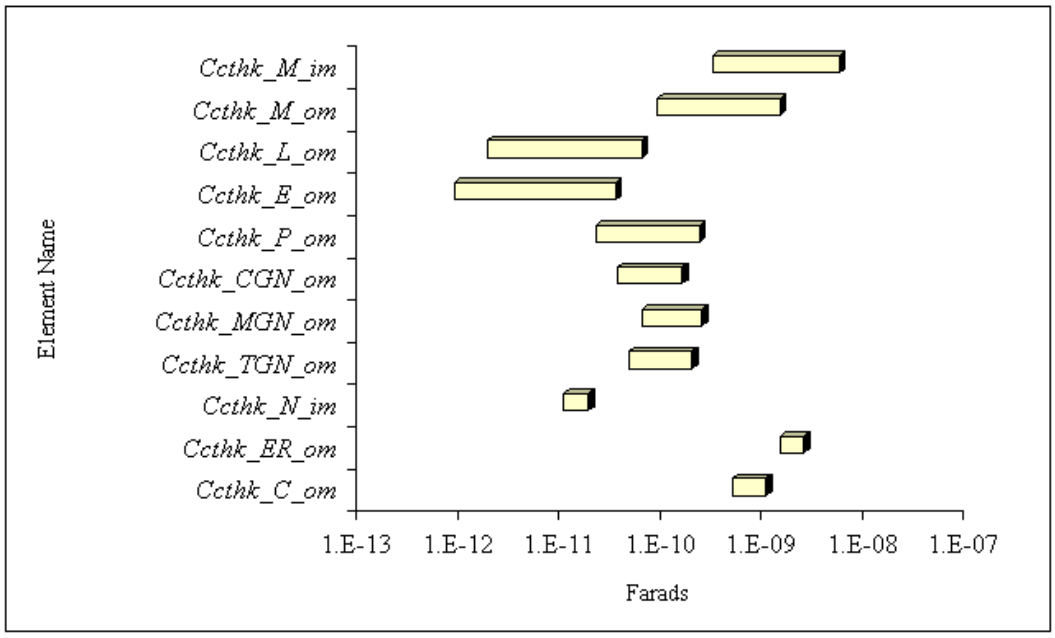

Fig. 12-12 Membrane capacitor value ranges for hyperkeratosis tissue

F. Necrotic Inflammation Tissue Model

Inflammation due to an acute injury such as a burn or an oral viral infection such as Candia can produce red lesions lasting weeks. During a routine oral examination a dentist can mistake a painless lesion for an oral cancer when the patient cannot recall a source of injury. Necrotic Inflammation is not as static as the other conditions that were previously modeled. There is an initial injury, which triggers an inflammation response involving monocytes, lymphocytes, eosinophils, basophils and fibroblasts [68, p. 256]. The inflammation may have a less stable impedance response as the tissue goes through the various stages of healing [43]. The stage of inflammation response that most likely physically resembles cancer is the early stage when the lesion is bright red and swollen [18]. The damaged cells undergo necrosis where cells rapidly swell and lysis [68, pp. 88-90]. The values for the primary variables in the necrotic inflammation model are shown in Table 12-14 and are continued on Table 12-15. Again the highlighted values are different from normal healthy tissue values.

Table 12-14
NECROTIC INFLAMMATION TISSUE PRIMARY VARIABLE VALUES PART I

Name of Variable	Units	Tissue Layer 1 Squamous Cell		Tissue Layer 2 Cuboidal Cell		Tissue Layer 3 Columinar Cell		Tissue Layer 4 Basal Cell		Variable Value References
		Max	Min	Max	Min	Max	Min	Max	Min	
t_m	nm	5	4	5	4	5	4	5	4	[7], [9], [50], [55], [95]
MC	uF/cm^2	1.15	0.85	1.15	0.85	1.15	0.85	1.15	0.85	[48], [50], [55], [89]
r_P	nm	250	100	250	100	250	100	250	100	[9], [68], [69], [99]
ρ_P	Ohm*cm	90	75	90	75	90	75	90	75	[1], [84], [85], [99]
MR_P	MOhm/cm^2	110	90	110	90	110	90	110	90	[48], [50], [55], [89]
P_{num}		300	240	500	400	500	400	500	400	[9], [68], [69], [71], [93]
r_E	nm	100	20	100	20	100	20	100	20	[9], [68], [69], [99]
ρ_E	Ohm*cm	90	75	90	75	90	75	90	75	[1], [84], [85], [99]
MR_E	MOhm/cm^2	110	90	110	90	110	90	110	90	[48], [50], [55], [89]
E_{num}		278	240	464	400	464	400	464	400	[9], [68], [69], [71], [93]
r_L	nm	400	100	400	100	400	100	400	100	[9], [68], [69], [99]
ρ_L	Ohm*cm	90	75	90	75	90	75	90	75	[1], [84], [85], [99]
MR_L	MOhm/cm^2	110	90	110	90	110	90	110	90	[48], [50], [55], [89]
L_{num}		36	23	45	29	45	29	45	29	[9], [68], [69], [71], [93]
r_{Mim}	nm	565	180	565	180	565	180	565	180	[9], [68], [69], [81], [99]
r_{Mom}	nm	600	200	600	200	600	200	600	200	[9], [68], [69], [81], [99]
t_{Mims}	nm	35	20	35	20	35	20	35	20	[9], [68], [69], [81], [99]
ρ_{Min}	Ohm*cm	90	75	90	75	90	75	90	75	[1], [84], [85], [99]
ρ_{Mmx}	Ohm*cm	30	10	30	10	30	10	30	10	[1], [84], [85], [99]
MR_{Mom}	MOhm/cm^2	110	90	110	90	110	90	110	90	[48], [50], [55], [89]
MR_{Mim}	MOhm/cm^2	110	90	110	90	110	90	110	90	[48], [50], [55], [89]
M_{num}		200	150	400	300	400	300	400	300	[9], [68], [69], [71], [93]
l_{GMC}	um	1.10	0.90	1.10	0.90	1.10	0.90	1.10	0.90	[9], [68], [69], [99]
d_{GMC}	um	0.80	0.70	0.80	0.70	0.80	0.70	0.80	0.70	[9], [68], [69], [99]
w_{GMC}	um	0.08	0.07	0.08	0.07	0.08	0.07	0.08	0.07	[9], [68], [69], [99]
$VxCGN$		1.7	1.5	1.7	1.5	1.7	1.5	1.7	1.5	[9], [68], [69], [99]
$VxTGN$		2.2	2	2.2	2	2.2	2	2.2	2	[9], [68], [69], [99]
$AxCGN$		1.9	1.7	1.9	1.7	1.9	1.7	1.9	1.7	[9], [68], [69], [99]
$AxTGN$		2.4	2.2	2.4	2.2	2.4	2.2	2.4	2.2	[9], [68], [69], [99]
MR_{MGN}	MOhm/cm^2	110	90	110	90	110	90	110	90	[48], [50], [55], [89]
MR_{CGN}	MOhm/cm^2	110	90	110	90	110	90	110	90	[48], [50], [55], [89]
MR_{TGN}	MOhm/cm^2	110	90	110	90	110	90	110	90	[48], [50], [55], [89]

Table 11-15
NECROTIC INFLAMMATION TISSUE PRIMARY VARIABLE VALUES PART II

Name of Variable	Units	Tissue Layer 1 Squamous Cell		Tissue Layer 2 Cuboidal Cell		Tissue Layer 3 Columinar Cell		Tissue Layer 4 Basal Cell		Variable Value References
		Max	Min	Max	Min	Max	Min	Max	Min	
ρ_{MGN}	Ohm*cm	90	75	90	75	90	75	90	75	[1], [84], [85], [99]
ρ_{CGN}	Ohm*cm	90	75	90	75	90	75	90	75	[1], [84], [85], [99]
ρ_{TGN}	Ohm*cm	90	75	90	75	90	75	90	75	[1], [84], [85], [99]
G_{num}		50	24	50	24	50	24	50	24	[9], [68], [69], [71], [93]
r_{nim}	um	1.12	0.96	1.44	1.56	2.00	2.04	1.80	1.40	[9], [68], [69], [81], [99]
KV_{NER}		0.5	0.4	0.5	0.4	0.5	0.4	0.5	0.4	[9], [71], [83], [93], [94]
KA_{NER}		190	170	190	170	190	170	190	170	[9], [71], [83], [93], [94]
Mr_{erom}	MOhm/cm^2	110	90	110	90	110	90	110	90	[48], [50], [55], [89]
ρ_{er}	Ohm*cm	90	75	90	75	90	75	90	75	[9], [68], [69], [71], [93]
Mr_{nim}	MOhm/cm^2	110	90	110	90	110	90	110	90	[48], [50], [55], [77], [89]
ρ_{n}	Ohm*cm	90	75	90	75	90	75	90	75	[1], [84], [85], [99]
G_{pore}	pS	1000	750	1000	750	1000	750	1000	750	[84], [85], [78]
Npd	pores/um^2	50	40	50	40	50	40	50	40	[9], [68], [71], [83], [94]
ER_{num}		1	1	1	1	1	1	1	1	[9], [68], [71], [83], [94]
N_{num}		1	1	1	1	1	1	1	1	[9], [68], [71], [83], [94]
LS_out	um	19.80	15.40	7.70	6.16	7.00	5.60	7.00	5.60	[9], [68], [69], [71]
H_cell	um	3.08	2.42	15.40	19.80	28.00	18.00	12.00	10.00	[9], [68], [69], [71]
Eg	nm	120	50	120	50	120	50	120	50	[9], [68], [69], [71]
PCV	percent	35%	15%	15%	10%	15%	10%	15%	10%	[9], [98], [99]
PECV	percent	45%	25%	20%	15%	15%	10%	25%	15%	[9], [69], [71], [101]
ρ_{CP}	Ohm*cm	70	35	70	35	85	60	85	60	[1], [84], [85], [96], [99]
MR_{PM}	MOhm/cm^2	110	90	110	90	110	90	110	90	[48], [50], [55], [89]
ρ_{ef}	Ohm*cm	80	55	80	55	80	55	80	55	[1], [84], [85], [99]
Yw	cm	0.2	0.2	0.2	0.2	0.2	0.2	0.2	0.2	[50], [55], [65]
Xl	cm	0.3	0.3	0.3	0.3	0.3	0.3	0.3	0.3	[50], [55], [65]
Ncz_n		55	55	20	20	4	4	20	20	[9], [98], [99]
Zh_n	um | percent	176	21%	310	37%	112	13%	242	29%	[9], [98], [99]
ANAm_n		1.10	1.10	1.10	1.10	1.00	1.00	1.00	1.00	[9], [68]
Mimpm_n		1.00	1.00	1.00	1.00	1.00	1.00	1.00	1.00	[9], [68], [69], [71], [93]
Mimrm_n		1.00	1.00	1.00	1.00	1.00	1.00	1.00	1.00	[9], [68], [69], [71], [93]
Nrm_n		1.00	1.00	1.00	1.00	1.00	1.00	1.00	1.00	[9], [68], [69], [71], [93]
Orm_n		1.00	1.00	1.00	1.00	1.00	1.00	1.00	1.00	[9], [68], [69], [71], [93]

Inflammation from an acute physical injury will likely remove some of the outer protective layers of squamous cells. The cells below will have had damaged membranes. The cells that die as a result swell and burst spilling their contents all over the neighbors. This causes the inflammatory response to destroy not only the dead cells but also its neighbors [9, p. 1011]. In the model the inflamed tissue is restricted to the first two layers. The values for the organelles are the same as normal tissue so there are no highlighted sections in table 13-13. The swelling cells are indicated by a modest anaplastic multiplier ANAm_*1* and *ANAm_2* of 1.1 for the first two tissue layers. The cells that burst cause intracellular fluid to spill out into the extracellular fluid, lowering the extracellular fluid resistivity. This is the only instance in the models that the resistivities: cytoplasm resistivity ρ_{CP} and extracellular fluid resistivity ρ_{ef} have changed. The first two layers of tissue have lysed cells and therefore a lower extracellular fluid resistivity in the model compared to normal. The numbers of cells in the first layer has decreased by 16% due to injury. The protein volume in the cell is higher than in normal tissue as keratin fiber production has slightly increased to protect the underlying tissue from further damage [68, pp. 446-448]. This small increase in protein displaces a modest amount of extracellular fluid. The primary variable reflecting the change in displacement is the protein extracellular volume variable *PECV*. The *PECV* for the squamous cell layer and the cuboidal cell layer is 6% higher in the model for necrotic inflammation compared to normal tissue.

The network element values for necrotic inflammation tissue corresponding to the primary element variables in Tables 12-14 and 12-15 are shown in Table 12-16 hyperkeratosis tissue resistor and capacitor network values.

Table 12-16
NECROTIC INFLAMMATION TISSUE NETWORK ELEMENT VALUES

Element	value	variance +-	units	Element	value	variance +-	units	Element	value	variance +-	units
Rctn_C_om	1.492E+01	4.201E+00	Ohms	*Rctn_C_ecf*	7.037E+03	8.048E+01	Ohms	*Cctn_C_om*	8.212E-10	2.920E-10	Farads
Rcn_ER_om	4.071E+01	9.204E+00	Ohms	*Rctn_C_cp*	8.357E+02	2.554E+02	Ohms	*Cctn_ER_om*	1.785E-09	4.885E-10	Farads
Rctn_N_im	2.782E-01	6.361E-02	Ohms	*Rctn_ER_iof*	9.397E+03	1.619E+02	Ohms	*Cctn_N_im*	1.474E-11	3.687E-12	Farads
Rctn_NP	1.906E+04	6.577E+03	Ohms	*Rctn_N_np*	6.041E+03	2.135E+02	Ohms	*Cctn_TGN_om*	1.160E-10	7.202E-11	Farads
Rctn_TGN_om	1.753E-03	1.019E-04	Ohms	*Rctn_TGN_iof*	8.250E+02	2.902E+02	Ohms	*Cctn_MGN_om*	1.475E-10	8.752E-11	Farads
Rctn_MGN_om	2.297E-03	2.328E-04	Ohms	*Rctn_MGN_iof*	7.282E+02	2.902E+02	Ohms	*Cctn_CGN_om*	9.140E-11	5.743E-11	Farads
Rctn_CGN_om	1.370E-03	6.310E-05	Ohms	*Rctn_CGN_iof*	9.051E+02	3.223E+02	Ohms	*Cctn_P_om*	1.269E-10	1.049E-10	Farads
Rctn_P_om	2.154E-05	1.603E-05	Ohms	*Rctn_P_iof*	1.263E+02	5.726E+01	Ohms	*Cctn_E_om*	1.765E-11	1.677E-11	Farads
Rctn_E_om	3.012E-06	2.792E-06	Ohms	*Rctn_E_iof*	8.315E+02	5.847E+02	Ohms	*Cctn_L_om*	3.143E-11	2.961E-11	Farads
Rctn_L_om	4.521E-04	3.856E-04	Ohms	*Rctn_L_iof*	1.692E+03	1.157E+03	Ohms	*Cctn_M_om*	7.898E-10	6.981E-10	Farads
Rctn_M_om	2.195E-04	1.720E-04	Ohms	*Rctn_M_iof*	1.193E+02	5.931E+01	Ohms	*Cctn_M_im*	3.020E-09	2.698E-09	Farads
Rctn_M_im	1.258E-03	1.007E-03	Ohms	*Rctn_M_mx*	2.080E+01	4.752E+00	Ohms				

The relative magnitudes and ranges of possible network values for the model contained in Table 12-16 are shown in Fig. 12-13 through Fig. 12-15. Each graphic uses a logarithmic x-axis scale because the wide ranging values. Fig. 12-13 Membrane resistor value ranges for necrotic inflammation tissue shows how small the organelle membranes values are and how they relate to each other. Fig. 12-14 Fluid and pore resistor value ranges for necrotic inflammation tissue shows they are much larger relative to the membrane resistors. Fig 12-15 Membrane capacitor value ranges for necrotic inflammation tissue shows the values are very similar to the other models.

The impedance response corresponding to the inflammation tissue model will be plotted on a common Nyquist, Bode magnitude and Bode phase plot with the other diseases for comparison at the end of this section.

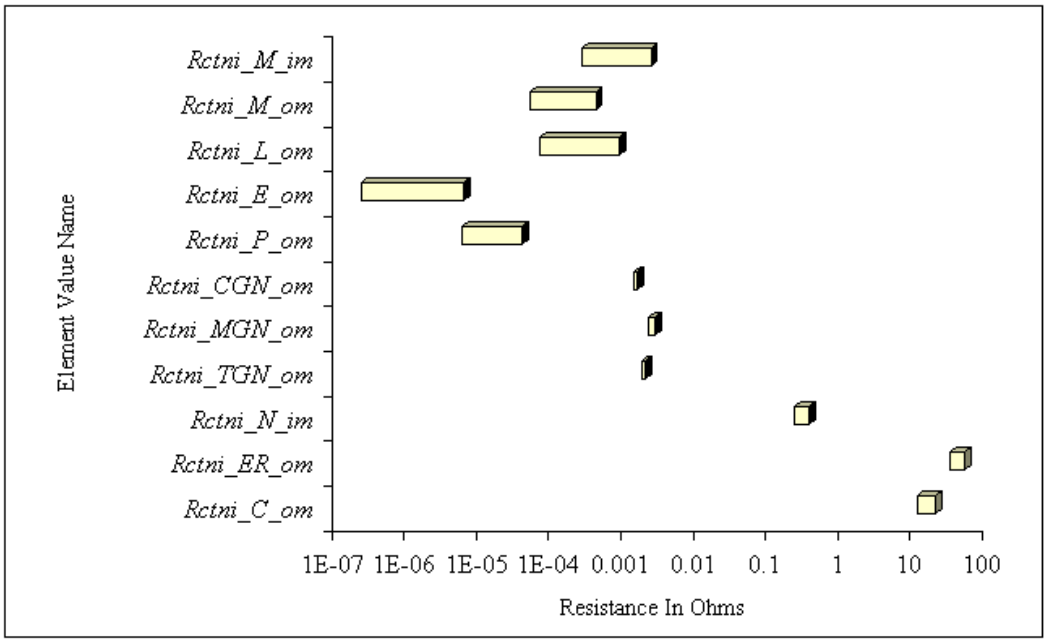

Fig. 12-13 Membrane resistor value ranges for necrotic inflammation tissue

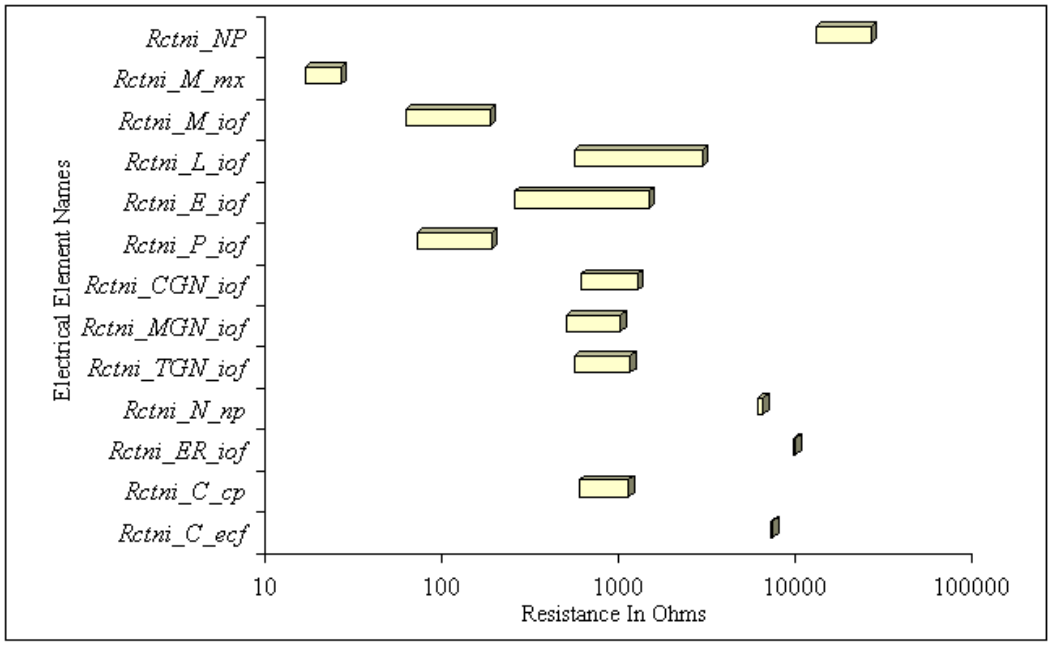

Fig. 12-14 Fluid and pore resistor value ranges for necrotic inflammation tissue

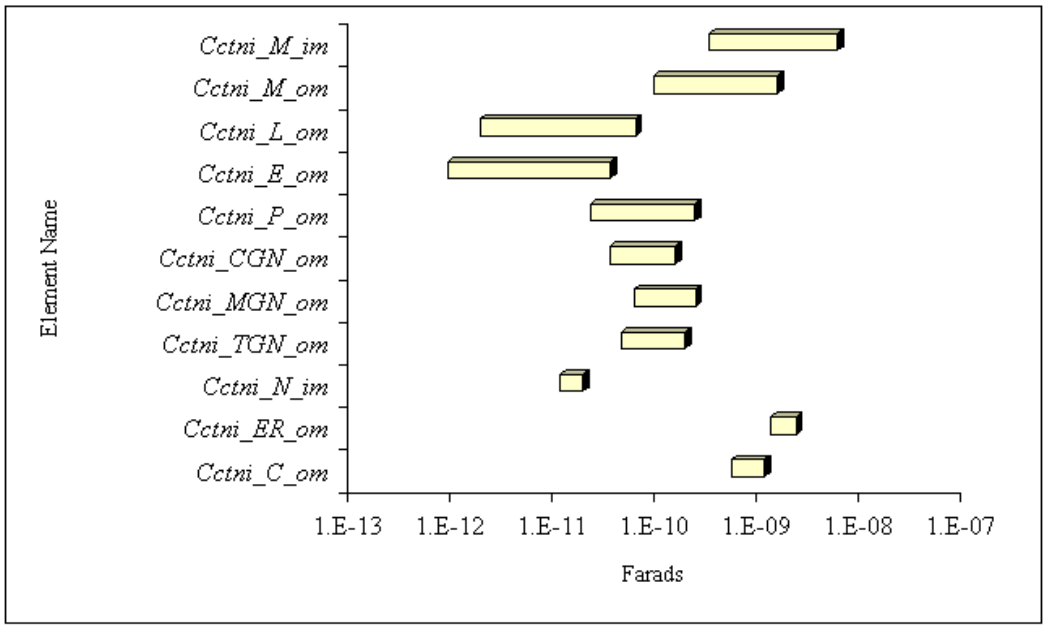

Fig. 12-15 Membrane capacitor value ranges for necrotic inflammation tissue

G. Hyperkeratosis Over Cancer Type 2 Tissue Model

Hyperkeratosis Over Cancer Type 2 Tissue (HK-CT2) is a compound condition. Hyperkeratosis is a benign oral disease that can hide the more serious oral cancers. A visual inspection will not detect the underlying cancer during a routine oral examination. Hyperkeratosis is a result of the over expression of keratin in the squamous cells. One of the cells response to a chronic irritant is the over expression of keratin. The long-term use of tobacco products irritates the oral mucosa and often leads to hyperkeratosis and may lead to dangerous cancer underneath the benign hyperkeratosis surface. The primary variables values for the model of hyperkeratosis affected squamous cell layer with type two-cancer are shown in Table 12-17 and are continued on Table 12-18. Again the highlighted values are different from normal healthy tissue values. The first layer (squamous cells) has primary variable values that look like that of the hyperkeratosis model. The rest of the remaining cell layers have values consistent with cancer type 2.

The hyperkeratosis affected cells show a decrease in the numbers of peroxisomes, endosomes, lysosomes and mitochondria [68, p. 447]. The Mitochondria numbers at the surface are low due to lower energy demand. The nucleus condenses to its smallest size as cells are fully differentiated [68, p. 446]. The protein volume inside and outside the cell is higher than in normal tissue as keratin fiber production has increased to protect the underlying tissue from chronic irritation [68, pp. 446-448]. The increase in protein displaces cytoplasm and organelles. The primary variable reflecting the change in displacement of the intracellular fluid is the protein cell volume variable *PCV*. Pathologists report the surface of hyperkeratosis tissue is tough and inelastic than normal oral mucosa [17]. The increase in structural protein makes the tissue surface appear translucent white sometimes granular and tough [17]. An increase in connective filaments between dead squamous cells prevents the normal sloughing off of individual dead cells at the surface of the oral mucosa. The extracellular protein cell volume variable *PCEV* displaces the volume of the extra cellular fluid resulting in increased resistance between cells. This dead skin cell layer gets tougher and thicker as more dead cells from lower layers get pushed up to replace old ones producing a callous thick layer of poorly conductive skin [44]. This model of hyperkeratosis tissue is moderate with an average *PCV* of 75% and an average *PECV* 55%. The underlying cancer is the medium grade of cancer it features considerable pleomorphism, less squamous cell differentiation it contains moderate mitoses distributed throughout the tissue and away from the basal membrane [11 p. 9]. The values for the primary variables in the cancer type 2 model are shown in the second and third layers of Table 12-17 and 12-18.

Table 12-17
HK-CT2 TISSUE PRIMARY VARIABLE VALUES PART I

Name of Variable	Units	Tissue Layer 1 Squamous Cell		Tissue Layer 2 Cuboidal Cell		Tissue Layer 3 Columinar Cell		Tissue Layer 4 Basal Cell		Variable Value References
		Max	Min	Max	Min	Max	Min	Max	Min	
t_m	nm	5	4	5	4	5	4	5	4	[7], [9], [50], [55], [95]
MC	uF/cm^2	1.15	0.85	1.15	0.85	1.15	0.85	1.15	0.85	[48], [50], [55], [89]
r_P	nm	250	100	213	83	213	80	250	100	[9], [68], [69], [99]
ρ_P	Ohm*cm	90	75	90	75	90	75	90	75	[1], [84], [85], [99]
MR_P	MOhm/cm^2	110	90	110	90	110	90	110	90	[48], [50], [55], [89]
P_{num}		250	200	650	520	550	440	500	400	[9], [68], [69], [71], [93]
r_E	nm	100	20	85	16.6	85	16	100	20	[9], [68], [69], [99]
ρ_E	Ohm*cm	90	75	90	75	90	75	90	75	[1], [84], [85], [99]
MR_E	MOhm/cm^2	110	90	110	90	110	90	110	90	[48], [50], [55], [89]
E_{num}		232	200	603	520	510	440	464	400	[9], [68], [69], [71], [93]
r_L	nm	400	100	340	83	340	80	400	100	[9], [68], [69], [99]
ρ_L	Ohm*cm	90	75	90	75	90	75	90	75	[1], [84], [85], [99]
MR_L	MOhm/cm^2	110	90	110	90	110	90	110	90	[48], [50], [55], [89]
L_{num}		27	17	29	19	41	26	45	29	[9], [68], [69], [71], [93]
r_{Mim}	nm	565	144	491	130	424	117	565	180	[9], [68], [69], [81], [99]
r_{Mom}	nm	600	200	690	220	600	200	600	200	[9], [68], [69], [81], [99]
t_{Mims}	nm	35	20	35	20	35	20	35	20	[9], [68], [69], [81], [99]
ρ_{Min}	Ohm*cm	90	75	90	75	90	75	90	75	[1], [84], [85], [99]
ρ_{Mmx}	Ohm*cm	30	10	30	10	30	10	30	10	[1], [84], [85], [99]
MR_{Mom}	MOhm/cm^2	110	90	110	90	110	90	110	90	[48], [50], [55], [89]
MR_{Mim}	MOhm/cm^2	110	90	110	90	110	90	110	90	[48], [50], [55], [89]
M_{num}		132	99	500	375	440	330	400	300	[9], [68], [69], [71], [93]
l_{GMC}	um	1.10	0.90	1.10	0.90	1.10	0.90	1.10	0.90	[9], [68], [69], [99]
d_{GMC}	um	0.80	0.70	0.80	0.70	0.80	0.70	0.80	0.70	[9], [68], [69], [99]
w_{GMC}	um	0.08	0.07	0.08	0.07	0.08	0.07	0.08	0.07	[9], [68], [69], [99]
$VxCGN$		1.7	1.5	1.7	1.5	1.7	1.5	1.7	1.5	[9], [68], [69], [99]
$VxTGN$		2.2	2	2.2	2	2.2	2	2.2	2	[9], [68], [69], [99]
$AxCGN$		1.9	1.7	1.9	1.7	1.9	1.7	1.9	1.7	[9], [68], [69], [99]
$AxTGN$		2.4	2.2	2.4	2.2	2.4	2.2	2.4	2.2	[9], [68], [69], [99]
MR_{MGN}	MOhm/cm^2	110	90	110	90	110	90	110	90	[48], [50], [55], [89]
MR_{CGN}	MOhm/cm^2	110	90	110	90	110	90	110	90	[48], [50], [55], [89]
MR_{TGN}	MOhm/cm^2	110	90	110	90	110	90	110	90	[48], [50], [55], [89]

Table 12-18
HK-CT2 TISSUE PRIMARY VARIABLE VALUES PART II

Name of Variable	Units	Tissue Layer 1 Squamous Cell		Tissue Layer 2 Cuboidal Cell		Tissue Layer 3 Columinar Cell		Tissue Layer 4 Basal Cell		Variable Value References
		Max	Min	Max	Min	Max	Min	Max	Min	
ρ_{MGN}	Ohm*cm	90	75	90	75	90	75	90	75	[1], [84], [85], [99]
ρ_{CGN}	Ohm*cm	90	75	90	75	90	75	90	75	[1], [84], [85], [99]
ρ_{TGN}	Ohm*cm	90	75	90	75	90	75	90	75	[1], [84], [85], [99]
G_{num}		50	24	50	24	50	24	50	24	[9], [68], [69], [71], [93]
r_{nim}	um	1.12	0.96	2.59	2.18	3.60	2.86	1.80	1.40	[9], [68], [69], [81], [99]
KV_{NER}		0.5	0.4	0.5	0.4	0.5	0.4	0.5	0.4	[9], [71], [83], [93], [94]
KA_{NER}		190	170	85.5	76.5	85.5	76.5	190	170	[9], [71], [83], [93], [94]
Mr_{erom}	MOhm/cm^2	110	90	110	90	110	90	110	90	[48], [50], [55], [89]
ρ_{er}	Ohm*cm	90	75	90	75	90	75	90	75	[9], [68], [69], [71], [93]
Mr_{nim}	MOhm/cm^2	110	90	110	90	110	90	110	90	[48], [50], [55], [77], [89]
ρ_{n}	Ohm*cm	90	75	90	75	90	75	90	75	[1], [84], [85], [99]
G_{pore}	pS	1000	750	3000	1000	3000	1000	1000	750	[84], [85], [78]
Npd	pores/um^2	50	40	50	40	50	40	50	40	[9], [68], [71], [83], [94]
ER_{num}		1	1	1	1	1	1	1	1	[9], [68], [71], [83], [94]
N_{num}		0.9	0.8	1.1	1.08	1.1	1.01	1	1	[9], [68], [71], [83], [94]
LS_out	um	18.00	14.00	7.00	5.60	7.00	5.60	7.00	5.60	[9], [68], [69], [71]
H_cell	um	2.80	2.20	14.00	18.00	28.00	18.00	12.00	10.00	[9], [68], [69], [71]
Eg	nm	120	50	120	50	120	50	120	50	[9], [68], [69], [71]
PCV	percent	80%	70%	8%	6%	12%	8%	15%	10%	[9], [98], [99]
$PECV$	percent	60%	50%	10%	6%	12%	10%	25%	15%	[9], [69], [71], [101]
ρ_{CP}	Ohm*cm	85	60	85	60	85	60	85	60	[1], [84], [85], [96], [99]
MR_{PM}	MOhm/cm^2	110	90	110	90	110	90	110	90	[48], [50], [55], [89]
ρ_{ef}	Ohm*cm	80	55	80	55	80	55	80	55	[1], [84], [85], [99]
Yw	cm	0.2	0.2	0.2	0.2	0.2	0.2	0.2	0.2	[50], [55], [65]
Xl	cm	0.3	0.3	0.3	0.3	0.3	0.3	0.3	0.3	[50], [55], [65]
Ncz_n		40	40	37	37	3	3	20	20	[9], [98], [99]
Zh_n	um | percent	117	12%	522	54%	84	9%	242	25%	[9], [98], [99]
$ANAm\_n$		1.00	1.00	1.00	1.00	1.00	1.00	1.00	1.00	[9], [68]
$Mimpm\_n$		1.00	0.80	0.75	0.65	0.75	0.65	1.00	1.00	[9], [68], [69], [71], [93]
$Mimrm\_n$		1.00	0.80	0.75	0.65	0.75	0.65	1.00	1.00	[9], [68], [69], [71], [93]
Nrm_n		1.00	1.00	1.80	1.40	1.80	1.40	1.00	1.00	[9], [68], [69], [71], [93]
Orm_n		1.00	1.00	0.85	0.83	0.85	0.80	1.00	1.00	[9], [68], [69], [71], [93]

There is an increase in the numbers of peroxisomes, endosomes and mitochondria for the middle two layers of tissue [70, p.51]. While the number of lysosomes in the cancer affected cell layers has decreased [70, p. 59]. The nucleus radius is on average larger because the DNA in the nucleus can no longer condense on the histones, the chromosomes themselves have mismatches, multiple copies and are damaged resulting in the failure of the nucleus to return to normal pre mitotic and pre cancer size, number and shape [9, p. 1316], [69, pp. 14-17]. Approximately one out of ten cuboidal cells will have multiple nuclei [12] hence N_{num} is 1.1 in cell layer two. The endoplasmic reticulum membrane area decreases as the nucleus membrane increases [100], [101]. This is shown in the model by a smaller nuclear to endoplasmic reticulum area multiplier $KA_{NER.}$ The protein volume in the cell is low, large keratin fiber production is further replaced by smaller fibers of actin and myosin [69, p. 7], [70, p.152]. This change in protein affects the displacement of cytoplasm. The primary variable reflecting the change in displacement is the protein cell volume variable *PCV*. There is a reduction in the extracellular connective proteins too. This is shown in the model by a lower *PECV* in the middle two layers of the model. The decrease in keratin makes the tissue feel softer pathologists report tumors are said to be noticeably more elastic from the keratin replacement by actin [12]. The drastic decrease in structural protein makes the tissue easy to rupture with moderate sheer forces but the tough Hyperkeratosis layer above mitigates this side effect. Like the cancer type two model the mitochondria have a reduced number and size of crista in the middle cell layers [69, p. 12]. The deformed mitochondria crista is implemented in the model with a reduced mitochondria inner membrane pleat multiplier *Mimpm_n* and a reduced mitochondria inner membrane radius multiplier *Mimrm_n.* Like cancer types one and two this cancer has not developed past the basal

membrane. Primary variable values in the forth layer still remain the same as that of the normal cell model.

The network element values for hyperkeratosis over cancer type two-tissue model are shown in Table 12-19 HK-CT2 tissue resistor and capacitor network values.

Table 12-19
HK-CT2 TISSUE NETWORK ELEMENT VALUES

Element	value	variance +-	units	Element	value	variance +-	units	Element	value	variance +-	units
Rctn_C_om	1.185E+01	2.933E+00	Ohms	*Rctn_C_ecf*	5.155E+03	9.896E+01	Ohms	*Cctn_C_om*	6.259E-10	2.067E-10	Farads
Rcn_ER_om	2.707E+01	6.120E+00	Ohms	*Rctn_C_cp*	1.798E+03	7.170E+02	Ohms	*Cctn_ER_om*	1.406E-09	3.849E-10	Farads
Rctn_N_im	4.098E-01	9.370E-02	Ohms	*Rctn_ER_iof*	9.303E+03	1.602E+02	Ohms	*Cctn_N_im*	3.064E-11	1.042E-11	Farads
Rctn_NP	6.719E+03	4.464E+03	Ohms	*Rctn_N_np*	4.429E+03	-9.454E+01	Ohms	*Cctn_TGN_om*	1.171E-10	7.274E-11	Farads
Rctn_TGN_om	1.736E-03	1.009E-04	Ohms	*Rctn_TGN_iof*	8.167E+02	2.873E+02	Ohms	*Cctn_MGN_om*	1.490E-10	8.841E-11	Farads
Rctn_MGN_om	2.274E-03	2.304E-04	Ohms	*Rctn_MGN_iof*	7.210E+02	2.873E+02	Ohms	*Cctn_CGN_om*	9.232E-11	5.801E-11	Farads
Rctn_CGN_om	1.357E-03	6.247E-05	Ohms	*Rctn_CGN_iof*	8.961E+02	3.191E+02	Ohms	*Cctn_P_om*	1.268E-10	1.054E-10	Farads
Rctn_P_om	2.239E-05	1.870E-05	Ohms	*Rctn_P_iof*	1.174E+02	5.378E+01	Ohms	*Cctn_E_om*	1.767E-11	1.681E-11	Farads
Rctn_E_om	2.084E-06	1.937E-06	Ohms	*Rctn_E_iof*	7.926E+02	5.645E+02	Ohms	*Cctn_L_om*	2.261E-11	2.132E-11	Farads
Rctn_L_om	4.901E-04	4.198E-04	Ohms	*Rctn_L_iof*	2.254E+03	1.548E+03	Ohms	*Cctn_M_om*	1.075E-09	9.569E-10	Farads
Rctn_M_om	2.185E-04	1.731E-04	Ohms	*Rctn_M_iof*	8.222E+01	4.231E+01	Ohms	*Cctn_M_im*	2.529E-09	2.334E-09	Farads
Rctn_M_im	6.042E-04	5.307E-04	Ohms	*Rctn_M_mx*	2.301E+01	7.700E+00	Ohms				

The relative magnitudes and ranges of possible network values for the model contained in Table 12-19 are shown in Fig. 12-16 through Fig. 12-18. Each graphic uses a logarithmic x-axis scale because the wide-ranging values being displayed. Fig. 12-16 Membrane resistor value ranges for HK-CT2 tissue shows how small the organelle membrane values are and how they relate to each other. Fig. 12-17 Fluid and pore resistor value ranges for HK-CT2 tissue shows they are much larger relative to the membrane resistors. Fig. 12-15 Membrane capacitor value ranges for HK-CT2 tissue shows the values is very similar to the other models. Because comparisons of these model network elements is difficult in this format Section XIII provides a direct side by side model comparison for each element. The side-by-side comparison makes it easier to notice the subtle changes to the network elements caused by the different conditions created by the changing primary variables.

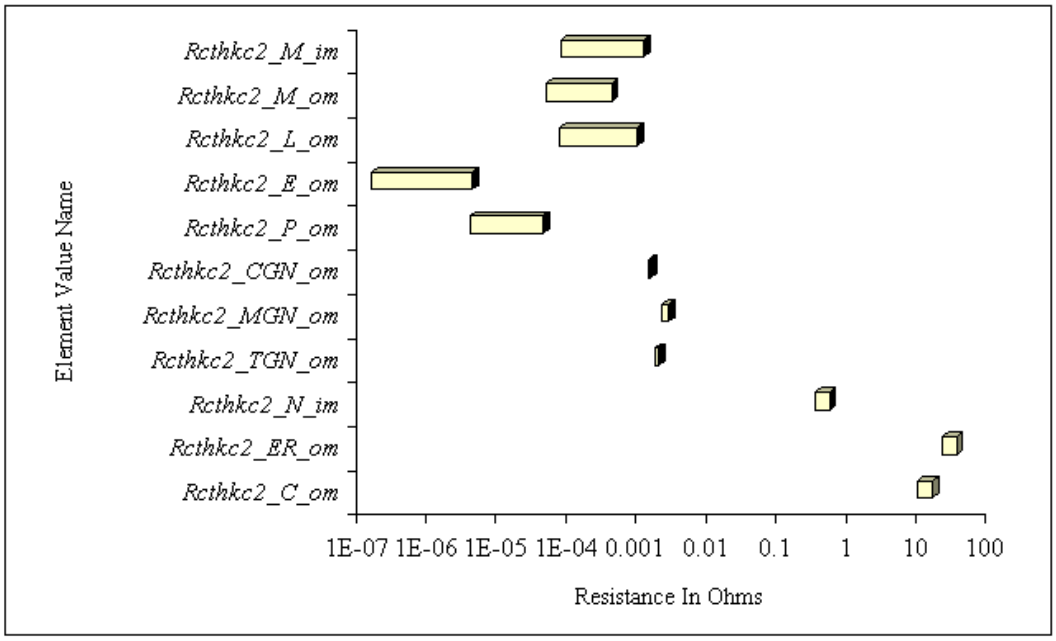

Fig. 12-16 Membrane resistor value ranges for HK-CT2 tissue

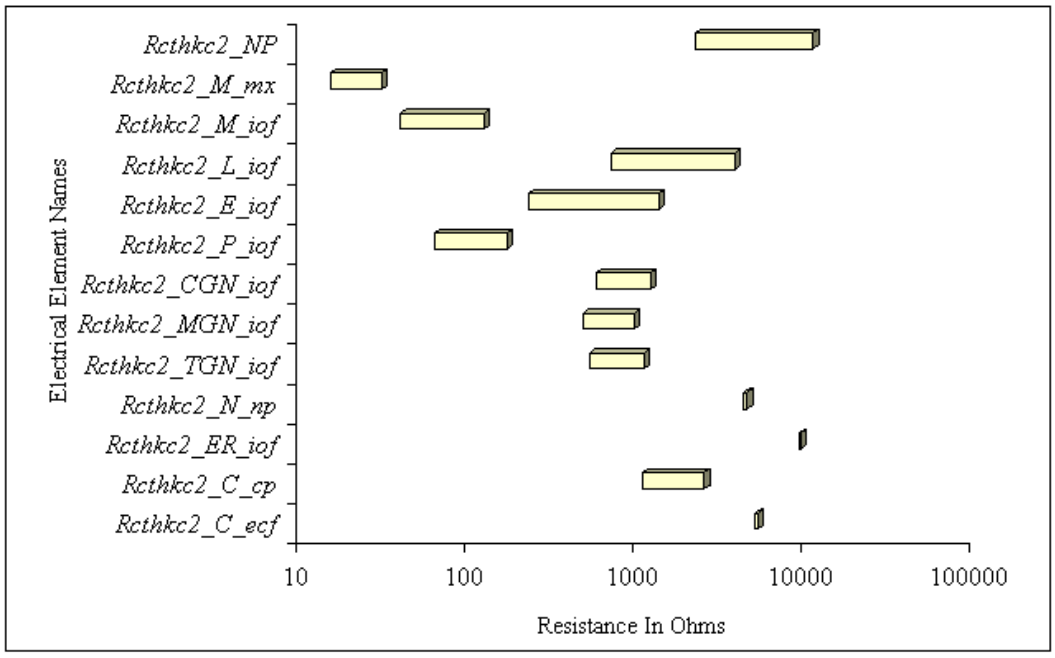

Fig. 12-17 Fluid and pore resistor value ranges for HK-CT2 tissue

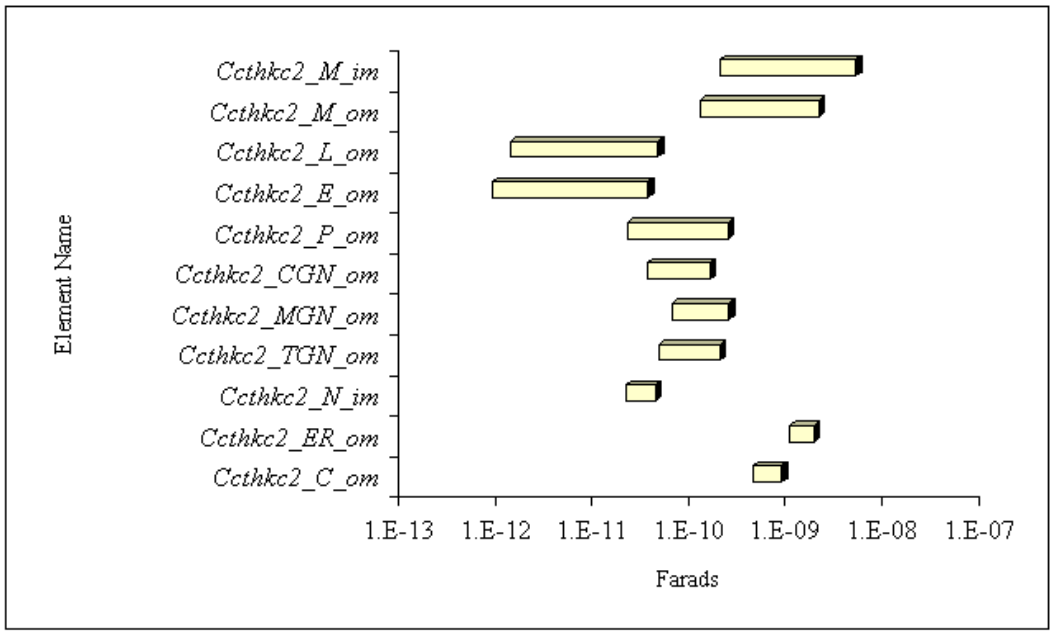

Fig. 12-18 Membrane capacitor value ranges for HK-CT2 tissue

Comparing the network elements will only provide some of what is going on. For this reason a network evaluation must be included with the electrical element evaluation; Section XIV provides this. The most practical way of evaluating the models is with frequency response analysis and this is provided next in this section.

H. Tissue Model Frequency Responses

It is difficult to interpret the differences in impedance responses by looking at the resistor and capacitor network values for each model alone. The Nyquist plot provides an ideal comparison for the impedance response of the tissue models. Fig. 12-19 Nyquist plot of the mean tissue impedance for each model shows the range of real and imaginary impedance values for each model. The network elements from each model were evaluated with the "Transparent Box" circuit topology in the frequency domain using P-spice® and Microsoft Excel®, the data was then plotted using Microsoft Excel®. The overall impedance response of the cancers including HK-CT2 is lower than the normal tissue. From casual inspection the impedance response for the inflammation and the

hyperkeratosis is slightly larger than the normal tissue response. It is highly plausible that these impedance response differences are large enough to prevent mistaking benign conditions such as hyperkeratosis and necrotic inflammation as cancerous lesions. A more detailed examination of the data will extract insight into developing ways of identifying disease from a simple series of impedance measurements with greater precision.

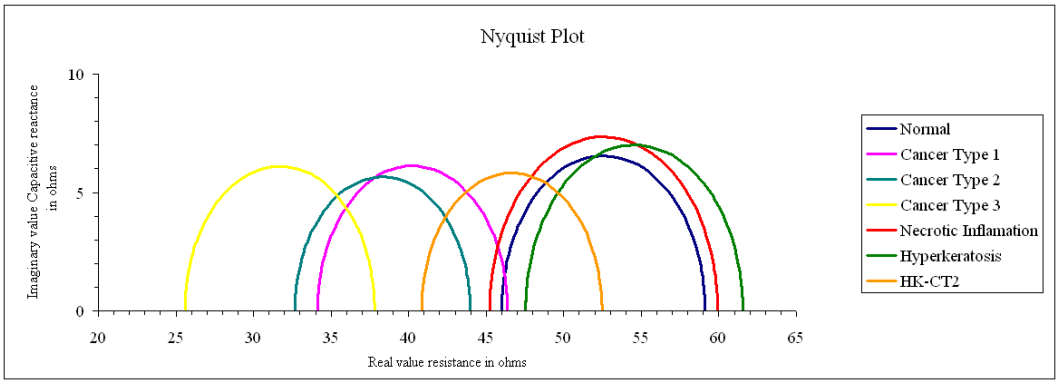

Fig. 12-19 Nyquist plot of the mean tissue impedance for each model

The Monte Carlo simulations for all the models produced families of waveforms from each model. Hundreds of random simulations were performed for each tissue model. These waveforms overlap and diverge from the mean sometimes smaller other times larger. The majority of waveforms (95% confidence interval) that result have a variance from the mean impedance that is less than ten percent. This is illustrated in Fig. 12-20 Nyqust plot with Monte Carlo simulation uncertainty. The overlapping bands creates a little uncertainty when it comes to identifying differences between the normal model, the hyperkeratosis model and the necrotic inflammation model especially at low frequencies. The difference between all the other cancerous models and the benign conditions is clearer with no overlap. Identification between cancer type 1 and cancer type 2 is less clear because there is a zone in-between each model where there is a 50%

overlap at all frequencies. Cancer type 3 is easily identified with no overlap with the low frequency regions of the other less malignant cancer grades.

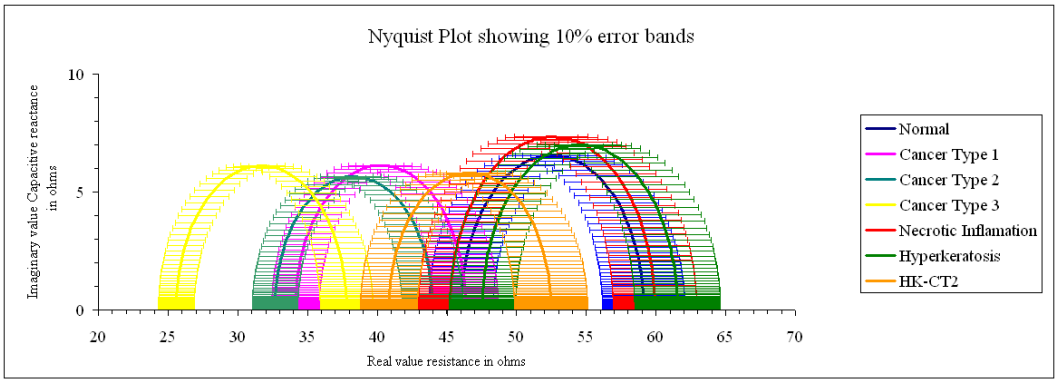

Fig. 12-20 Nyqust plot with Monte Carlo simulation uncertainty

Another way to visualize the impedance is by using the Bode plot. The Bode magnitude plots the magnitude of impedance as a function of the log of the frequency as shown in Fig. 12-21 Mean tissue impedance Bode magnitude plot for all the models.

The Bode phase plot provides the phase angle shift in degrees as a function of frequency as shown in Fig. 12-22 Bode phase plot. Fig. 12-23 Bode plot with Monte Carlo simulation uncertainty shows a 10% band of uncertainty again like the Nyqust plot this shows the resolution between the benign conditions make it difficult to separate the responses from the normal response.

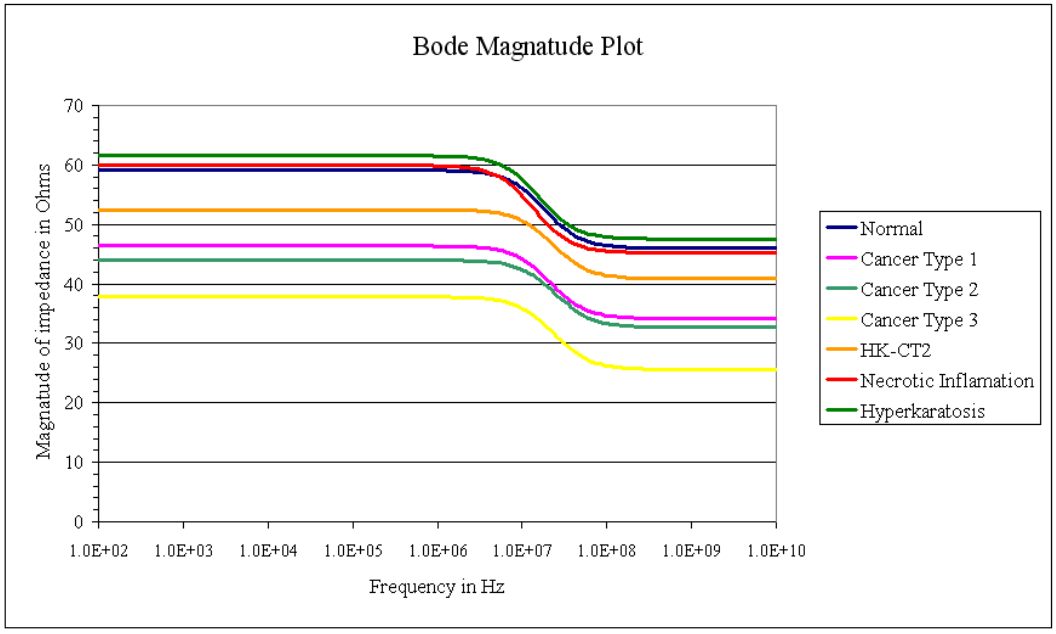

Fig. 12-21 Mean tissue impedance Bode magnitude plot for all the models

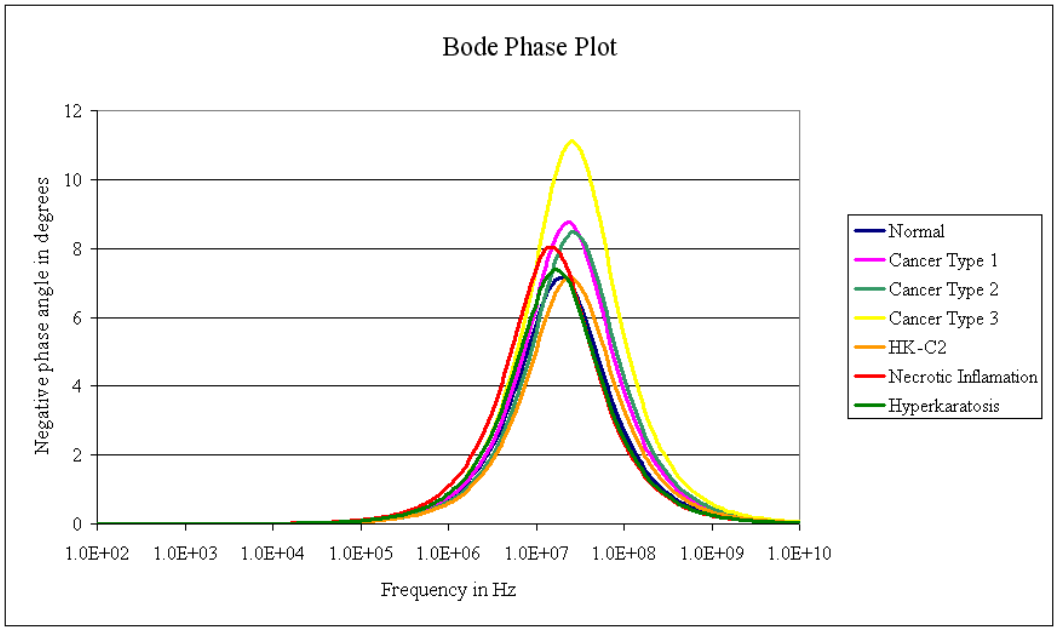

Fig. 12-22 Bode phase plot

Identification of cancers type 1 and type 2 is difficult from the close overlap between these responses. From all the Bode plots one may notice the maximal amount of phase change occurs in about one decade of frequency. The maximum magnitude difference between tissues happens before or after this phase shift; this can be seen in Fig. 12-21 Percent difference in the magnitude of impedance. Fig. 12-21 is a modified Bode plot where the frequency responses are normalized by the normal tissue model frequency response. From this plot one can see that measuring the magnitude at high frequency after the dispersion will give the poorest separation between models. To effectively identify tissue health with a single frequency it may be better to choose a frequency at least one to two decades lower than the frequency dispersion.

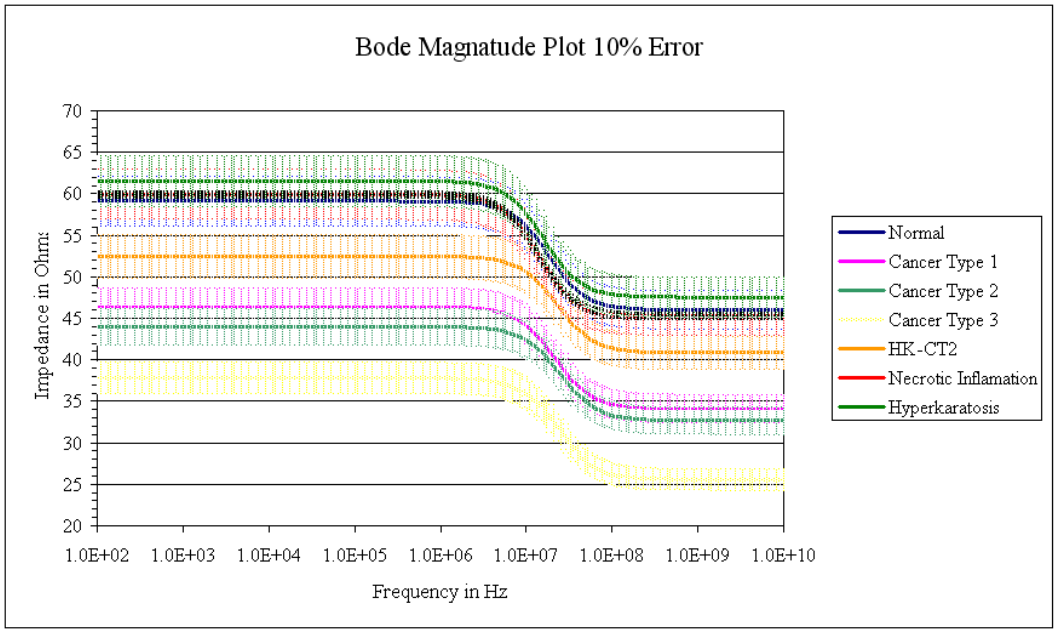

Fig. 12-23 Bode magnitude plot with Monte Carlo simulation uncertainty

Note as the tissue sample size increases (probe electrode spacing increases) this dispersion will shift to the left toward lower frequencies. One can use other parameters to identify tissue health rather than a single frequency; one can use multiple frequencies to

identify tissues. The percent difference in the magnitude of the impedance shown in Fig. 12-24 has both imaginary and real parts. One can evaluate the contribution given by just the real part or just the imaginary part in order to identify what dominates the response at the various frequencies.

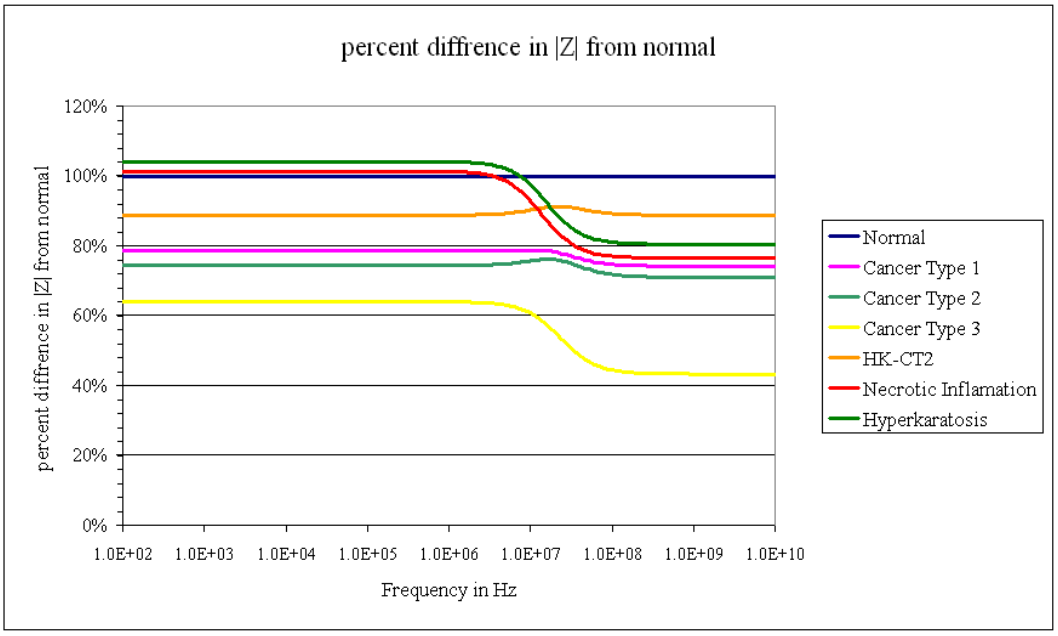

Fig. 12-24 Percent difference in the magnitude of impedance

The contribution of the real part of impedance is illustrated in Fig. 12-25 The percent difference in the resistance from the normal tissue. The contribution to the impedance by the imaginary part is given in Fig. 12-26 The percent difference in reactance from the normal tissue. The part that stands out is the reactance of the cancer tissue models dominates the impedance at high frequency.

If one wanted to determine the difference between inflammation and hyperkeratosis when frequency responses are similar to a normal healthy tissue response, then a simple visual inspection of the patients' lesion in a clinical setting will provide the answer. Red

lesions (erythroplakic) are from inflammation and white (leukoplakic) lesions are likely hyperkeratosis. There are subtle differences in the component parts of the impedance. The inflammation response has a much larger imaginary component than normal or hyperkeratosis tissues. Hyperkeratosis tissues have a larger low frequency resistance than the normal or inflamed tissues.

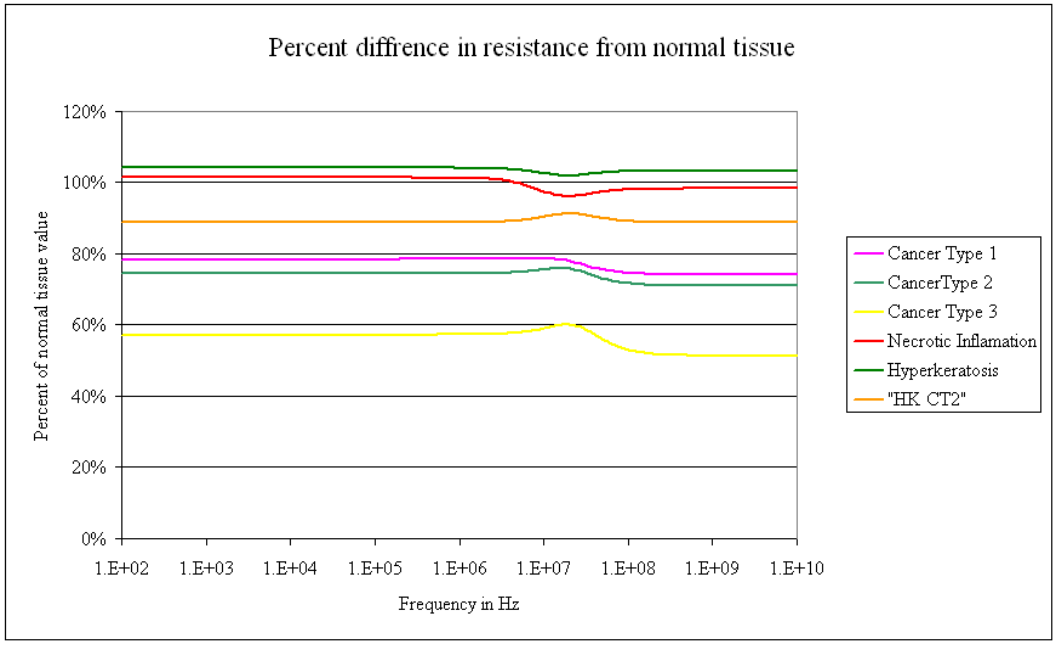

Fig. 12-25 The percent difference in the resistance from the normal tissue

When one carefully examines the percent difference in resistance from the normal tissue curves in Fig. 12-25 one may notice that derivative tests would be helpful. By examining the first derivatives of the curves leading up to the dispersion frequency it becomes clear that a negative first derivative indicate benign conditions.

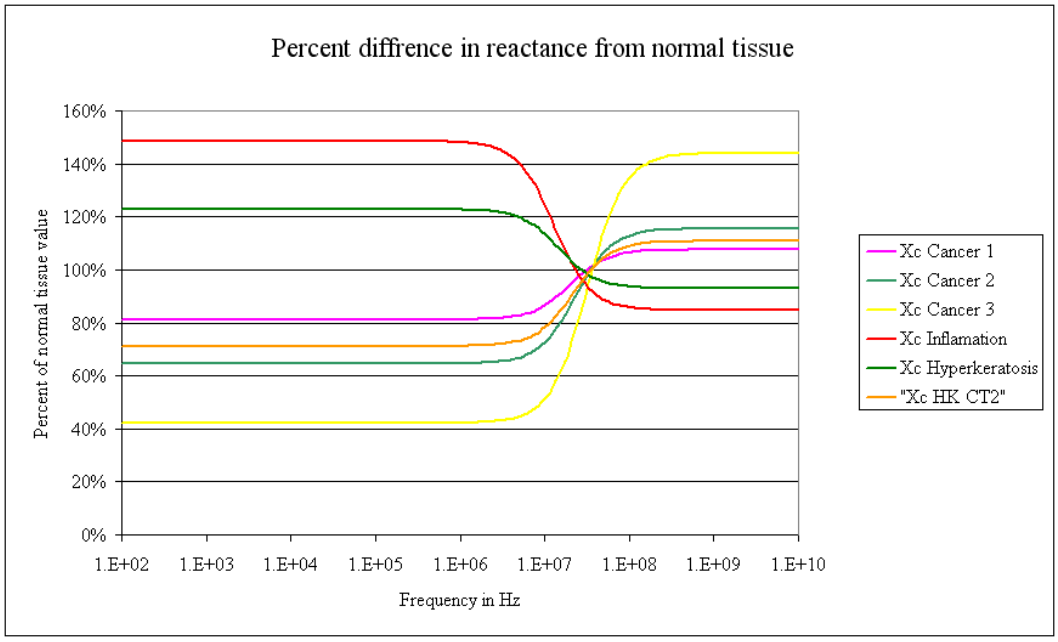

Fig. 12-26 The percent difference in reactance from the normal tissue

And the curves that have positive first derivatives leading up to the dispersion frequency come from malignant or cancerous conditions. Notice how the compound diseased tissue model of hyperkeratosis with cancer type 2 has a resistance value close to that of normal tissue. If you overlay HK-CT2 with a positive 10% uncertainty caused by randomness in the Monte Carlo experiments one could get resistances close to a normal value and one might be fooled into predicting that this is the signature of a benign condition. But if one were to take the first derivative of the curve leading up to the dispersion frequency it would show that it is positive and therefore the tissue must be cancerous or at the very least pre-cancerous and necessitates further investigation through a biopsy. This same logic can be applied to the imaginary component as well. The percent difference in reactance from the normal tissue shown in Fig. 12-26 suggests the same behavior negative first derivative leading up to the dispersion frequency suggests this is the signature of a benign condition whereas a positive first derivative suggests that it is the signature of a malignant condition.

When identifying the differences between the tissues and tissue models it is helpful to obtain the largest difference in the measured signal. One technique might be to use the peak product of the real part multiplied by the imaginary part this is shown in Fig. 12-27 R*Xc Product. There is a noticeable shift to the right in the peak as the tissue models become cancerous. Using a single impedance measurement with the resistance reactance product method may be problematic. There is good separation between the curves at frequencies between about 1 MHz and 8 MHz with the 1mm electrode spacing. Measurements after the peak have lower separation and would not be recommended.

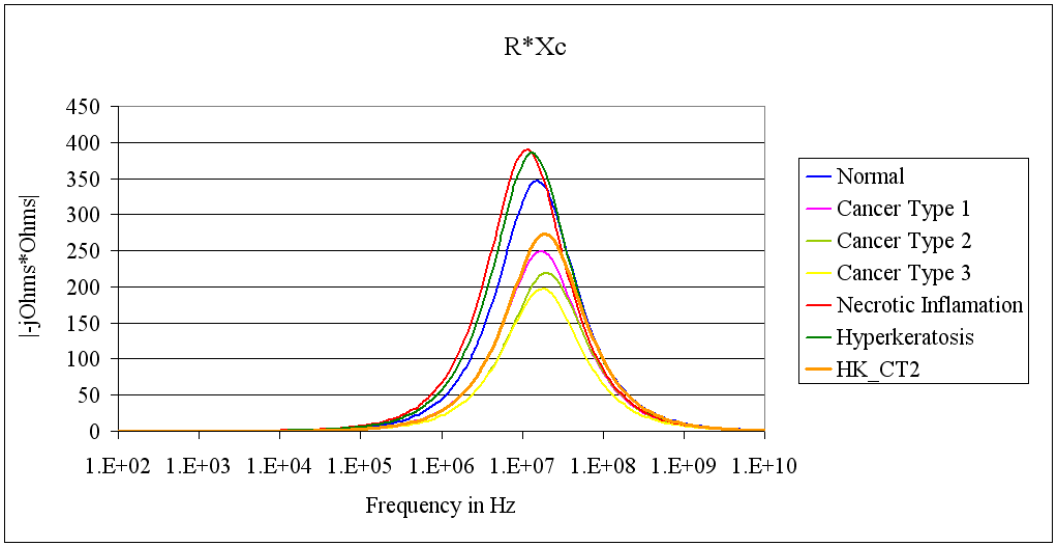

Fig. 12-27 R*Xc Product

The lack of separation between waveforms is better illustrated by viewing the same data from Fig. 12-27 but normalized by the product of the real impedance times the imaginary impedance of the normal tissue model. This modification produces Fig. 12-28 Percent difference between R*Xc from the normal tissue model. It shows clear separation and therefore identification between normal tissue and cancers at low frequency. It shows clear separation between normal tissue and both hyperkeratosis and necrotic

inflammation models at low frequencies. But at low frequencies there is no separation between cancer type 1 and HK-CT2 as well as between cancer type 2 and cancer type 3. But there is separation from those same pairs at high frequency. This type of analysis would require measurements be made at both high and low frequencies. Two frequency measurements will increase time to measure and probably increase the cost of the instrumentation.

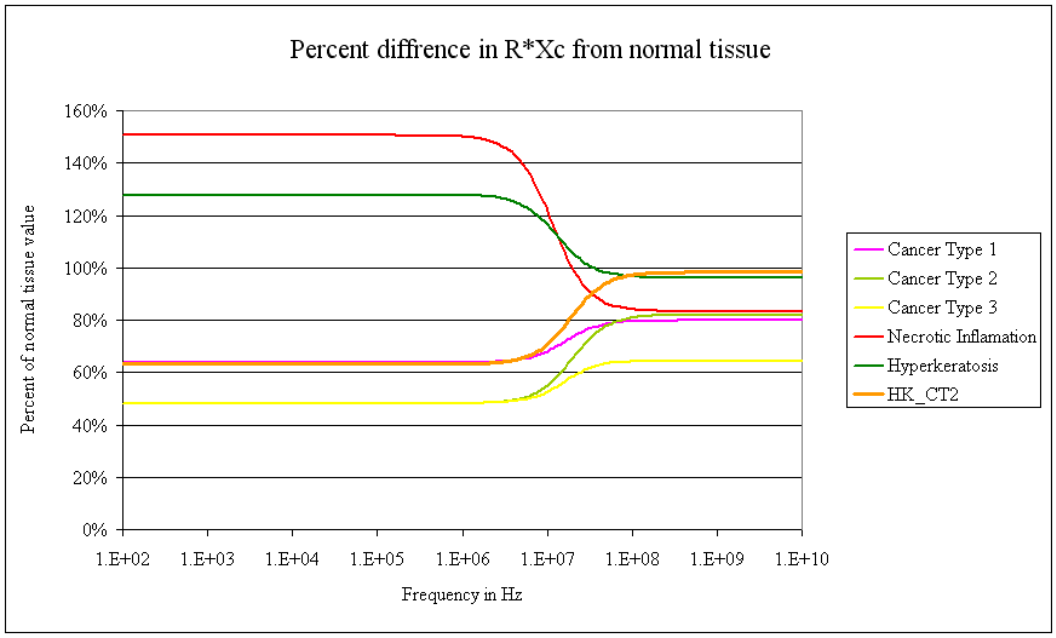

Fig. 12-28 Percent difference between R*Xc from the normal tissue model

One can get away from the influence of frequency shifts and Ohmic shifts in order to identify tissue by impedance. Notice the Ohmic shift of impedance curves in the Nyquist plots of Fig. 12-19 and Fig. 12-20. The various curves for each model form arches of different sizes that are shifted so one could not only characterize a tissue by its real and imaginary values at high and low frequencies and by its shift, one could also characterize a tissue by the area under the curve. The area under the curve can be viewed independent of the shifts in ohmic value. The area can be calculated unit less by normalizing. The

area under the curve for the Nyqust plot in Fig. 12-19 can be normalized by dividing the area under the curve for each diseased model by the area under the curve for the normal healthy tissue model. The comparison of the curves can be seen in the bar chart in Fig. 12-29 Normalized area under the curve of the nyquist plot.

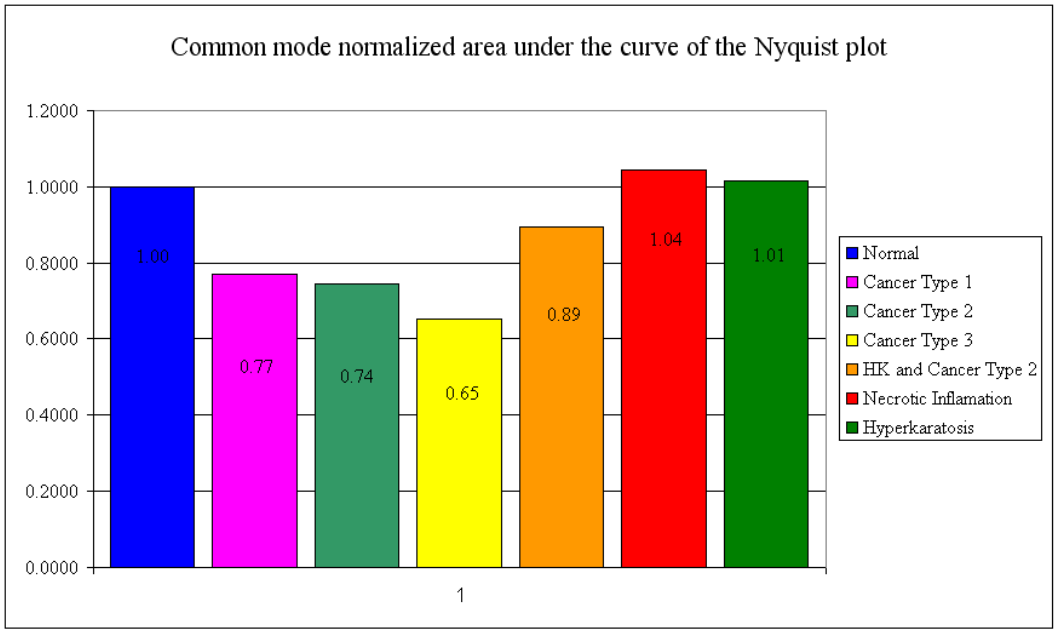

Fig. 12-29 Normalized area under the curve of the Nyquist plot

One drawback of this method would be the need to sample at several frequencies to form a good Nyquist plot; this will increase the time it takes to make an impedance measurement. To simplify this measurement dilemma one can measure the impedance at a relatively low frequency around 5kHz then normalizes the measured impedance by the normal healthy tissue; this is shown in Fig. 12-30 Normalized maximum low frequency resistance. Since the measurement is single frequency it is quick and the resolution between the various diseases is surprisingly good.

To increase the signals spacing between benign and cancerous tissues one can take the product of Fig. 12-29 and Fig. 12-30 this makes the benign conditions signals larger

and the cancerous conditions smaller. The results of this product can be seen in Fig. 12-31 Product of the common modes of normalized area under the Nyquist plot times the normalized maximum low frequency resistance. This can be a helpful method for determining if a lesion was benign or dangerous especially if environmental factors might have increased the uncertainty of the measurement.

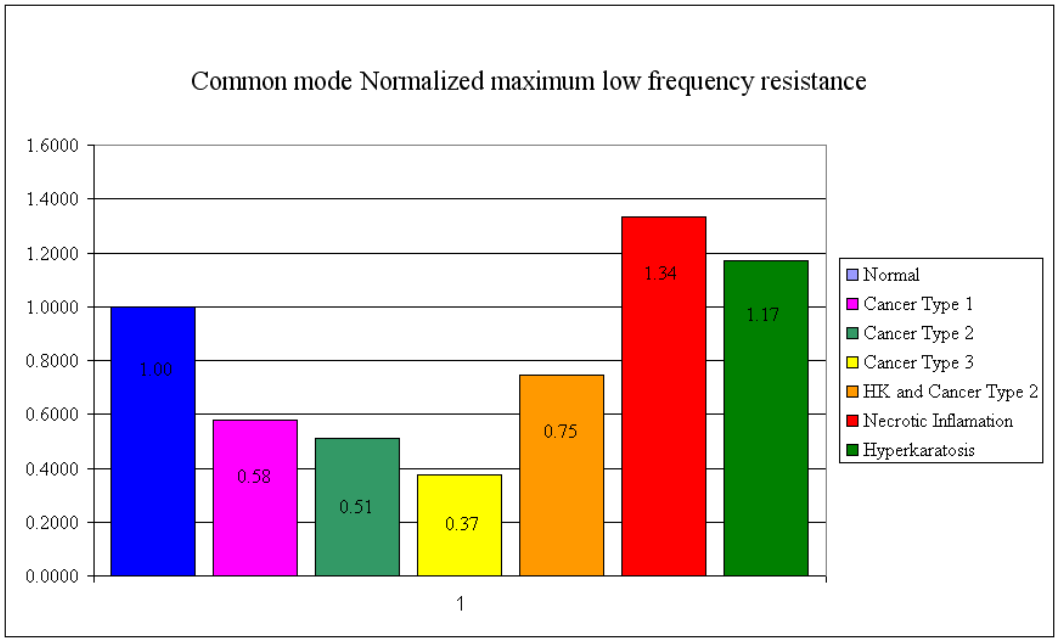

Fig. 12-30 Normalized maximum low frequency resistance

The power of using impedance to screen oral tissue is the variety of methods that can be used to identify differences in tissue. All these methods come from a simple magnitude and phase measurement at various frequencies.

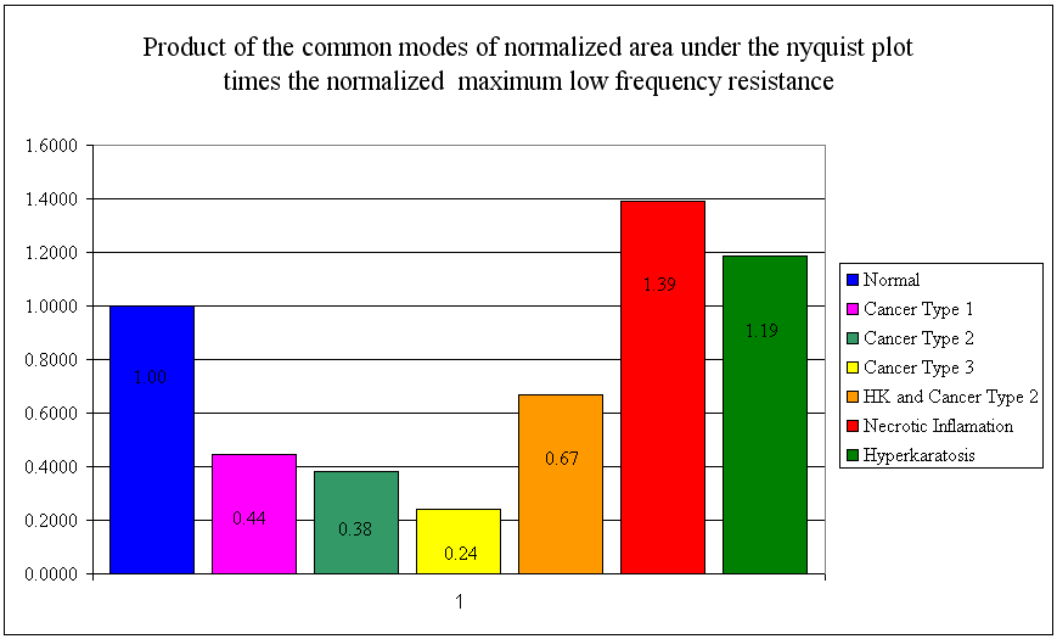

Fig. 12-31 Product of the common modes of normalized area under the Nyquist plot times the normalized maximum low frequency resistance

I. Review of the "Transparent Box" Model for Diseased Tissue

This section started with the introduction of some simple multipliers that act on primary structural variables. In this way the normal tissue model is in effect unchanged when the multipliers are equal to one. These multipliers act as a shortcut to the tedious changing of the individual primary variables in the worksheets by hand. The majority of the chapter was explaining the small differences in the primary variables that are indicators of a specific disease or condition. Models for cancer type 1, cancer type 2, cancer type 3, hyperkeratosis necrotic inflammation and hyperkeratosis combined with cancer type 2 were developed and compared. A brief analysis of different graphing and data display and manipulation methods showed how these various methods could be used to identify disease types by differences in the impedance. The last method shown was the area under the curve of a Nyquist plot this method is independent of electrolyte Ohmic shifts.

An analysis algorithm can be constructed using these methods to evaluate the key features that identify the specific disease based entirely on impedance. The models here simply suggest the factors are structural and that have a relatively large influence on the differences in impedance measurement from normal and are not intended to predict the absolute impedance of a tissue.

XIII. TISSUE MODEL NETWORK ELEMENT COMPARISON

A. Network Element Comparison

In order to evaluate the “Transparent Box” model for possible network reduction or modification it is important to compare the magnitudes of the individual resistor and capacitor elements. An element-by-element comparison will help identify typical maximum and minimum element ranges within the various tissue models. This evaluation coupled with the network evaluation will identify the dominant features affecting impedance. The “Transparent Box” model has thirty five total circuit elements; eleven membrane capacitor elements, eleven membrane resistor elements, twelve fluid resistor elements and one nuclear pore resistor element. All of them have an effect on the overall impedance measurement. Some elements regardless of size have a dominant effect some elements because of network location have very little effect. It is important to note that it is best to keep the model intact and not to reduce it based on the few diseases that were modeled here.

B. Membrane Resistances

The membrane resistances for the tissue model network are typically small because of the large numbers of membranes in parallel. The small values have a huge effect when they are in parallel with other network elements and of course a miniscule effect when in series. One of the most important membrane resistors has to be the cell plasma membrane. The resistor values for each tissue model representing the outer membrane *R_C_om* is compared in Fig. 13-1 Cell outer membrane resistor comparison. What is striking about this set of resistor values is their similarity between models; each model’s cell plasma membrane practically overlaps the other only the cancer models have smaller ranges and slightly smaller averages.

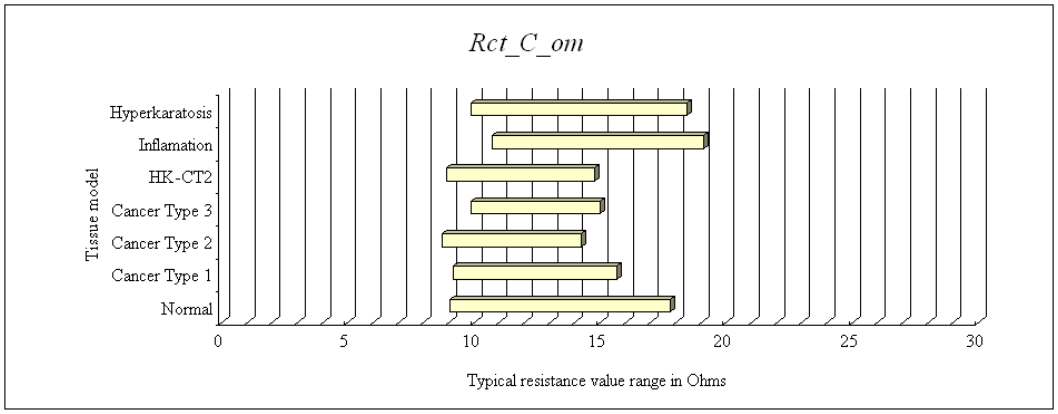

Fig. 13-1 Cell outer plasma membrane resistor comparison

The resistor values for each tissue model representing the endoplasmic reticulum outer membrane *R_ER_om* is compared in Fig. 13-2 Endoplasmic reticulum outer membrane resistor comparison.

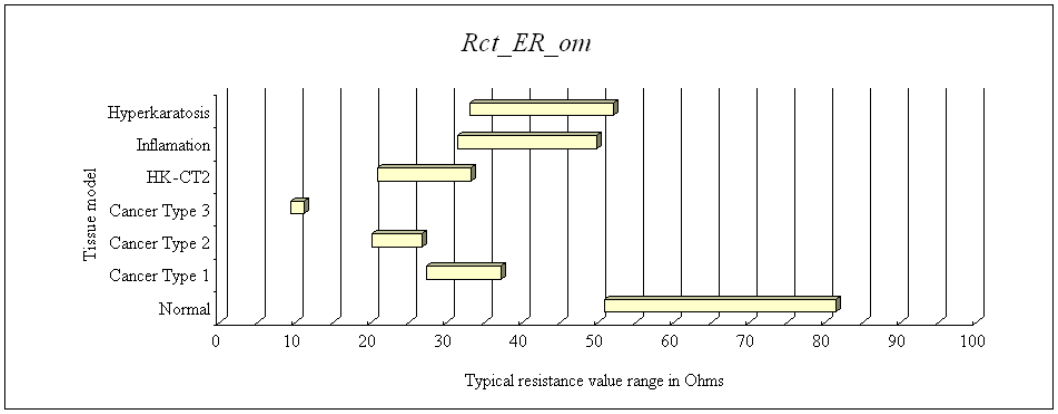

Fig. 13-2 Endoplasmic reticulum outer membrane resistor comparison

Notice there is a wide range of values. The normal cell model has the largest range of possible values and the largest average value. Cancer type 3 has the smallest possible value and range. There is less overlap between these models for each tissue type. Cancerous diseases are on the left and benign conditions are on the right.

The resistor values for each tissue model representing the nuclear envelope inner membrane *R_N_im* is compared in Fig. 13-3 Nuclear envelope inner membrane resistor comparison. This network element comparison looks interesting. The cancer type 3 inner membrane resistor has no overlap with the other models.

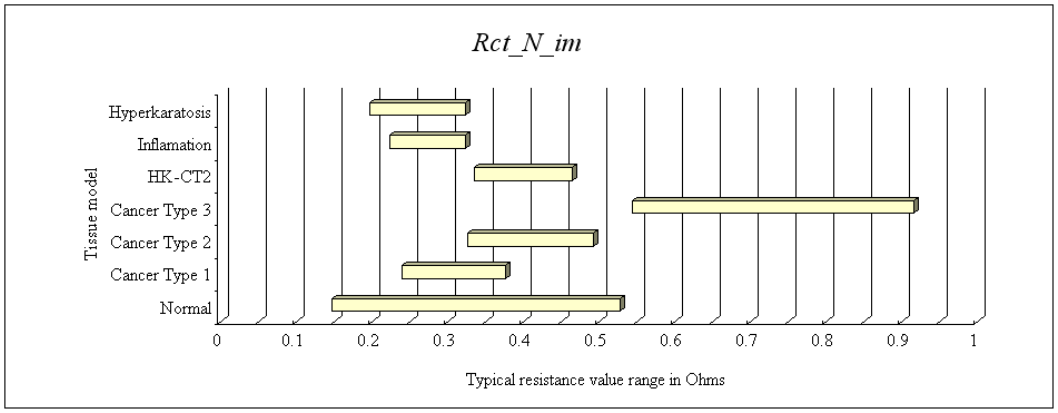

Fig. 13-3 Nuclear envelope inner membrane resistor comparison

The trans Golgi network outer membrane resistors *R_TGN_om* are compared in Fig. 13-4 Trans Golgi network resistor value comparison.

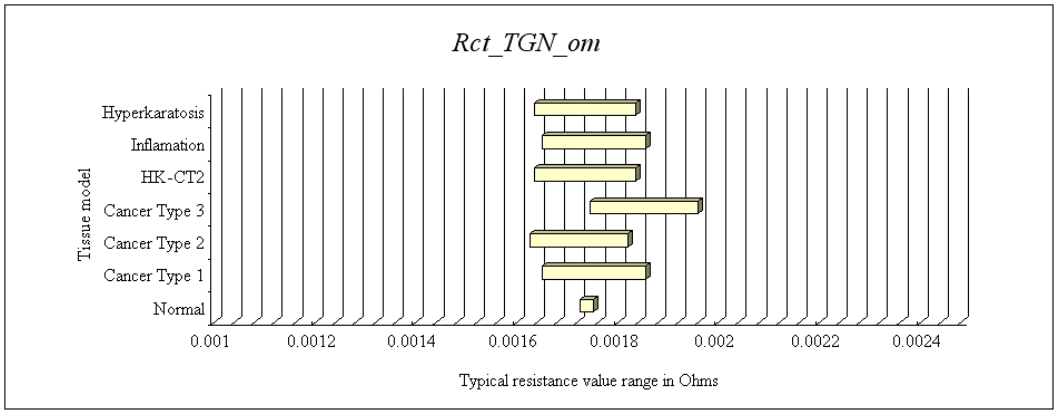

Fig. 13-4 Trans Golgi network resistor value comparison

The medial Golgi network outer membrane resistors *R_MGN_om* are compared in Fig. 13-5 Medial Golgi network resistor value comparison.

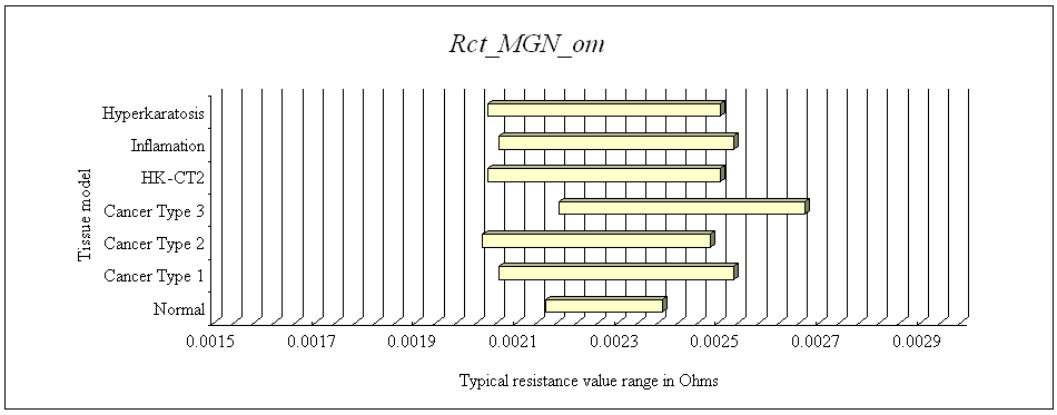

Fig. 13-5 Medial Golgi network resistor value comparison

The cis Golgi network outer membrane resistors *R_CGN_om* are compared in Fig. 13-6 Cis Golgi network resistor value comparison.

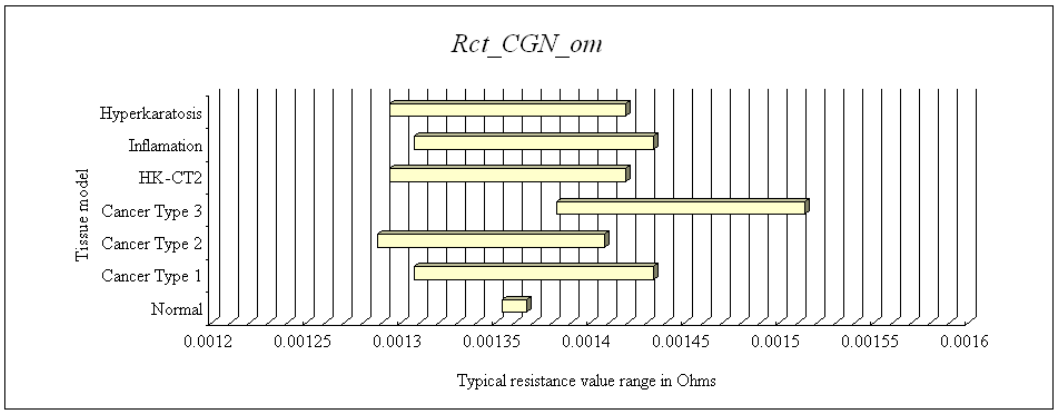

Fig. 13-6 Cis Golgi network resistor value comparison

The peroxisome outer membrane resistors *R_P_om* are compared in Fig. 14-7 Peroxisome outer membrane resistor value comparison.

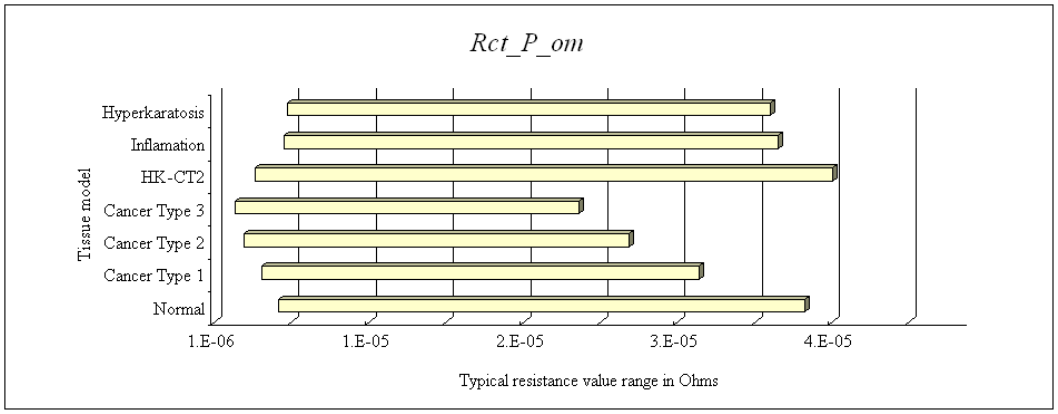

Fig. 13-7 Peroxisome outer membrane resistor value comparison

The endosome outer membrane resistors *R_E_om* are compared in Fig. 12-8 Endosome outer membrane resistor value comparison.

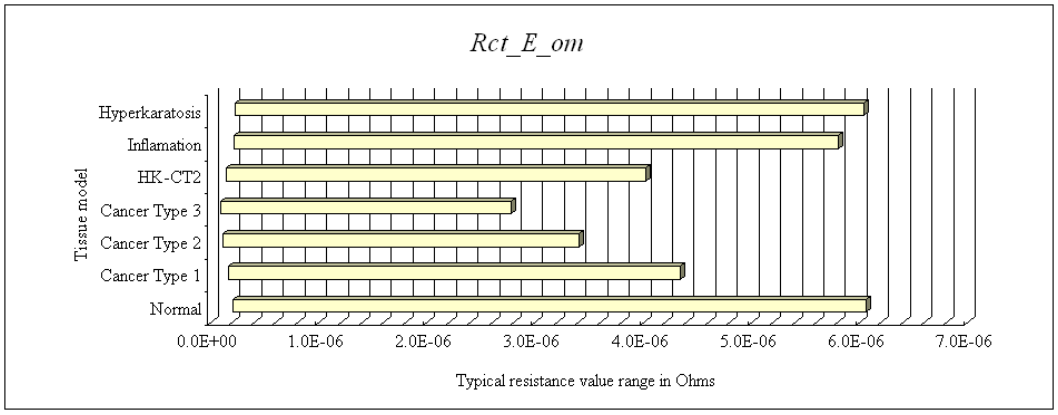

Fig. 13-8 Endosome outer membrane resistor value comparison

The lysosome outer membrane resistors *R_L_om* are compared in Fig. 13-9 Lysosome outer membrane resistor value comparison.

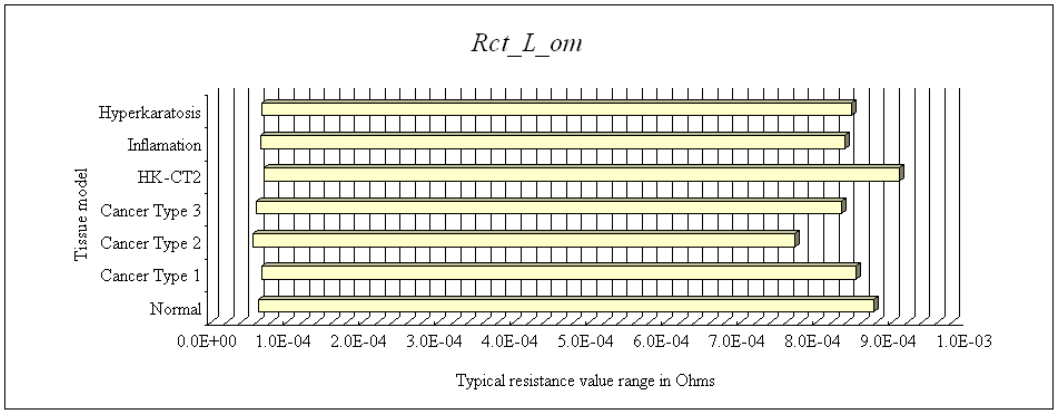

Fig. 13-9 Lysosome outer membrane resistor value comparison

The mitochondria outer membrane resistors *R_M_om* are compared in Fig. 13-10 Mitochondria outer membrane resistor value comparison.

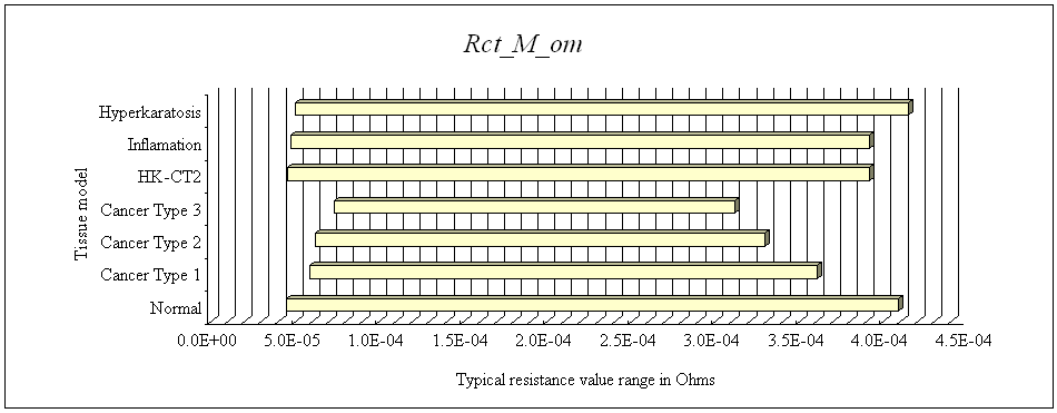

Fig. 13-10 Mitochondria outer membrane resistor value comparison

The mitochondria inner membrane resistors *R_M_im* are compared in Fig. 13-11 Mitochondria inner membrane resistor value comparison. It appears all of the diseases affect the mitochondria inner membranes relative to normal.

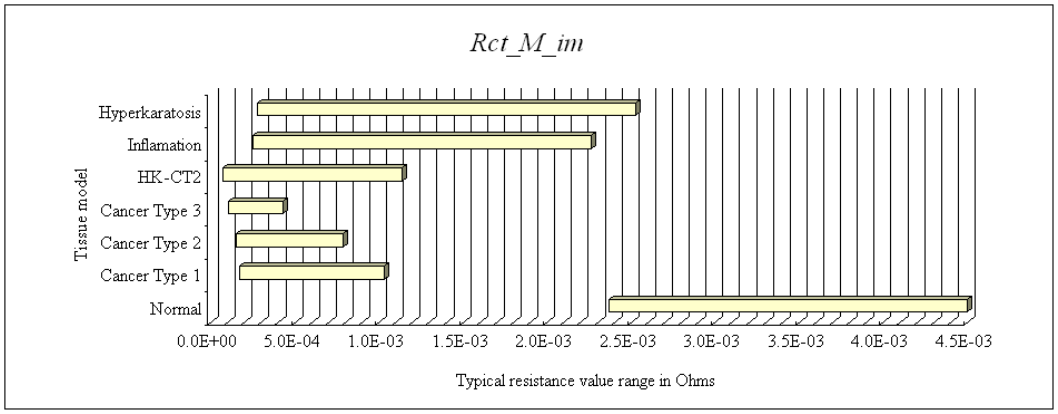

Fig. 13-11 Mitochondria inner membrane resistor value comparison

C. Fluid and Pore Resistances

The tissue model fluid resistances are larger than the membrane resistances. And as one might expect the fluid resistors that represent large numbers of organelles produce lower resistances because there are so many of theses organelles electrically in parallel. The extra cellular fluid resistors for the cell *R_C_ecf* for the various tissue models are compared in Fig. 13-12 Extra cellular fluid resistor value comparison. There are large clear differences between each model for the extracellular fluid resistors.

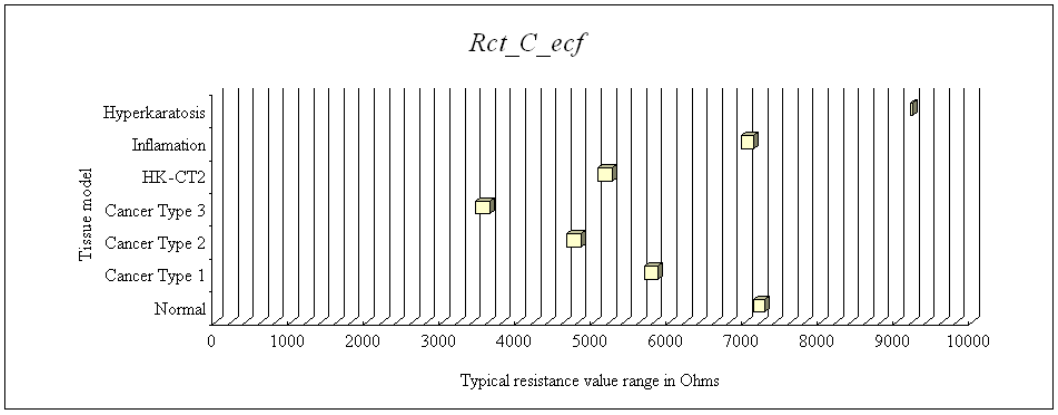

Fig. 13-12 Extra cellular fluid resistor value comparison

The intracellular fluid of the cell or cell cytoplasm resistor comparison is shown in Fig. 13-13 Cell cytoplasm fluid resistor value comparison.

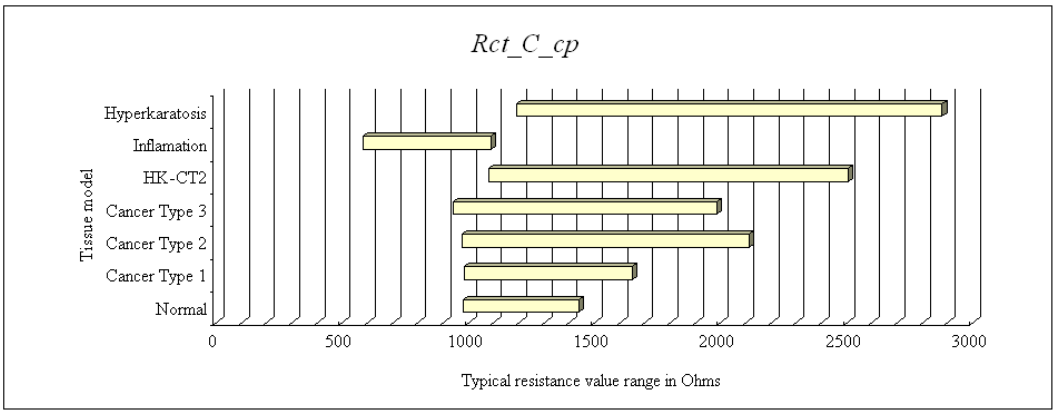

Fig. 13-13 Cell cytoplasm fluid resistor value comparison

The endoplasmic reticulum inter-organelle fluid resistor *R_ER_iof* comparison for the tissue models is provided in Fig. 13-14 Endoplasmic reticulum intra-organelle fluid resistor value comparison.

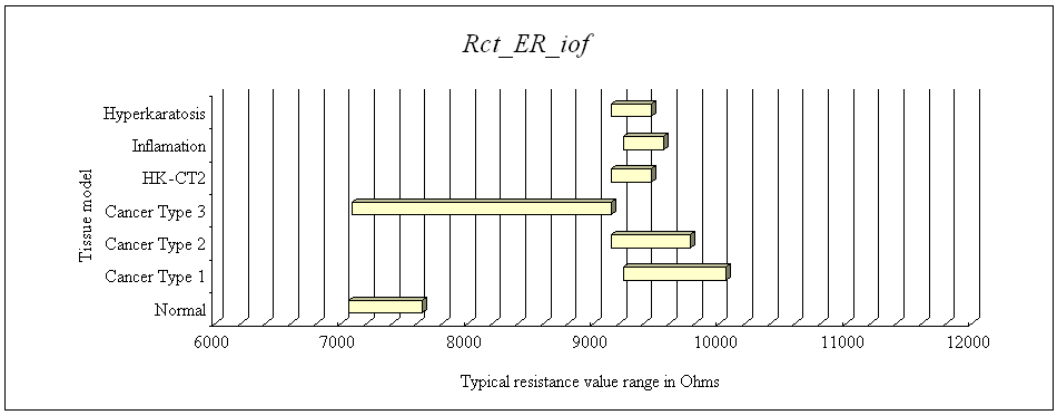

Fig. 13-14 Endoplasmic reticulum intra-organelle fluid resistor value comparison

The Nucleoplasm fluid resistor *R_N_np* comparison for the tissue models is provided in Fig. 13-15 Nucleoplasm fluid resistor value comparison. There are clear differences

between the nucleoplasm resistors average values and their ranges for most of the models.

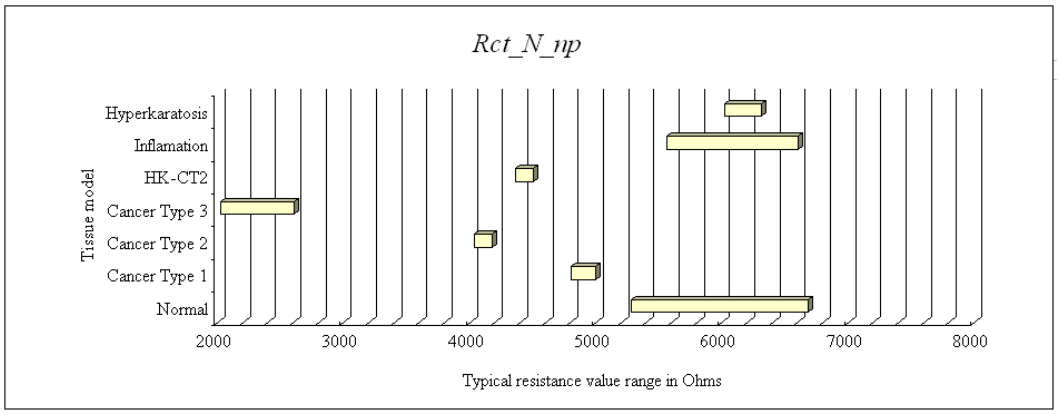

Fig. 13-15 Nucleoplasm fluid resistor value comparison

The trans Golgi network inter-organelle fluid resistor *R_TGN_iof* comparison for the tissue models is provided in Fig. 13-16 Trans Golgi network inter-organelle fluid resistor value comparison.

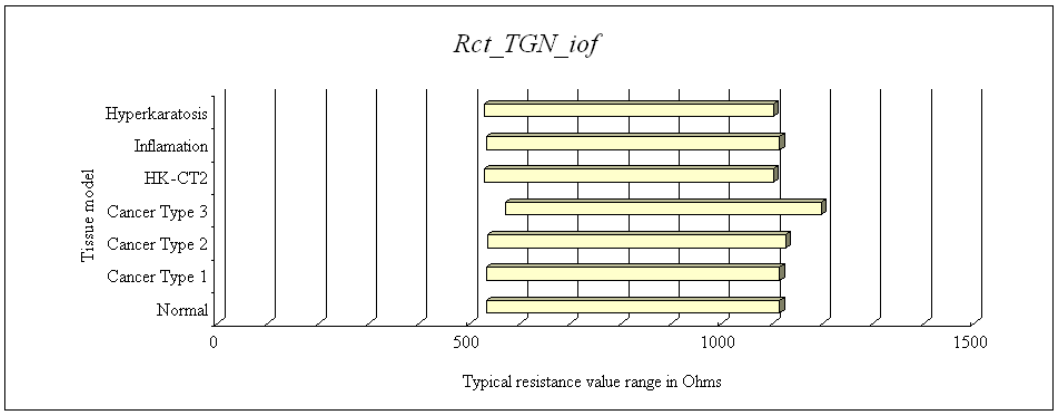

Fig. 13-16 Trans Golgi network inter-organelle fluid resistor value comparison

The medial Golgi network inter-organelle fluid resistor *R_MGN_iof* comparison for the tissue models is provided in Fig. 13-17 Medial Golgi network inter-organelle fluid resistor value comparison.

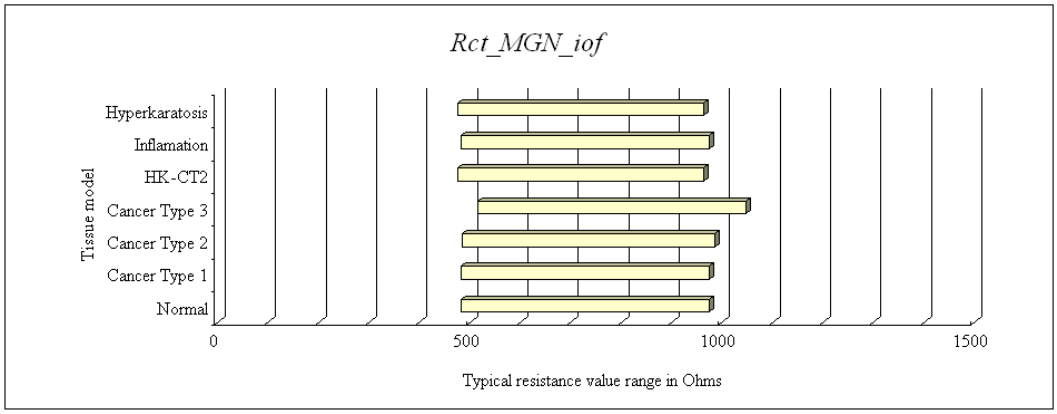

Fig. 13-17 Medial Golgi network inter-organelle fluid resistor value comparison

The cis Golgi network inter-organelle fluid resistor *R_CGN_iof* comparison for the tissue models is provided in Fig. 13-18 Cis Golgi network inter-organelle fluid resistor value comparison.

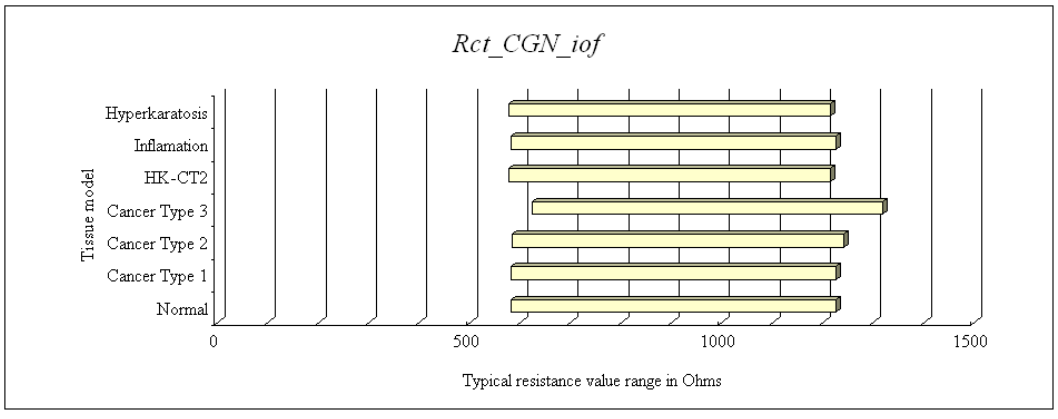

Fig. 13-18 Cis Golgi network inter-organelle fluid resistor value comparison

The peroxisome inter-organelle fluid resistor *R_P_iof* comparison for the tissue models is provided in Fig. 13-19 Peroxisome inter-organelle fluid resistor value comparison.

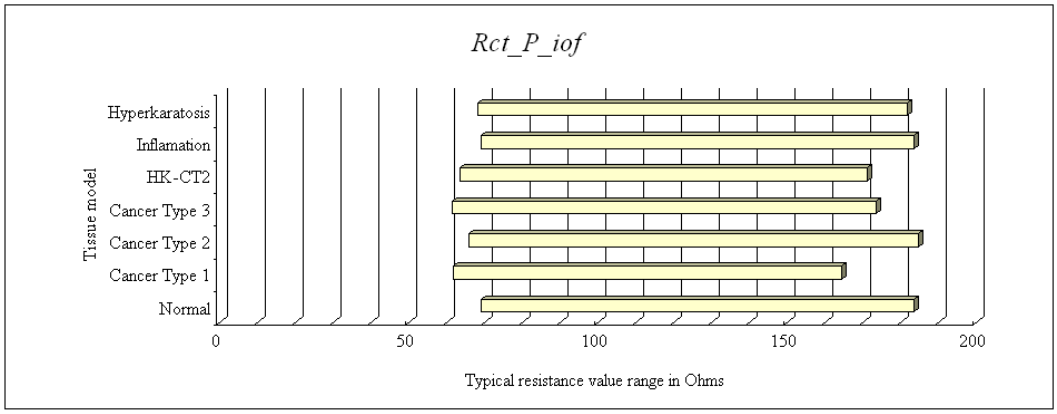

Fig. 13-19 Peroxisome inter-organelle fluid resistor value comparison

The endosome inter-organelle fluid resistor *R_E_iof* comparison for the tissue models is provided in Fig. 13-20 Endosome inter-organelle fluid resistor value comparison.

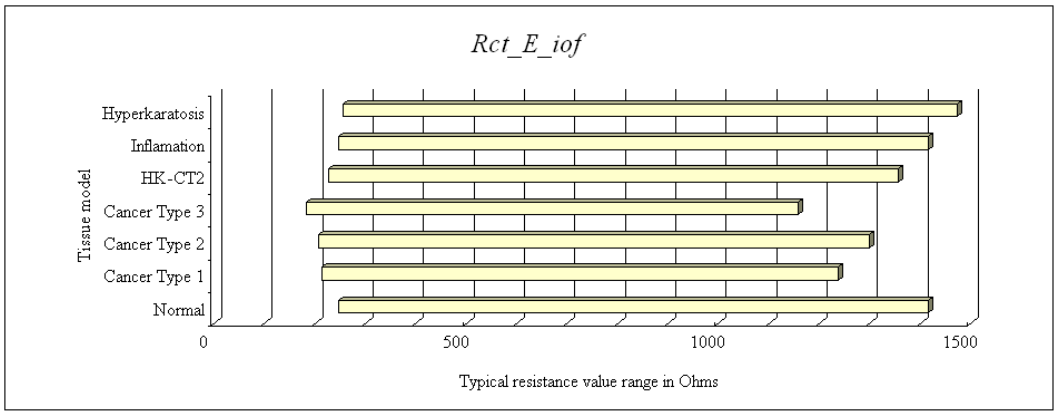

Fig. 13-20 Endosome inter-organelle fluid resistor value comparison

The lysosome inter-organelle fluid resistor *R_L_iof* comparison for the tissue models is provided in Fig. 13-21 Lysosome inter-organelle fluid resistor value comparison.

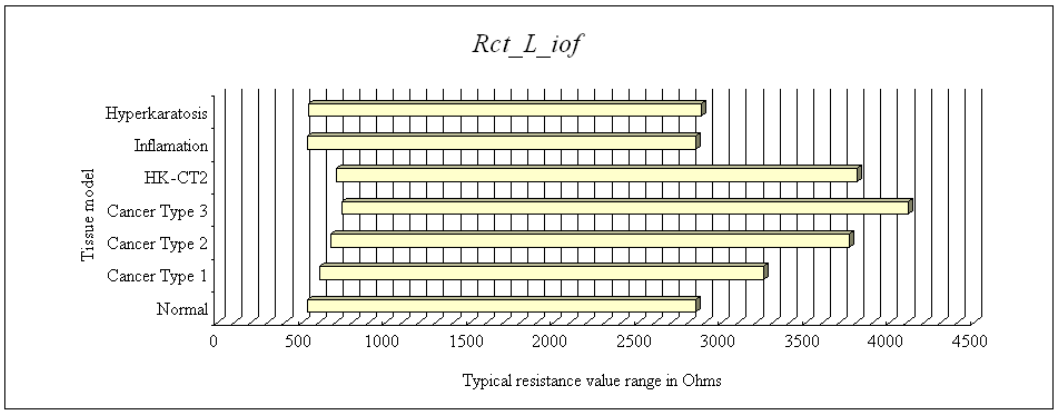

Fig. 13-21 Lysosome inter-organelle fluid resistor value comparison

The mitochondria has two fluid compartments the very core is called the matrix the fluid in the inter-membrane space is the inter-organelle fluid. The mitochondria inter-organelle fluid resistor *R_M_iof* comparison for the tissue models is provided in Fig. 13-22 Mitochondria inter-organelle fluid resistor value comparison. Notice how much smaller and shorter the cancer mitochondria inter-organelle fluid resistor is.

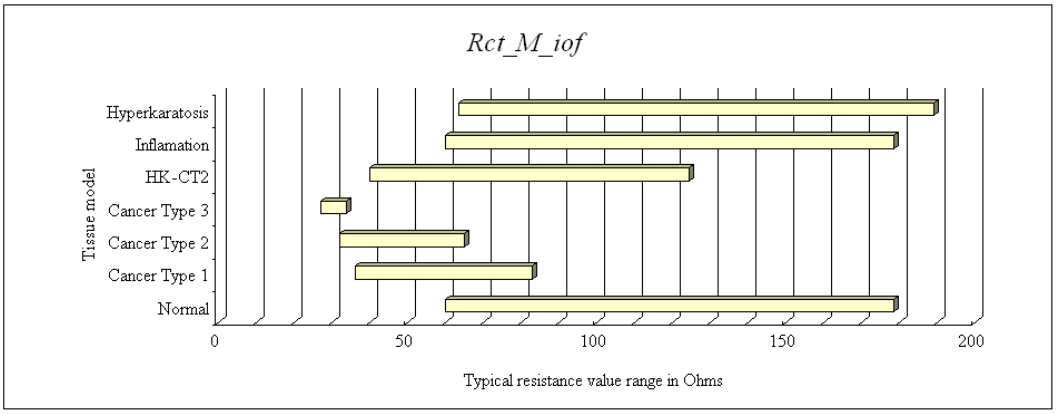

Fig. 13-22 Mitochondria inter-organelle fluid resistor value comparison

The mitochondria matrix fluid resistor *R_M_mx* comparison for the tissue models is provided in Fig. 13-23 Mitochondria matrix fluid resistor value comparison. The matrix

fluid resistor values show a clear separation between the benign and malignant tissue models

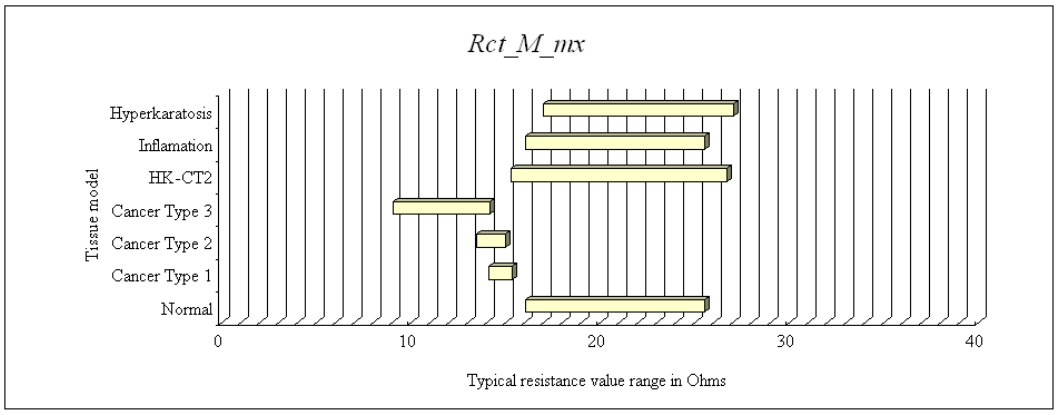

Fig. 13-23 Mitochondria matrix fluid resistor value comparison

The nuclear pore resistor *R_NP* comparison for the tissue models is provided in Fig. 13-24 nuclear pore resistor value comparison. The nuclear pore forms a fluid connection from the cytoplasm to the nucleoplasm across the outer membrane of the endoplasmic reticulum and the inner membrane of the nucleus. Therefore it is electrically in parallel with these two membranes. So even though the nuclear pore resistor value is large the membrane resistors dominate by providing an easier path for current to flow. There are large differences in the average values and allowable ranges for the nuclear pore resistor. The more malignant tissue models have the lowest average value and the shortest allowable ranges of values. The normal tissue model has the largest average value and the largest allowable range of values.

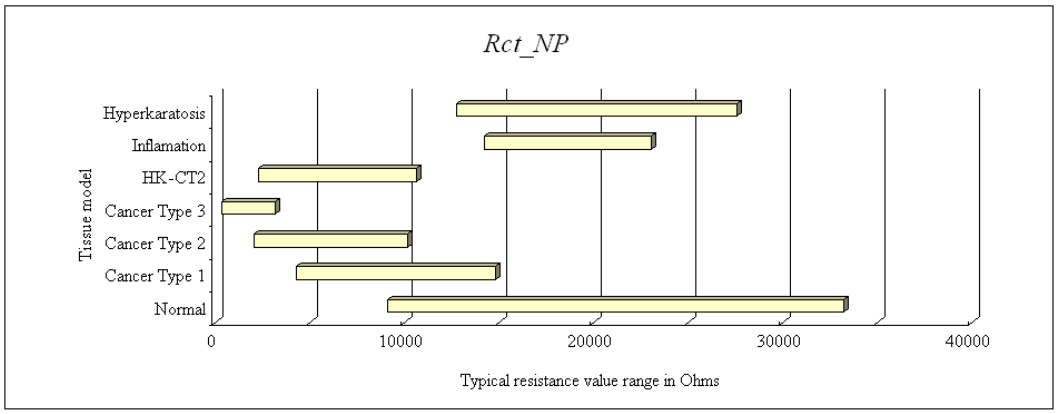

Fig. 13-24 Nuclear pore resistor value comparison

D. Membrane Capacitances

The membrane capacitance for the tissue model network are proportional to surface area of the cell or organelles the most important membrane capacitor is the cell plasma membrane capacitor element not because it is the largest but because it is not electrically in parallel with a tiny membrane resistor element which would negate its effect. The tissue model elements representing the outer membrane capacitor *C_C_om* is compared in Fig. 13-25 Cell outer membrane capacitor comparison.

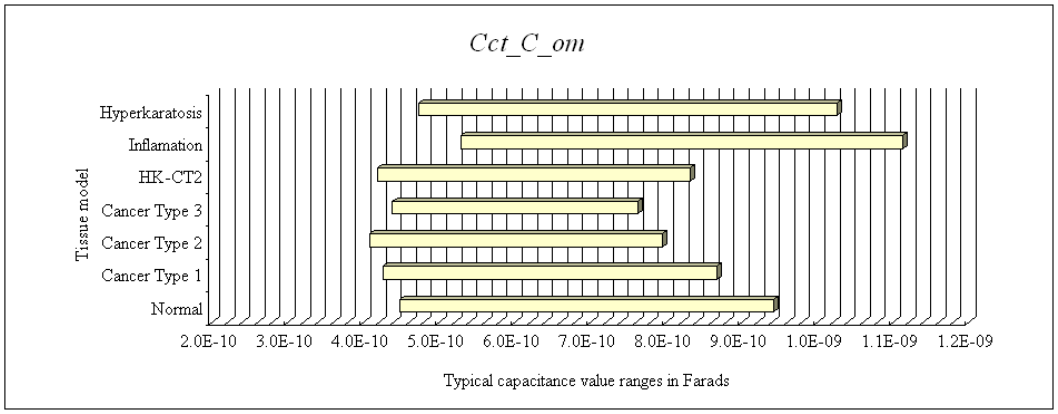

Fig. 13-25 Cell outer membrane capacitor comparison

The capacitor representing the endoplasmic reticulum outer membrane capacitor *C_ER_om* for the tissue models is compared in Fig. 13-26 Endoplasmic reticulum outer membrane capacitor comparison. The normal tissue model ER capacitor is three times larger than the cancer type 3 model.

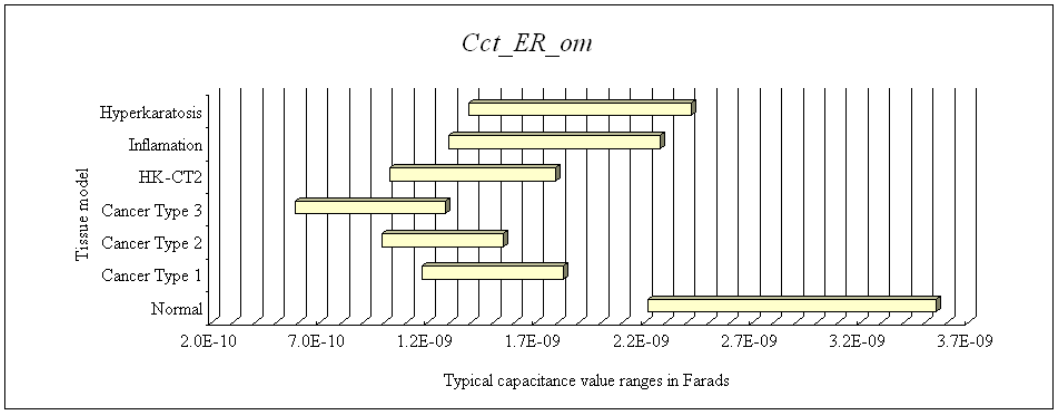

Fig. 13-26 Endoplasmic reticulum outer membrane capacitor comparison

The capacitor representing the nuclear envelope inner membrane capacitor *C_N_im* for the tissue models is compared in Fig. 13-27 Nuclear envelope inner membrane capacitor comparison. The cancer type 3 model nuclear inner membrane capacitor is four times larger than the normal tissue model.

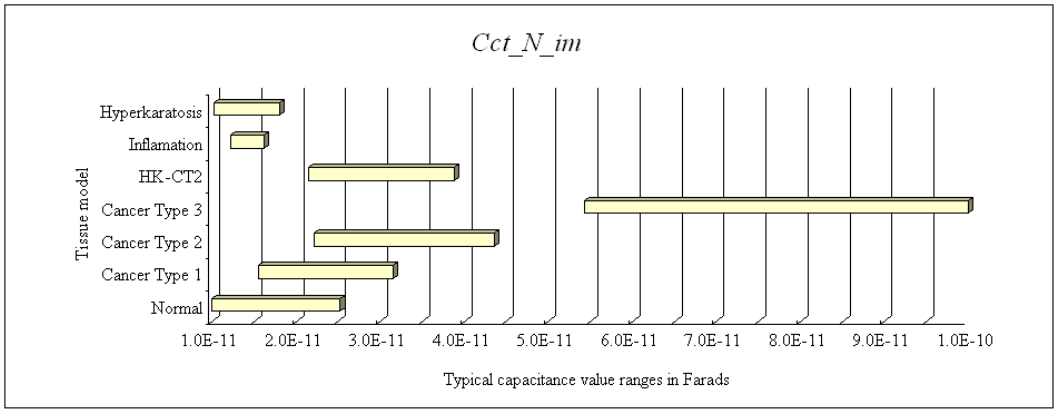

Fig. 13-27 Nuclear envelope inner membrane capacitor comparison

The capacitor representing the trans Golgi network outer membrane capacitor *C_TGN_om* for the tissue models is compared in Fig. 13-28 trans Golgi network outer membrane capacitor comparison.

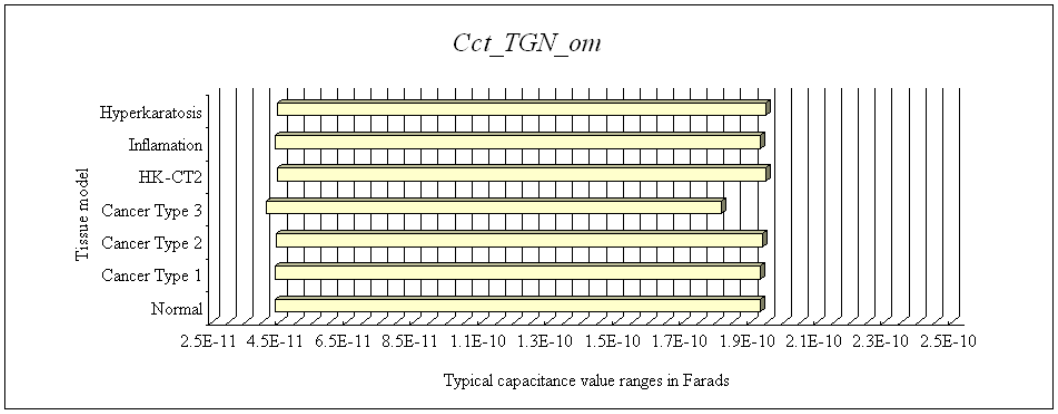

Fig. 13-28 Trans Golgi network outer membrane capacitor comparison

The capacitor representing the medial Golgi network outer membrane capacitor *C_MGN_om* for the tissue models is compared in Fig. 13-29 trans medial network outer membrane capacitor comparison.

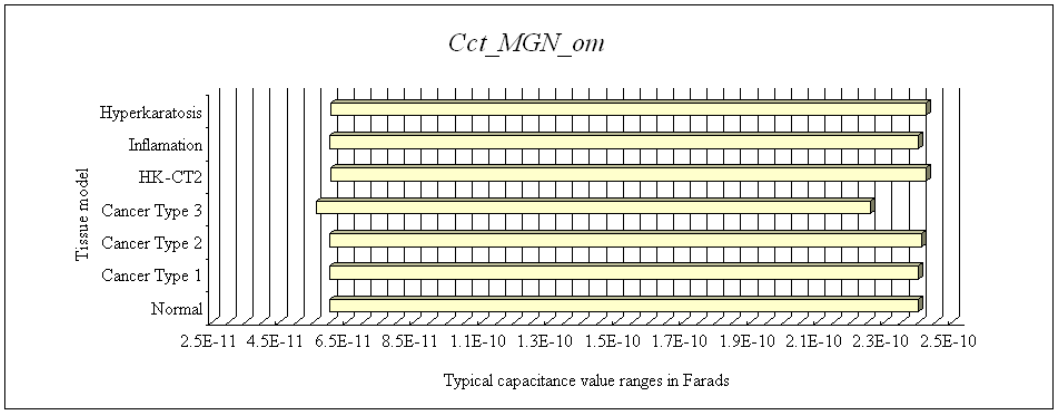

Fig. 13-29 Medial Golgi network outer membrane capacitor comparison

The capacitor representing the cis Golgi network outer membrane capacitor *C_CGN_om* for the tissue models is compared in Fig. 13-30 Cis Golgi network outer membrane capacitor comparison.

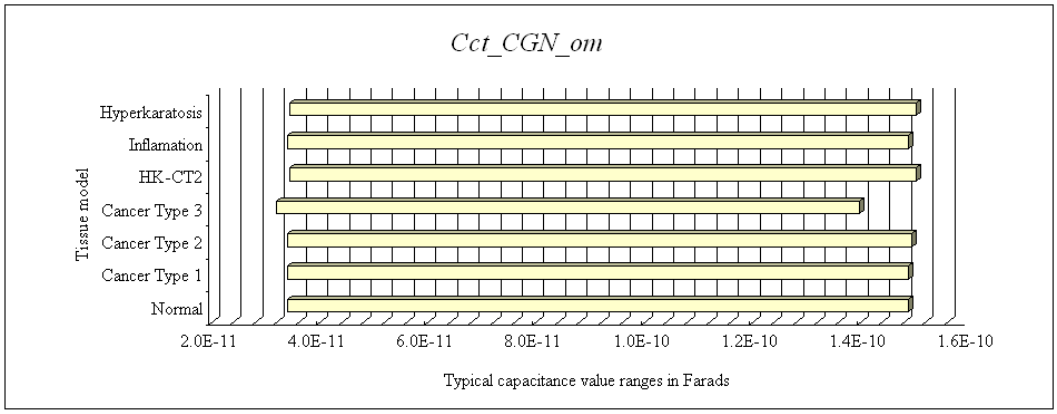

Fig. 13-30 Cis Golgi network outer membrane capacitor comparison

The capacitor representing the peroxisome outer membrane capacitor *C_P_om* for the tissue models is compared in Fig. 13-31 Peroxisome outer membrane capacitor comparison.

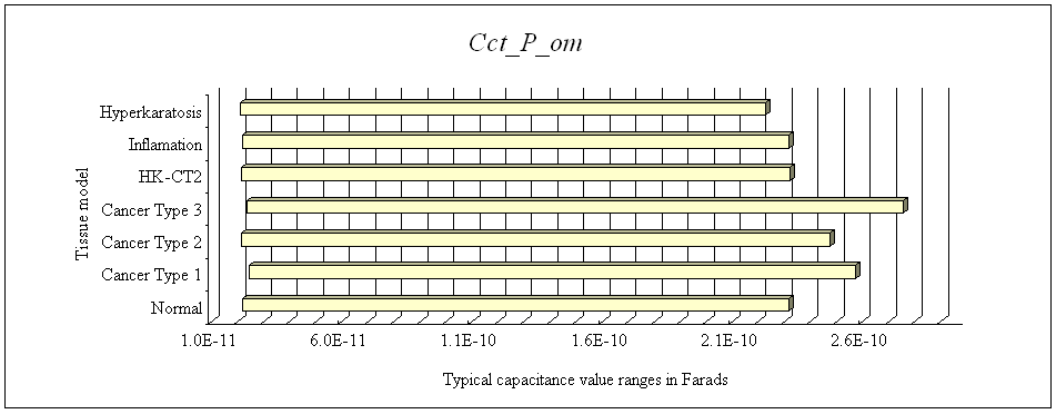

Fig. 13-31 Peroxisome outer membrane capacitor comparison

The capacitor representing the endosome outer membrane capacitor *C_E_om* for the tissue models is compared in Fig. 13-32 Endosome outer membrane capacitor comparison.

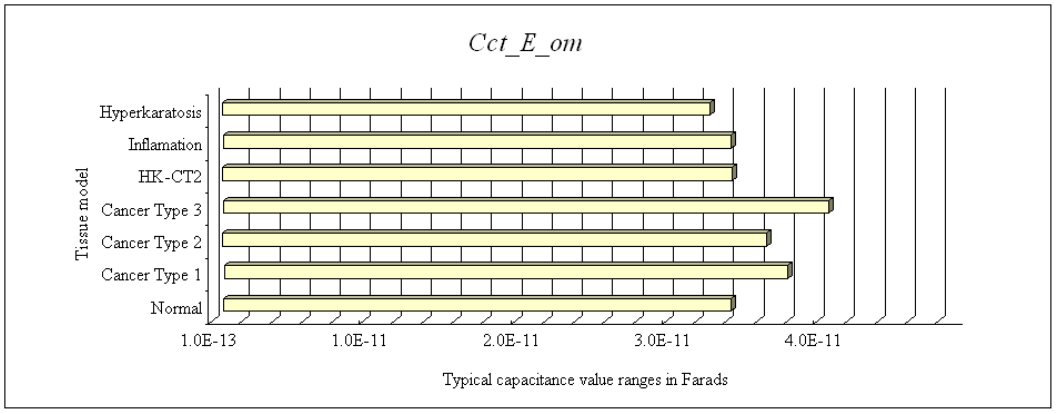

Fig. 13-32 Endosome outer membrane capacitor comparison

The capacitor representing the lysosome outer membrane capacitor *C_L_om* for the tissue models is compared in Fig. 13-33 Lysosome outer membrane capacitor comparison.

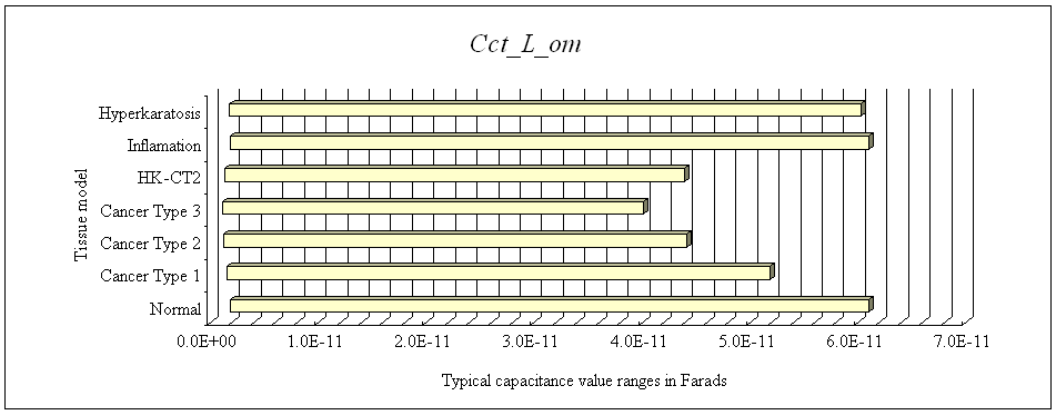

Fig. 13-33 Lysosome outer membrane capacitor comparison

The capacitor representing the mitochondria outer membrane capacitor *C_M_om* for the tissue models is compared in Fig. 13-34 Mitochondria outer membrane capacitor comparison.

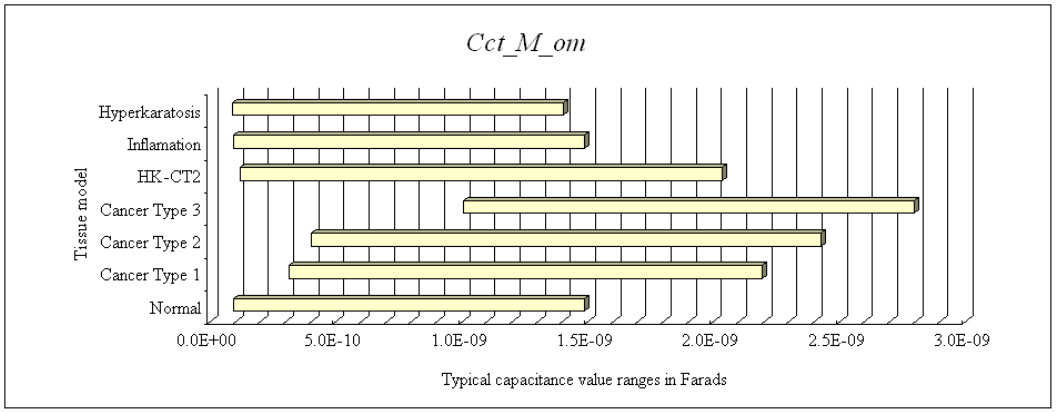

Fig. 13-34 Mitochondria outer membrane capacitor comparison

The capacitor representing the mitochondria inner membrane capacitor *C_M_im* for the tissue models is compared in Fig. 13-35 Mitochondria inner membrane capacitor comparison.

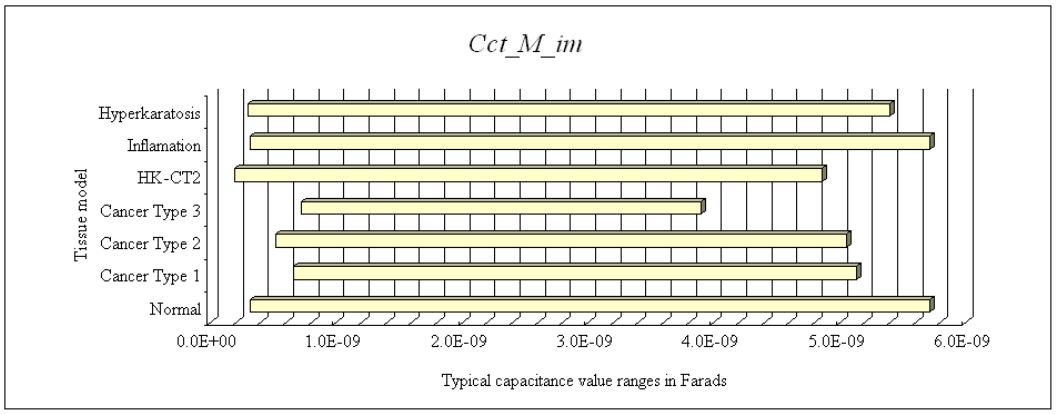

Fig. 13-35 Mitochondria inner membrane capacitor comparison

E. Tissue Model Network Element Comparison Review

It appears that twenty-two of the total thirty five network elements differ very little from tissue model to tissue model. Only thirteen network elements are noticeably changing from model to model. The network elements that have different values are those elements related to the mitochondria, endoplasmic reticulum, the nuclear membrane, the plasma membrane, the cytoplasm and the extracellular fluid. It is hard to make the determination of what is most important without considering the network structure. But it is doubtful that network elements that are constant from model to model will have an important roll in the changes of the impedance. Some of these static network elements may change if a new model of a disease is created that affects different organelle types. Section XIV will address the influence the network topology has on impedance. The overall impedance response is dependent on both the network topology as well as the element values.

XIV. EVALUATION OF NETWORK TOPOLOGY

A. Introduction to the Evaluation of the Network Topology

With the typical range of the various circuit elements known it becomes easy to evaluate the network topology for the tissue models. The network topology can be evaluated for several reasons including whether the models make intuitive sense as well as to find out what cell structures have a dominant affect on the overall impedance measured. A quick efficient evaluation of an electrical network can be performed using simple frequency analysis.

B. Introduction Model Evaluation in the Frequency Domain

A helpful analytical method for determining the relative importance of individual resistive elements in the "Transparent Box" model is to evaluate the network responses at the extremes in frequency, both DC and infinity or high frequency. The analytical procedure is to convert the circuit into the frequency domain where the reactive elements are evaluated at $\omega = 0$ and $\omega = \infty$. To convert a capacitor into capacitive reactance use equation (14-1)

$$Xc(\omega) = \frac{1}{j \cdot \omega \cdot C} \tag{14-1}$$

where

$Xc(\omega)$	is the capacitive reactance
j	is the imaginary number the square root of –1
C	is the capacitance in Farads
ω	is the radial frequency 2πHz

At low frequencies capacitors look like open circuits. At high frequencies capacitors behave like shorts. To evaluate the circuit at DC open the capacitors the result will be that the resistors in parallel to the capacitors will dominate in DC resulting in a higher overall resistance. Key points to consider are the membrane resistances are relatively low. Only the cell's outer plasma membrane, the endoplasmic reticulum membrane and the nuclear membrane have resistance values greater than one Ohm. The rest of the membrane resistor values are in the mili-Ohm and micro-Ohm ranges. The high frequency effects that cause the membranes to look like short circuits will not be much of a factor for the small plentiful organelles since they already have minuscule membrane resistances.

C. Low Frequency Model Evaluation

The "Transparent Box" tissue network with typical resistor element values in Fig. 14-1 Low frequency network approximation shows the capacitors are open circuited (not connected) in order to evaluate DC response $\omega = 0$

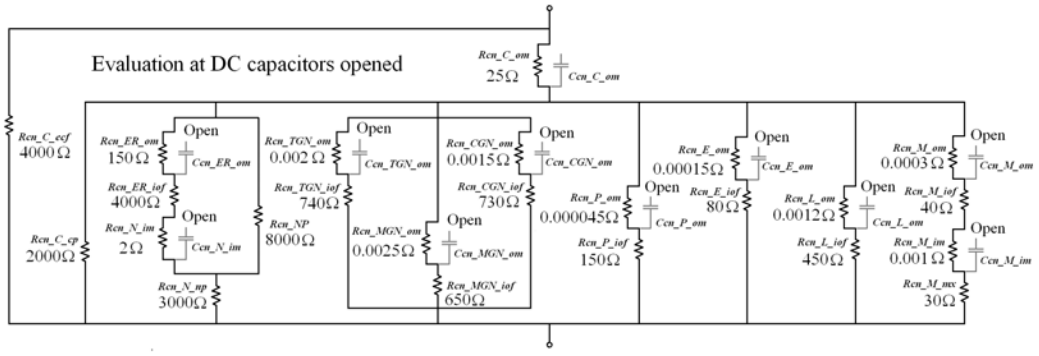

Fig. 14-1 Low frequency network approximation

Calculate the series resistors of the mitochondria in parallel with the other organelles the peroxisome, endosome, lysosome and Golgi networks (14-2).

$$740\Omega \,//\, 650\Omega \,//\, 730\Omega \,//\, 150\Omega \,//\, 80\Omega \,//\, 450\Omega \,//\, (40\Omega + 30\Omega) = 25\Omega \qquad (14\text{-}2)$$

calculate the series of the endoplasmic reticulum outer membrane in series with the intra organelle fluid and the inner nuclear membrane all in parallel with the nucleopore resistor in series with the nucleoplasm resistor (14-3)

$$((150\Omega + 4000\Omega + 2\Omega) // 8000\Omega) + 3000\Omega = 5733\Omega \qquad (14\text{-}3)$$

The organelles from (14-2) and (14-3) are in parallel with the cell cytoplasm resistor (13-4)

$$25\Omega // 5733\Omega // 2000\Omega = 24.9\Omega \qquad (14\text{-}4)$$

The series combination of the outer membrane resistor and the inner cell contents calculated in (14-4) in parallel with the extracellular fluid provide the overall impedance shown (14-5)

$$(25\Omega+24.9\Omega) // 4000\Omega = 49\Omega \qquad (14\text{-}5)$$

This overall impedance at DC makes sense and is consistent with the other tissue models.

D. High Frequency Model Evaluation

The "Transparent Box" tissue network in Fig. 14-2 high frequency network approximation shows shorted capacitors with a black wire. The network is shown with typical resistor element values for a 3mm electrode spacing in normal tissue as an example to evaluate high frequency response $\omega = \infty$. Calculate the series resistors of the mitochondria in parallel with the other organelles the peroxisome, endosome, lysosome and Golgi networks.

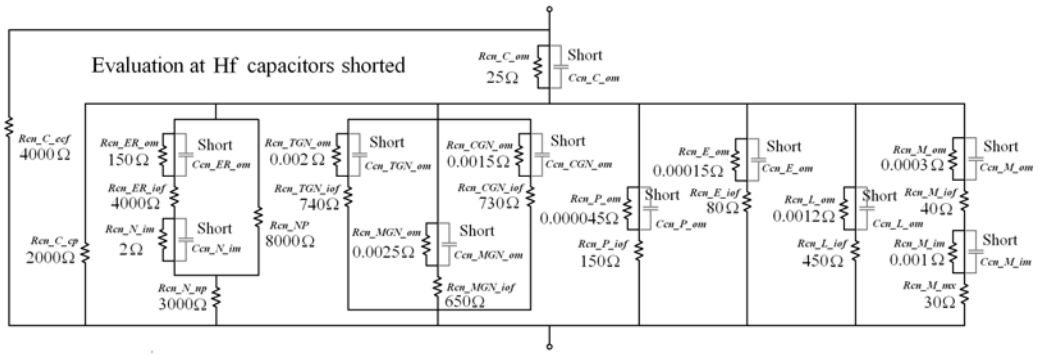

Fig. 14-2 High frequency network approximation

Notice it is the same as the low frequency evaluation since the organelle membrane resistors are negligible and a short has little effect on the membrane resistors (12-2).

740Ω // 650Ω // 730Ω // 150Ω // 80Ω // 450Ω // (40Ω + 30Ω) = 25Ω (12-6)

the endoplasmic reticulum and the nucleus inner membrane resistors are shorted so only the endoplasmic reticulum intra organelle fluid resistor is in parallel the nucleopore resistor which is in series with the nucleoplasm resistor (12-7)

(4000Ω // 8000Ω) + 3000Ω = 5667Ω (12-7)

The organelles from (12-6) and (12-7) are in parallel with the cytoplasm resistor (12-4)

25Ω // 5667Ω // 2000Ω = 24.7Ω (12-8)

The short circuit of the outer membrane resistor by the capacitor at high frequency results in the parallel combination of the extracellular fluid resistor and the inner cell contents from (12-8) provide the overall high frequency impedance shown (12-9)

24.7Ω // 4000Ω = 24.6Ω (12-9)

This overall impedance at $\omega = \infty$ makes sense and is consistent with the other tissue models.

E. High and Low Frequency Evaluation Insights

The simple frequency response exercise done in sections *C* and *D* shows the small influence of the organelle membranes on the overall impedance response. The organelle

that seems to have the largest effect other than the outer plasma membrane is the endoplasmic reticulum. The endoplasmic reticulum is a large membrane organelle and cells have only one perhaps two of these organelles. Being highly parallel dilutes the effect of the membranes by numerous type organelles such as the peroxisome. So typically the more numerous an organelle is the less membrane influence, the larger the organelle membrane the more membrane influence. The more organelles there are within a cell the more parallel the structure and therefore the lower its impedance is. This means diseases that affect the number of organelles will more likely affect both the high frequency and low frequency resistance. Whereas diseases that primarily affect the outer cell membrane will have a disproportionately larger affect on the low frequency resistance. More insight into parameter effects can be performed to find out the limits of the "Transparent Box" model as well as the effects of certain specific organelles by using parameter sweeps.

F. Intro to Sub Cellular Parameter Sweeps

The geometric or biochemical parameter sweep will highlight the dynamic electrical elements. Individual electrical elements values can be "swept" from lowest to highest values dependent on the range of allowable geometric or biochemical factors that made up the model. There are over 256 individual parameters that can be "swept." This will give a good indication of the dominance of the element in the overall transparent model. To save time and trouble it is wise to use the structure of the electrical network to weed out parameters that will effect the electrical elements that have very little influence on the overall impedance. Some network elements have a less dominant location within the electrical network no mater how large the parameter sweep is, very little will happen to the overall impedance. It's important to perform a sweep or at the very least a high then low value test since some parameters are proportional and others are inversely

proportional to the overall impedance. It is beneficial to expand the sweep range of a parameter outside the normal range by a factor such as ten. Divide the low value by the factor and multiply the high value by the factor. For example, if the number of mitochondria in a normal cell ranges from 300 to 500 then sweep from 30 to 5000. Through this sweep one can ether observe the mitochondria dependent network elements or monitor the overall impedance outputs. It is better to monitor the overall impedance output and not just the directly affected electrical elements because many other indirect elements will be affected in this complex integrated model. For example, sweeping the number of mitochondria will change the cytoplasm volume thus affecting fluid resistance elements. This exercise can be done to evaluate each electrical element while keeping the other elements fixed. One must be aware that there is often more than one factor (multiple primary values) affecting the sweep of an individual electrical element. Again using the mitochondria organelle as an example it will have biochemical as well as geometric size ranges that affect the electrical element maximum and minimum ranges. Typically the quantity of organelles within a cell will have the most dominant effect on electrical element ranges. One may perform nested sweeps to test multiple primary variables simultaneously. The parameter sweep procedure will highlight the static electrical elements. Static elements can be defined as values that change impedance less than 1% from a full geometric or biochemical primary variable parameter sweep.

The most interesting electrical elements are the elements that have a wide range of possible values in a location that schematically has a strong influence on impedance. Examples of interesting electrical elements are the resistor representing the plasma outer cell membrane and the resistor representing the endoplasmic reticulum membrane. When the primary variables influencing these network elements have a large range of possible

values the overall impedance changes are quite noticeable. This makes the primary variables that affect these elements very important when it comes to disease.

G. Tissue Model Network Evaluation Review

In this section the electrical network was reviewed to determine which circuit elements have a dominant effect on the measured impedance at both high and low frequencies. Parameter sweeps were introduced to determine the importance of the primary variables effect on overall impedance.

The evidence by these evaluations suggests impedance measurements can easily detect diseases that affect the largest and less numerous organelles. The impedance measurement changes are highly sensitive to differences in the endoplasmic reticulum, the outer cell plasma membrane and are moderately sensitive to the nucleus and the mitochondria. The impedance measurement is less sensitive to changes affecting the smaller organelles.

XV. CONCLUSIONS

A. Introduction

The research goal was to develop an ultra-structurally based tissue model for oral mucosa that is versatile enough to be easily modified to mimic the passive electrical impedance response of multiple benign and cancerous cell tissue types. This research produced seven ultra-structurally based “Transparent Box” tissue models to support the use of minimally invasive impedance measurements as an early cancer-screening tool. This new model provides answers to biologically meaningful questions related to the impedance response of healthy and diseased tissues. It appears to provide a measure of confidence for the further development of impedance based measurement tools as a diagnostic and screening aid for both benign and invasive oral tissue abnormalities.

B. The Modeling Goal

The goal of this research is to produce and explore a detailed “Transparent Box” passive element electrical model for both healthy and diseased oral mucosal tissues; where an electrical network represents the passive physical and ionic makeup of each cell structure. All the electrical networks for each cell structure were combined into the organelle networks then further combined into the cell and then tissue networks. This allows for the manipulation of structurally and electrochemically based parameters so that detailed questions related to the changeable parameters can be answered. The model was enhanced with Monte Carlo random variable techniques applied to the primary structural and electrochemically based variables. Employing the Monte Carlo method into the “Transparent Box” model more closely mimics the uncertainty of real tissue responses. The randomness of the inputs produces less deterministic outputs. The elevated uncertainty demands that the methods developed to identify the diseased tissue from healthy tissue with impedance be more robust.

C. Answers to the Analytical Questions

Construction of the detailed ultra structurally based “Transparent Box” passive element electrical model for both healthy and diseased tissues was just the first part of the project. Evaluating the “Transparent Box” tissue model when applied to various diseased tissues for comparison to normal tissue was the second part of the project. The third part of the project is to finally answer important questions that have both medical and scientific significance for using impedance in a clinical setting for the screening of cancer and other oral tissue diseases.

The ten analytical questions to be asked by the ‘Transparent Box” model from section 1 and the answers are provided by the model from the evaluation normal and diseased tissues

1) What factors dominate the apparent decrease in impedance response of cancer tissue compared to the impedance response of normal healthy tissue?

The question was answered by [3] before the inquiries of cell structure as a factor were raised. It was traditionally assumed that cancer cells were more conductive because of an increase of ions within the cell; the theory behind this ionic concentration increase is a result of increased signaling for growth [1]. Microprobe analysis on rat tissue has shown invasive cancerous tissue similar to cancer type 3 has an increase in ion concentration over normal tissue for the ions, Na^+ by 200% for Cl^- by 50% and K^+ by 33% [1, p450]. A higher concentration of ions theoretically would increase conductivity and decrease resistance [44], [55] but those conditions in the model do not appreciably lower resistance. All the “Transparent Box” models for all the diseases have the same

identical primary variable resistivities (see the primary variable tables in section eleven and section twelve). All the impedance differences seen in the models are a result of only the structural changes and not changes in fluid resistivities. Network analysis in section fourteen suggests membrane resistances due to structure are the primary cause for the differences in impedance and not the increased ion concentrations.

2) What changes in the cells and tissues are responsible for decreasing impedance are they structurally related?

The answer to question two is related to question number one, the changes that are responsible for decreasing the impedance are structurally related. It appears the membranes for the endoplasmic reticulum and the cell outer membrane have the largest effect on the impedance. It appears the membrane differences in the more numerous organelles such as the mitochondria have less influence. The electrolyte related primary variables have an even lower influence on decreasing impedance.

3) Are the observed impedance differences in cancer solely dominated by electrolyte increases as a result of increased cell signaling as suggested by [1-3]?

No, it would appear from the “Transparent Box” models impedance differences are dominated by structural changes such as decreases in endoplasmic reticulum surface areas.

4) Are the impedance differences mainly because of biochemical differences in the various membranes of the cells and the organelles [4-7]?

All the membrane resistances per square cm between different diseases were the same as the normal tissue for each organelle and cell. This means the differences observed between diseases are structurally based.

5) Are the numbers, sizes and structures of the organelles within the cell responsible for the observed lower impedance responses [8-12]?

Yes, the more there is of a small organelle in a cell the smaller the membrane resistance. This small resistance is in parallel with the membrane capacitance so this resistance effectively short-circuits the organelles capacitive contribution at all frequencies (see section fourteen evaluation of network topology).

6) Does the large nuclear to cytoplasmic ratio feature common in all cancer cell tissues cause the observed decrease in impedance [13]?

No, the nuclear to cytoplasmic ratio is a good tool for a histo-pathologist to make a quick determination about the health of a tissue. It was theorized that only the cell outer plasma membrane and the cells nuclear membrane could be measured by impedance but from these models it has become apparent that the shrinking of the endoplasmic reticulum membrane area is more important. It is possible the ER membrane shrinks as it gives up lipids to the ever-growing nuclear envelope. But whatever the mechanism the ER gets smaller in cells affected by cancer and impedance can measure those differences.

7) Can impedance be used to differentiate between other benign diseases that often get misdiagnosed as cancer because their lesions have similar physical appearances to cancer [14]?

Yes, this research has shown that while a benign tissue may look like cancer the structural differences at the cellular and sub cellular levels are significant. Impedance can identify these differences related to cancer and other diseases. Necrotic inflammation looks red and swollen like many cancers but the two have vastly different impedance responses. Impedance can also detect the signature of cancer in compound diseased tissues. The model of hyperkaratosis over cancer type 2 tissues showed the impedance signatures of cancer despite having the physical appearance of a benign disease.

8) Can impedance be used to screen for and detect innocuous lesions before they become apparent by a visual inspection for the earliest detection of oral cancer?

In principle yes the cancer type one model affects mainly the second cell layer in the model the squamous cell layer closest to the surface would appear normal but an impedance measurement would show otherwise. The probe spacing in the model is adjustable thus the sample that can be measured is adjustable. These impedance results were made with sample probe spacing of one mm. It could be argued that lesions smaller than one mm are innocuous and may appear to be small candidis lesions in a clinical setting. Lesions that are small would require narrow probe spacing this would be problematic because the dispersion would be seen at high frequencies where complications arise due to molecular effects.

9) What frequency or frequencies would be best for an impedance based oral cancer-screening tool?

This would depend on the method used for detection of cancer and other diseases. The location of the frequency dispersion will be a function of electrode spacing; small electrode spacing means small samples, lower capacitances and higher frequencies. Larger electrode spacing translates to larger samples with larger capacitances and shifts the dispersion toward lower frequencies. The Bode plots of all the models in section 12 indicate it may be suitable to choose a relatively low 5kHz sinusoidal excitation signal for the measurement. The clinician taking the measurements would first choose a location or locations for normal healthy tissue impedance measurements as a comparative baseline then compare that with the impedance measurement from the suspicious lesion. More detailed disease identification techniques covered at the end of section 12 will require multiple frequency measurements.

10) What methods of data display or manipulation would provide the best identification of tissue anomalies for possible disease identification?

Normalization of the impedance at low frequency seems to produce the best separation between the diseases this can be seen in Fig 12-27 Normalized maximum low frequency resistance. This method would also be the fastest and cheapest to implement.

D. Closing Observations

This “Transparent Box” model can be used in other tissue impedance applications especially the network topology. The model can be applied to other cell types, alternative geometric shapes may be used. More layers of different cell types can be used. The

model can be continually improved upon as biological researchers make new discoveries related to the organelles within the cell and the electrochemical properties specific to the particular membranes within the cell. These discoveries can be used to update the values and the ranges of the primary variables for the specific cells and layers. This flexibility will make the model incrementally more accurate since many of the organelle membranes in this research shared identical primary variable values. More tissue diseases and conditions can be evaluated with the “Transparent Box” model in the future for possible identification by impedance.

The results of this research should provide more confidence for those developing impedance as an early cancer-screening tool. The “Transparent Box” models show good separation between benign and cancerous tissues this should increase the confidence that there will be fewer false positives by using comparative impedance scanning. The techniques covered here should maximize the opportunity for minimally invasive early detection of cancer by impedance.

Caution should be exercised while using this model there is no inclusion of the electrode impedance in this model. The selection of electrodes and electrode geometry is very important if one wants to minimize the effects of the electrode impedance while maximizing the signal changes due to the tissue itself. It is difficult to separate the electrode impedance from the overall measurement. The subject of electrode electrolyte transduction is a very complex matter in the simplest of electrochemical cells. The discussion is extremely complex when the interface also involves a tissue or layers of cells. The consensus is when examining the impedance spectra of a tissue or even a cell suspension the first dispersion is generally due to the electrode electrolyte interface effects [61], [62]. The second dispersion is due to the cellular and biological effects [50], [61], [62]. The third dispersion is due to the molecular effects [50], [61]. This model is

concerned with the second dispersion any data extrapolated at very low or very high frequency is very suspect. Fig. 15-1 Impedance spectrum of *Gallus gallus domesticus* (chicken) breast skeletal muscle with 2mm probe spacing shows the three dispersions of the impedance response using a four point probe arrangement that is detailed in [105] the impedance was measured and recorded with a Core Technologies frequency response analyzer.

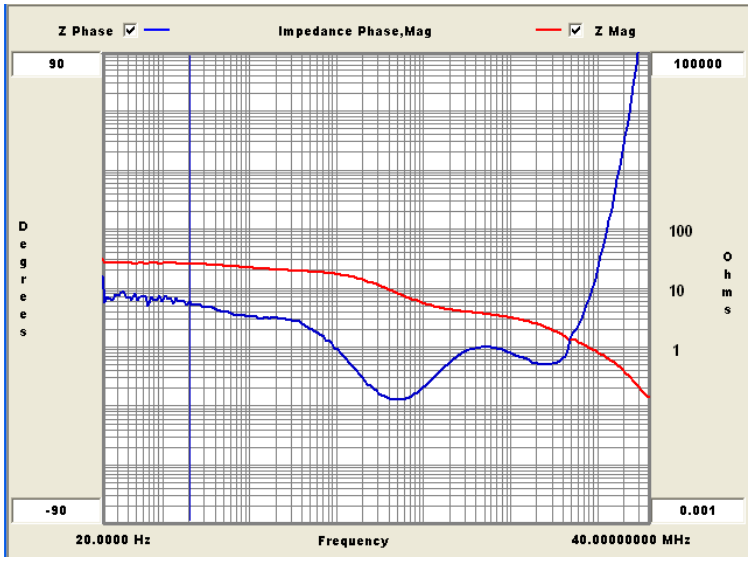

Fig. 15-1 Impedance spectrum of *Gallus gallus domesticus* (chicken) breast skeletal muscle

The magnitude of impedance at the beta dispersion is 20 Ohms at 2000 Hz and 3 ohms at 1 MHz. Electrode and molecular effects dominate the impedance response outside this range. The magnitude of the impedance response is comparable to the "Transparent Box" model impedance response for normal tissue at 2mm spacing but it must be noted there are extreme differences structurally between human oral epithelial cells and chicken skeletal muscle cells. It would be better to construct a "Transparent Box" model for a tissue and cell type that can be easily experimentally verified but the entrepreneurial aspects for impedance measurements of skeletal muscle are low. The

entrepreneurial aspects of cancer detection are much stronger this is why the model was developed for cancer. Unfortunately the availability of cancer tissue for tissue impedance is non-existent [40].

Single cell impedance analysis has been performed on the cancer breast cell lines MCF-10A, MCF-7, MDA-MB-231, and MDA-MB-435 over a frequency range of 100 Hz to 3.0MHz [26], [24]. The Transparent Box" model applied to a single cuboidal epithelial cell trends the data in [26] closely despite the differences in cell shapes. Most of the differences can be attributed to electrode effects and structural differences between breast cells and epithelial cells.

The "Transparent Box" model is meant for comparative analysis of healthy tissue and diseased tissue this point cannot be emphasized enough. In a clinical setting base line normal tissue impedance must be taken from the patient opposite or adjacent from the suspect lesion. For example if the left bucal mucosa has a suspicious lesion then the mirror opposite location should be used (right bucal oral mucosa) for the normal baseline measurement. In some instances an area adjacent to the lesion can be used for the normal impedance baseline [106]. Getting a base line from each individual patent is important because the differences in quantity and distribution of adipose tissue within the epithelial tissue will vary greatly from person to person. Increased amounts of adipose tissue will increase both the normal and diseased tissue impedance response. Other factors affect the baseline impedance response includes the level of hydration of the individual and capillary density. The combination of these factors makes it imperative to take at least three baseline readings.

Moving away from tissues and examining cell suspensions of brewers yeast *sacchraromyses Cerevisiae* may be the best method for evaluating the structural principles used in the "transparent Box" model. Another technique would be to construct

artificial cells liposomes with multiple membrane bound internal structures analogous to organelles. The background of these techniques and measuring cell suspensions can be seen in my masters thesis “impedance mapping and performance analysis of electroporated cells” [105]. A future paper comparing the impedance prediction of the “Transparent Box” model for cell suspensions to the impedance response of a cell suspension of brewers yeast *sacchraromyses Cerevisiae* is under way.

REFERENCES

[1] P. Ingram, J. D. Shelburne, V. L. Roggli and A. LeFurgey, *Biomedical Applications of Microprobe Analysis* chapter 14 Ionic Regulation of Proliferation in Normal and Cancer Cells. San Diego: Academic Press, 1999.

[2] S. V. Gandhi, D. C. Walker, B. H. Brown and D. Anumba, "Comparison of human uterine cervical electrical impedance measurements derived using two tetrapolar probes of different sizes," *BioMedical Engineering Online,* vol. 5, no. 62, 2006.

[3] C. Waterhouse, A. Raymond-Terepka and C. D. Sherman, Jr, "The Gross Electrolyte Composition of Certain Human Malignant Tissues" *Cancer Res*., vol.15, pp. 544-549, September 1955.

[4] A. K. Brewer and R. Passwater, "Physics of the Cell Membrane: Mechanisms Involved in Cancer," *Am. Lab.* pp. 37-45. April 10, 1976.

[5] G. K. Ojakian, "Tumor Promoter-Induced Changes in the Permeability of Epithelial Cell Tight Junctions," *Cell*, vol. 23, pp. 95-103, January 1981.

[6] A. P. Soler, R. D. Miller, K.V. Laughlin, N.Z. Carp, D. M. Klurfeld and J. M. Mullin, "Increased Tight Junctional Permeability is Associated with the Development of Colon Cancer," *Carcinogenesis*, vol.20, no.8, pp.1425–1431, 1999.

[7] R. B. Gennis, *Biomembranes: molecular structure and function*, New York: Springer-Verlag, 1989.

[8] A. C. Buchholz, C. Bartok and D. A. Schoeller," The Validity of Bioelectrical Impedance Models in Clinical Populations," *Nutr. Clin. Pract*., vol. 19, no. 5, pp. 433-446, Oct. 2004.

[9] B. Alberts, A. Johnson, J. Lewis, M. Raff, K. Roberts and P. Walter, *Essential Cell Biology: An Introduction to the Molecular Biology of the Cell*, 4th ed. New York: Garland, 1998.

[10] L. M. Broche, N. Bhadal, M. P. Lewis, S. Porter, M. P. Hughes and F. H. Labeed, "Early Detection of Oral Cancer – Is Dielectrophoresis the Answer?" *Oral Oncology*, vol. 43, pp. 199–203, 2007.

[11] I. Damjanov and F. Fan, *Cancer Grading Manual.* New York: Springer, 2007.

[12] D. Hanahan and R. A. Weinberg, "The hallmarks of cancer," *Cell*, vol. 100, pp. 57-70, 2000.

[13] G. Bussolati, C. Marchiò , L. Gaetano , R. Lupo and A. Sapino, "Pleomorphism of the Nuclear Envelope in Breast Cancer: A New Approach to an Old Problem," *J. Cell Mol. Med.*, vol. 12, no. 1, pp. 209-218, Jan.-Feb. 2008.

[14] S. B. Toal, et al. Centers for Disease Control and Prevention Oral Cancer Background Papers. http://oralcancerfoundation.org/presskit/CDC%20Media%20Kit/CDC%20Backgrounder.pdf 2011.

[15] "Preventing and Controlling Oral and Pharyngeal Cancer" U.S. Department Of Health And Human Services, Centers for Disease Control and Prevention (CDC) *morbidity and mortality weekly report*, vol.47, no. 14, Aug. 28, 1998.

[16] A. Mashberg and L. Garfinkel, "Early Diagnosis of Oral Cancer: The Erythroplastic Lesion in High Risk Sites," *CA-A Cancer Journal For Clinicians*, vol. 28, no.5, Sept./Oct. 1978.

[17] C. Scully and D. H. Felix, "Aphthous and other common ulcers," *British Dental Journal* vol. 199, no. 5, Sept. 10, 2005.

[18] R. M. Craig Jr, V. A. Vickers and R. W. Correll, "Erythroplastic lesion on the mandibular marginal gingival," *J. Am. Dent. Assoc*., vol. 119, no. 4, pp 543-544. Oct, 1989.

[19] A. Kauzman, M. Pavone, N. Blanas and G. Bradley, "Pigmented Lesions of the Oral Cavity: Review, Differential Diagnosis, and Case Presentations," *Journal of the Canadian Dental Association*, vol. 70, no. 10, pp. 682-683, Nov. 2004.

[20] C. A. Squier, M. J. Kremer, "Biology of Oral Mucosa and Esophagus," *Journal of the National Cancer Institute Monographs*, no. 29, pp.7-16, 2001.

[21] M.W. Lingen , J. R. Kalmar, T. Karrison and P. M. Speight "Critical Evaluation of Diagnostic Aids for the Detection of Oral Cancer," *Oral Oncology*, June 2007.

[22] R. J. Oliver, P. Sloan and M. N. Pemberton, "Oral Biopsies: Methods and Applications," *British Dental Journal*, vol. 196 no. 6, 27, March 2004.

[23] B. Blad and B. Baldetorp, "Impedance spectra of tumour tissue in comparison with normal tissue; a possible clinical application for electrical impedance tomography," *Physiol. Meas.* Suppl 4A pp. A105-115. Nov. 17 1996.

[24] C. Younghak, K. Hyun Soo, A. B Frazier, Z.G. Chen, S. Dong Moon and A. Han. "Whole-Cell Impedance Analysis for Highly and Poorly Metastatic Cancer Cells," *Journal of Microelectromechanical Systems* Vol. 18, no. 4, pp. 808 – 817, 2009.

[25] B. Blad, "Impedance spectra of cancerous and normal tissues from a mouse, " *Bioelectrochemistry and Bioenergetics*, vol. 45, pp. 169–172 1998.

[26] A. Han, L. Yang, and A. B. Frazier, "Quantification of the Heterogeneity in Breast Cancer Cell Lines Using Whole-Cell Impedance Spectroscopy," *Clinical Cancer Research*, vol. 139, no. 13, Jan. 1, 2007.

[27] N. Chauveau, L. Hamzaoui, P. Rochaix, B. Rigaud, J. J. Voigt, J. P. Morucci." Ex vivo discrimination between normal and pathological tissues in human breast

surgical biopsies using bioimpedance spectroscopy." *Annals of the NY Acad. Sci*., vol. 873, pp. 42-50. 20 April 1999.

[28] R. J. Halter, A. Schned, J. Heaney, A. Hartov, S. Schutz and K. D. Paulsen, "Electrical Impedance Spectroscopy of Benign and Malignant Prostatic Tissues," *The Journal Of Urology*, vol. 179, pp. 1580-1586, April 2008.

[29] R. J. Davies, R. Joseph, D. Kaplan, R. D. Juncosa, C. Pempinello, H. Asbun, and M. M. Sedwitz, "Epithelial Impedance Analysis In Experimentally Induced Colon Cancer," *Biophysical Journal*, vol. 52 1987.

[30] S. Abdul, B. Brown, P. Milnes and J. Tidy. "The use of Electrical Impedance Spectroscopy in the Detection of Cervical Intraepithelial Neoplasia," *Int. J. Gyneco.l Cancer*, vol. 16, no.5, pp. 1823-1832, 2006.

[31] A. J. Barrow and S. M. Wu, "Impedance measurements for cervical cancer diagnosis" *Gynecologic Oncology*, vol. 107, pp. S40–S43, 2007.

[32] B. H. Brown, P. Milnes, S. Abdul and J. A. Tidy. "Detection of cervical intraepithelial neoplasia using impedance spectroscopy: a prospective study." *British journal of obstetrics and gynaecology*. Vol. 112, no. 6, pp. 802–606, June 2005.

[33] S. Tai-Ping, C. Tak-Shing, C. Chi-Sheng, H. Su-Hua, C. Yi-Juai, H. Chin-Sung, C. Ching-Haur, H. Shiow-Yuan, S. Hsiu-Li, L. Wei-Hao, L. Chia-Ming and C. Chung-Yuan, "The use of bioimpedance in the detection/screening of tongue cancer," *Cancer Epidemiology*, vol. 34, pp. 207–211, 2010.

[34] L. Yang, L. R. Arias, T. S. Lane, M. D. Yancey and J. Mamouni, "Real-time electrical impedance-based measurement to distinguish oral cancer cells and non-cancer oral epithelial cells," *Anal Bioanal Chem*., vol. 399, no. 5, pp. 1823-1833 Feb, 2011.

[35] L. Yang, L. Renea Arias, T. S. Lane, M. D. Yancey and J. Mamouni, "Real-time electrical impedance-based measurement to distinguish oral cancer cells and non-Cancer oral epithelial cells," *Chemistry and Materials Science Analytical and Bioanalytical Chemistry* Speciation Analysis in Healthcare, vol. 399, no 5, pp. 1823-1833, 2010.

[36] P. Aberg ,I Nicander , J. Hansson, P. Geladi , U. Holmgren and S. Ollmar, "Skin cancer identification using multifrequency electrical impedance--a potential screening tool," *IEEE Trans. Biomed. Eng.*, vol. 51, no.12, pp. 2097-2102, Dec. 2004.

[37] M. Orazem and B. Tribollet, *Electrochemical Impedance Spectroscopy.* New York: John Wiley & Sons, 2008.

[38] E. Barsoukov and J. R. Macdonald, *Impedance Spectroscopy: Theory, Experiment, and Applications*, 2nd ed., New Jersey: John Wiley & Sons, 2005.

[39] W. He and J. Ferna´ndez, "Electron Tomography" *Encyclopedia of Life Sciences (ELS)*. Chichester: John Wiley & Sons, Ltd, January 2010.

[40] Origene "Tissue blocks price and availability," 2011 http://www.origene.com/tissue/tissue_blocks.aspx

[41] American Dental Association "2009 Distribution of Dentists in the U.S. by Region and State", Item code: DOD-2009/DOD-2009D. Available as a free download from http://www.ada.org/1444.aspx

[42] R. D. Juncosa, "Apparatus for epithelial tissue impedance measurements," U.S. Patent 4,690,152, September 1, 1987 - American Mediscan, Inc.

[43] K. R. Foster, "Dielectric Properties of Tissues." *The Biomedical Engineering Handbook: 2nd ed.*, Editor J. D. Bronzino, Boca Raton: CRC Press, 2000.

[44] B. J. Roth, "The Electrical Conductivity of Tissues."" *The Biomedical Engineering Handbook: 2nd ed.* ,Editor Joseph D. Bronzino, Boca Raton: CRC Press, 2000.

[45] C. Polk and E. Postow, *Handbook Of Biological Effects Of Electromagnetic Fields*. Boca Raton: CRC press, 1986.

[46] J. Tsai, J. A. Will, S. Hubbard-Van Stelle, H. Cao, S. Tungjitkusolmun, ,Y. Bin Choy, D. Haemmerich, V. R. Vorperian, and J. G. Webster, "Error Analysis of Tissue Resistivity Measurement," *Ieee Transactions On Biomedical Engineering*, vol. 49, no. 5, May 2002.

[47] E. T. McAdams and J. Jossinet, "Tissue Impedance: A Historical Overview," *Physiol. Meas.*, vol. 16, no. 1, 1995.

[48] K. Cole, *Membranes Ions and Impulses*, London: University of California Press, 1972.

[49] A. R. Waterworth, R. H Smallwood, P. Milnes and B. H. Brown, "Cole Equation Modelling to Measurements Made Using an Impulse Driven Transfer Impedance System," *Phys. Meas.*, vol. 21, no. 1, pp. 137-144, 2000.

[50] O. Schanne, and E. P.-Ceretti, *Impedance Measurements in Biological Cell*. New York: John Wiley and Sons, 1978.

[51] J. R. Macdonald, *Impedance spectroscopy*. New York: John Wiley & Sons, 1987.

[52] H. Fricke and S. Morse, "The Electric Resistance and Capacity of Blood for Frequencies Between 800 and 41/2 Million Cycles," *J. Gen. Physiol.*, vol. 9, pp. 153-167, 1925.

[53] H. Fricke, "A Mathematical Treatment of Electrical Conductivity and Capacity of Disperse Systems. II. The Capacity of a Suspension of Conducting Spheroids

Surrounded by a Non-Conducting Membrane for a Current of Low Frequency," *Phys. Rev*. vol. 26, pp. 678-681 1925.

[54] K. H. Schoenbach, R. P. Joshi, J. F. Kolb, N. Chen, M. Stacey, P. F. Blackmore, E. S. Buescher, and S. J. Beebe, "Ultrashort Electrical Pulses Open a New Gateway Into Biological Cells," *Proceedings of the IEEE*, vol. 92, no. 7, July 2004.

[55] R. Plonsey and R. Barr, *Bioelectricity A Quantitive Approach*. New York: Kluwer Academic / Plenum Publishers, 2000.

[56] D. Jones, R. Smallwood, D. Hose, B. Brown and D. Walker. "Modeling of Epithelial Tissue Impedance Measured Using Three Different Designs of Probe," *Physiol. Meas.*, vol. 24, no. 2, pp. 605–623, 2003.

[57] D. C. Walker, B. H. Brown, R. H. Smallwood, D. R. Hose and D.M. Jones, "Modeled Current Distribution in Cervical Squamous Tissue." *Physiol. Meas*., vol. 23, no. 1, pp. 159-168. 2002.

[58] D. C. Walker, "Modelling the Electrical Properties of cervical epithelium." Ph.D. dissertation, Univ. of Sheffield, Medical Engineering dept., Sheffield, 2001.

[59] A. Ivorra, R. Gomez, and J. Aguilo," Computer Modeling of Bioimpedance: A SPICE netlist generator to simulate living tissue electrical impedance." *Proceedings of the 12 International Conference on Electrical Bioimpedance*, Gdansk, Poland. pp. 317-320, 20 July 2004.

[60] S. Grimnes and Ø. G. Martinsen, "Cole Electrical Impedance Model—A Critique and an Alternative," IEEE Transactions On Biomedical Engineering, vol. 52, no. 1, pp.132-135 Jan. 2005.

[61] M. Osypka and E. Gersing, "Tissue impedance spectra and the appropriate frequencies for EIT," *Physiol. Meas*., vol. 16, pp. A49-A55, 1995.

[62] A. Ivorra, M. Genesc, A. Sola, L. Palacios, R. Villa, G. Hotter and J. Aguil´o, "Bioimpedance dispersion width as a parameter to monitor living tissues," *Physiol. Meas*. vol. 26, pp. 1-9, 2005.

[63] H. Thielecke, J. Fleckenstein, P. Bartholomä andC. Rübe "Evaluation of Impedance Spectroscopy for the Characterization of Small Biological Samples in Tissue-based Test Systems," *Proc. 26th Annual Int. Conf of the IEEE EMB*, pp. 2070- 2073, Sept. 1-5, 2004.

[64] A. R. Abdur-Rahman, C. M. Lo, and S. Bhansali, "Detailed Model for High-Frequency Impedance Characterization of Ovarian Cancer Epithelial Cell Layer Using ECIS Electrodes" *IEEE Transactions On Biomedical Engineering*, vol. 56, no. 2, Feb. 2009.

[65] H. P. Schwan, "Electrical Properties of Tissues and Cell Suspensions: Mechanisms and Models," *Proceedings of the 16th Annual International*

Conference of the IEEE Engineering in Medicine and Biology Society, vol.1, pp. A70 - A71, 3-6 Nov 1994.

[66] H. P. Schwan, "Mechanisms Responsible for Electrical Properties of Tissues and Cell Suspensions," *Med. Prog. Technol*., vol. 19, pp. 163-165, 1993.

[67] T. M. Mayhew "Quantitative description of the spatial arrangement of organelles in a polarised secretory epithelial cell: the salivary gland acinar cell," *J. Anat.* vol. 194, pp. 279-285, 1999.

[68] M. H. Ross and W. Pawlina, *Histology: A Text and Atlas: With Correlated Cell and Molecular Biology*, 6th ed. London: Wolters Kluwer/Lippincott Williams & Wilkins Health, 2011.

[69] N. F. Cheville, *Ultrastructural Pathology: An Introduction to Interpretation*, Ames Iowa: Iowa University Press, 1994.

[70] F. N. Ghadially, *Diagnostic Electron Microscopy of Tumours*, 2nd ed. Oxford: Butterworth-Heinemann, February 1986.

[71] F. N. Ghadially, *Ultrastructural Pathology Of The Cell And Matrix: A Text And Atlas Of Physiological And Pathological Alterations In The Fine Structure Of Cellular And Extracellular Components, 2nd ed.* Oxford: Butterworth-Heinemann, February 1982.

[72] D. W. Henderson and J. M. Papadimitriou, *Ultrastructural Appearances of Tumours: A Diagnostic Atlas.* New York: Churchill Livingstone, 1982.

[73] E. Hunter and M. Silver, *Practical electron microscopy a beginners illustrated guide.* New York: Cambridge university press 1993.

[74] J. A. King, "Role of transmission electron microscopy in cancer diagnosis and research," *Microscopy And Microanalysis*, p. 20, 2007.

[75] E. R. Weibel "Stereological Methods in Cell Biology: Where are we -Where are we going?" *The Journal of Histochemistry and Cytochemistry*, vol. 29, no. 9, pp. 1043-1052, 1981.

[76] W. He and J. Ferna´ndez, "Electron Tomography" *Encyclopedia of Life Sciences (ELS)*. Chichester: John Wiley & Sons, Ltd, January 2010.

[77] W. R. Loewenstein and Y. Kanno. "The Electrical Conductance and Potential Across the Membrane of Some Cell Nuclei," *J. Cell Biology*, Feb 1963.

[78] M. Mazzanti, J. O. Bustamante, and H. Oberleithner, "Electrical Dimension of the Nuclear Envelope." *Physiological Reviews*, vol. 81, no. 1, Jan. 2001.

[79] D. Zink, A. H. Fischer and J. A. Nickerson "Nuclear Structure in Cancer Cells," *Nature Reviews Cancer*, vol. 4, pp. 677 –787, Sept. 2004.

[80] S. Timonen and E. Therman," The Changes in the Mitotic Mechanism of Human Cancer Cells," *Cancer Res*., vol. 10 pp. 431-439, 1950.

[81] G. A. Perkins, and T. G. Frey, "Recent structural insight into mitochondria gained by microscopy, ” *Micron*, p. 9731, 2000.

[82] D. Koga, and T. Ushiki, "Three-dimensional Ultrastructure of the Golgi Apparatus in Different Cells: High-Resolution Scanning Electron Microscopy of Osmium-Macerated Tissues,” *Archives of Histology and Cytology*, p. 357, 2006.

[83] K. Gohari and F. H. White, "A Morphometric Study of Alterations in Rough Endoplasmic Reticulum During Differentiation in Stratified Squamous Epithelium," *Archives of Dermatological Research*, vol. 275, no.5, pp. 303-312, Aug. 1984.

[84] M. Grabe and G. Oster, "Regulation of Organelle Acidity," J. Gen. Physiol. vol. 117, pp. 329–343, April 2001.

[85] M. Blank, and I. Vodyanoy, *Biomembrane Electrocheistry*. Washington DC: American Chemical Society, 1994.

[86] G. Gabbiani, C. Chaponnier, and I. Huitner, "Cytoplasmic Filaments and Gap Junctions in Epithelial Cells and Myofibroblasts During Wound Healing." *Journal Of Cell Biology*, vol. 76, pp. 561-568, 1978.

[87] D. S. Friend And N. B. Gilula, " Variations In Tight And Gap Junctions In Mammalian Tissues," *Journal Of Cell Biology*, vol. 53, pp. 758-776, 1972.

[88] K. Kaufmann, W. Hankeand A. Corcia, *Book 3: Ion Channel Fluctuations in Pure Lipid Bilayer Membranes: Control by voltage*, Caruaru: 1989. available on line at http://membranes.nbi.dk/Kaufmann/publications.html

[89] H. Fricke, “The Electrical Capacity of Suspensions of Red Corpuscles of a Dog,” *Phys. Rev*. vol. 26, pp. 682-687, 1925.

[90] K. Cole, “Electric Impedance of Suspensions of Spheres,” *J. Gen. Physiol*., vol. 12 pp. 29-36, 1928.

[91] K. Cole, “Electric Conductance of Biological Systems,” *Cold Spring Harbor Symp*. *Quant. Biol.* Vol. 1, pp. 107-116, 1933.

[92] K. Asami, "Characterization of heterogeneous systems by dielectric spectroscopy," *Progress in Polymer Science*, vol. 27, no. 8, pp. 1617-1659, Oct. 2002.

[93] P. Nelson, *Biological Physics: energy, Information, Life*, New York: W.H. Freeman 2004.

[94] M. Mazzanti, J. O. Bustamante, and H. Oberleithner, "Electrical Dimension of the Nuclear Envelope." *Physiological Reviews*, vol. 81, no. 1, January 2001.

[95] H. Frlcke, “Thickness Of The Red Blood Corpuscle Membrane,” *J. Gen. Physiol*., vol. 9, p. 137, 1925.

[96] K. R. Foster, J. M. Bidinger and D. O. Carpenter,"The Electrical Resistivity Of Cytoplasm," *Biophysical Journal,* vol. 16, pp. 991-1001, 1976.

[97] D. Halliday, and R. Resnick, *Physics: Parts 1 and 2*. 3rd ed., New York: John Wiley and Sons, 1978.

[98] R. J. Ellis, "Macromolecular Crowding: Obvious but Underappreciated," *Trends Biochem. Sci*. vol. 26, no. 10, pp. 597–604, Oct. 2001.

[99] T.Y. Aw, "Intracellular Compartmentation of Organelles and Gradients of Low Molecular Weight Species," *Int. Rev. Cytol.* vol. 192 pp. 223–53, 2000

[100] R. S Cotran, V. Kumar and T. Collins, *RobbinsPathologic Basis of Disease. 6th ed.*, New York: W.B. Saunders, 1999.

[101] S.Y. Chen and R. D. Harwick, "Ultrastructure of oral squamous-cell carcinoma," *Oral Surg Oral Med Oral Pathol*. vol. 44, pp.744-53. Nov. 1977

[102] A. Doucet, N. Freitas, N. Gordon, *Sequential Monte Carlo methods in practice*, New York: Springer, 2001.

[103] D. P. Kroese, T. Taimre and Z. I. Botev, *Handbook of Monte Carlo Methods*, New York: John Wiley & Sons, 2011.

[104] W. L. Winston, *Microsoft Office Excel 2007 Data Analysis and Business Modeling*, Redmond: Microsoft Press, 2007

[105] P. R. Pelletier, “Impedance Mapping and Performance Analysis of Electroporated Cells,” Masters thesis, Arizona State University, Tempe, 2008. [UMI Proquest]

[106] I. Nicander, L. Rundquist and S. Ollmar “Electric impedance measurements at six different anatomic locations of macroscopically normal human oral mucosa,” *Acta Odontol Scand.* vol. 55, 1997.

APPENDIX

NOTES ON THE “TRANSPARENT BOX” MODEL IN EXCEL

TISSUE MODELS IN EXCEL® SPREADSHEETS ON CD

NOTES ON THE "TRANSPARENT BOX" MODEL IN EXCEL

A. Introduction

All the "Transparent Box" tissue models were developed in Excel® making it convenient for some aspects such as mathematical transparency and tedious for others such as repeated random simulations. The CD only contains the Excel® workbooks for each model. The Excel® files allow for the user to change the input variables and other model parameters to calculate the network element values. The frequency response analysis has to be performed in P-spice® or other circuit analysis software. P-spice® and schematics® is not included in the CD but a student version can be downloaded for free off the Internet from Cadence® at www.cadence.com

B. The Model Layout Within The Workbooks

One will notice for each model there are seventeen worksheets in each workbook. They can be generally categorized as output worksheets and input worksheets. The input worksheets comprise of the organelle level models, the cell level models and the tissue level models. There are four tissue layers in this model so there are four organelle level worksheets with tabs labeled; 'OL1' is for the squamous cell layer organelle construction, 'OL2' is for the cuboidal epithelial cell layer organelle construction, 'OL3' is for the columnar epithelial cell layer organelles and 'OL4' is for the basal cell layer organelle construction. There are also four cell level model worksheets with tabs labeled; 'CL1,' 'CL2,' 'CL3' and 'CL4' one representing each cell type in each layer. Finally there is a tissue layer models for each cell specific tissue; 'TL1,' 'TL2,' 'TL3' and 'TL4.' The tissue level worksheet is both an input and output worksheet one will input electrode spacing and tissue sample size data in X, Y, Z values, the outputs include the network element values. The 'tissue level' worksheet includes the network schematic for the tissue model and a reduced network model with respective network element values. The

element values would be exported to circuit analysis software for the appropriate network topology. The 'circuit elements' worksheet has the output in a convenient table form. The 'graph element' worksheet gives a graphical representation of the network element values it presents the values as a range and gives perspective of the relative values for each component. The 'primary variables' worksheet shows a convenient viewing table for the primary values from each of the levels of the model.

C. Changing Primary Input Variables

To change primary input variables it is simplest to go to the primary variable worksheet tab workbook and find the variable you want to change this will allow one to find the location of the variable value in the formula bar for an example one can find the source cell block in the model for the maximum resistivity of the peroxisome by clicking in the cell see Fig A-1 Finding the variable location.

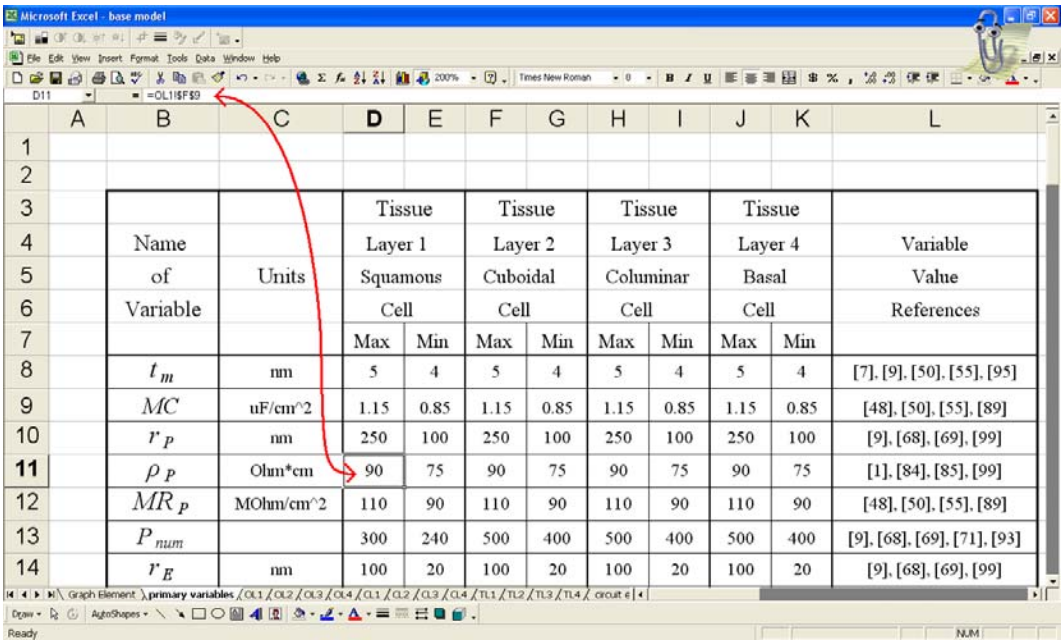

Name of Variable	Units	Tissue Layer 1 Squamous Cell Max	Tissue Layer 1 Squamous Cell Min	Tissue Layer 2 Cuboidal Cell Max	Tissue Layer 2 Cuboidal Cell Min	Tissue Layer 3 Columnar Cell Max	Tissue Layer 3 Columnar Cell Min	Tissue Layer 4 Basal Cell Max	Tissue Layer 4 Basal Cell Min	Variable Value References
t_m	nm	5	4	5	4	5	4	5	4	[7], [9], [50], [55], [95]
MC	uF/cm^2	1.15	0.85	1.15	0.85	1.15	0.85	1.15	0.85	[48], [50], [55], [89]
r_P	nm	250	100	250	100	250	100	250	100	[9], [68], [69], [99]
ρ_P	Ohm*cm	90	75	90	75	90	75	90	75	[1], [84], [85], [99]
MR_P	MOhm/cm^2	110	90	110	90	110	90	110	90	[48], [50], [55], [89]
P_{num}		300	240	500	400	500	400	500	400	[9], [68], [69], [71], [93]
r_E	nm	100	20	100	20	100	20	100	20	[9], [68], [69], [99]

Fig A-1 Finding the variable location

The formula bar shows the value comes from the organelle layer one worksheet (OL1) in cell F9. Click on the OL1 tab in the workbook click in the cell F9 and change the value as shown in Fig A-2 Editing values. Note for some primary variables like the membrane thickness variable t_m the task is not as simple. Each organelle and structure has its own specific t_m changing one does not change them all. One will have to search each cell layer and organelle level to adjust the values for the particular structure of interest.

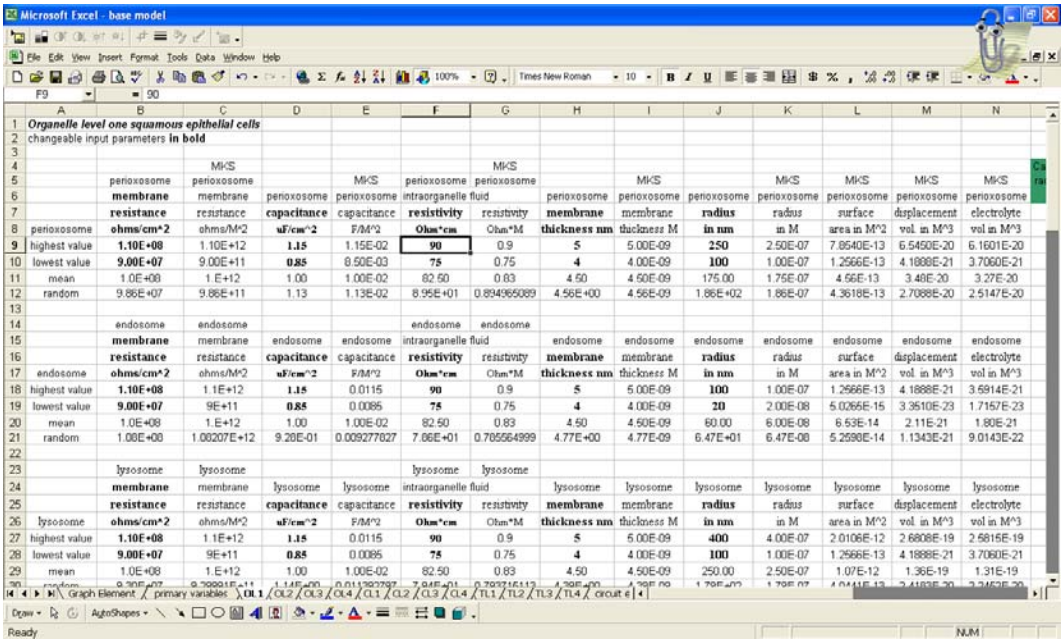
Microsoft Excel - base model

F9 = 90

	A	B	C	D	E	F	G	H	I	J	K	L	M	N
1	***Organelle level one squamous epithelial cells***													
2	changeable input parameters **in bold**													
3														
4			MKS				MKS							
5		perioxosome	perioxosome		MKS	perioxosome	perioxosome		MKS		MKS	MKS	MKS	MKS
6		**membrane**	membrane	perioxosome	perioxosome	intraorganelle fluid		perioxosome	perioxosome	perioxosome	perioxosome	perioxosome	perioxosome	perioxosome
7		**resistance**	resistance	**capacitance**	capacitance	**resistivity**	resistivity	**membrane**	membrane	**radius**	radius	surface	displacement	electrolyte
8	perioxosome	**ohms/cm^2**	ohms/M^2	**uF/cm^2**	F/M^2	**Ohm*cm**	Ohm*M	**thickness nm**	thickness M	**in nm**	in M	area in M^2	vol. in M^3	vol in M^3
9	highest value	**1.10E+08**	1.10E+12	**1.15**	1.15E-02	**90**	0.9	**5**	5.00E-09	**250**	2.50E-07	7.8540E-13	6.5450E-20	6.1601E-20
10	lowest value	**9.00E+07**	9.00E+11	**0.85**	8.50E-03	**75**	0.75	**4**	4.00E-09	**100**	1.00E-07	1.2566E-13	4.1888E-21	3.7060E-21
11	mean	1.0E+08	1.E+12	1.00	1.00E-02	82.50	0.83	4.50	4.50E-09	175.00	1.75E-07	4.66E-13	3.48E-20	3.27E-20
12	random	9.86E+07	9.86E+11	1.13	1.13E-02	8.95E+01	0.894965089	4.56E+00	4.56E-09	1.86E+02	1.86E-07	4.3618E-13	2.7088E-20	2.5147E-20
13														
14		endosome	endosome			endosome	endosome							
15		**membrane**	membrane	endosome	endosome	intraorganelle fluid		endosome	endosome	endosome	endosome	endosome	endosome	endosome
16		**resistance**	resistance	**capacitance**	capacitance	**resistivity**	resistivity	**membrane**	membrane	**radius**	radius	surface	displacement	electrolyte
17	endosome	**ohms/cm^2**	ohms/M^2	**uF/cm^2**	F/M^2	**Ohm*cm**	Ohm*M	**thickness nm**	thickness M	**in nm**	in M	area in M^2	vol. in M^3	vol in M^3
18	highest value	**1.10E+08**	1.1E+12	**1.15**	0.0115	**90**	0.9	**5**	5.00E-09	**100**	1.00E-07	1.2566E-13	4.1888E-21	3.6914E-21
19	lowest value	**9.00E+07**	9E+11	**0.85**	0.0085	**75**	0.75	**4**	4.00E-09	**20**	2.00E-08	5.0265E-15	3.3510E-23	1.7157E-23
20	mean	1.0E+08	1.E+12	1.00	1.00E-02	82.50	0.83	4.50	4.50E-09	60.00	6.00E-08	6.63E-14	2.11E-21	1.80E-21
21	random	1.08E+08	1.08207E+12	9.20E-01	0.009277627	7.66E+01	0.765564999	4.77E+00	4.77E-09	6.47E+01	6.47E-08	5.2598E-14	1.1343E-21	9.0143E-22
22														
23		lysosome	lysosome			lysosome	lysosome							
24		**membrane**	membrane	lysosome	lysosome	intraorganelle fluid		lysosome	lysosome	lysosome	lysosome	lysosome	lysosome	lysosome
25		**resistance**	resistance	**capacitance**	capacitance	**resistivity**	resistivity	**membrane**	membrane	**radius**	radius	surface	displacement	electrolyte
26	lysosome	**ohms/cm^2**	ohms/M^2	**uF/cm^2**	F/M^2	**Ohm*cm**	Ohm*M	**thickness nm**	thickness M	**in nm**	in M	area in M^2	vol. in M^3	vol in M^3
27	highest value	**1.10E+08**	1.1E+12	**1.15**	0.0115	**90**	0.9	**5**	5.00E-09	**400**	4.00E-07	2.0106E-12	2.6808E-19	2.5815E-19
28	lowest value	**9.00E+07**	9E+11	**0.85**	0.0085	**75**	0.75	**4**	4.00E-09	**100**	1.00E-07	1.2566E-13	4.1888E-21	3.7060E-21
29	mean	1.0E+08	1.E+12	1.00	1.00E-02	82.50	0.83	4.50	4.50E-09	250.00	2.50E-07	1.07E-12	1.36E-19	1.31E-19

Graph Element / primary variables / OL1 / OL2 / OL3 / OL4 / CL1 / CL2 / CL3 / CL4 / TL1 / TL2 / TL3 / TL4 / circuit e

Ready

Fig A-2 Editing values

Note all changeable primary variables are shown in bold. These changeable values are listed in appropriately sized units that have historically been used in the literature. The calculated values and the MKS unit values in adjacent cells for the same variables are not shown in bold. This can be seen in Fig A-2 Editing values. One will notice there is a row of maximum values followed by a row of minimum values. The next row is average values the following row is a random value between the max and min values.

D Using Multipliers

In the diseased models there are various multipliers that effect individual variables or entire groups of variables. For example in the cancer type 1 model at the organelle level worksheet for the cuboidal epithelial cells there are multipliers that will act globally on all organelles. Fig A-3 organelle level 2 worksheet in the cancer type 1 model shows the cancer radius reduction multiplier shaded in green it will act on each organelle within the tissue layer.

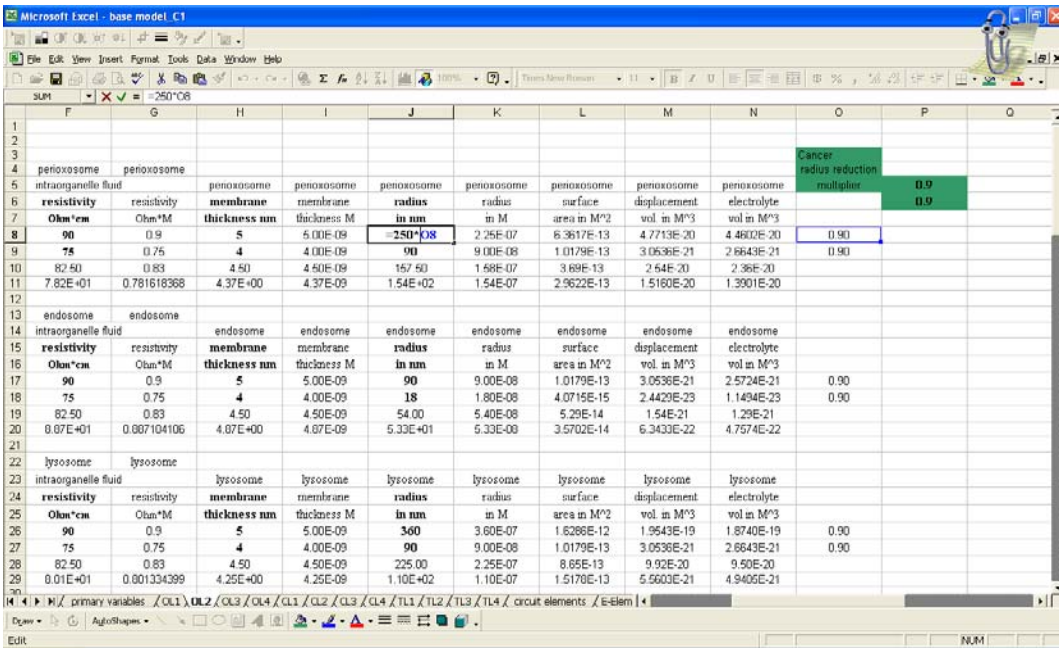

Fig A-3 organelle level 2 worksheet in the cancer type 1 model

In this case the multiplier is 0.9 so all the organelle radiuses will be 10% shorter. The organelle radiuses can still be manipulated individually it just happens to be more convenient to use the multiplier in situations of systematic changes. One will notice there are multipliers that act on both the maximum possible value and on the minimum possible value. These multipliers do not need to be symmetrical at the maximum and minimum ranges as shown in Fig A-3. Having separate multipliers for the max and min

value ranges provides a more flexible means of primary variable range control. All variables and formulas are traceable this is the advantage of a spread sheet program one can find all the interconnectivity fairly easily.